FAP24

Government of the People's Republic of Bangladesh

Water Resources Planning Organization

European Commission

Delft Hydraulics

Danish Hydraulic Institute

Hydroland

Approtech

Osiris

RIVER SURVEY PROJECT

Special Report No.11

Optimization of hydraulic measurements

October 1996

Special Report 11

Optimization of Hydraulic Measurements

October 1996

6

Contents

Contents, Annexure A: Turbulent structure and optimal measuring time

Contents, Annexure B: Some aspects of turbulent flow structure in large alluvial rivers

Contents, Annexure C:
Optimal vertical and horizontal distribution of velocity measurements in discharge estimation

Contensts, Annexure D: Analysis of Tidal Survey Data

Figures

9

Tables

Acronyms and abbreviations

ADCP	: Acoustic Doppler current profiler
BIWTA	: Bangladesh Inland Water Transport Authority
BTM	: Bangladesh Transverse Mercator (a geodetic grid)
BWDB	: Bangladesh Water Development Board
CEC	: Commission of the European Communities (presently the EC)
DELFT	: DELFT Hydraulics, The Netherlands
DGPS	: Differential Global Positioning System
DHA, DHB...	: Names of RSP survey vessels
DHI	: Danish Hydraulic Institute
EC	: The European Commission (formerly the CEC)
ELAC	: Brand name of an echo sounder instrument
EMC	: Electromagnetic current meter
EMF	: Electromagnetic flow meter
FAO	: Food and Agriculture Organization
FAP	: Flood Action Plan
FAP24	: Flood Action Plan project no. 24 (= RSP)
FPCO	: Flood Plan Coordination Organization (presently WARPO)
HYMOS	: Name of a hydrological software package and of a FAP24 database
IO	: Inter-Ocean (manufacturer of the S4 instrument)
ISO	: International Organization for Standardization
LAZ	: Name of a specific echo sounder instrument
O&M	: Operation and maintenance
PEMS	: Name of an EMF instrument
PSD24	: Processed Survey Data of FAP24, a FAP24 database
PWD	: Public Works Department (and name of a datum)
RDI	: RD Instruments (manufacturer of an ADCP instrument)
RSP	: River Survey Project (= FAP24)
RSPMU	: River Survey Project Management Unit
SEBA	: Name of a propeller type current meter
SLW	: Standard Low Water (a datum)
SPE	: Standard pulsation error
S4	: Brand name of an electronic current meter
VHF	: Very high frequency
WARPO	: Water Resources Planning Organization
WMO	: World Meteorological Organization

Summary

This report considers hydraulic measurements for routine gauging of velocity, depth, water level, and width, taken to obtain discharge information, stage-discharge relationships, and to produce bathymetric maps. The optimization of those hydraulic measurements covered four basic, but inter-related, activities: (1) optimization of measurement networks, (2) optimization of measurement frequencies, (3) optimization of equipment and methods, and (4) optimization of survey operations.

A multi-criteria optimization analysis technique was developed and applied for screening these activities. The criteria determined that the equipment and methods used in this study should allow for high data quality at low procurement and operational and maintenance costs. In addition, the equipment and methods should be easy to operate, take minimal measurement time, require little maintenance, and should well represent the hydraulic parameters.

Since this report covers the final evaluation of hydraulic measurements, different activities were further screened on a multi-criteria sustainability analysis technique. The applied criteria were:

- the affordability of investment and operational and maintenance costs
- operational and maintenance institutional capabilities
- technological compatibility
- optimal technique and survey results
- justifying results against incurred expenses
- environmental suitability

The findings and recommendations are based on the routine gauging of water level and flow, as well as several programmes of special measurements that were made in order to account for equipment and method accuracy within the River Survey Project (RSP) and between RSP and BWDB. The results should only be interpreted as indicative.

One result was that through several inter-comparison measurements of the instruments, velocity variations were within seven percent only. The variations may have been the result of systematic biases of each instrument, random variation of the instruments, or the fact that the instruments did not measure at the same place. A second result was that the PEMS-EMF velocity had the least relative standard deviation at ± 2.5 percent, but the Ott-propeller velocity had the highest at ± 6.5 percent. Other relative standard deviations included the RDI-ADCP 600 velocity at ± 4.6 percent, the IO-EMC (S4) velocity at ± 5.1 percent, the RDI-ADCP 600 direction at ± 1.0 percent, and the IO-EMC (S4) direction at ± 1.3 percent.

A third result was that joint measurements by the River Survey Project (RSP, or FAP24) and the Bangladesh Water Development Board (BWDB) indicated that the discharge estimation between the two techniques (traditional velocity-area by BWDB and the ADCP-EMF moving boat method by FAP24) were comparable and within 8.5 percent.

A fourth result was that investigations on the Type I error, due to limited exposure, indicated that the error decreased as the exposure is increased. For a 50 s exposure time, the error varied from ± 4.7 percent near the surface to ± 13.8 percent near the bottom.

A fifth result was that the Type II error, which was due to the limited numbers of vertical measuring points, appeared to be insignificant. The maximum variation was only about five percent. The last result was that the Type III error, which was due to the limited numbers of measuring verticals in a transect, was significant if few verticals were sampled.

Although the current gauging network involving primary stations is working, it would be beneficial to relocate some sites. The annual measurement frequency should be carried out according to the distinct phases of the hydrograph. This report suggests gauging discharge on a fortnightly schedule during flat low stages, weekly gauging during slow rising and falling stages, and bi-weekly gauging during rapid rising, falling stages, and peak stages.

During multi-criteria optimization analyses of equipment and methods, the Differential Global Positioning System (DGPS) was found to be optimal in positioning survey vessels because of its accuracy and ease of operation. ADCP was considered the best for measuring velocity, although other devices had close scores. The acoustic system proved optimal for measuring depths, while water level observation were best obtained with sensors involving acoustic and pressure devices. In addition, the ADCP-EMF moving boat method was found optimal for measuring discharge.

In conclusion, similar analyses of sustainability show that a DGPS positioning system should be applied as it is accurate and easy to operate. Although propeller-type current meters were found reasonable for measuring velocity, other instruments are developing quickly and should be considered in the future. The same is true for manual staff gauges. Also, an acoustic-type depth-measuring instrument (echo sounder) should be used. A velocity-area method of discharge estimation could be followed, but it needs improvement in instrumentation. A cost-effective application of the ADCP-EMF moving boat method could be sustainable under similar circumstances. Bathymetric surveys should be carried out in specific locations during rising, peak, and falling river stages.

It is also recognized that human factor is an important consideration in survey. A sophisticated and high-tech method can fail if the equipment and method are not operated correctly. Therefore, training is fundamental for a sustainable survey. In addition, careful consideration should be given with selecting a survey vessel. Utmost care should be given when measuring hydraulic parameters at the primary gauging stations. If necessary, certain stations should be relocated. Discharge measurements should be made bi-weekly, weekly, or fortnightly, depending on the season.

22

1 Introduction

1.1 General

The River Survey Project (RSP, or FAP24) was initiated on June 9, 1992. The Project was executed by the Flood Plan Coordination Organisation (FPCO), later merged with Water Resources Planning Organization (WARPO), under the Ministry of Irrigation, Water Development, and Flood Control, later the Ministry of Water Resources. Funding was granted by the European Union (formerly the Commission of the European Communities). The FAP 24-A Consultant was Delft Hydraulics and Danish Hydraulic Institute (DELFT-DHI Consortium) in association with Osiris, Hydroland and Approtech. The Project is supervised by a Project Management Unit with participation by FPCO/WARPO, FAP 24-B Consultants consisting of a Project Advisor, and a Resident Project Advisor.

The objective of the Project is to establish detailed, accurate field data for Flood Action Plan projects, and in general for any planning, impact evaluation, or design activities within national water resource and river engineering activities.

The Project comprises:

- A survey component, comprising a comprehensive field survey programme of river hydrology, sediment transport, and morphology
- A study component, comprising investigations of processes and effects within river hydrology, sediment transport, and morphology
- A training component

The scope of the study component was developed in a dialogue with the Client and the Project Advisor, who stressed the importance of survey in large alluvial rivers (Peters, 1993a) and also undertook supervision and rendered comprehensive professional advice during its execution. The advice was rendered in several of the Project Advisor's mission reports (e.g., Peters, 1994, 1995). The proceedings are reported in a series of *RSP Study Reports*.

The present RSP Study Report 11 describes an optimization study on hydraulic measurements for routine gauging of water level and flow in Bangladesh. A closely related study on optimization of sediment transport measurements is reported in Study Report 12.

The study was managed and reported by Dr. Dilip K. Barua with participation by several other members of the RSP study team. Annexure B of the present report was prepared together with Khalid H. Rahman. This Annexure was submitted for publication in the IAHR journal. Other Annexure contributions are as follows: Annexures A and C - Dr. Dilip K. Barua; Annexure D - Mr. Carsten Staub.

1.2 Background

BWDB has collected hydraulic data systematically since 1964 under the initiative of the Food and Agriculture Organization (FAO, 1964). The collected data form an appreciable data-base that has been used extensively by different water sector planners, designers, and managers. Still, there is room for modifications or supplements (River Survey Project, 1994), for example when

- detailed data are required over space and time
- more hydraulic parameters are needed than those measured by BWDB

- the high water and flood stages of the rivers need to be measured
- special data are needed for different water-sector projects and studies

The River Survey Project (FAP24, or RSP) began operation in Bangladesh in June 1992 with the objectives to collect all-season data on river hydraulics and morphology. The survey area covered the main rivers of Bangladesh — the Ganges, the Brahmaputra, and the Padma — and their major tributaries and distributaries (Figure 1.1).

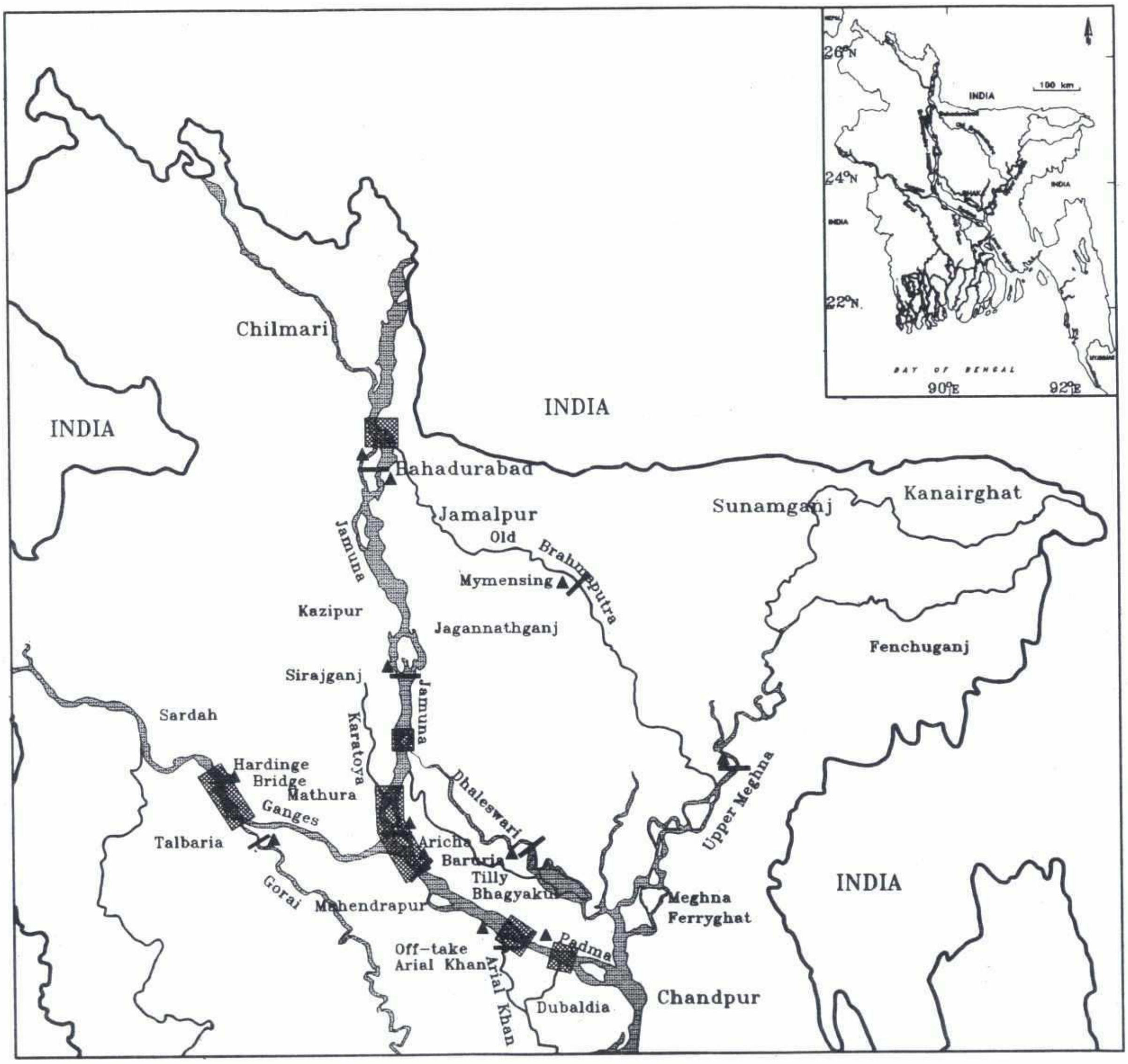

LEGEND:

Figure 1.1: Main rivers of Bangladesh the Ganges, the Brahmaputra and the Padma and their major tributaries and distributaries and the study area of the River Survey Project

ƏG

The mobilized equipment used for hydraulic measurements is shown in Figure 1.2

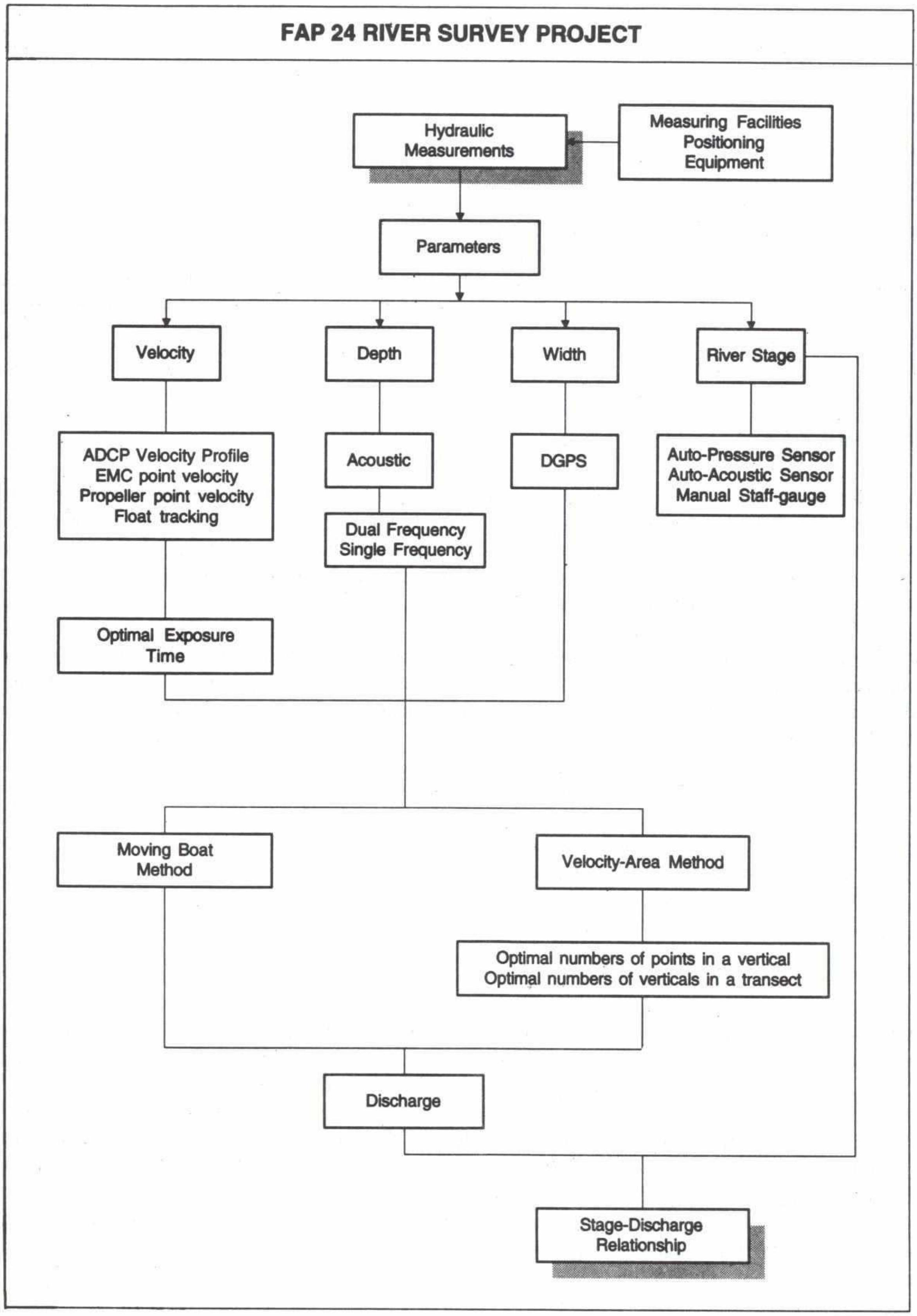

Figure 1.2: Flow-chart of hydraulic measurements and mobilized equipment by FAP24

and includes instruments to measure four different hydraulic parameters: velocity, depth, width, and river stage. In several cases, multiple instruments were mobilized to pursue an optimal measurement after evaluating the instrument performance against optimization criteria. It was necessary to examine the measurement options against sustainability criteria so that a sustainable measuring technique could be recommended for Bangladesh agencies. This report discusses the discharge and bathymetric maps that have resulted from these measurements.

Optimization of overall survey techniques is a continuous process when each instrument and method is evaluated to pursue an optimal option. In the River Survey Project, the process began by selecting instruments before the initial mobilization phase, followed by evaluating instrument performance during the test gauging phase, resulting in the subsequent selection and mobilization during Phase II of the project. Finally, during phase II, further evaluation took place, using both routine surveys and special measurements. The selection and initial mobilization are described in RSP (1991). During the initial test phase, equipment was mobilized, tests were made, and results were reported (RSP, 1993c; RSP 1993d).

1.3 Objectives

The objectives of this report were to present an evaluation of the RSP experience with respect to equipment and methods for optimal, sustainable hydraulic measurements, and to suggest an optimal, sustainable hydraulic measurements strategy with the intent that the suggested instruments and methods will be adopted by agencies such as BWDB and the Bangladesh Inland Water Transport Authority (BIWTA), or private organizations (Figure 3).

When designing a field-data collection plan, it should be clear as to whether the objectives are general monitoring, special studies or project requirements, or research, as each has definite data requirements and desired accuracy levels. In this report, hydraulic measurements were examined mainly for the purpose of long-term routine data generation.

The optimization process considered the following four sets of data-collection activities:

- optimizing the measurement network
- optimizing the measurement frequency
- optimizing equipment and methods
- optimizing the survey operations

FAP24's routine gauging measurements were used and analyzed for the purpose of the present study. Also, some special dedicated surveys were made to support the optimization process. These included measurements to determine the uncertainty level of velocity-measuring instruments and to make inter-comparisons between them, and measurements made to compare instruments and methods used by BWDB and FAP24. It also included the use of electronic current meter sensors to take time-series measurements of flow velocities in low and high river stages to determine the turbulent flow structure and an optimal exposure time for instruments. And, last, special measurements were made to determine the optimal numbers of points in a vertical, and the optimal number of verticals in a transect that were required for an optimal velocity-area discharge method. Details of the special measurements can be found in the Annexures to the present report.

2 Principles of optimization

Optimization is a process of finding the most favourable solution to a problem that will meet pre-determined quantified objectives. It implies obtaining appropritae data at a minimum cost. It is a well-established discipline of science that applies rigorous numerical techniques (e.g. Fletcher, 1987) to practical heuristic approaches (e.g. Delft Hydraulics, 1990). Figure 2.1 shows the optimization principle in the form of a flow-chart.

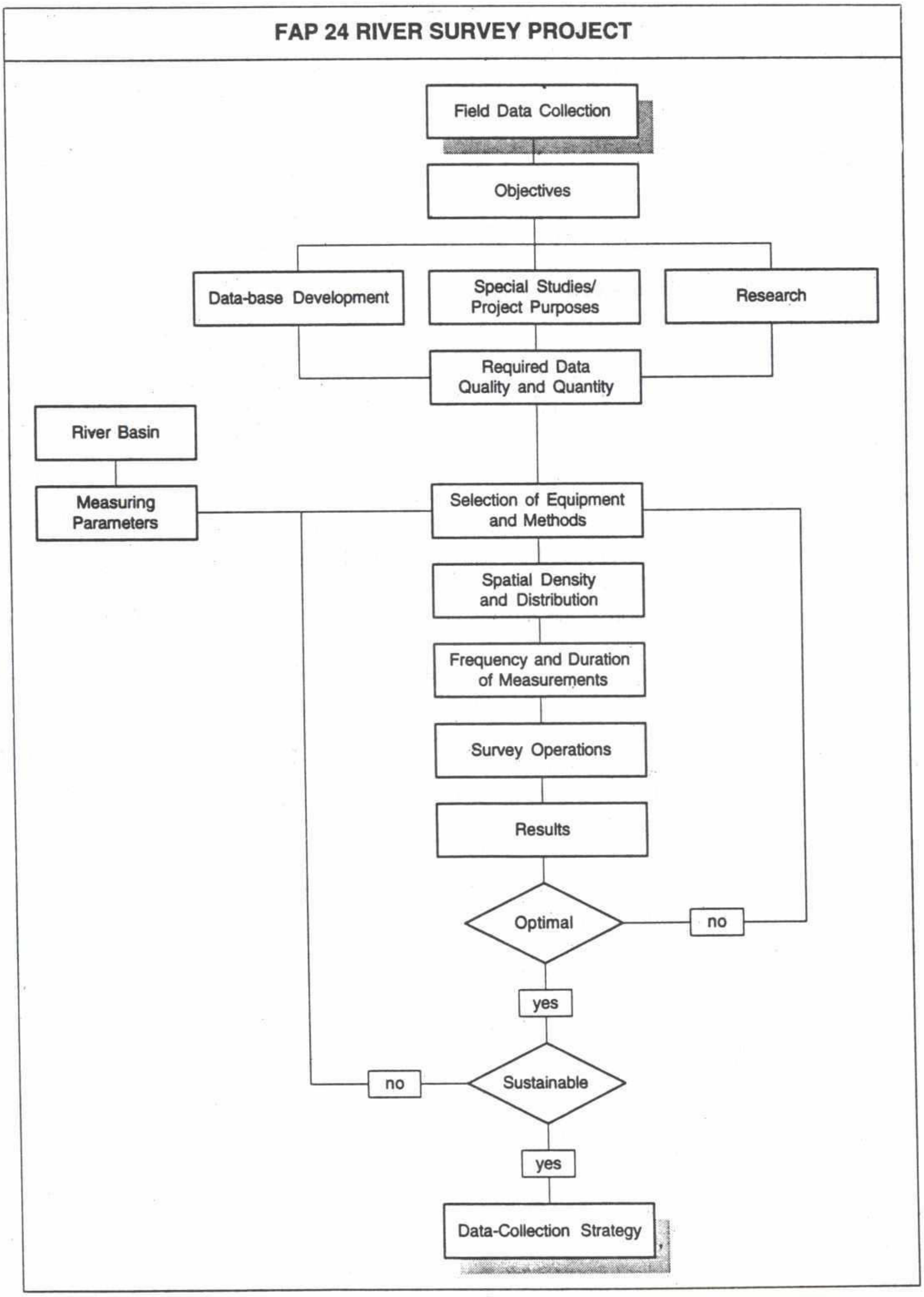

Figure 2.1: Flow-chart indicating the general optimization principle

It consists of a series of activities that are evaluated from optimization criteria, and repeated, if necessary, at an advanced level, thus forming a loop. An external loop could be imposed on the chart to examine the activities on the basis of sustainability criteria (see chapter 9). Such criteria could lead to developing a data collection strategy for an institution or country. Therefore, it is suggested that optimization is necessary for sustainability.

The quality and quantity of data collection can be defined relative to the following three basic objectives of the measurements:

- routine measurements for long-term, data-base development may be less detailed in space, time, and accuracy (whereas the data consistency is a main quality characteristic)
- data for special studies or project requirements should fulfil specific quality and quantity objectives
- data required for research purposes often should include details on space and time, and be of a high quality

The examination is based on the principle that,

- appropriate data means basically comparing the required data with available data (= survey results) in terms of quality and quantity
- if the optimum solution is not sustainable, the requirements regarding data quality and quantity need to be adjusted (e.g. by accepting less data or less accuracy)
- data quality means accuracy, but also timely availability (level of automation of data processing).

Once the desired data quality and quantity are defined, the variability and range of the river parameters to be measured should be recognized before selecting equipment and methods. Once recognized, the activities can be pursued in four distinct disciplines: (1) selecting equipment and methods, (2) determining spatial density and distribution of measuring stations, (3) determining frequency and temporal distribution of measurements, and (4) conducting the actual survey operations.

Each of these activities should be evaluated on some optimization criteria. This study used a multi-criteria format and identified six basic criteria (Table 2.1). The equipment or method selected should have the least procurement, and operation and maintenance costs, but maintain sufficient accuracy. In addition, the equipment and methods should be easy to operate, should take little measurement time, should require little maintenance and should represent the hydraulic parameters well.

Optimization Criteria
1. Investment, operation and maintenance costs
2. Required accuracy according to the objectives
3. Operational ease
4. Measurement duration
5. Maintenance
6. Representativity of parameters being measured

Table 2.1: Optimization criteria for hydraulic measurements

Each instrument and method was evaluated by the optimization criteria listed in Table 1. For this study, cost and accuracy received higher priority than the others. Detailed application of the proposed method and results are discussed in Chapter 8.

3 River characteristics

3.1 River hydraulics and survey

The survey planning, equipment mobilization, and execution of the measurements are dependent on the hydraulic characteristics of the rivers. The more complicated the rivers are, the more difficult is the survey. In particular, the flow structure in large alluvial rivers is three-dimensional and turbulent (Peters and Goldberg, 1989), which makes accurate measurements difficult.

In the rivers of Bangladesh, there are multiple channels in most reaches, especially in the Jamuna and Padma Rivers, with no easy navigation between them especially during low river stages. The confluence and off-take flow situations created by multiple channel junctions, river bends, and transitional reaches from wide to constricted or from constricted to wide, cause accelerating and decelerating flows and makes it difficult to locate an ideal measuring station. Shallow, wide secondary, or storage channels, are difficult to navigate and measure. Also, channels and banks migrate at such a high rate that during one measurement interval a completely new channel configuration could form, necessitating repeated reconnaissance.

In addition, there is a high variability in space and time when measuring Bangladesh river parameters. For example, the seasonality of rivers creates an important difference in wet cross-sectional areas. High sediment concentrations, specially during the monsoon season, may require special instruments to counter common instrument sensitivities. For studies located in the lowermost reach of the fluvial system, that cover both tidal and nontidal reaches, it is necessary to design a different survey spread.

These important river characteristics were recognized at the initiation of this project and influenced the selection of equipment and methods as described in the technical specifications and technical proposal of the River Survey Project (RSP, 1991a; RSP, 1991b).

3.2 Variability of major hydraulic parameters

It is esssential to understand the various characteristics of the hydraulic parameters, such as water level, velocity, and discharge variability, and how they relate in space, time, and range in order to determine an optimum measuring technique. Table 3.1 shows the range of water level, velocity, discharge, depth, and width in the major rivers of Bangladesh. The measurement stations were located at Bahadurabad on the Jamuna River, Mymensingh on the Old Brahmaputra River, Tilly on the Dhaleswari River, Hardinge Bridge on the Ganges River, Kushtia Railway Bridge on the Gorai River, Baruria on the Padma River, the Arial Khan off-take, and Bhairab Bazar on the Upper Meghna River.

The largest variations occurred in the Ganges River. The highest velocity was measured in the Ganges River near Hardinge Bridge, while the highest flood-time discharge was recorded in the Padma River at Baruria. Confluences and bend scour holes kept maximum depth measurements in all rivers to about 40 m. The largest width measurement was taken over the major channel of the multi-channelled Jamuna River during the bankfull discharge.

River system	River	Water level range (m)	Maximum velocity (m/s)	Discharge variability (1000 m^3/s)	Maximum depth (m)	Maximum width (km)
Brahmaputra-Jamuna	Jamuna	6	3.5	8 - 100	40	5
	Old Brahmaputra	4	3.0	0 - 10	30	1
	Dhaleswari	4	3.0	0 - 15	30	1
Ganges	Ganges	8	4.0	1 - 70	40	3
	Gorai	5	3.0	0 - 20	30	1
Padma	Padma	4	3.0	10 - 120	40	5
	Arial Khan	3	2.0	0 - 15	20	1
Meghna	Upper Meghna	4	2.5	0 - 30	30	1

Table 3.1: Range of water level, velocity, discharge, depth, and width in the major rivers of Bangladesh

It should be understood that in the course of the proeject-period, a lot of additional information on the variability became available from the following sources.

- planforms
- cross-sections
- bed-profiles (side-scan, dune tracking)
- velocities at different stations
- discharge (hydrographs of several years)

Water levels in different Bangladesh rivers varied seasonally with the lowest levels occurring from February to April, and the highest occurring from July to August. The water level slope is important for hydraulic computations and for use in bathymetric surveys. Overall surface water slopes depicting time and space averages are shown in Table 3.2. The upper Meghna River had the least slope at 2.3 x 10^{-5}, while the upper reaches of the Brahmaputra-Jamuna River had the highest slope at 7.6 x 10^{-5}. In addition, local slopes are important indicators of morphological developments (Peters, 1993). The local and the seasonal slopes have been recognized (RSP, 1996a).

River	Surface water slopes
Brahmaputra-Jamuna upper reaches	7.6×10^{-5}
Brahmaputra-Jamuna lower reaches	6.5×10^{-5}
Ganges	5.5×10^{-5}
Padma	4.0×10^{-5}
Upper Meghna	2.3×10^{-5}

Table 3.2: Average surface-water slopes of the major rivers in Bangladesh

4 Selection and mobilization of equipment

Equipment and methods were suggested either as a reference method, the traditional method followed by BWDB, or a recommended method, which was the method eventually applied by the RSP.

4.1 Basic considerations

A survey vessel is a mobile platform for deployment of instruments. When selecting and procuring a survey vessel, careful consideration was made of the hydraulic environment of Bangladesh rivers; the propulsion system; the draft of the vessel; the overall stability and stability during hazardous situations; speed of the vessel; deck space for survey operations; data-processing, and office work-space; accommodations for crew and surveyors; procurement, operation, and maintenance costs; modification possibilities to install survey equipment, availability of spare parts and local repairs; and other facilities.

When selecting an instrument either for velocity, depth, width (positioning), or river stage measurements, the basic considerations were: Accuracy, cost, operational conditions, repair and maintenance constraints, and the hydraulic environment of Bangladesh rivers.

In this chapter, only a brief description of the mobilized equipment used for Phase I and II of the Project is given. Details of the initial mobilized equipment used are discussed in the First Interim Report (RSP, 1993a).

4.2 Measuring facilities

Table 4.1 shows the measuring facilities used by FAP24. Included, but not shown, were guest houses rented or renovated to accommodate surveyors and vessel crews.

Facilities		Phase I	Phase II
Vessels:	DHA	x	x
: DHB			x
: DHC		x	x
: DHD			x
: DHE		x	x
: Zodiac		x	x
System support:			
:	Gyro compass & auto-pilot	x	x
:	On-line data logging and navigation system	x	x
:	Software package for data logging, processing navigation and quality assurance	x	x
:	Safecom, VHF radios, walkie-talkies	x	x

Table 4.1: Measuring facilities mobilized and used by FAP24

The largest survey vessel used by FAP24 was DHA. This vessel had a draft of 1.5 m, a screw-type propulsion system, crew sleeping accommodations, wheel-house space for data-logging and on-line data processing, deck space, and winches and davits for deploying instruments and sampling. After installing different survey instruments, it became a well-equipped vessel able to carry out discharge measurements, bathymetric surveys, and sediment measurements.

The DHB is a flat-bottomed vessel with a draft of 1.0 m and a Z-drive propulsion system that was procured during Phase II of the project. Deck-space and other facilities were limited on this vessel.

The DHC is a catamaran that works well in shallow water. It was equipped with a Navtrack DGPS receiver, a SIMRAD single frequency echosounder, and different communication hardware.

The DHD and DHE were equipped, when needed, with portable positioning systems, single frequency echosounders, and propeller-type current meters for measuring discharge in shallow water and for carrying out bathymetric surveys.

In DHA, DHB and DHC vessels, excellent steering were achieved by installing a modern steering machine and an advanced steering automat. For further details on the on-line data processing equipment, see Chapter 6 and RSP First Interim Report (1993a).

4.3 Instruments

Various hydraulic measurement instruments mobilized and used by FAP24 are shown in Table 4.2. A brief description of each follows.

On survey-vessel DHA, the following instruments are installed.

- 300 kHz ADCP
- Trimble 300E DGPS receiver
- ELAC LAZ 4420 dual frequency echosounder
- S4 electromagnetic sensor deployed at the aft of the vessel
- EMF electromagnetic sensor deployed at the bow of the vessel
- various communication hardware

On survey-vessel DHB, the following instruments are installed.

- 600 kHz ADCP
- Navtrack DGPS receiver
- SIMRAD EA 300 P single frequency echosounder
- S4 electromagnetic sensor deployed at the aft of the vessel
- EMF electromagnetic sensor deployed at the bow of the vessel
- different communication hardware

A summary of the installed instrument is shown in Table 4.2 during Phase I and Phase II.

Purpose	: Instrument	Phase I	Phase II
Positioning:	: Trimble DGPS	x	x
Echosounding:	: ELAC LAZ 4420	x	x
	: SIMRAD EA 300 P	x	x
Velocity:	: RDI-ADCP	x	x
	: IO-EMC (S4)	x	x
	: PEMS-EMF	x	x
	: Ott-propeller	x	x
	: Float-tracking	x	x
River-stage:	: Auto-pressure level-log		x
	: Auto-acoustic level-log		x
	: Manual staff-gauge	x	x

Table 4.2: Instruments mobilized and used by FAP24

4.3.1 Positioning

Traditionally, Bangladesh agencies use two types of positioning systems for hydraulic and hydrographic measurements. The Bangladesh Inland Waterways Transport Authority (BIWTA) and BWDB bathymetric surveys use the Decca Navigation System. For transect discharge gauging, BWDB used sextants. While the Decca Navigation System has a 100 m accuracy range, the accuracy of sextant system depends on the observer and conditions in the field. Sextant sighting is usually effective on smaller channels and rivers when measuring short distances by observing angles. On large rivers, such as the Jamuna, the system is not accurate, although BWDB uses the system for hydrological survey and cross-sectional measurements. FAP24 introduced the DGPS, a system that offers coordinates with a standard deviation of $\pm$ 3 m (determined in a stationary mode). The DGPS system described in River Survey Project (1993a) consists of space, control, user, and reference station segments. The positioning was made from the shore-based reference stations that monitored and modulated the GPS signals to the desired accuracy level.

Applying a DGPS system for absolute positioning implies that the easting and northing position of the shore-based stations are known. But, no such stations existed prior to this study. In addition, the projection system used a WGS84 ellipsoid, which differs from the Everest ellipsoid used by Bangladesh. Therefore, the initial test phase of the project was devoted to establishing the reference stations by land-survey and transferring the WGS84 eastings and northings to the Everest ellipsoid. The reference stations were installed at Fulchari near Bahadurabad, Sirajganj, Aricha, Hardinge Bridge, and Mawa.

4.3.2 Water level gauging

BIWTA and BWDB are the government agencies that gauge river stages. BIWTA operates about 35 recording gauges that primarily collect tidal data in coastal areas. BWDB operates about 28 gauges, primarily in the inland rivers. Float or bubble-type recording gauges are the main instruments used at these stations where analogue data are collected. However, none of these stations were located in places that could be used effectively by the River Survey Project. Though some BWDB stations were suitably located, such as the one at Hardinge Bridge, a continuous auto-record was often not available. Moreover, FAP24 objectives to establish stage-discharge relations, estimate local and overall hydraulic gradients, reduce bathymetric survey data, and design hydraulic modelling and morphological computations were often different from BWDB or BIWTA objectives.

To attain its objectives, FAP24 installed 11 permanent recording stations that are shown in Table 4.3.

Serial Number	River System	River	Station	Sensor
01	Brahmaputra-Jamuna	Jamuna	Bahadurabad and Gabgachi	Pressure/ Acoustic
02	-	Jamuna	Sirajganj/ Bhuapur	Pressure
03	-	Jamuna	Teota (Aricha)	Pressure
04	-	Old Brahmaputra	Mymensingh	Acoustic
05	-	Dhaleswari	Tilly	Pressure
06	Ganges	Ganges	Hardinge Bridge	Acoustic
07	-	Gorai	Kushtia R.B.	Acoustic
08	Padma	Padma	Baruria	Pressure
09	-	Padma	Mawa	Pressure
10	-	Arial khan	Off-take	Pressure
11	Meghna	Upper Meghna	Bhairab Bazar R.B.	Acoustic

Table 4.3: Water level observation stations along the major rivers and there distributaries

Pressure or acoustic sensors were installed at these recording stations. Details of the selected sensors are discussed in River Survey Project (1995). At each station, the recording gauges were supplemented by manual staff gauge readings. In addition to these permanent stations, gauges also were installed in some locations to record local slope. Figures 4.1, 4.2 and 4.3 show some inter-comparison of different sensors and manual staff gauging at Bahadurabad and Gabgachi.

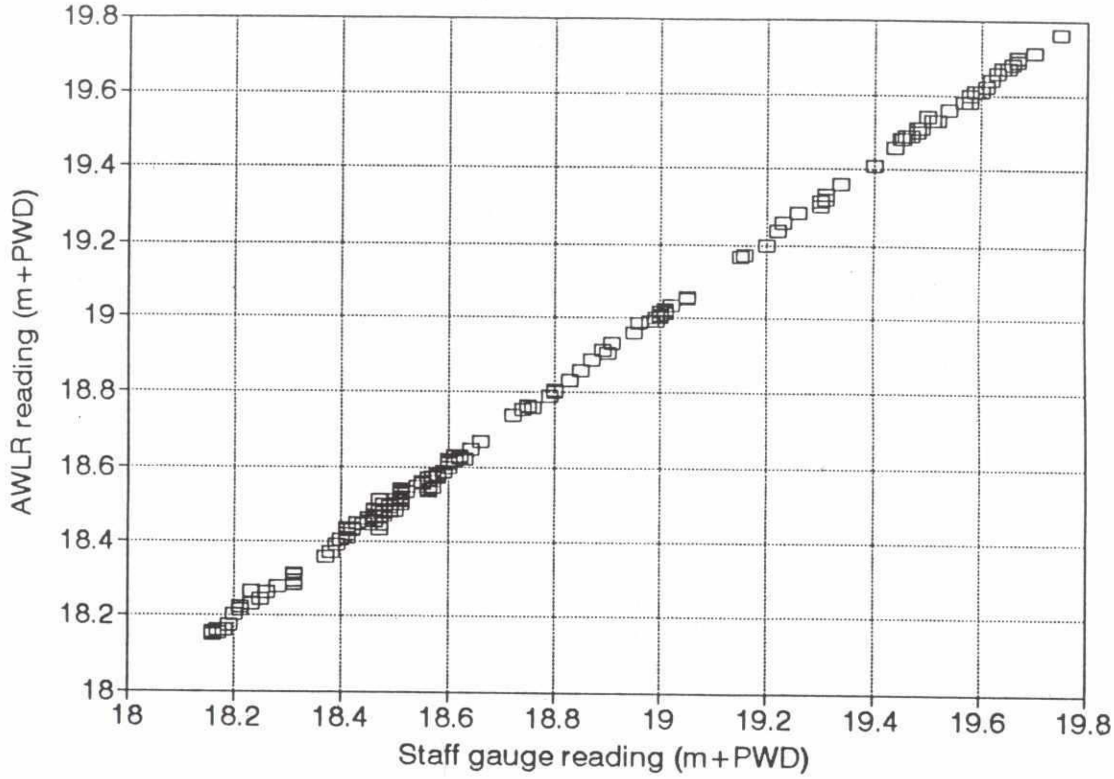

Figure 4.1: Comparison of raw pressure sensor water level data and manual staff gauge reading at Bahadurabad

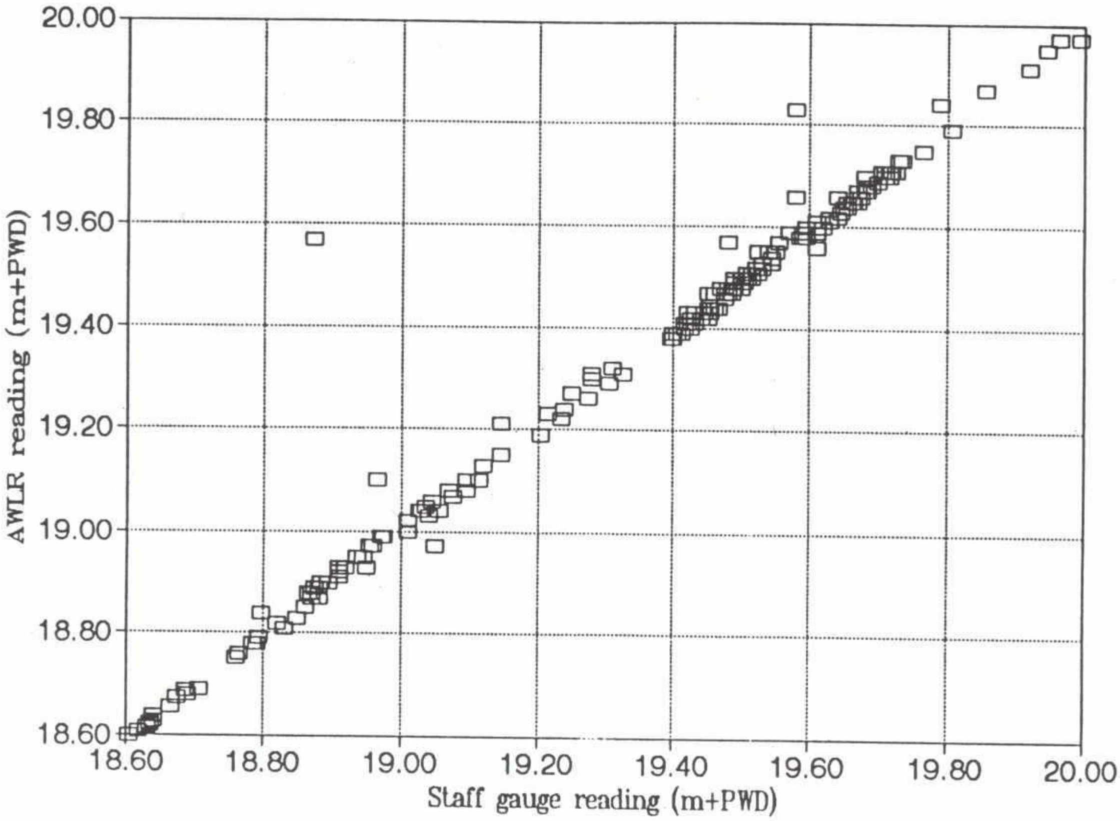

Figure 4.2: Comparison of raw acoustic sensor water level data and manual staff gauge reading at Gabgachi

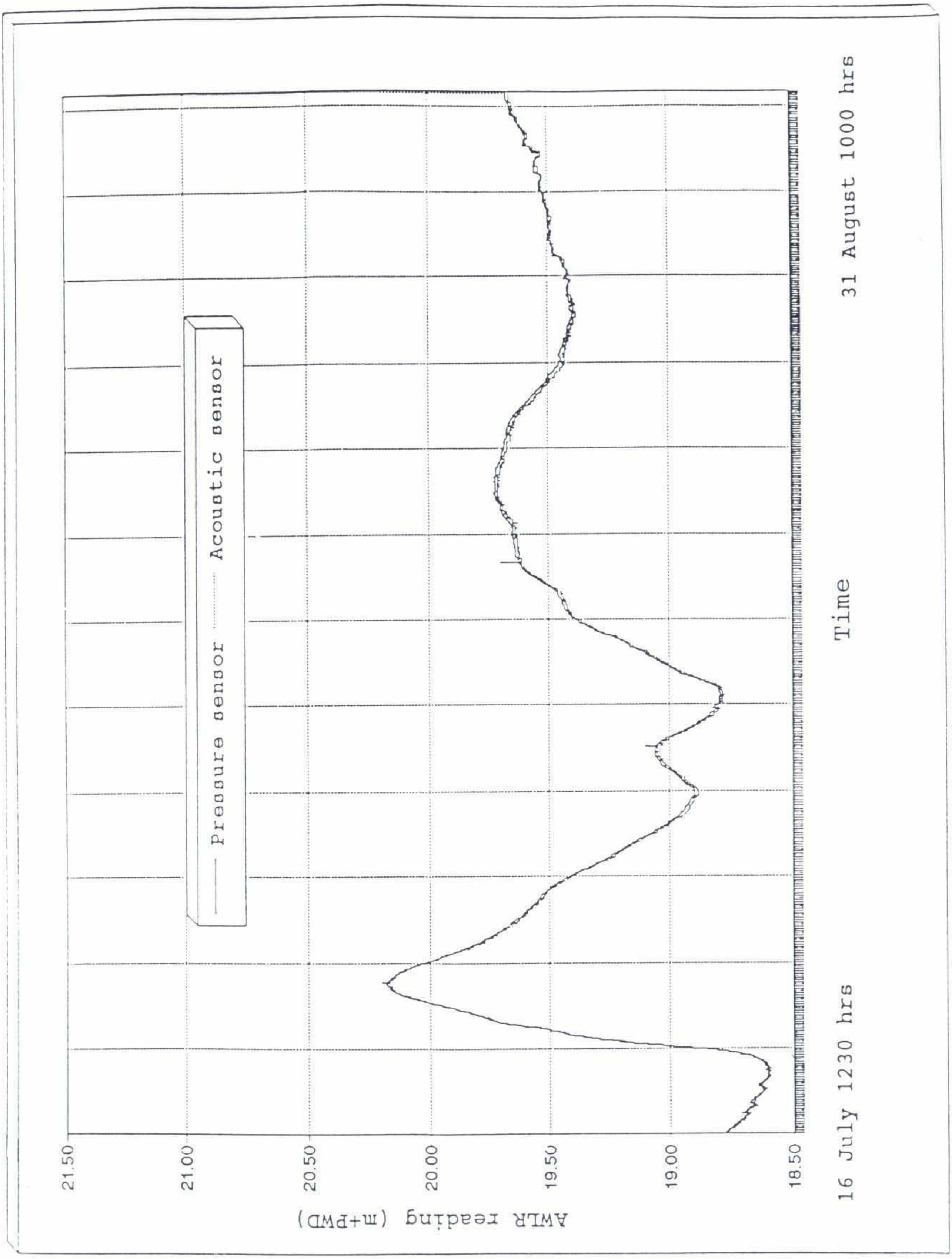

Figure 4.3: 1/2 hourly water level data of acoustic and pressure sensor data at Gabgachi

4.3.3 Depth measurements

The mobilized equipment for depth measurements included two types of echosounders: The dual frequency ELAC LAZ 4420 in DHA and the single frequency SIMRAD EA 300 P in DHB, DHC, and DHD. The echosounder output is given in analogue depth-profiles and in digital display. The selection of a dual frequency echosounder was prompted by the possibility of cohesive sediment layers and high-concentration moving sediment layers near the bed, which, if forming a sharp interface, could be recognized by the echosounder. It was found, however, that such a situation did not exist and consequent echosounding was based on single frequency mode.

Acoustic depth resolution by an echosounder is dependent on the angle of the acoustic beam. The opening angles of the acoustic beam in FAP24 echosounders varied from 7° to 24°, depending on frequency. No experimental investigation was made to determine the accuracy of FAP24 echosounders. Detailed investigations by Sauer and Meyer (1992) indicates that an acoustic system can make a 10 percent error in mobile stream bed conditions.

4.3.4 Velocity measurements

Velocity measurements, used for discharge estimations, were made in 10 transects along the main rivers of Bangladesh as shown in Figure 1. The ADCP-EMF moving boat method was used to estimate discharge in the main rivers. In the distributaries, a velocity-area method was followed, using an S4 current meter or an Ott-propeller current meter. A brief description of each instrument selected by FAP24 follows:

ADCP

The Acoustic Doppler Current Profiler (ADCP) measures flow velocity using the principle of the Doppler effect (Urik, 1975). The velocity is measured using the following principle (RD Instruments, 1989):

$$F_D = 2F_s\left(\frac{V}{C}\right)\cos A$$

where
F_D = Doppler frequency shift;
F_s = transmitted frequency of the sound when everything is still;
V = relative velocity between the sound source and the sound receiver;
C = speed of the sound wave; and
A = angle between the relative velocity vector and the acoustic beam.

When F_D and the angle A are measured, and F_s and C are known, the relative velocity V can be determined. If the velocity of the vessel is known either from bottom track or from the DGPS, the absolute velocity of the scatterers can be computed. Applying the principle, each beam computes one velocity component. With 3-beam ADCP, three orthogonal velocity components u, v, and w are measured. The set-up in FAP24 vessels used four beams to measure velocity and to compensate for errors. FAP24 procured and installed broadband ADCPs with 300 and 600 kHz frequencies.

During Phase I of the project, a 300 kHz RDI-ADCP was installed in the DHA. This ADCP was operated with a bin size of 0.5 m and 10 pings (profiles) were made in five to six seconds. The first bin was located about 2.8 m below the surface and the last bin was located at the 94 percent water-depth level. The average of the 10 pings was stored at about five to six second intervals. The standard deviation of the acquired velocity was 30 cm/s per ping. It was reduced to 9.5 cm/sec for the time-averaged situation of five to six seconds.

During the first mobilization phase of the project, some implications of the limitations of the ADCP became clear. It was not able to measure higher than 2.8 m from the water surface or with a bin size less than 0.5 m, and the instrument was not portable.

Possible instrument failure was anticipated in case of high sediment concentrations and therefore, for safety reasons, a 300 kHz instrument was bought and installed in the large survey vessel DHA. To overcome the unmeasured surface zone of 2.8 m, the EMF was installed. Obviously, a higher frequency with smaller sensor is preferable, especially for smaller boats. The advantages are smaller bin height and smaller unmeasured zone. The disadvantage is that the system is more sensitive for higher sediment concentrations. We tested, therefore, a portable 1200 kHz instrument (borrowed from RD Instruments) and based on the experience with the 300 and 1200 kHz, a 600 kHz RDI-ADCP was installed in the DHB. The advantage of this instrument were that the unmeasured surface zone was reduced to 1.8 m and the bin height was reduced to 0.25 m. The instrument was portable and could be deployed in other vessels.

Point-velocity measurements

To measure point-velocity, electromagnetic sensors and mechanical rotor current meters were used. The electromagnetic sensors used were the Inter-Ocean S4 current meter and the Delft Hydraulics PEMS-EMF. The mechanical rotor-types used were the Ott and the Valeport propeller meters. A brief description of these instruments follows:

Electromagnetic sensors

An electromagnetic sensor works according to Faraday's Induction Law:

$$E = \psi I v$$

where
E = electromotive force
I = magnetic field intensity
v = flow velocity
ψ = a factor

A magnetic field is generated by a pulsed current meter through a small coil inside the body of the sensor. In the PEMS-EMF, two pairs of diametrically opposed platinum electrodes sense the voltage produced by the flow past the sensor (Delft Hydraulics, 1992). The sensor is designed so that these voltages are proportional to the horizontal orthogonal components of the velocity vector at the plane of the electrode. The accuracy of the instrument is ± 1 percent of the reading, or ± 0.5 cm/s. It can measure velocity in the range of 0 to 3.5 m/s. During routine flow gauging, the instrument serves as a supplement to the ADCP. For this purpose, it is deployed at the bow of the vessel to sample 0.5 m below the surface.

The InterOcean S4 worked on the same principle as the above equation. It was equipped with additional sensors to measure water-depth, velocity direction, and temperature and conductivity. It was deployed to measure flow during an anchored position, and especially to measure the flow velocity during sediment sampling. With a resolution of 0.2 cm/s, the range of the instrument was from 0 to 3.5 m/s (InterOcean, 1990), which can be increased up to 6 m/s at the cost of a reduced resolution. Its accuracy was ± 2 percent of the reading, or ± 1 cm/s. Direction by S4 was measured by flux-gate compass with a resolution of 0.5°, and it had an accuracy of 2°.

Mechanical rotor current meter

Ott and Valeport propeller-type meters were mobilized to measure flow velocity while anchored, especially in shallow areas when using a shallow-draft vessel. This technology is widely used by BWDB. The operation principle of the current meter is that the rotation of the propeller is proportional to the flow velocity. A calibration formula was made after testing the equipment in calibration tanks. The main disadvantages of these current meters were their inability to measure direction, and the fact that they require frequent calibration and maintenance.

Float tracking

Flow velocity can be measured by floats according to the principle that the float velocity is equal to the ambient flow velocity. This is achieved by choosing a float that has an appropriate dimension and a specific weight. The float is released in the water and its position is traced at some suitable intervals of time. From the measured travel distance and time, the velocity is computed:

$$V=\frac{\Delta s}{\Delta t}$$

This method provides a so-called Lagrangean description of the flow, by illustrating the trajectory of the moving water, as basically opposed to the Euleran description of the current vector at a fixed point.

A good accuracy requires that the displacement of the float is large as compared with the positioning accuracy. This, in turn, requires a time increment that is related to the current speed. Hereby, the time and space resolution of the method depends on the current speed. Obviously, the above computed velocities represents an average velocity over the depth level interval of the vane. The vane must be rather big in order to reduce the effect of wind drift (which becomes excessive if the wind drag force is significant as compared with the current drag force). Therefore, the method is not well suited for describing the vertical variation of the current, and in general it cannot provide detailed information about time and space variations. Tracking of multiple floats can indicate parallel, diverging, or converging flow lines thus providing a flow pattern, and the data are well suited for validation of hydrodynamic models with their inherent finite length and time increments. In areas with strong depth variation, grounding of floats is a problem. Also, in case of considerable wind, no float tracking should be made. Details of the method can be read in Liu and Martin (1968), Hayes (1978) and El-Haddi (1990).

5 Selection of measuring method

5.1 Bathymetric survey

The sites for regular bathymetric surveys by RSP are indicated in Figure 1.1. The surveys covered seven sites: The left bank of the Jamuna River near Bahadurabad, the right bank of the Jamuna near Kamarjani, the Dhaleswari off-take at the Jamuna, the Jamuna near the Hurasagar off-take, the Jamuna-Ganges confluence near Aricha, the Gorai River off-take at the Ganges River, and the Arial Khan off-take at the Padma River (RSP, 1996). Optimization exercises were made at these sites in order to:

- find suitable sounding track densities
- reduce bathymetric charts to a suitable datum
- find suitable locations for gauges in order to reduce bathymetric charts
- obtain a suitable measurement frequency

Sounding tracks at spacings of 100 m and 200 m followed for 1:10,000 and 1:20,000 scale bathymetric maps, respectively. Echosounder depths were recorded at every two metres along the survey lines. The interval of sounding-track spacing was determined after some optimization exercises, so as to avoid missing of important bathymetric details. Figures 5.1, 5.2 and 5.3 show some examples of the Jamuna River bathymetry near Bahadurabad.

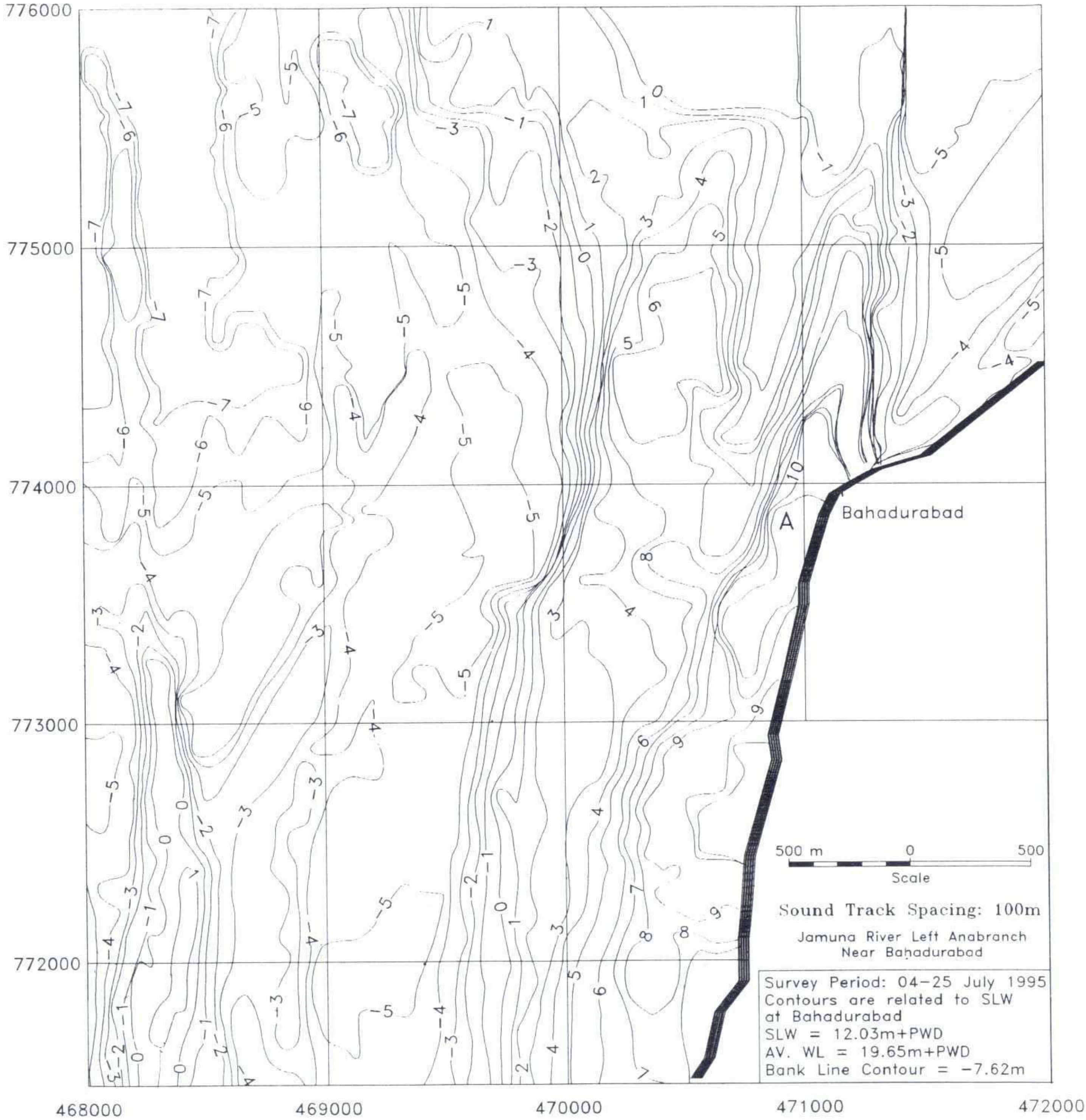

Figure 5.1: Jamuna River left channel bathymetry at Bahadurabad measured on 04-25 July 1995 at 100 m spacing

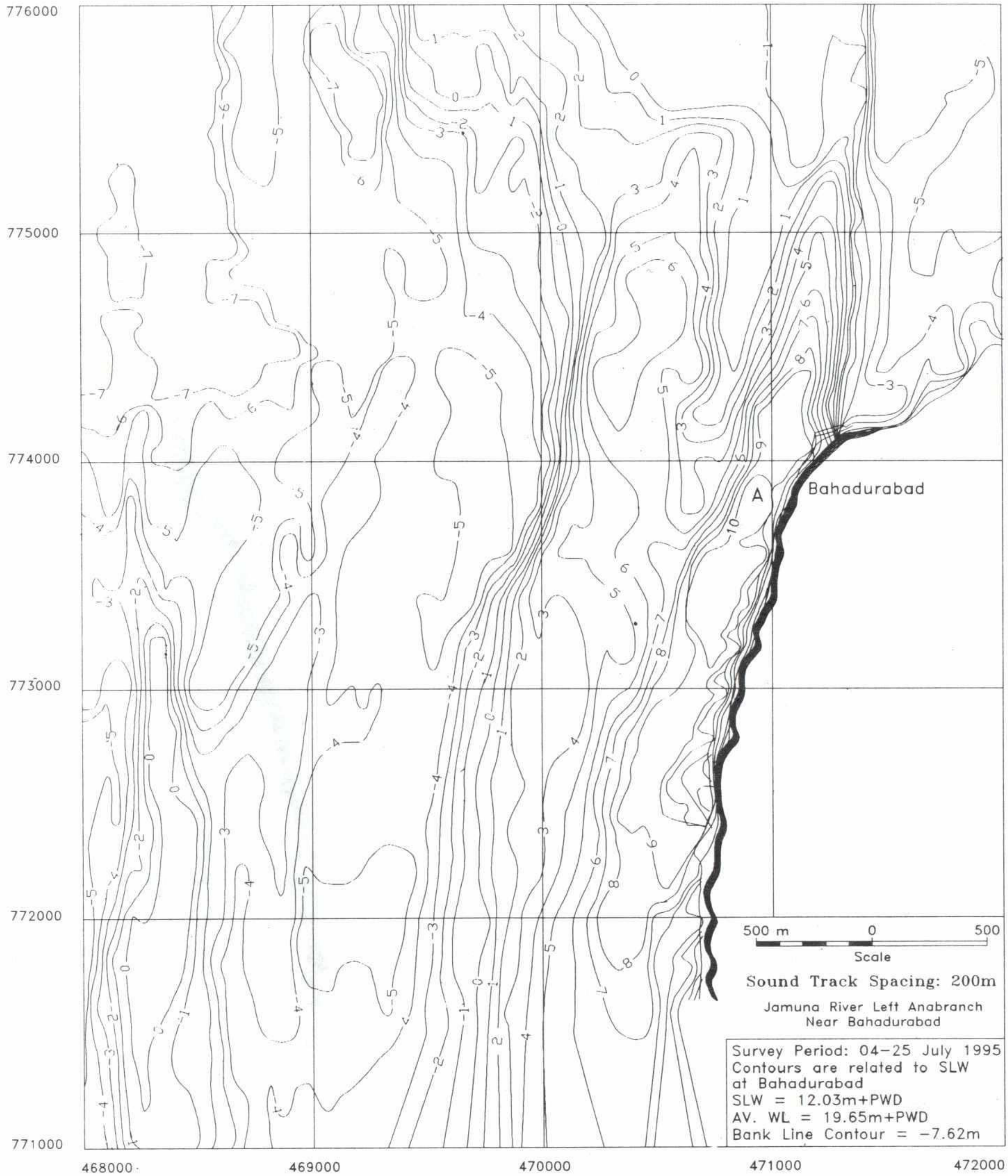

Figure 5.2: Jamuna River left channel bathymetry at Bahadurabad measured on 04-25 July 1995 at 200 m spacing

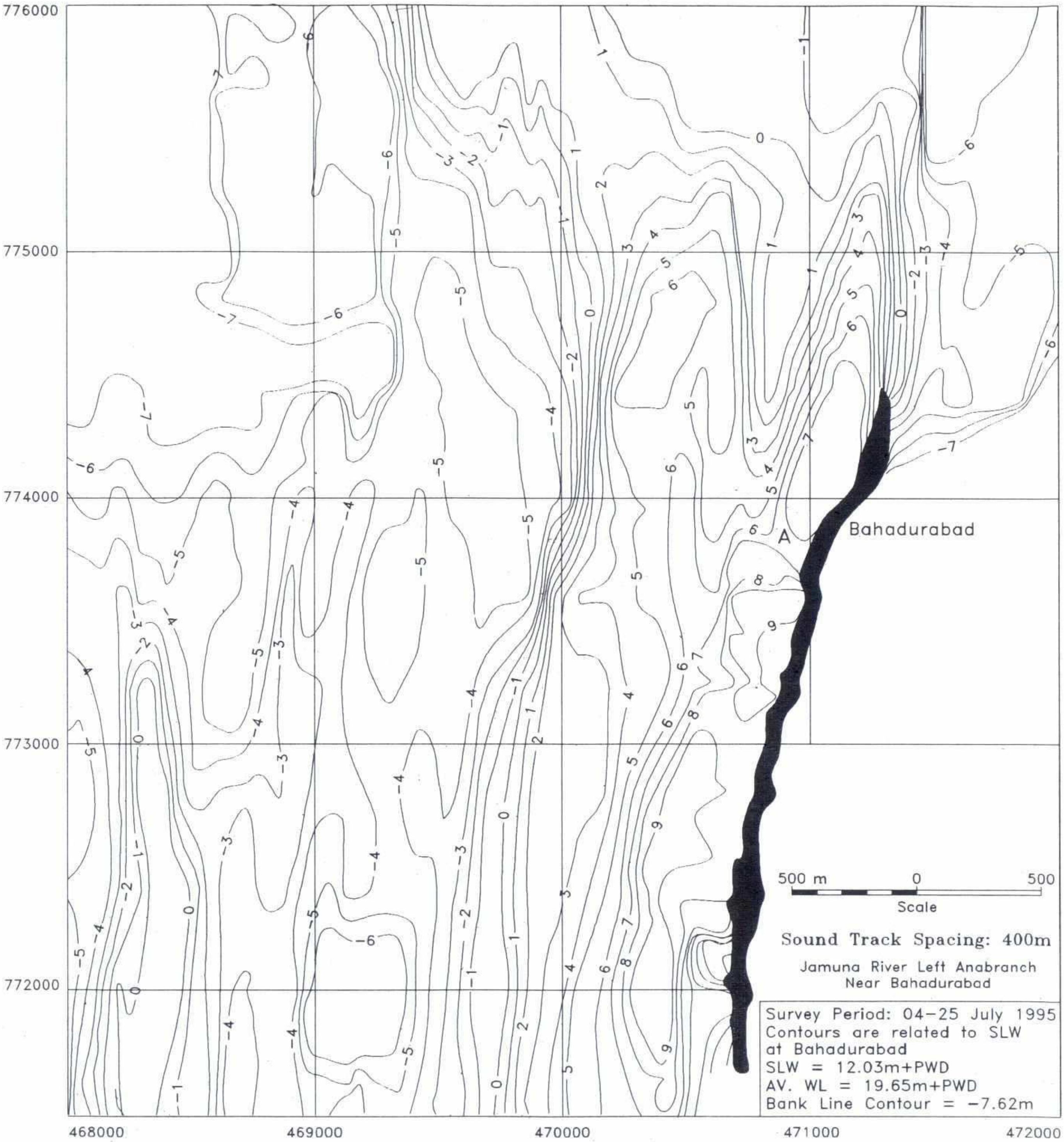

Figure 5.3: Jamuna River left channel bathymetry at Bahadurabad measured on 04-25 July 1995 at 400 m spacing

The survey was made in the monsoon season at 100 m spacing. Figure 5.1 shows the contour plot utilizing all the sounding information made at 100 m interval. Figure 5.2 shows the contour plot utilizing the alternate sounding tracks (200 m spacing). In Figure 5.3, only the sounding tracks at every 400 m were utilized. Comparison of the charts indicates that hardly any information is missed between Figures 5.1 and 5.2. However, when a sounding track spacing of 400 m was used considerable information is missed. Consider, for example, the location at A. In the 400 m spacing (Figure 5.3) a shallow area is depicted between the 7 m contours which is unrealistic (Figures 5.1 and 5.2). The horizontal control of the bathymetric surveys were made in the Bangladesh Transverse Mercator (BTM) system, using the Everest 1830 ellipsoid. The vertical control was made relative to the Standard Low Water (SLW) datum. The relation between SLW and Public Works Datum (PWD), established at different stations by INTERCONSULT (1991), was used by FAP24 for definition of the SLW datum in the field.

Various specific water level stations were used for reducing bathymetric charts. For large survey areas (e.g., areas as large as 160 km^2 near Kamarjani in the Jamuna River), one gauge was not enough, because the significance of surface slope variations increase over large distances. Therefore, the actual surface-water slope (discussed in section 3.2) was used to determine the water level in places other than the gauging station.

Initially, only two surveys per year were scheduled: Pre-monsoon and post-monsoon. Later, after discussion with the River Survey Project Management Unit (RSPMU), a monsoon season survey was added.

Survey results and the current bathymetric survey strategy are reported in detail in River Survey Project (1996b).

5.2 Discharge measurements

ADCP-EMF moving boat method

The moving boat method used by this study to measure discharge is referred to as the *'ADCP-EMF moving boat method'*. It is different from the conventional moving boat method, where a moving platform measures velocity at one measuring point at a fixed depth across the transect, first in the one direction and afterwards in the opposite one. The ADCP-EMF application used by FAP24, however, samples the 'entire' vertical current profile as the boat sails one time across the channel (except for the lowermost part, as described in Section 4.3.4). The detailed methodology is discussed in the 1st Interim Report (RSP, 1993a) and the principle of the method is indicated in Figure 5.4.

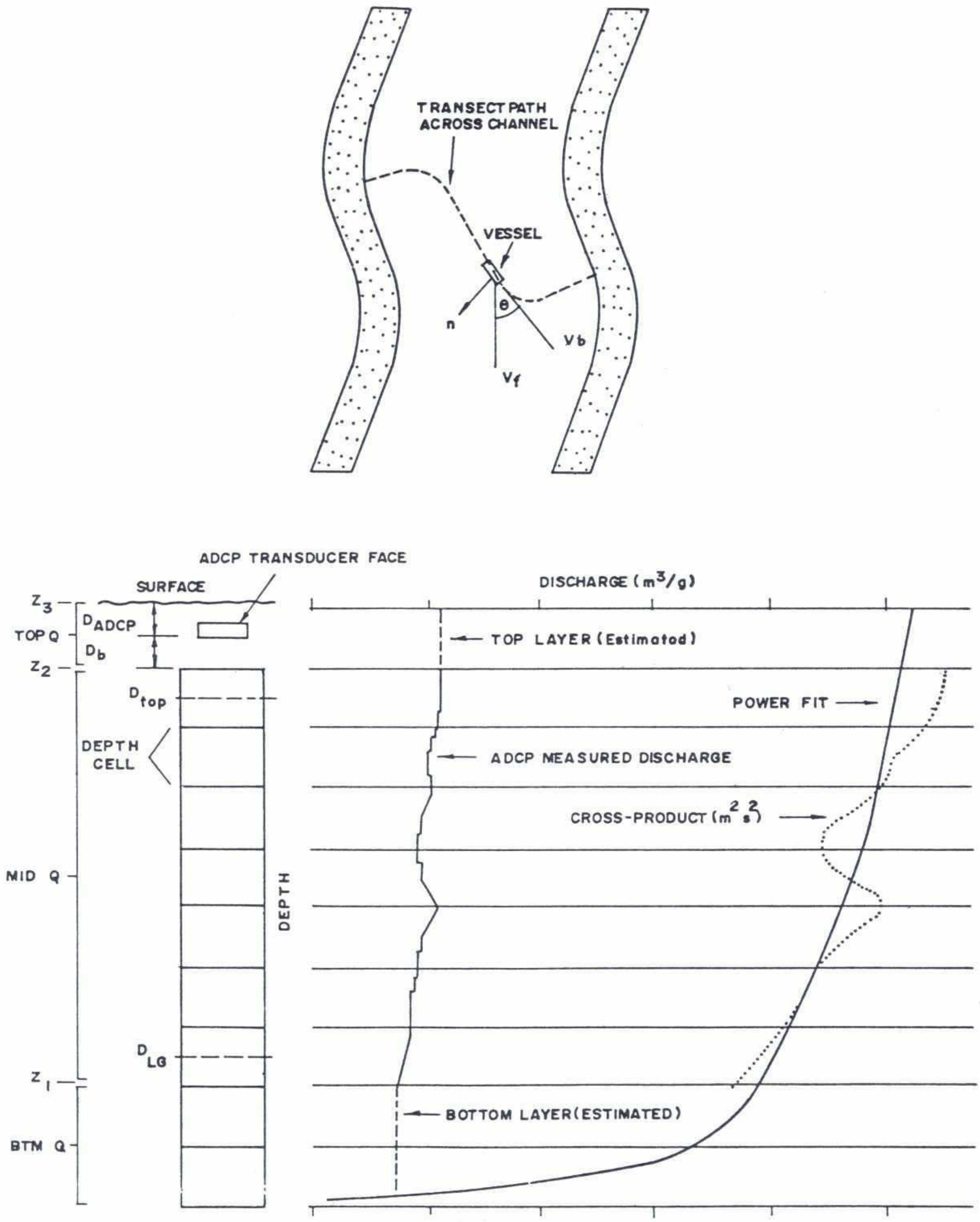

Figure 5.4: ADCP-EMF moving boat discharge measurement principle

V_b = mean vessel velocity vector, V_f = mean water velocity vector, n = unit vector normal to transect path at a general point, D_{ADCP} = depth of the ADCP transducer face from the water surface, D_b = blank beyond transmit, D_{top} = depth of the center of the first bin, D_{LG} = depth of the last good bin, TOP Q = estimated discharge for the unmeasured data at the top of the profile, BTM Q = estimated discharge for the unmeasured data at the bottom of the profile.

The test phase and subsequent surveys proved that the ADCP-EMF method is fast and can be used during adverse hydraulic conditions, such as a flood. Also, because of its 'instantaneous' and detailed coverage of the flow field, it is much less dependent on a regular cross-sectional flow distribution. As opposed to the conventional moving boat method, transversing does not need to follow a straight course (although this was done wherever possible). This is of some significance in the Bangladesh rivers, where a straight, regular cross-section is not always immediately at hand, both due to hydraulic irregularities and due to navigational obstacles, such as shallow banks or fishing nets.

It does have a few limitations, however. In a mobile bed condition during the monsoon season, the system underestimated the flow velocity because the measurements were made relative to the mobile bed. That problem was solved by measuring the vessel speed with a DGPS rather than relating it to the mobile bed. Another problem was since the mobile sediment layer was recognized as the bed, the ADCP underestimated the depth. That, however was insignificant to the discharge estimate.
The ADCP instrument left unmeasured zones in the top and bottom layers, but an additional EMF was introduced to measure in the top layer. The bottom layer, comprising six percent of the water-depth (but a few percent of the flow), was estimated by fitting a power curve (Chen, 1991).

A final problem was that in the shallow channels, the method could not be applied due to vessel draft limitations. Instead, in those channels, the velocity-area method was applied.

Velocity-area method

The velocity-area method is the standard method used by BWDB. In general, the method is very effective, however, in large channels with high flow velocity, the method was inefficient considering the time required to carry out the discharge measurements and the actual number of vessels needed (see further RSP, 1996c). Different aspects and limitations of the method are addressed in Annexure C.

In FAP24, the method was applied to measure shallow channels using Ott/Valeport current meters, floats, or the S4 current meter.

6 Different aspects of hydraulic measurements

6.1 Survey programming

Based on the RSP objectives and data requirements, a survey programme composed of a proper design of the survey spread, logistical arrangements, data collection procedures, and data storage and transfer arrangements were made. The programme was executed under the responsibility of the project's operational management team.

Below are listed some questions which were examined in the course of the programme and which are discussed in the present report:

1. What are the uncertainty levels of different instruments?

2. When measuring a given parameter, how do different instruments differ from each other? Relevant in this respect is the inter-comparison between RSP instruments, and between BWDB and RSP instruments

3. What is the optimal exposure time of a current measurement device, taking into account the particular turbulence pattern encountered in the Bangladesh rivers?

4. What is the optimal density and distribution of points in a vertical, and of verticals in a transect? This question is of particular importance for the velocity-area method

5. When estimating a given parameter, how do different methods differ from each other? Like it is the case with instrumentation, the inter-comparison between RSP instruments, and between BWDB and RSP instruments is relevant in this respect

In order to address such issues, some special surveys were made in addition to the routine gauging programme. For such special surveys, proposals were made specifying objectives, data collection procedures, expected outputs, and required resources, as a basis for a dialogue with RSPMU about scope and execution.

6.2 Operational Aspects

Collection of accurate information through field measurements depends on an efficient and competent management of survey operations. It involves (1) designing a suitable survey spread according to the requirements, (2) administering survey vessels, crew and hydrographers, (3) overlooking book keeping of survey records, (4) arranging logistics, (5) overlooking the proper transfer of data and samples from the field to the processing office, (6) maintaining survey vessels and instruments in operable conditions, and (7) maintaining day-to-day contact with survey operations and providing necessary backstopping. The hydrographers and the survey crew have the responsibility of collecting the information as desired. Some of their on-board responsibilities include:

- Maneuvering of the vessel for accurate positioning both during navigation and anchoring. This was achieved successfully by FAP24 with advanced navigational aids and on-line display of vessel-movement.
- Closely monitor the ADCP and EMF velocities and discharges such that useful data are collected.
- Accurately deploying the instrument at the desired depth and location.

- Ensuring a sampling rate such that it is equal to the ambient flow velocity. This is required, especially during suspended sediment sampling.
- Determining suitable sampling duration during Delft-Bottle and Helley-Smith sampling.
- Recording survey details on a log-book.
- Keeping the supervising office informed on the progress and problems of survey.

In the execution and overseeing the activities often problems were encountered. some of them include

- On establishing the reference stations problems were encountered regarding the availability of a reliable reference station, keeping the stations operational and obtaining conversion factor to switch from one projection system to the other.

- ADCP registering less velocity due to a highly mobile bed. The problem was later solved by referring to the positioning coordinates.

6.3 Data collection

Execution of the hydraulic measurements in the field involved the following tasks:

- activating reference stations and checking positioning quality
- determining or checking transect perpendicularity at discharge transects
- ensuring that water level gauging stations functioned well
- preliminarily checking instruments and software
- actually executing work and logging data
- on-line data processing, quality checking and recording on PC hard disks
- storing data and making two back-up tapes
- maintaining a record of executed observations in the log-book

All instruments were connected to a PC through an interface. Data acquisition software enabled the sampling of the various signals with a time interval of one second. The HYDRO software package controlled the synchronization of all systems.

There were some problems discovered in the data collection process. It took more time than expected to activate some reference stations and keep them operational during the surveys. The HYDRO software, an on-line data-logging system, was often down, and making back-up data tapes took a great deal of time.

6.4 Data elaboration

The actual data elaboration was performed in the office as an off-line procedure. It involved retrieving and filtering data from the back-up tapes, and computing discharge, preparing bathymetric maps, and storing data in the PSD24 database. A specially designed ADCP-EMF moving boat software package was used for discharge measurements, while Grapher and MIKE 21 software were used for processing bathymetric survey data. PSD24 is a specially designed software with a specific application of PARADOX 4.5 for WINDOWS.

The data elaboration also involved assuring quality, validating data, preparing survey bulletins with texts and figures, preparing data books, and preparing figures or arranging processing for special studies or projects.

6.5 Capacity building

With the objective of continued capacity building within river surveys, Bangladesh organizations received on-the-job-training as the surveys were being executed. This capacity building included training Bangladesh navigation and survey crews to maintain and operate their survey vessels. It also included training these crews to assist in hydrographic surveys. Bangladesh hydrographers were trained to measure flow and sediment transport, and to make bathymetric surveys, and to operate relevant software. In addition, Bangladesh personnel were trained in data elaboration.

The persons that received such training comprised government employees from BWDB, individually employed project team members, and employees representing Bangladesh subcontractors.

7 Measurements and results

Table 7.1 lists the surveys that were made and used for examining the questions listed in Section 6.1. Special survey reports or survey bulletins were prepared for each of these surveys.

Date	Location	River	Measurement type
1 APR 1994	Bahadurabad	Jamuna	Turbulence and optimal measuring time
13 APR 1994	Aricha	Jamuna	---------do-----------
13 AUG 1994	Bahadurabad	Jamuna	---------do------------
17-23 OCT 1994	Bahadurabad	Jamuna	FAP24-BWDB joint measurements
17-18 FEB 1995	Mawa	Padma	FAP24-BWDB 26-hours tidal measurements
18-19 MAR 1995	Bhairab Bazar	Upper Meghna	---------do------------
15 APR 1995	Bahadurabad	Jamuna	Inter-comparison velocity measuring instruments
17-20 JUL 1995	Bahadurabad	Jamuna	FAP24-BWDB joint measurements
27-30 JUL 1995	Bahadurabad	Jamuna	Density of numbers of points in a vertical and numbers of verticals in a transect
21 OCT 1995	Mawa	Padma	FAP24-BWDB joint measurements
-	-	-	Relevant routine measurements

Table 7.1: Special surveys for optimization of hydraulic measurements

7.1 Accuracy and intercomparison of instruments

Production of accurate data is the aim of any river survey. Therefore, the accuracy of an individual instrument to measure parameters is a key consideration when selecting an instrument or a method. Accuracy in this context is understood as a measure of the degree of error. Error is an unintentional deviation from what is correct, right or true. It is often expressed as a relative standard deviation in percentage. Another word 'uncertainty' is often used synonymously. Uncertainty results from unknown or unidentified sources of errors (instrumental, measuring or human) and unexplained natural variability.

In echosounding, the data quality depends on

- the accuracy of the echosounder itself
- the accuracy of the positioning system
- the accuracy of the water level recording

The quality of the processing and the preparation of bathymetric charts depends on

- the sounding line density
- the resolution of the echosounder
- the procedure applied for reducing bathymetric charts to a reference datum
- the procedures applied for contour plotting, interpolation, and extrapolation

Mueller (1989) identified three basic sources of errors that can influence a velocity measurement or a derived quantity such as the discharge in turbulent flow:

- instrument and calibration errors
- *Error Type I* (by ISO 1983), which involves statistical uncertainty that depends upon the properties of the random velocity field, and on the sampling time that determines the integration time for the statistical mean
- method errors that are used to evaluate derived quantities. For the velocity-area method of discharge estimation, this error is due to the limited numbers of sampling points in a vertical *(Error Type II)* or to the limited numbers of verticals in a transect *(Error Type III)*

In order to reduce instrumental errors, an instrument should be chosen based on the following seven criteria (Mueller, 1989):

- the range of velocities to be measured
- the instrument's calibration
- the spatial and temporal resolution
- the sensitivity to magnitude and velocity direction
- behaviour in a high turbulent flow field
- water properties
- field application of the instrument

Such quality considerations were regarded when selecting, mobilizing, and evaluating instruments.

An outline of the evaluation is given below. It is noted that the analysis is entirely based on field tests. Hereby, an insight is gained with respect to the instrument performance in the actual physical environment, rather than about potential instrument performance under ideal operating conditions (which would require laboratory tests under controlled conditions).

Figures 7.1 to 7.6 show some intercomparisons of velocity measuring instruments based on measurements in the in the Jamuna River left channel near Bahadurabad on 30 April 1995.

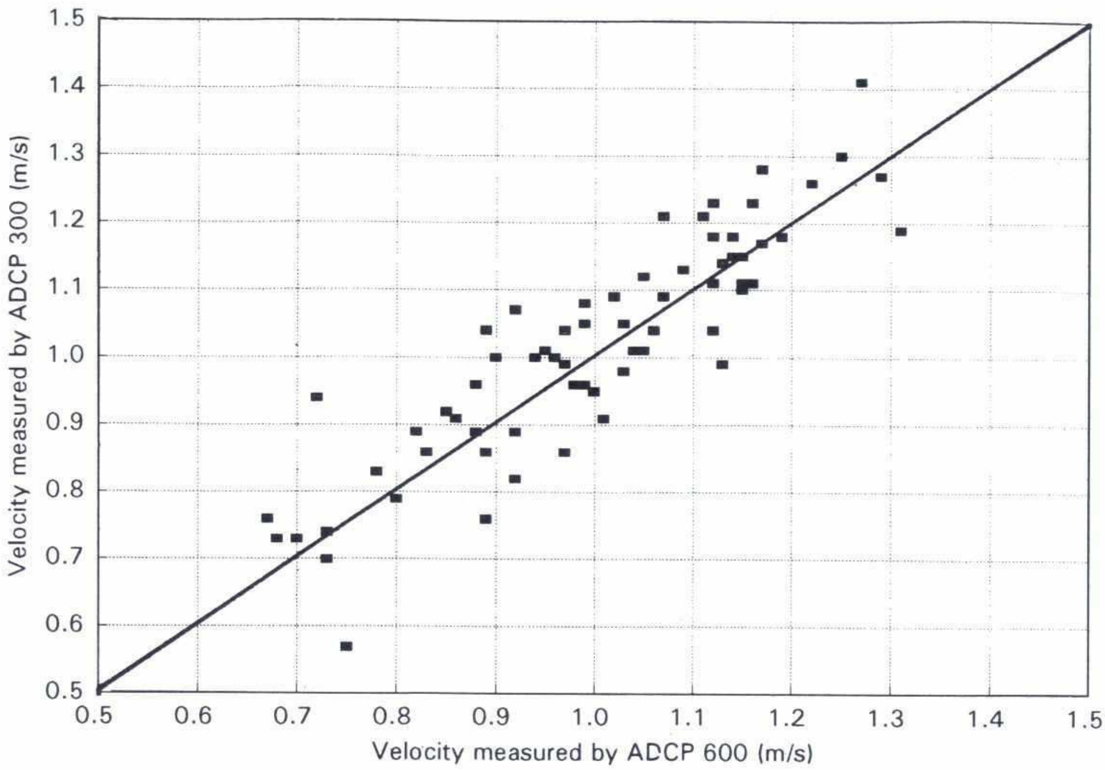

Figure 7.1: Inter-comparison of velocity between 300 kHz-ADCP and 600 kHz-ADCP measured on 30 April 1995 in the Jamuna River left channel near Bahadurabad.

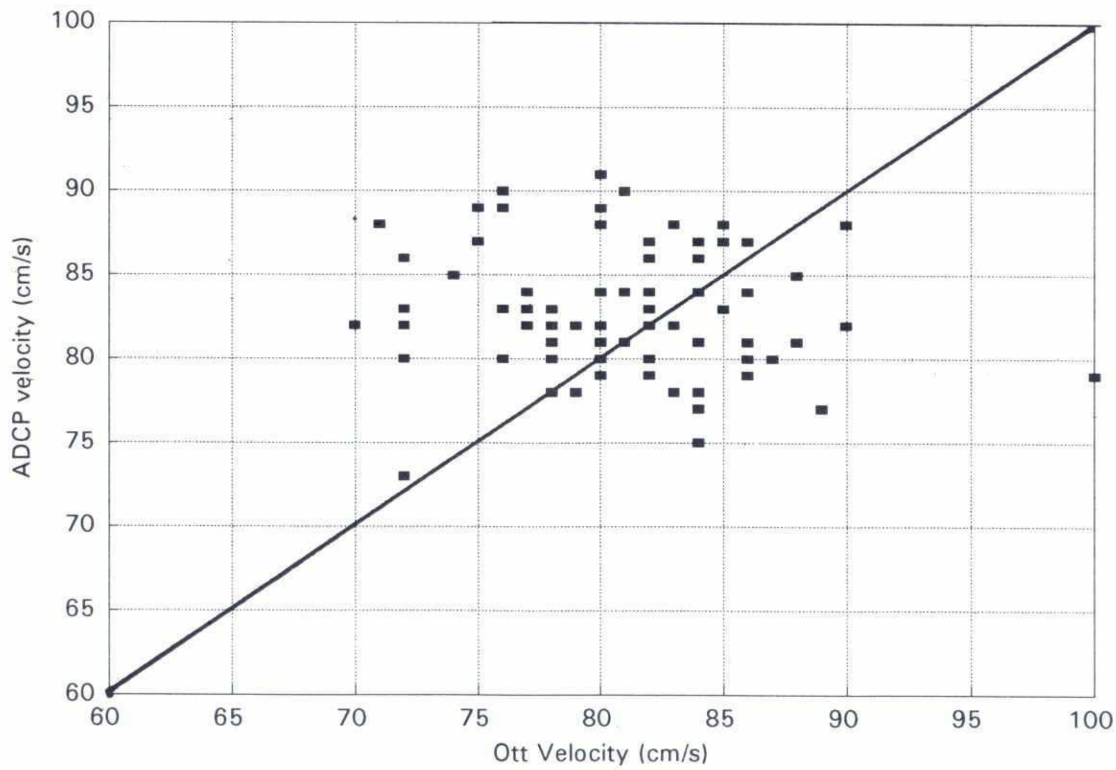

Figure 7.2: Inter-comparison of velocity measured by an Ott-propeller and the 300 kHz ADCP on-board DHA measured on 30 April 1995 in the Jamuna River left channel near Bahadurabad.

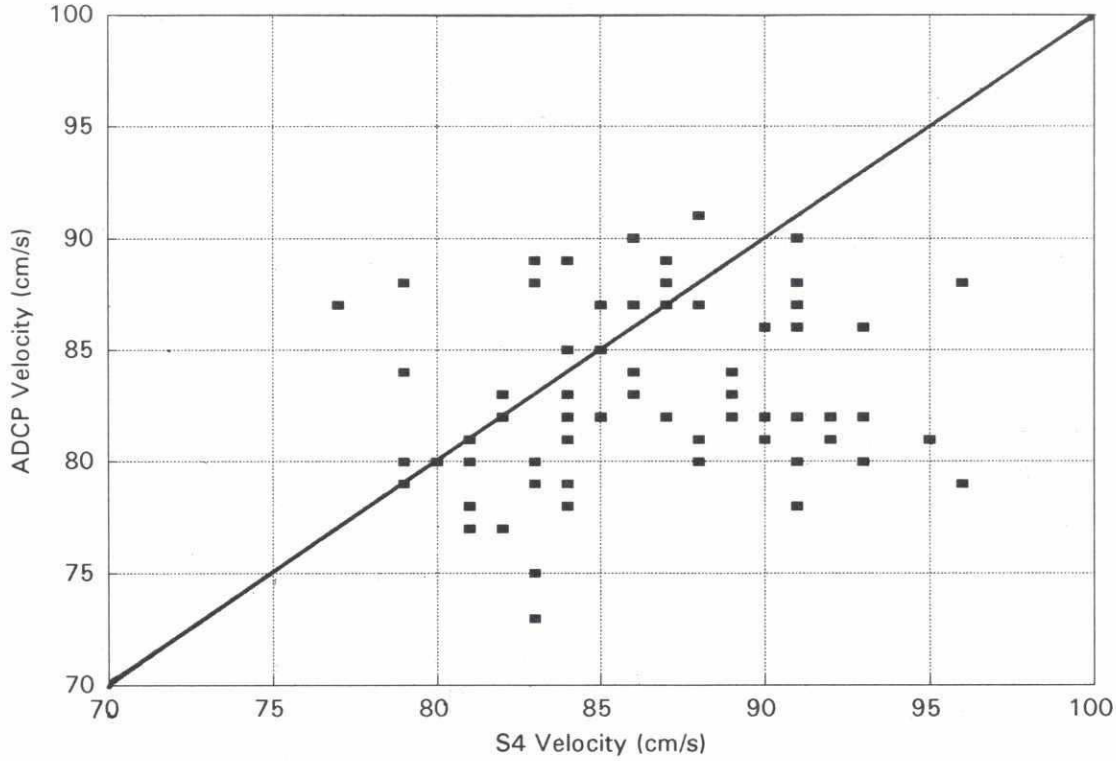

Figure 7.3: Inter-comparison of velocity measured by the S4 current meter and the 600 kHz ADCP on-board DHA measured on 30 April 1995 in the Jamuna River left channel near Bahadurabad.

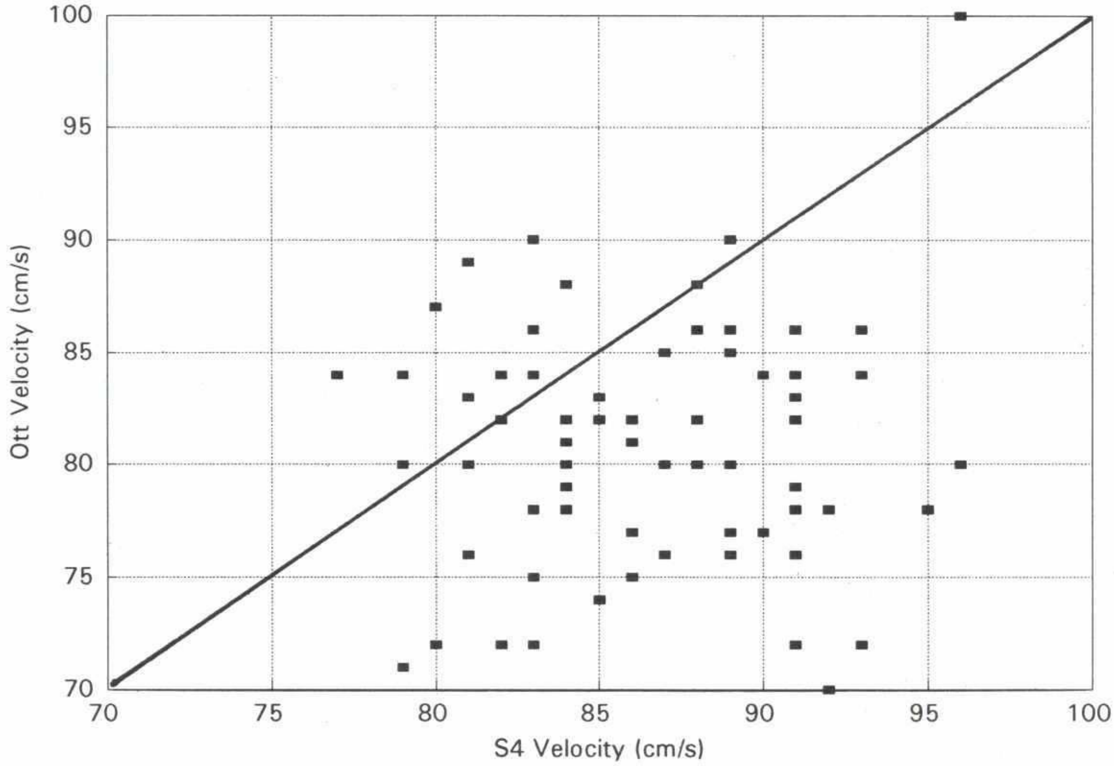

Figure 7.4: Inter-comparison of velocity measured by the S4 current meter and an Ott-propeller measured on 30 April 1995 in the Jamuna River left channel near Bahadurabad.

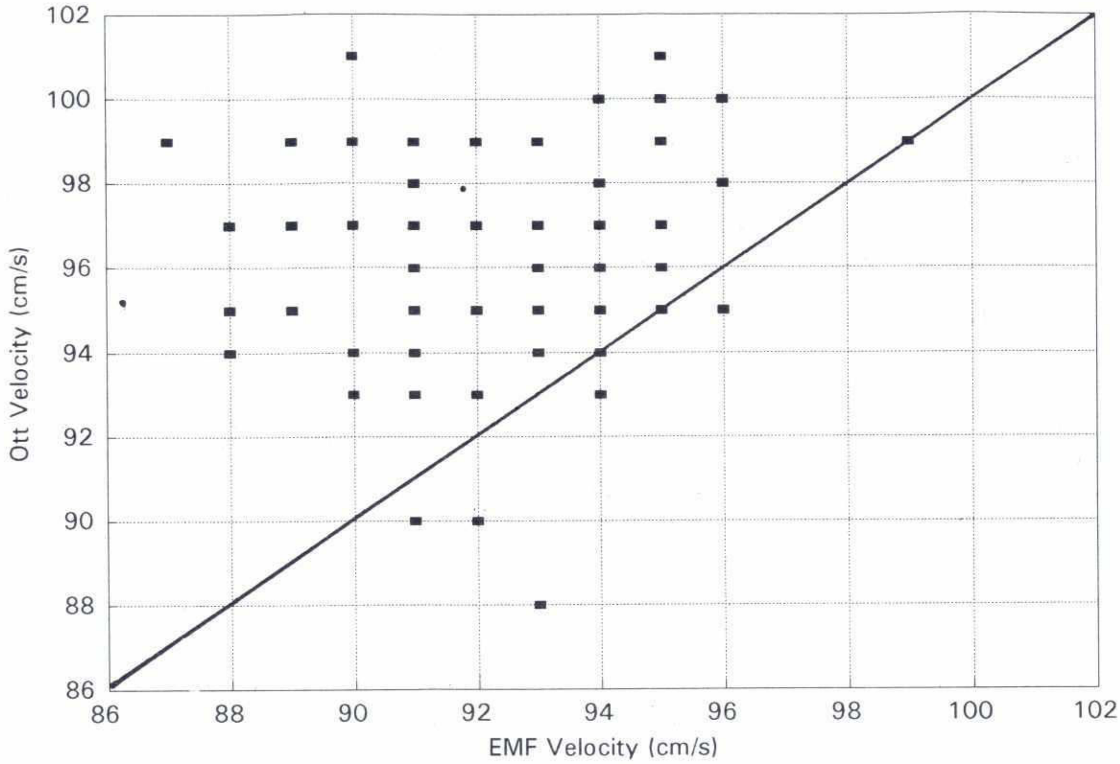

Figure 7.5: Inter-comparison of velocity measured by S4 and EMF measured on 30 April 1995 in the Jamuna River left channel near Bahadurabad.

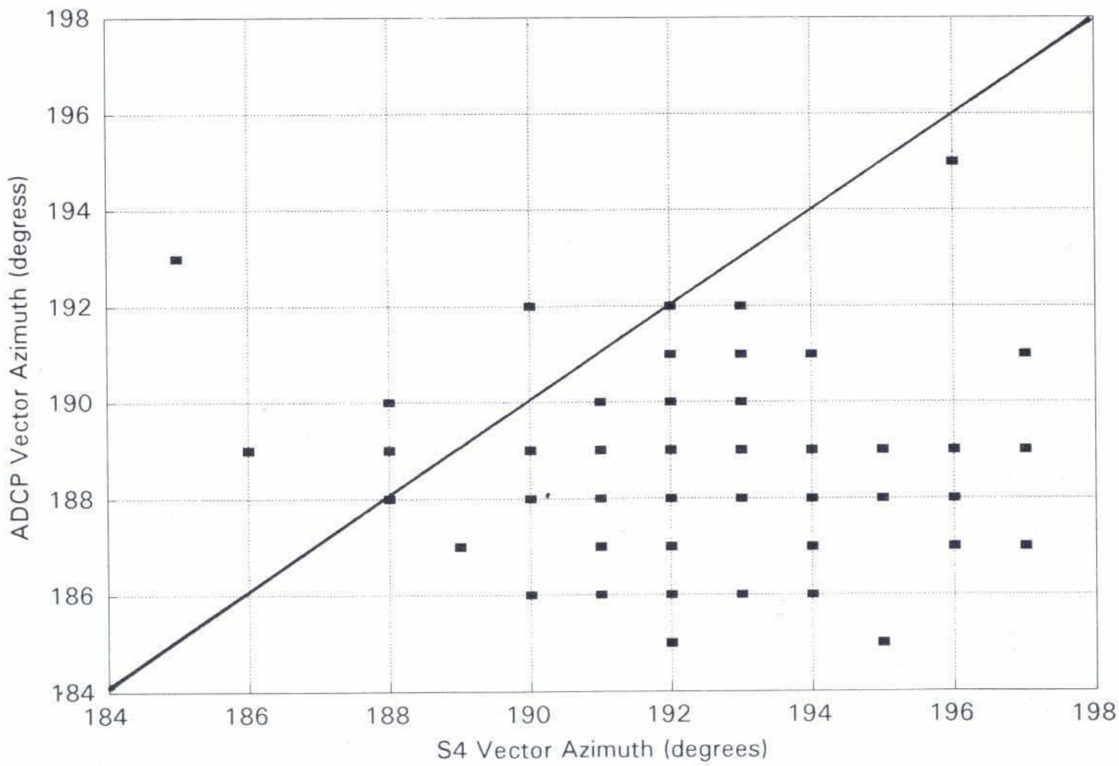

Figure 7.6: Inter-comparison of current azimuth measured by ADCP and S4 measured on 30 April 1995 in the Jamuna River left channel near Bahadurabad.

Figure 7.1 shows the intercomparison between the RDI-ADCP 300 installed in DHA and the RDI-ADCP 600 installed in DHB. Velocities were taken at coinciding bins from about 50% water depth (It may be mentioned that the bin-sizes of 300 and 600 kHz ADCPs are 0.5 and 0.25 m, respectively. The measured velocities represent a 10-ping average. This comparison is made in the velocity range of 0.7 to 1.4 m/s. The result indicate a close agreement between the two, despite some scatter. The average deviation was -1.3 percent of ADCP 300 velocity. This means that, on the average, ADCP 300 measured 1.3 percent higher than the ADCP 600.

The intercomparisons shown in Figures 7.2 to 7.6 were made by deploying some instruments simultaneously at 50% water depth, except the comparison made in Figure 7.5 which were deployed at 1 m below surface. Figure 7.2 shows the comparison of velocity between the Ott-propeller and ADCP 300 in the velocity range of 0.7 m/s to about 1.0 m/s. On the average, the Ott-propeller measurements were 2.1 percent lower than the ADCP 300. Figure 7.3 shows the comparison between the RDI-ADCP 300 and IO-EMC (S4) in the velocity range of 0.8 to about 1.0 m/s. It indicates that, on the average, the S4 instrument measured 4.8 percent higher than the ADCP velocity. A similar comparison between the Ott and the S4 (Figure 7.4) indicates that, on the average, the S4 measured seven percent higher than the Ott. Figure 7.5 shows that the Ott measured some 4.3 percent higher than the PEMS-EMF. In vector directions, the S4 measures a 2.1 percent higher direction than the ADCP (Figure 7.6).

In Figure 7.7, the S4 and the ADCP corresponding point velocities are compared using routine measurements data taken by FAP24 in the range of 0.5 to 2.5 m/s.

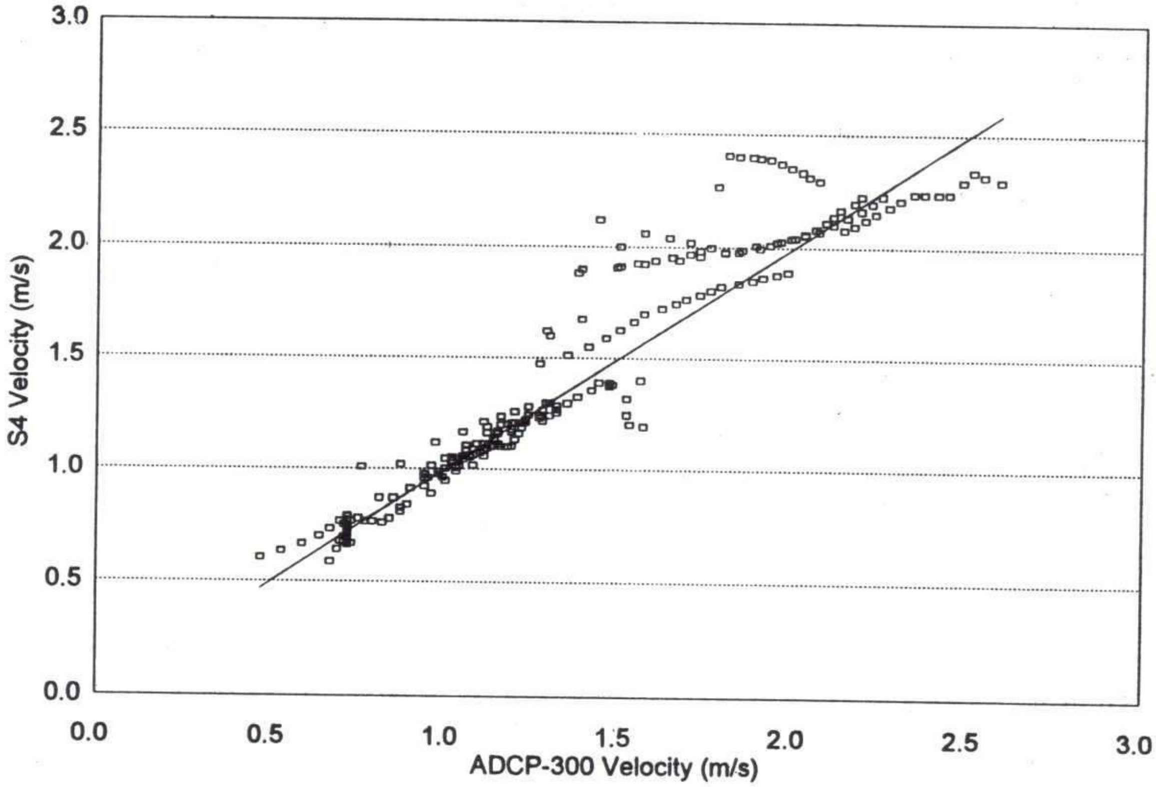

Figure 7.7: Inter-comparison of S4 and ADCP 300 velocity based on 1994 measurements in the reference verticals of the routine measurements in the Jamuna River near Bahadurabad.

It indicates that, in low velocity ranges, the agreement between the two instruments is better than at high velocities. Figures 7.8 to 7.11 show some examples of velocity profiles measured by ADCP-300 and S4 in routine transects.

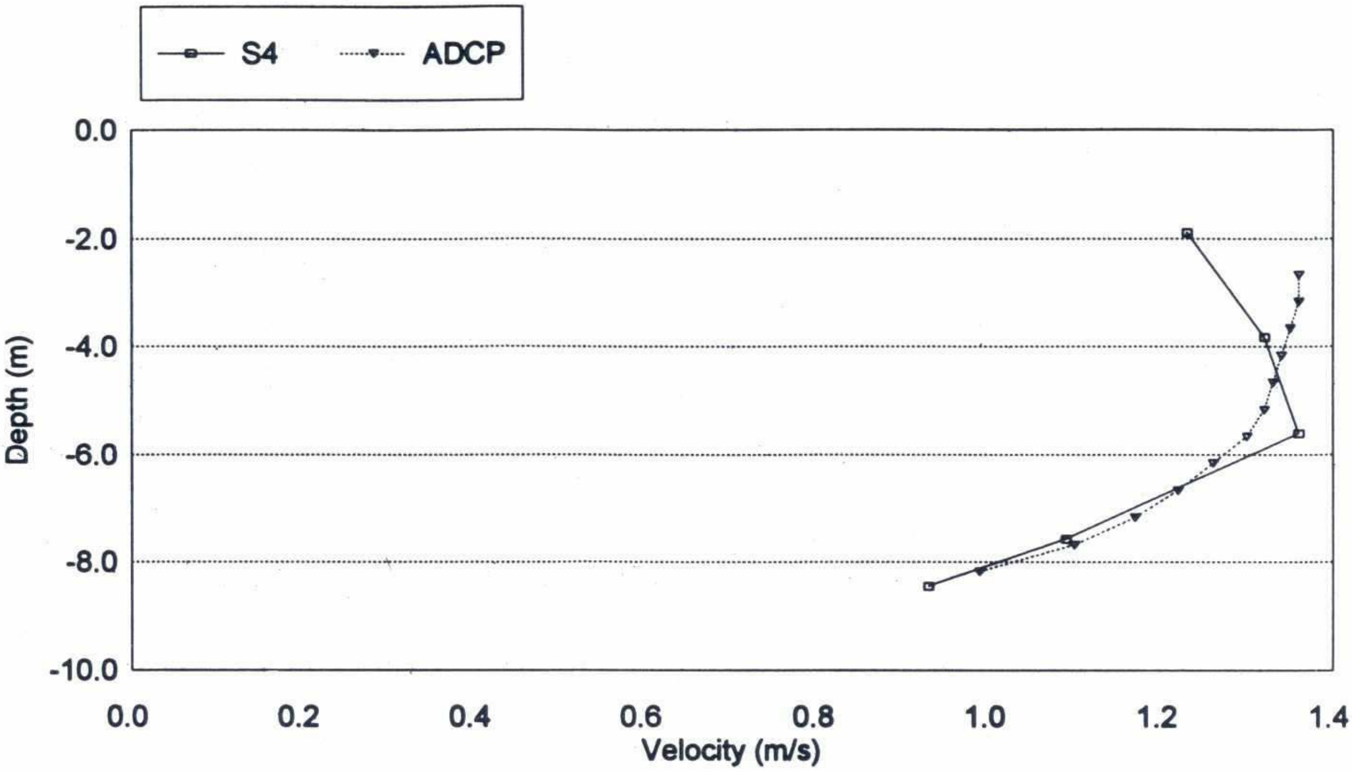

Figure 7.8: Velocity profiles measured by S4 and ADCP in a reference vertical (V-3) measured on 27 April 1994 is the Jamuna river at Bahadurabad.

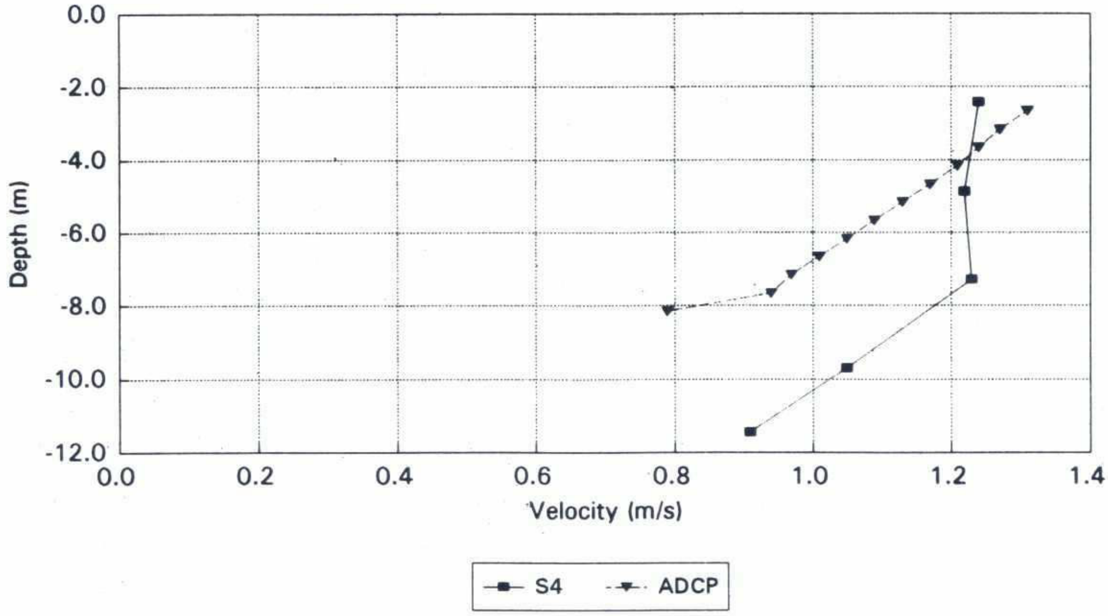

Figure 7.9: Velocity profiles measured by S4 and ADCP in a reference vertical (V-5) measured on 20 May 1995 at Sirajgonj.

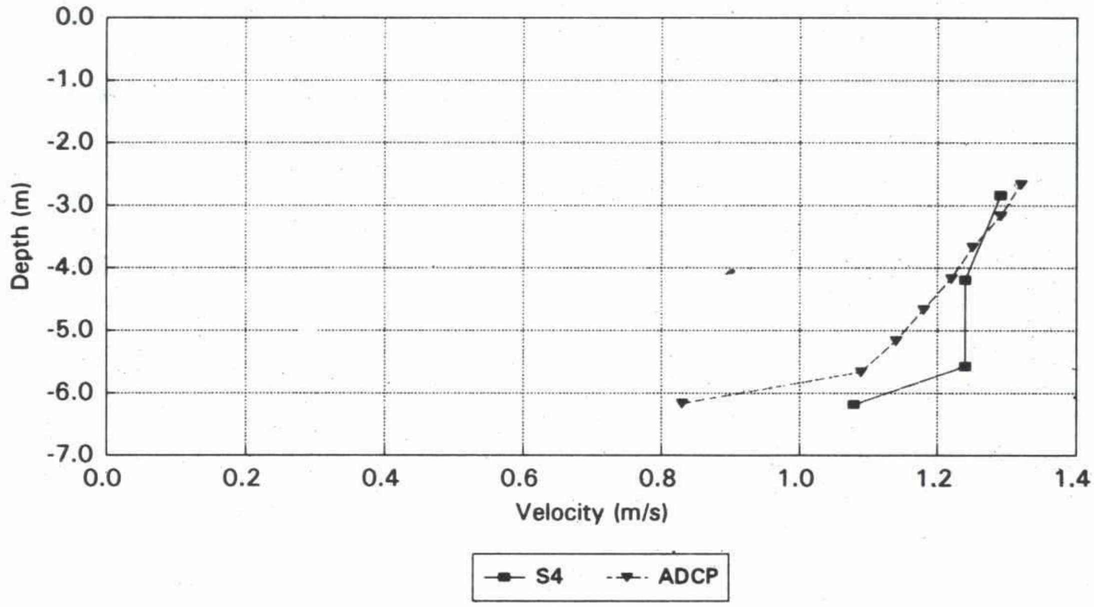

Figure 7.10: Velocity profiles measured by S4 and ADCP in a reference vertical (V-7) measured on July 6, 1994 at Aricha

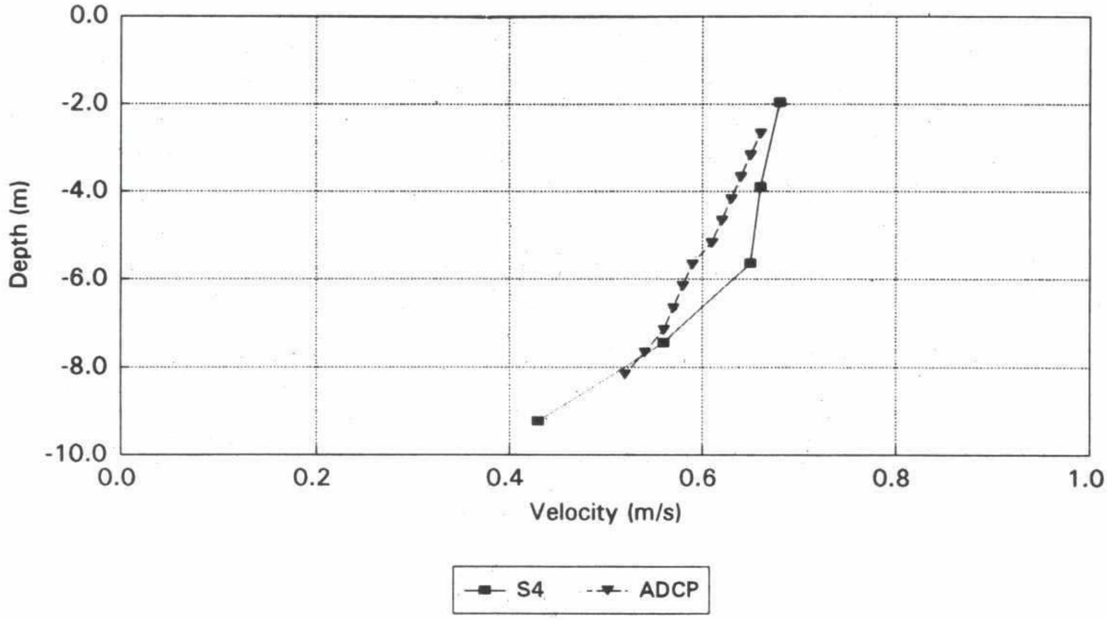

Figure 7.11: Velocity profiles measured by S4 and ADCP in a reference vertical (V-3) measured on 14 April 1994 at Baruria

Figure 7.8 shows a good agreement between the two instruments in the Jamuna River, although near the surface, the S4 measured a significantly lower velocity. On an other occasion, in the Jamuna River near Sirajganj, the agreement between the two was poor (Figure 7.9). Here, the S4 measured a higher velocity than the ADCP on most occassions. At Aricha, a similar but smaller variation was noticeable between the two instruments (Figure 7.10). At Baruria, the agreement between the instruments was close, but the S4 was still lower than the ADCP (Figure 7.11).

In April 1995, an intercomparison measurement was made in the Jamuna River near Bahadurabad. In one set of measurements, ADCP, S4, and Ott-propeller current meters were deployed simultaneously at 50 percent water-depth. Seventy-two samples were taken at 50 s instrument exposure time. In another set of measurements, the EMF and the Ott were deployed at one metre below the surface. Table 7.2 shows the relative standard deviations (at 67 percent confidence level). Figures 7.12 to 7.17 show the data and the relative standard deviations which are summarized in Table 7.2.

Instrument	Time-mean values	Relative standard deviation
ADCP velocity	0.83 m/s	± 4.6%
S4 velocity	0.87 m/s	± 5.1%
EMF velocity	0.92 m/s	± 2.5%
Ott-propeller velocity	0.81/0.96 m/s	± 6.5%
ADCP direction	189°	± 1.0%
S4 direction	193°	± 1.3%

Table 7.2: Relative standard deviations of instruments of different velocity measuring instruments at 67% confidence level, based on measurements in the Jamuna River left channel near Bahadurabad on 30 April 1995

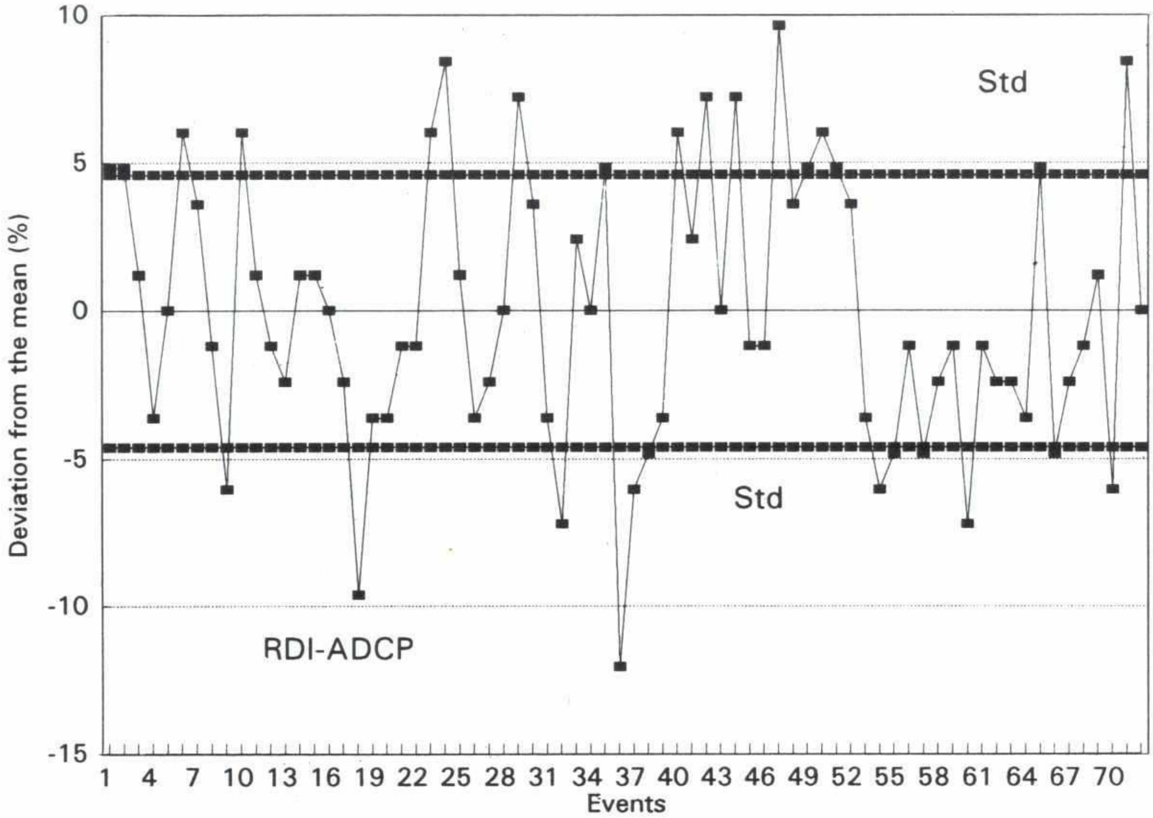

Figure 7.12: Relative standard deviation of ADCP velocity based on measurements in the Jamuna River left channel near Bahadurabad on 30 April 1995.

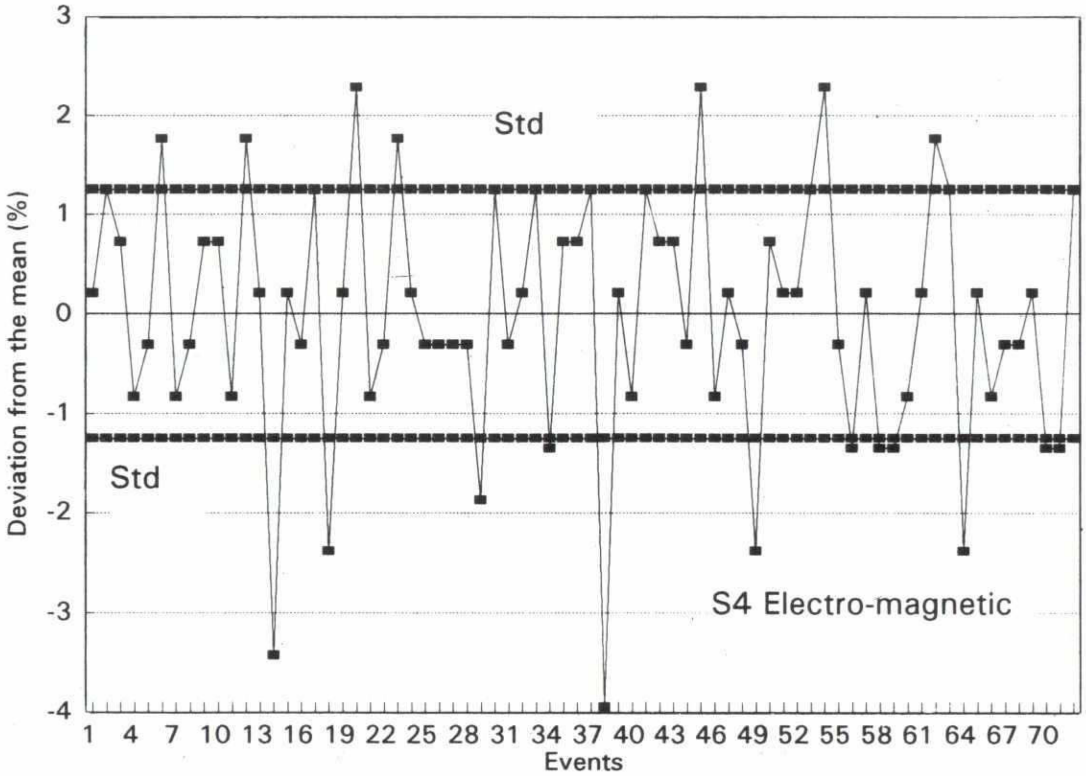

Figure 7.13: Relative standard deviation of S4 velocity based on measurements in the Jamuna River left channel near Bahadurabad on 30 April 1995.

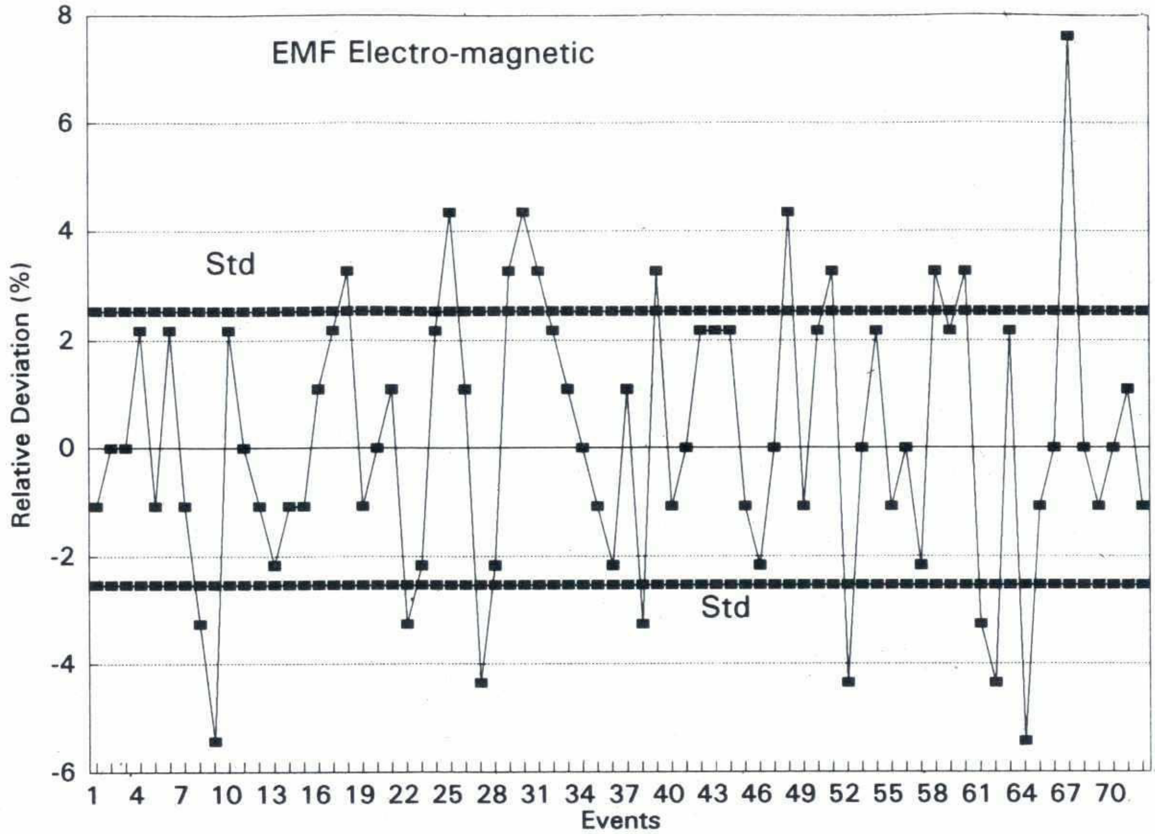

Figure 7.14: Relative standard deviation of EMF velocity based on measurements in the Jamuna River left channel near Bahadurabad on 30 April 1995.

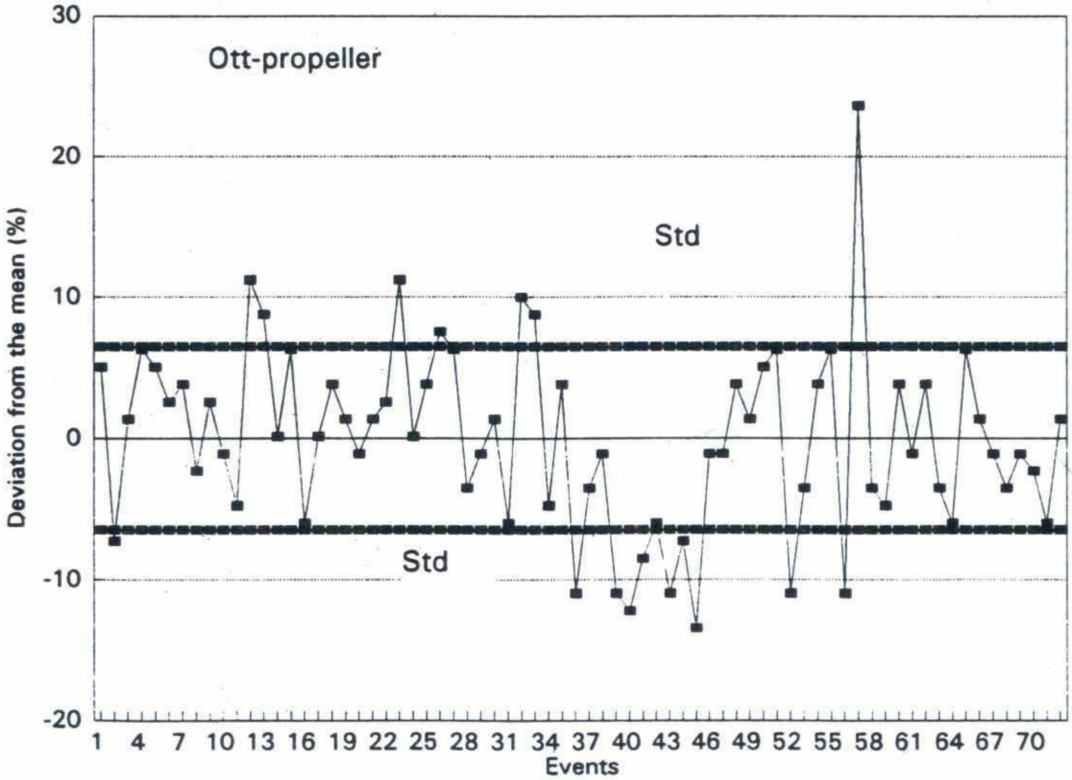

Figure 7.15: Relative standard deviation of an Ott-propeller current meter based on measurements in the Jamuna River left channel near Bahadurabad on 30 April 1995.

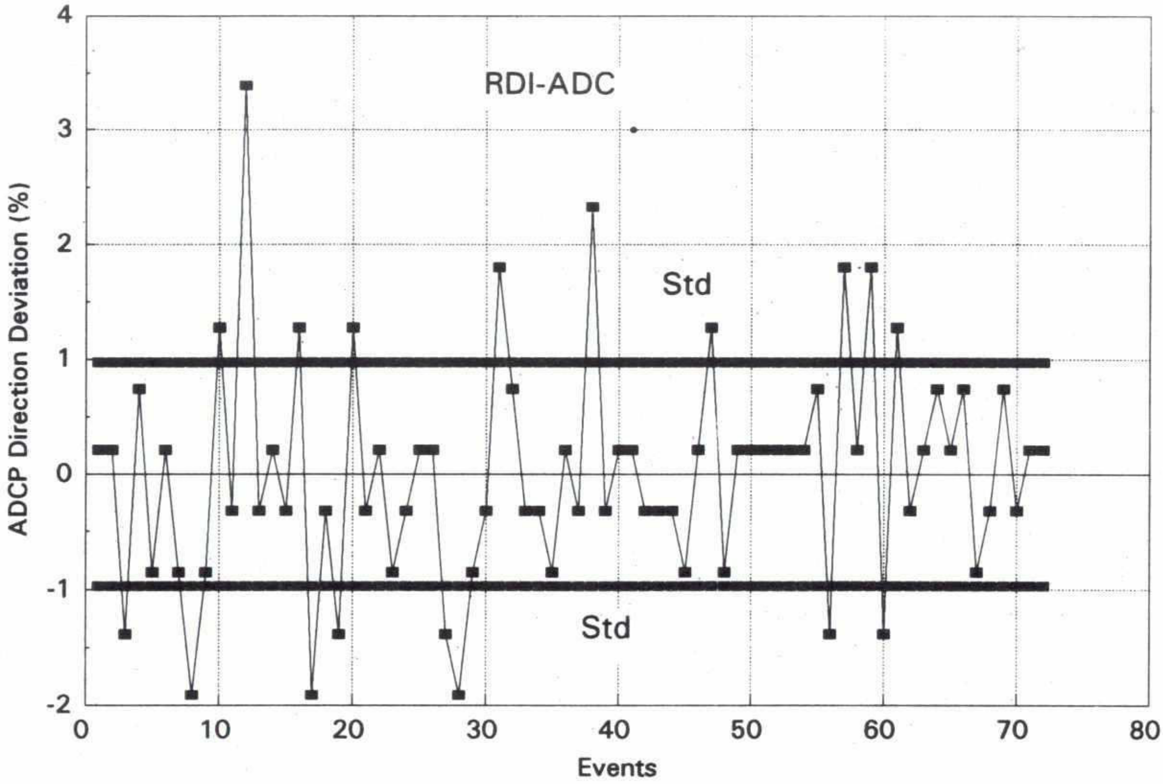

Figure 7.16: Relative standard deviation of ADCP direction measurements based on measurements in the Jamuna River left channel near Bahadurabad on 30 April 1995.

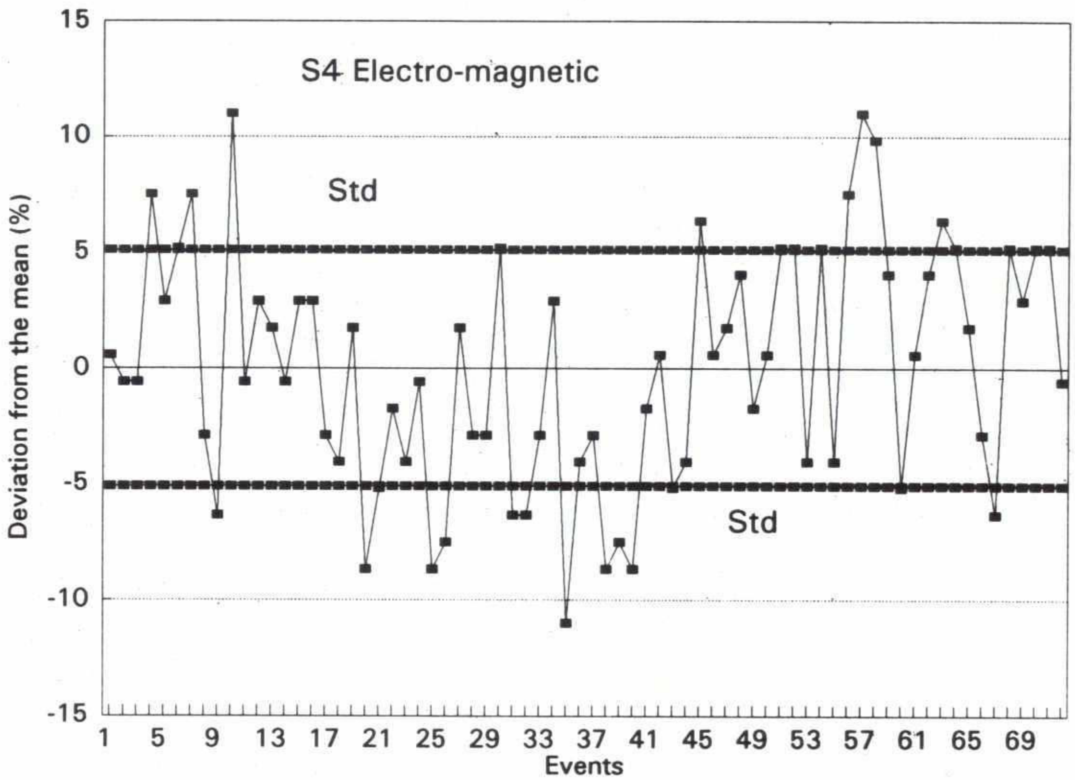

Figure 7.17: Relative standard deviation of S4 direction based on measurements in the Jamuna River left channel near Bahadurabad on 30 April 1995.

These intercomparisons or individual standard deviations of the instruments give only some indicative results. They are far from conclusive as one or two measurements could hardly give conclusive results.

The relative standard deviation (termed as standard error if compared with a true value) measured in the natural river indicates the natural variation in flow as well as the individual accuracy of the instrument. It is difficult to explain the variability among the instruments or to say that this instrument measured better than the other. Certainly, one reason is that the nonhomogeneity of flow affected the instruments that were deployed at different locations. But that does not fully explain the systematic deviation between the registrations. Also, the basic instrument characteristics play a role. If one assumes the natural variation to be the same in all the cases, then Table 7.2 indicates that Ott-propeller has a relatively higher inaccuracy than the others.

The ADCP uses the Doppler shift principle of scatterers. The scatterers include sand particles that usually have less velocity than the water particles. Therefore, a lower registration is conceivable. However, the ADCP velocity is not affected by the movement of the platform, because (under most operating conditions), the instrument registers the velocity relative to the river bed rather than to the position of the vessel. Under extreme operating conditions, however, the ADCP suffers from limitations related to mobile bed conditions, where it is certain to underestimate the flow velocity. FAP24 solved this problem by measuring the velocity relative to the vessel position determined by DGPS.

The flow, when measured by any point-measuring device, is affected by at least four factors:

- individual bias of the instrument
- the movement of the survey vessel (sway, roll, pitch)
- flow irregularities caused by the presence of the vessel
- small-scale flow fluctuations (the problem of flow homogeneity)

The electromagnetic sensors are not significantly affected by the roll and pitch as these effects are filtered out. But, the results are affected by the presence of the vessel.

Mechanical rotor current meters, such as the Ott or the Valeport propeller-types, are affected by all the four factors. Studies show that propeller-type current meters measure as much as 10 percent more velocity in highly turbulent flow (Jepson, 1967; Gordon and Bornhoft, 1991). Discharge measurements (980 m^3/s) in the Rhine River near Brohl in 1991 indicated similar discrepancies between a 1200 kHz Broadband ADCP, and an Ott propeller current-meter (Gordon and Bornhoft, 1991). Comparison of one velocity profile indicated that the Ott velocities were nine percent higher than the ADCP, and that the discharge measured by the Ott was about 10 percent higher. Similar results were obtained in Jepson's laboratory experiments (1965). He found that Ott over-registered velocity by as much as 10 percent due to velocity fluctuations on the axis of the Ott current meter.

7.2 FAP24 - BWDB joint measurements

Some simultaneous discharge measurements were executed by FAP24 and BWDB with the purpose to make intercomparisons between their instruments and methods. The detailed comparisons and results are reported in RSP Special Report 19.

The comparison measurements included

- special joint measurements at Bahadurabad in October 1994
- routine but coinciding measurements at Bahadurabad in June, July, and August 1994
- special joint measurements at Bahadurabad in July 1995

The comparisons primarily involved BWDB's velocity-area method and FAP24's ADCP-EMF moving boat method. Table 7.3 shows the comparison of instruments deployed and the measuring methods pursued.

In Figures 7.18 to 7.20, the velocity profile measurements are shown.

Items	BWDB	FAP24
Vessels	Catamaran	DHA
Sampling mode on a vertical	No anchoring	ADCP-EMF moving boat in deep channels and anchored while using S4 current meter
Vessel positioning	One angle measurement using sextant	DGPS
Depth/transect profiling	Length of current-meter wire at the verticals	Continuous profiling by echosounders
Current meter positioning in the vertical	Length of current-meter wire	Complete profiling by ADCP-EMF and by pressure sensor while using S4.
Flow velocity	SEBA propeller type	ADCP - acoustic Doppler EMF, S4 - electro-magnetic
Flow direction	SEBA directional current meter/ or measuring at the surface by floats	ADCP in 3 orthogonal directions S4 in 2 orthogonal directions
Points in a vertical	20% and 80% of water-depth	Vertical profile by ADCP 6 points by S4

Table 7.3: Intercomparison of BWDB and FAP24 instruments and methods as applied during joint measurements on 19 July 1995 in the left anabranch near Bahadurabad.

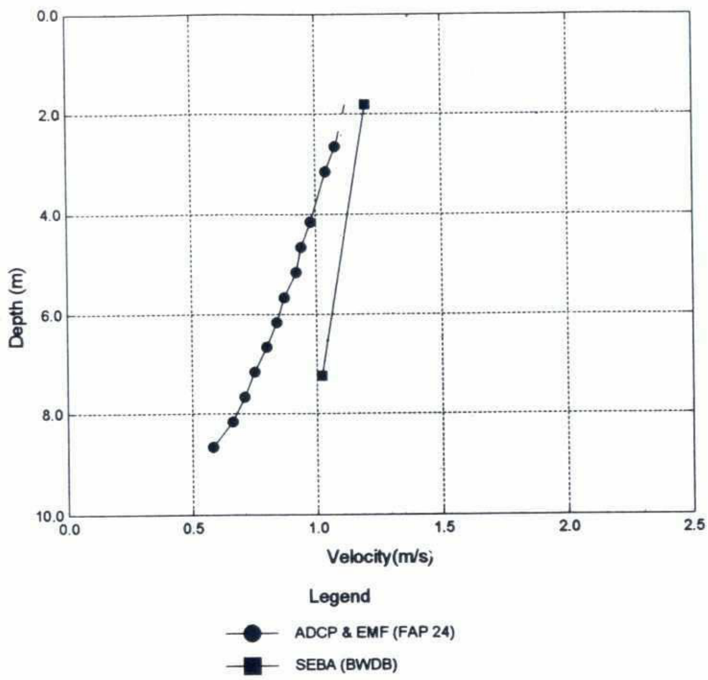

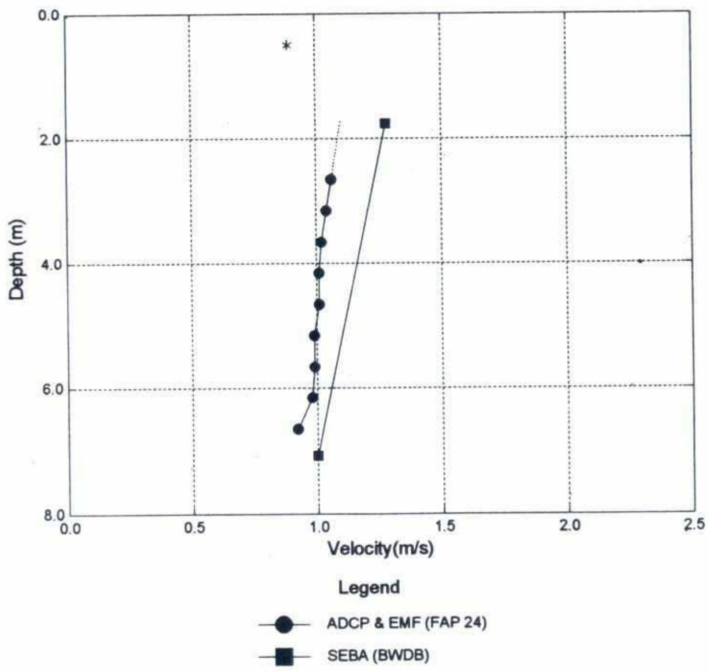

Figure 7.18: ADCP-EMF velocity profile of FAP24 vs. SEBA-propeller velocity of BWDB as obtained during joint measurements on 17 July 1995 in the right anabranch near Fulchari

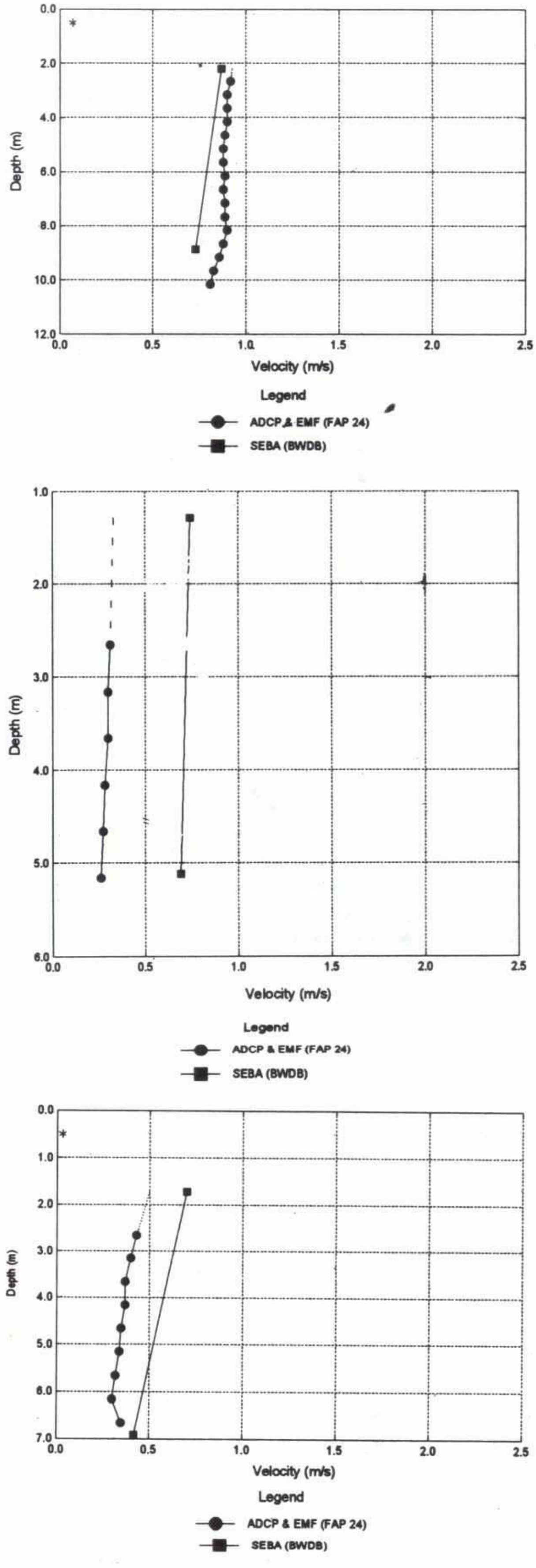

Figure 7.19: ADCP-EMF velocity profile of FAP24 vs. SEBA-propeller velocity of BWDB as obtained during joint measurements on 18 July 1995 in the left anabranch near Bahadurabad

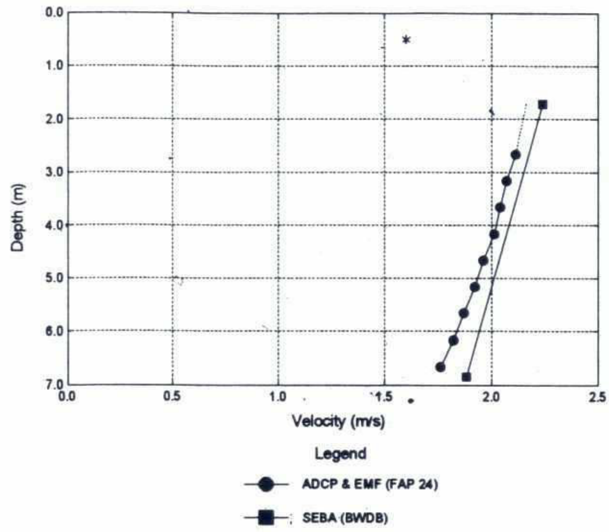

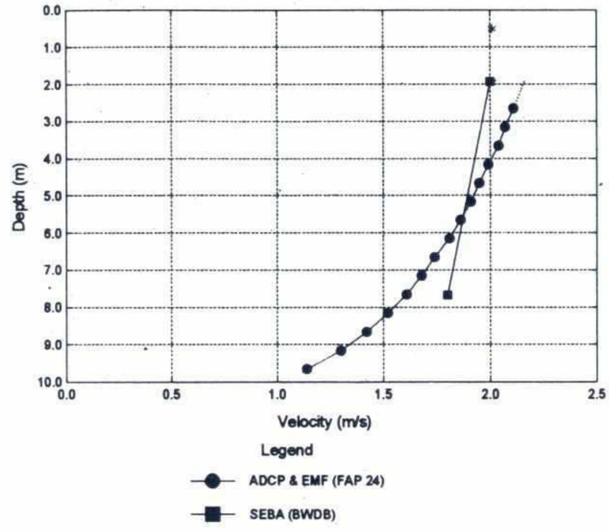

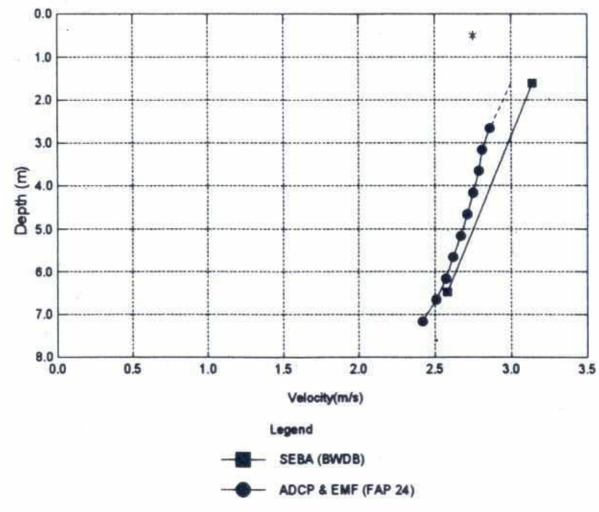

Figure 7.20: ADCP-EMF velocity profile of FAP24 vs. SEBA-propeller velocity of BWDB as obtained during joint measurements on 19 July 1995 in the left anabranch near Bahadurabad

In most cases, the ADCP measured lower velocities than the SEBA. Figure 7.21 presents the stage-discharge relationship based on joint and simultaneous measurements, indicating that the BWDB discharge was systematically higher than the FAP24 discharge.

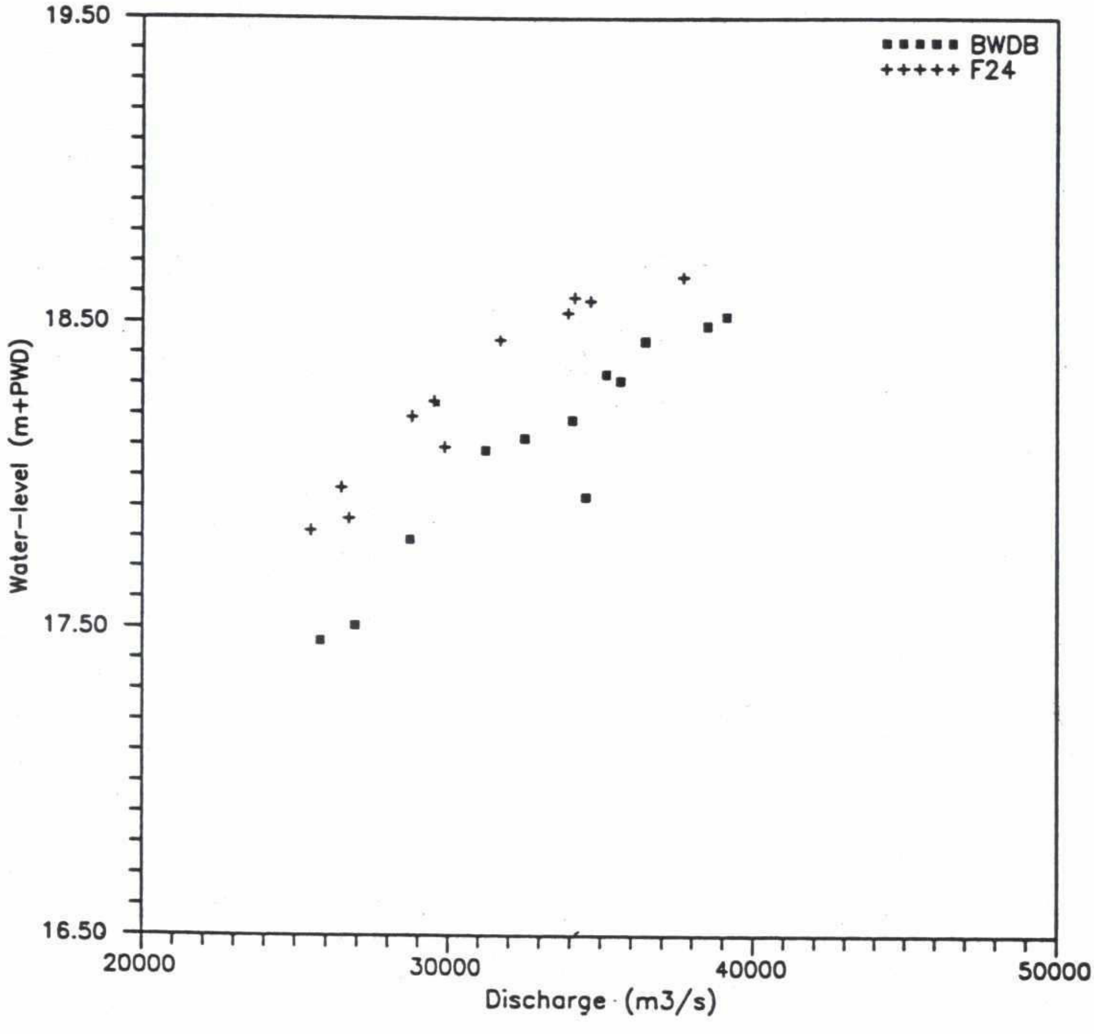

Figure 7.21: Stage-discharge relationship based on joint measurements by FAP24 and BWDB

The discharge difference between the two methods varied between 3.6 percent and 8.5 percent.

7.3 Optimal measuring time

When measuring discharge, an error usually occurs due to the limited exposure time of the sensor. This *Type I error* (ISO, 1983) is known as a *standard pulsation error* that occurs due to the turbulent flow field being more intense at the bed than at the surface. This error can be examined by considering different windows of time. Studies by Carter and Anderson (1963) confirmed that the standard pulsation error lessens as the exposure time increases. Their studies indicated that at 60 percent water depth, the standard error (ϵ) is related to the exposure time (τ) as,

$$\epsilon = 16.6\ \tau^{-0.28}$$

The standard error is in percentage and the exposure time is in seconds. The relation indicates that with 50 s exposure time, the standard error is 5.6 percent. Although such studies and error ranges were found elsewhere in the world, no such data were gathered for Bangladesh rivers. However, FAP24 has made several special surveys and determined turbulence flow fields and optimal exposure times. Measurements and detailed results are described in Annexure A, and are elaborated in Annexure B.

Special turbulence measurements were made at three locations in the Jamuna River near Bahadurabad on 1 April and 13 August 1994 (Figure 7.22).

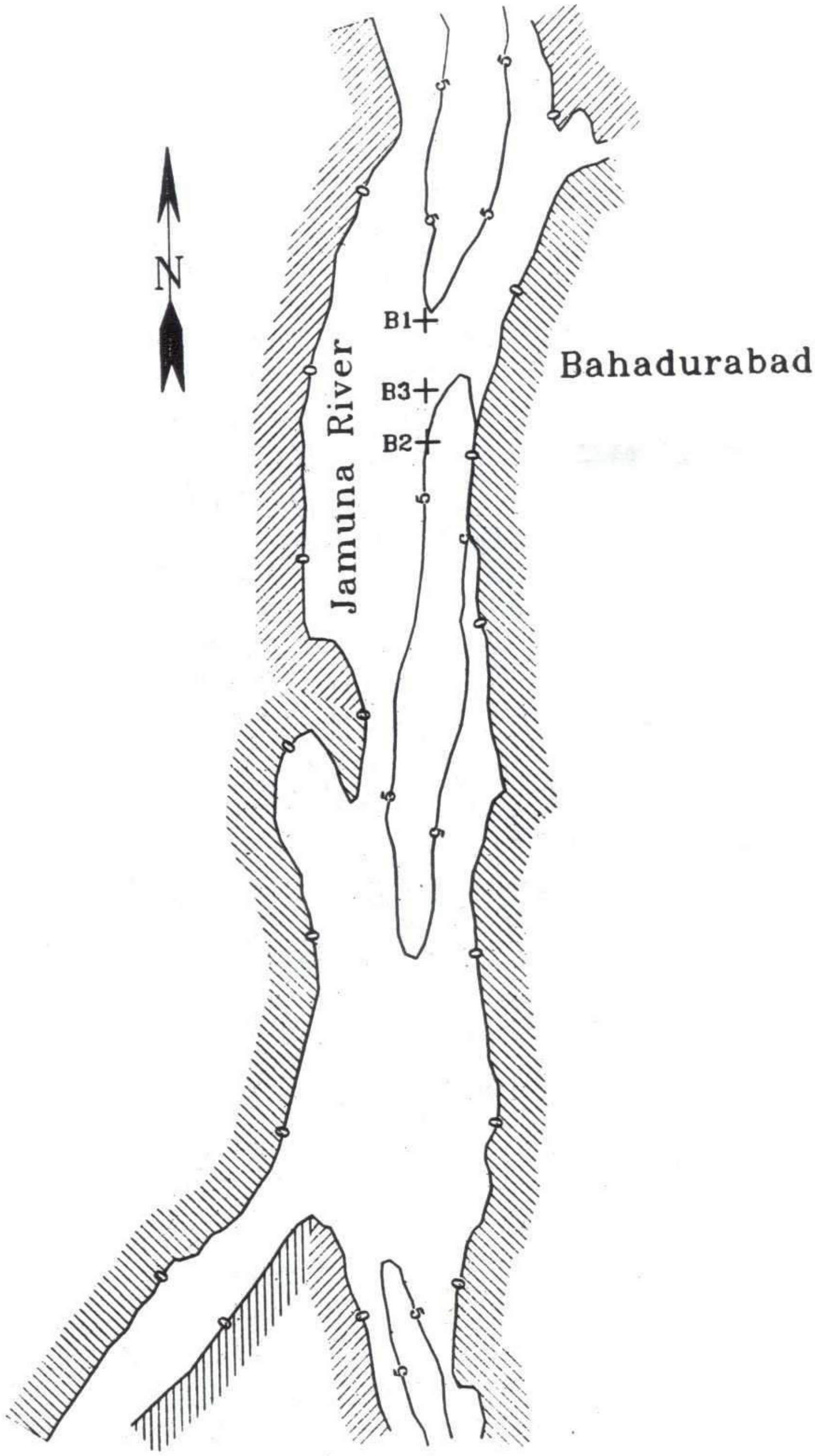

Figure 7.22: Stations B1, B2 and B3 in the Jamuna River left channel near Bahadurabad measured on 1 April 1994 and 13 August 1994.

Measurements also were taken at the Ganges-Jamuna confluence near Aricha on 13 April 1994 (Figure 7.23).

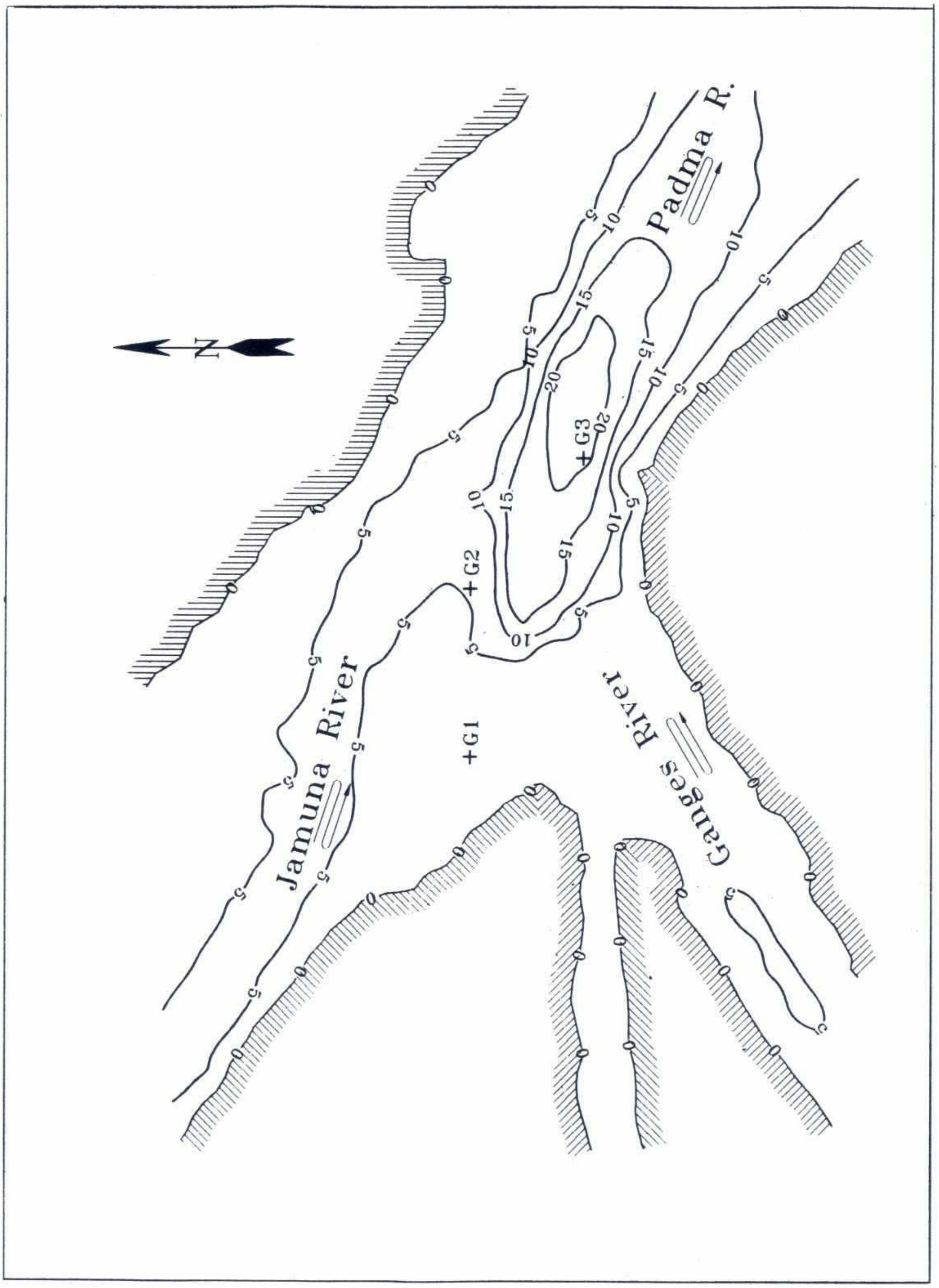

Figure 7.23: Turbulence measurement locations at the Ganges-Jamuna Confluence near Aricha on 13 April 1994.

The measurements were executed during the rising and peak river stages as shown in Figure 7.24.

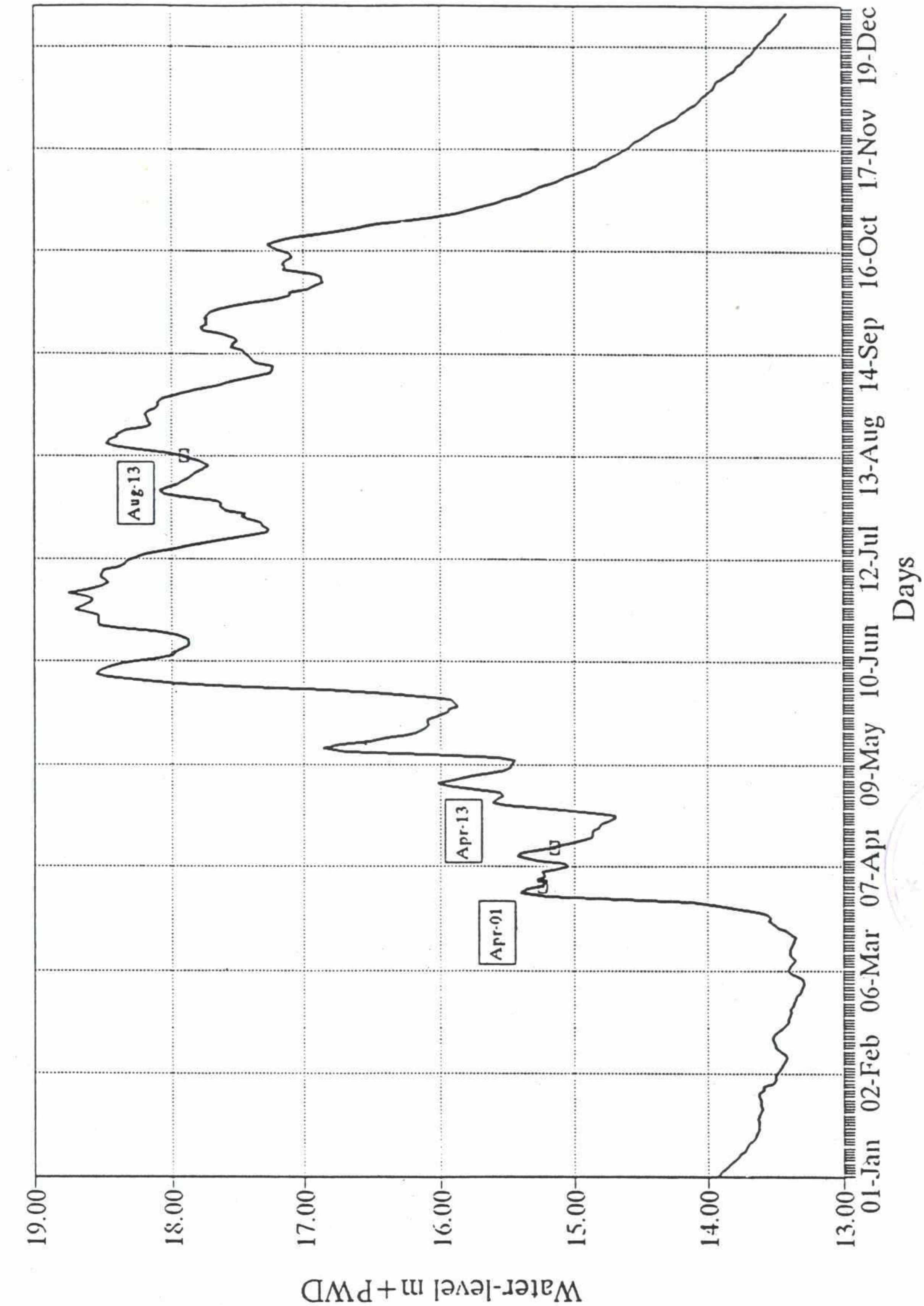

Figure 7.24: Water level stage during which the turbulence measurements were made

The exposure time relative to the time-scale of turbulence is used to determine the standard pulsation error for ADCP and EMF velocities. To determine the standard pulsation error, three regions of the boundary layer were chosen for measurement: One near the wall-region representing 88 percent to 93 percent water-depth, one in the free-stream region representing five percent water-depth, and one in the intermediate region. The results are given in Table 7.4; it is seen that a higher pulsation error was found near the river bed.

Fractions of depth (h)	SPE equation	SPE at 50 s exposure time	SPE at 100 s exposure time
5% h	$\epsilon_v = 26\ \tau^{-0.44}$	± 4.7%	± 3.4%
28% - 68% h	$\epsilon_v = 80\ \tau^{-0.65}$	± 6.3%	± 4.0%
88% - 93% h	$\epsilon_v = 269\ \tau^{-0.76}$	± 13.8%	± 8.1%

Table 7.4: Standard pulsation error (SPE) at different water-depths obtained by ADCP and EMF measurements

Figures 7.25 and 7.26 show standard pulsation errors as a function of exposure time. The negative exponents imply that as the exposure time increased, the standard pulsation error decreased.

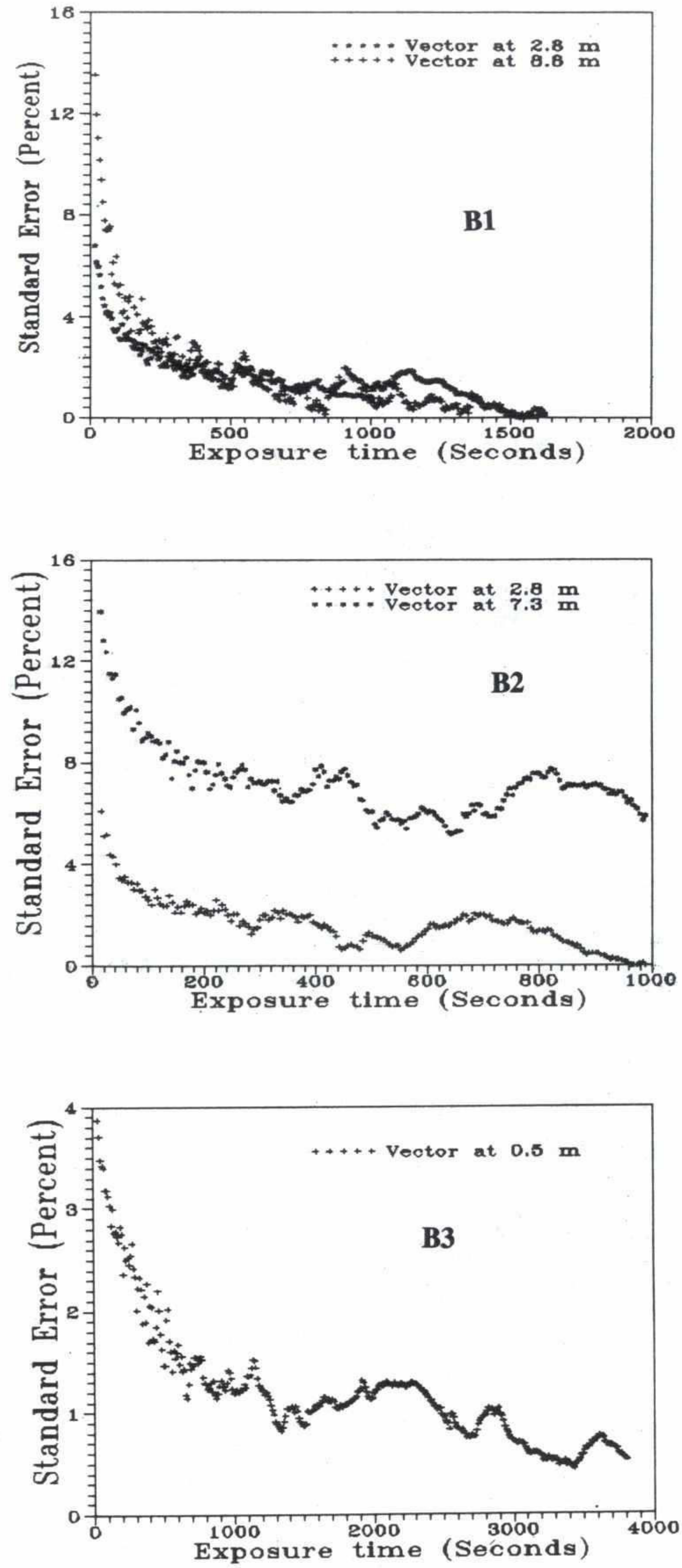

Figure 7.25: Standard pulsation error vs exposure time at stations B1, B2 and B3 in the Jamuna River left channel near Bahadurabad measured on 1 April 1994 and 13 August 1994

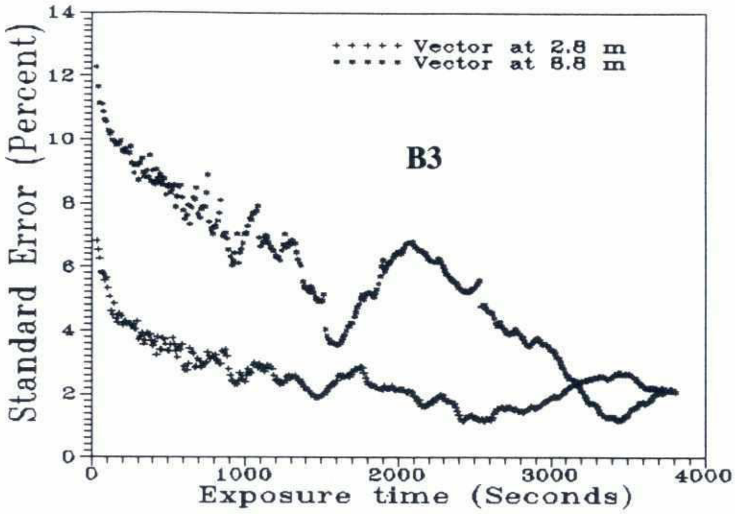

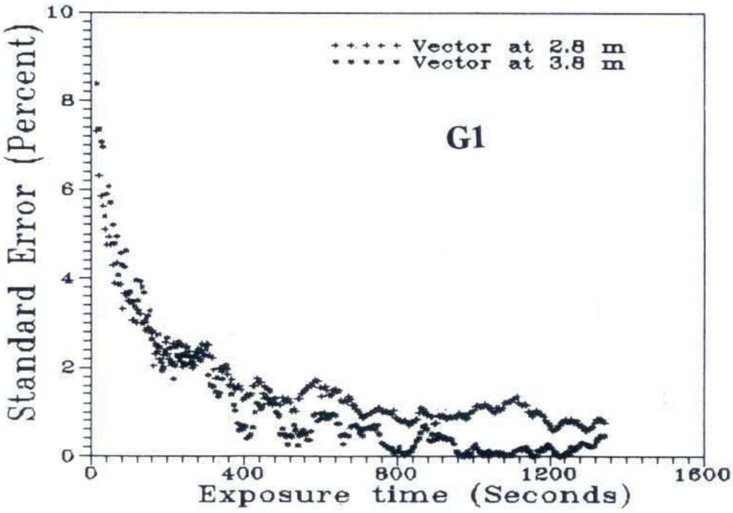

Figure 7.26: Standard pulsation error vs exposure time at station B3 in the Jamuna River left channel near Bahadurabad (on 13 August 1994) and at station G1 in the Ganges-Jamuna confluence (on 13 April 1994).

7.4 Optimal vertical and horizontal distribution

Special measurements were made of the flow distribution in vertical and horizontal directions, in order to optimize the number of points in a vertical, and the number of verticals in a transect. This is a requirement of velocity-area method of discharge estimation which is primarily used by BWDB. FAP24 used the method in shallow channels. Figure 7.27 shows the locations of special measurements made in July 1995.

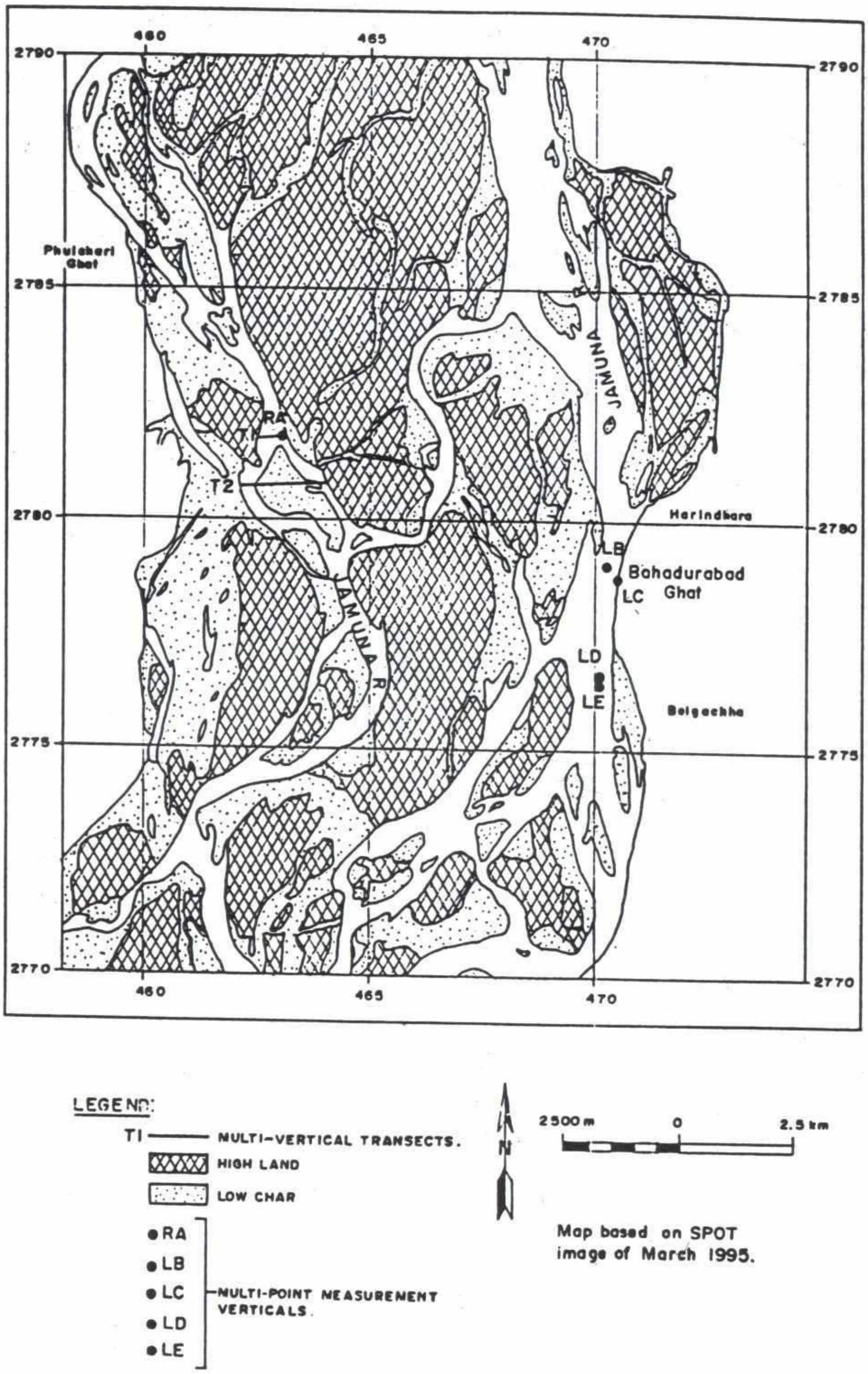

Figure 7.27: Locations of optimization measurements on spatial density in the Jamuna River near Bahadurabad

Annexure C provides detailed analyses and results of the Type II and Type III discharge measurement errors. Some findings are summarised as follows:

- To limit the relative deviation of the depth-averaged velocity estimation to ± 1 percent, the minimum numbers of points in a vertical should be at least five. The maximum deviation is well within five percent, however. On average, an underestimation occurs when fewer points are measured. The present analyses indicated that when only two points are measured (20 percent and 80 percent water-depth) it is no better than when one point is measured (50 percent water-depth). This is contrary to the observations by Carter and Anderson (1963).

- Estimating the total discharge using the mid-section method appeared to be dependent on choosing the vertical numbers. In the two cases compared, overestimation occurred when the number of verticals were reduced. The dependence on the vertical numbers is described in the following linear equations:

  At transect T1: $Y = 22 - 2.1\ X$
  At transect T2: $Y = 34 - 2.7\ X$

  where Y is the percentage discharge deviation from the discharge using 12 verticals, and X is the number of verticals. Figures 7.28 and 7.29 show the discharge deviation as a function of the numbers of verticals

- The total discharge estimates made using the ADCP-EMF moving boat method and the two velocity-area methods were comparable in magnitude. However, the velocity-area method appeared to slightly underestimate the flow

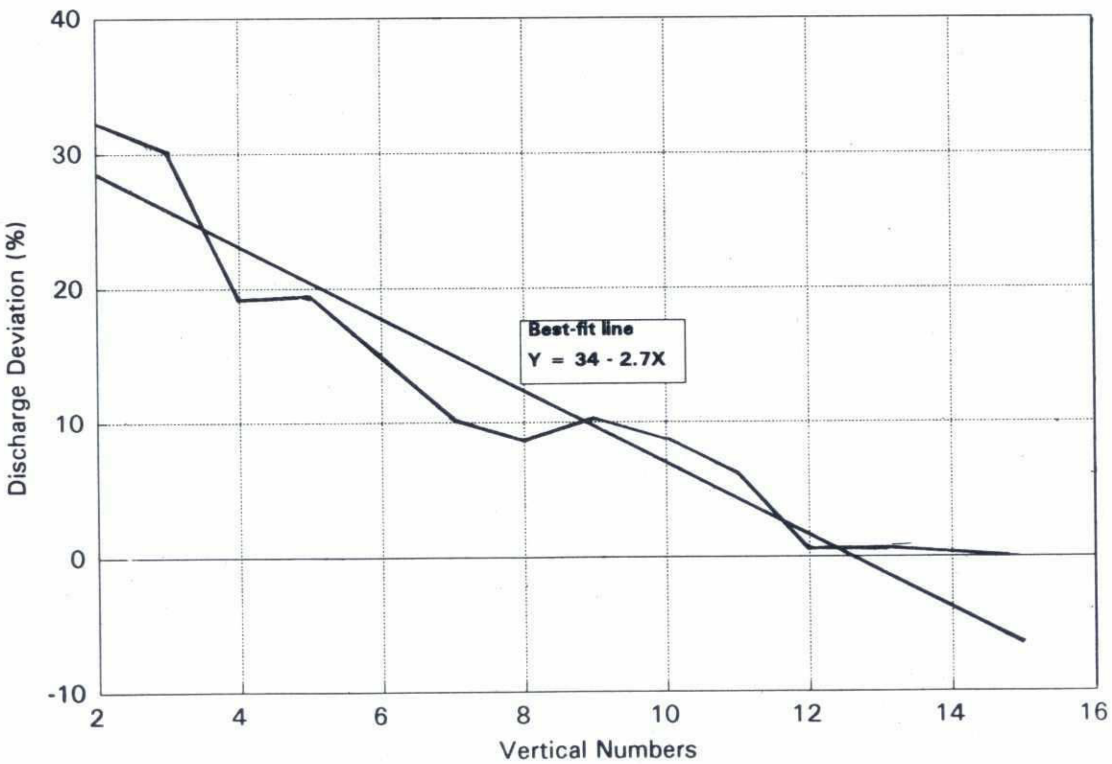

Figure 7.28: Percentage deviation of discharge estimates as a function of the numbers of verticals at T1 measured on 27-30 July 1995 in the Jamuna River at Bahadurabad

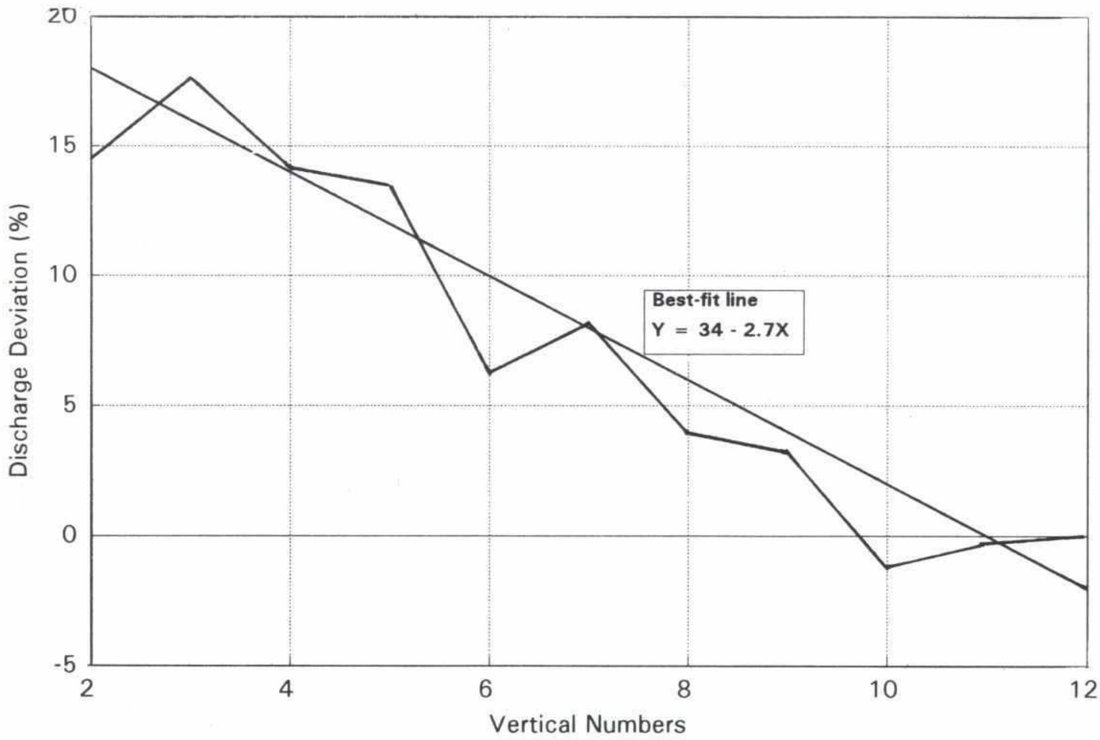

Figure 7.29: Percentage deviation of discharge estimates as a function of the numbers of verticals at T2 measured on 27-30 July 1995 in the Jamuna River at Bahadurabad

7.5 Tidal Surveys

The main objectives of the RSP tidal measurements are to assess the errors made using traditional methods, to justify the need for detailed measurements to improve balances and the net flow and sediment transport rates in different tidal situation. In this context, tidal measurements were carried out to provide a 'sufficient' picture of the variation of flow and sediments in time as well as in space. The following Table (Table 7.5) shows the tidal surveys carried out by RSP.

Station	Period	Survey Bulletin No.	Remarks
Bhairab Bazar	27-28 April 1993	5	Phase 1
Bhairab Bazar	10 February 1994	34	Phase 1
Baruria	21-22 March 1994	43	Phase 1
Arial Khan Offtake	18-19 April 1994	53	Phase 1
Baruria	3-5 May 1994	56	Phase 1
Mawa	17-18 February 1995	134	Phase 2
Arial Khan Offtake	23 February 1995	136	Phase 2
Bhairab Bazar	17-20 March 1995	139	Phase 2
Mawa	30-31 January 1996	254	Phase 3
Mawa	7-8 February 1996	256	Phase 3

7.5 Tidal Surveys in the Padma River at Mawa and in the upper Meghna River at Bhairab Bazar from 1993 to 1996

Among the tidal measurements done at different stations, a detailed analyses were only carried out at Mawa and Bhairab Bazar in Phase 2 surveys. The analyses of Phase 3 measurements were limited. These analyses include water levels and discharge variations, river bed profiles changes, sediment concentration and transport variations in Mawa and Bhairab Bazar. A comparison of the water level records from the left and right banks clearly shows a water level difference of up to 0.25 m which is clearly correlated with the discharge (highest at the highest discharge) as shown in Figure 7.30. The grain size distribution of the Delft bottle, bed material and Helley-Smith samples were analyzed for Mawa during the spring tide on 17-18 February 1996. Figure 7.31 shows that grain sizes of the Delft bottle are similar to the grain sizes of the bed material and fairly constant over the tidal cycle. The grain sizes of the Helley-Smith samples are significantly higher than the grain sizes of the bed material samples and the Delft bottle samples. The total suspended sediment concentration at different levels with the variation of time is shown in Figure 7.32. This Figure indicates that there is a phase lag of the sediment concentrations behind the discharges of the order of a few hours. The discharge time series at Bhairab Bazar has a clear indication of reversing flow with a higher discharge during flooding than during ebbing. The grain sizes for bed material and near bed suspended material were found to be lower during flooding than for ebbing.

Some other observations can be summarized as follows:

- With respect to flow measurements, the half-hourly measurements over 13 or 26 hours of discharges and water levels provides a good short-term description of flow conditions. For a long-term description the detailed tidal measurements should be combined with long-term flow velocity measurements, for instance by a self-recording current meter at a fixed location 1-2 metres below surface. A one-dimensional model will be a strong tool for long-term tidal flow analysis. Long-term water level data along the river will be required for setting up the model, see also Tajeda-Guibert (1994).

- With respect to sediment transport measurements, measurements in two verticals is insufficient to establish the integrated transport rates over the entire cross section in a main river. Measuring at a large number of verticals requires large resources. Ad a compromise it may be possible to measure regularly at few verticals and less frequently at a number of additional verticals. This method requires scaling during analysis, and has not been tested.

A detailed bathymetric survey covering a reach of minimum 2 times the width of the river upstream and downstream is useful for interpreting the measurements of sediment transport.

- The use of dune tracking to determine bed load and near bed transport proved less useful. The results will be dominated by measuring inaccuracies when the transport rate is relatively low and the measuring period is short.

The following detailed conclusions can be drawn from the measurements carried out at the two locations:

Phase 2, Mawa

- The flow in the minor channel seems to be ahead of the overall flow by 10-15 minutes.
- The average flow is 4000-4200 m^3/s and not much different with 24.8 hours averaging compared with 12.4 hours averaging. Reversed flow occurred under this condition (approximately 1000 m^3/s).
- The median grain sizes of the Delft Bottle samples are nearly the same as for the bed sediment. There is a tendency that it is lower at high flow rate.
- The median grain sizes for the Helley Smith samples are much higher than for the Delft Bottle samples. It tends to be highest at high flow rate/high Helley Smith catch.
- For the suspended sediment, the grain size of only the coarsest fraction varies with the flow. The d_{90} increases with the flow velocity with a phase lag which depends on the level above bed (1 and 9 metres above bed in main channel).
- The sediment flux measured by Helley Smith, Delft Bottle ($kg/m^2/s$) and from pump samples (multiplied by velocities) are generally of the same magnitude. All three methods show clear dependence on flow rate, but there are no clear phase shifts.
- It is not possible accurately to estimate the total transport over a more than two kilometres cross section based on measurements at only two verticals.
- The sand fraction of concentrations is up to 20 per cent one metre above bed; up to 10 per cent at higher levels (in main channel).
- There is a clear phase lag of the concentrations compared to the discharge.
- In the secondary channel there is no distinct temporal variation of concentrations.

Phase 2, Bhairab Bazar

- Grain sizes of both bed material and near bed suspended material seem to be lower during flood flow than during ebb flow (only few data).
- The coarse fractions of suspended material tend to be coarser during ebb flow than at any other time.
- The measurements indicate that the sediment balance may be different for the wash load and for bed material load.

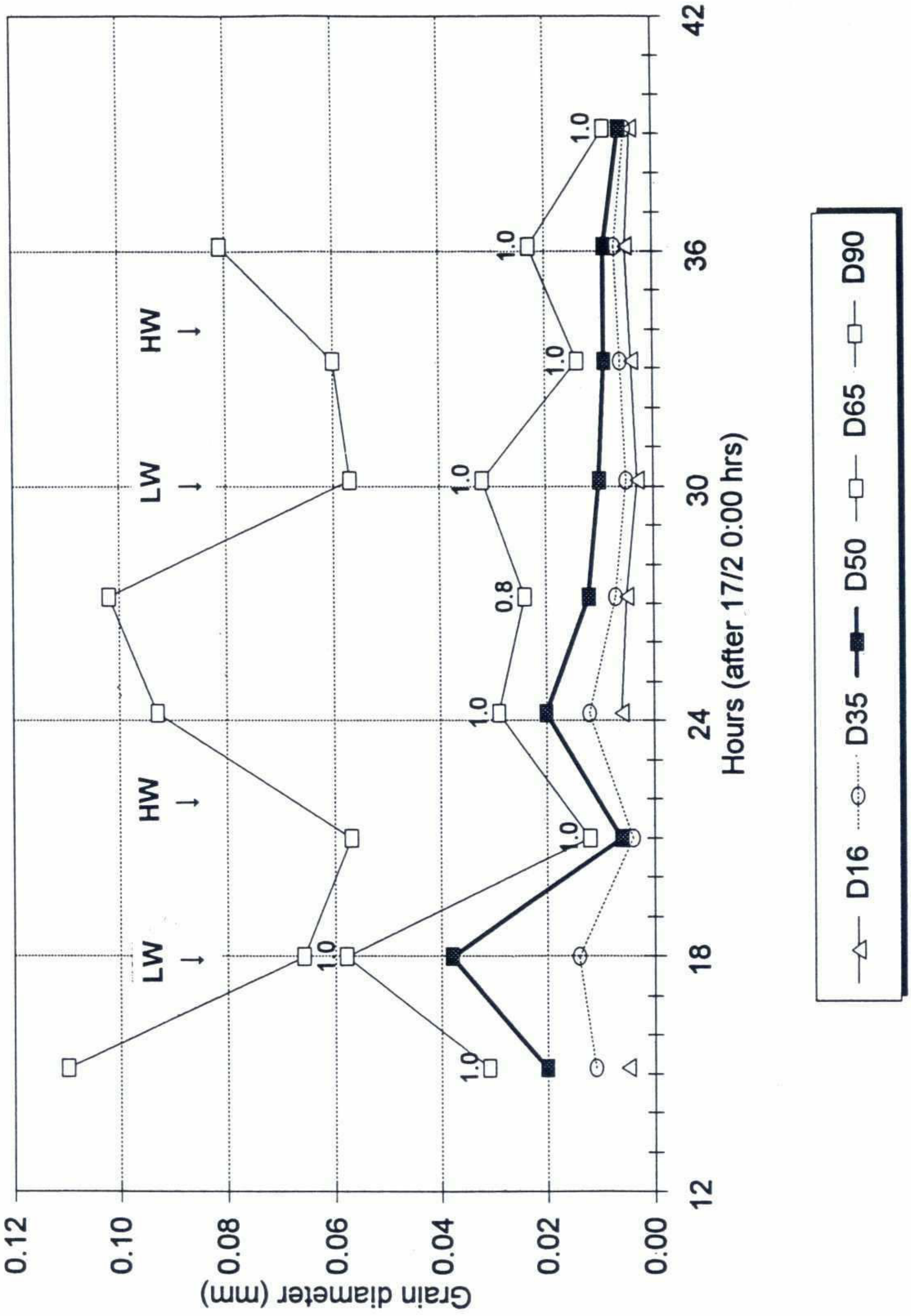

7.30 Water level changes as a function of discharge during a spring tide measurements on 17-18 February 1995 in the Padma River at Mawa.

49

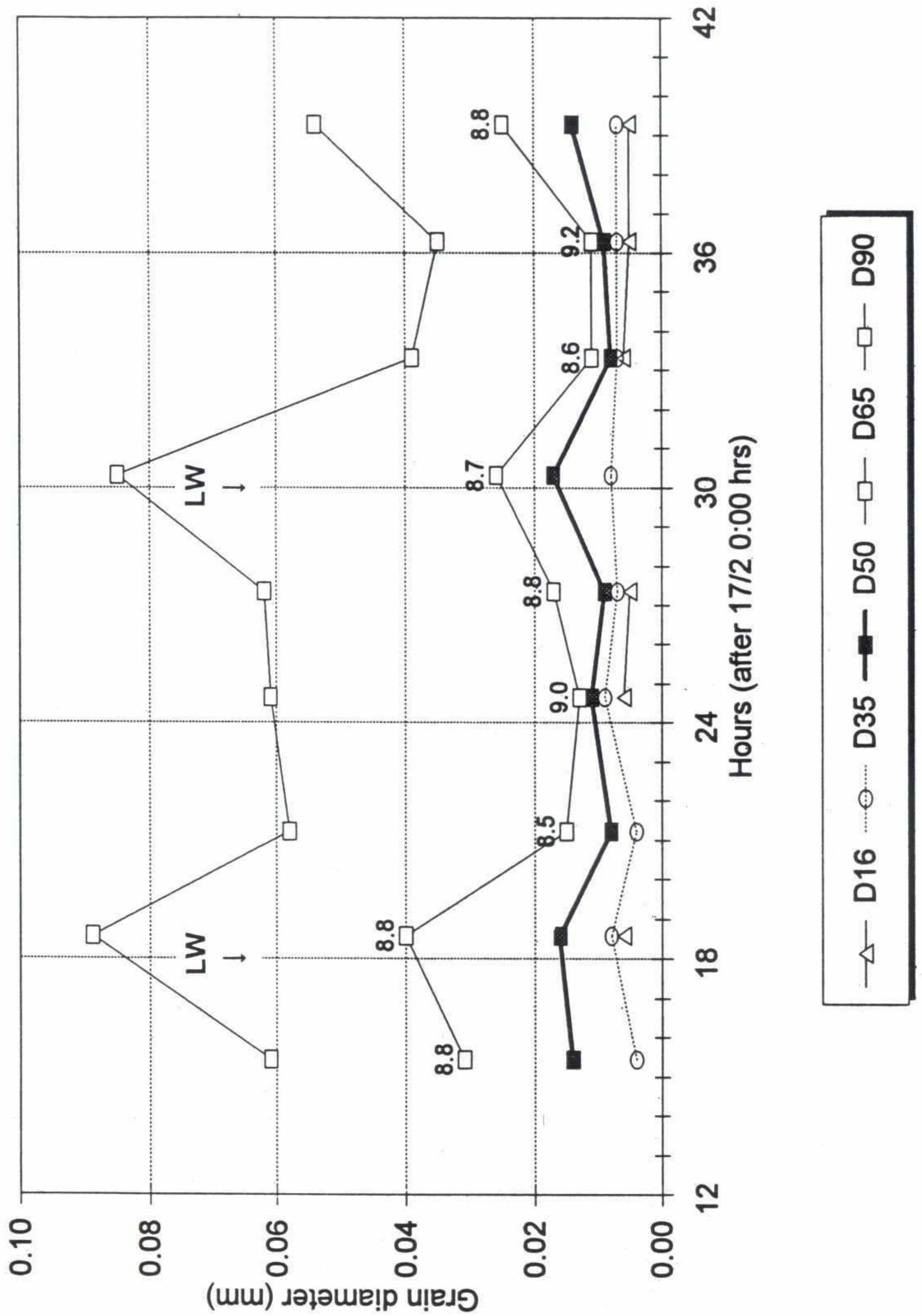

7.31 Median grain sizes of the bed materials, Delf-bottle samples at 5 and 15 cm above bed, and Helly-Smith samples taken in the Padma River at Mawa during measurements on 17-18 February 1995

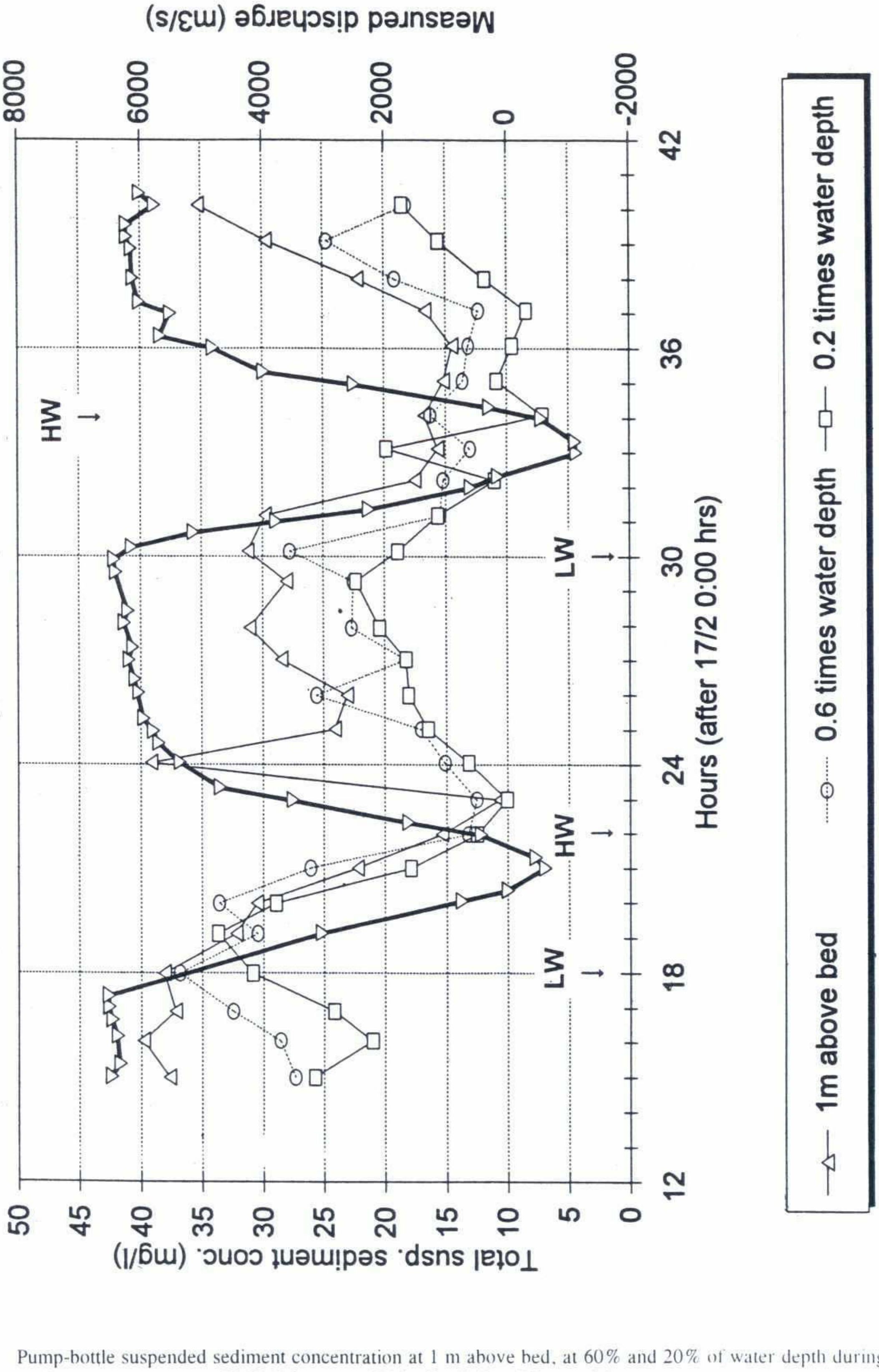

7.32 Pump-bottle suspended sediment concentration at 1 m above bed, at 60% and 20% of water depth during a tidal cycle measurements on 17-18 February 1996 in the Padma River at Mawa.

8 Optimization of hydraulic measurements

8.1 Network optimization

Hydraulic measurements in natural rivers comprise two components: River-stage and discharge gauging networks. Discharge gauging networks invariably include river-stage measurements, whereas river-stage measuring networks can stand alone, depending on the purpose of the monitoring. As indicated in River Survey Project (1995), a river-stage network can have the following five purposes:

- to monitor river stages for navigation and flood forecasting
- to estimate water resources by discharge measurements
- to estimate hydraulic gradients
- to reduce bathymetric survey data
- to make special hydraulic modelling and morphological computations

FAP24 objectives for river-stage networking include all of the above, except monitoring for navigation and flood forecasting.

A discharge gauging network, on the other hand, can have two basic purposes:

- to estimate the water resources (via stage-discharge relationships determined by simultaneous water level observations)
- to estimate sediment transport (via simultaneous sediment concentration or sediment transport measurements)

Figure 8.1 shows the optimization principle based on these two objectives.

20

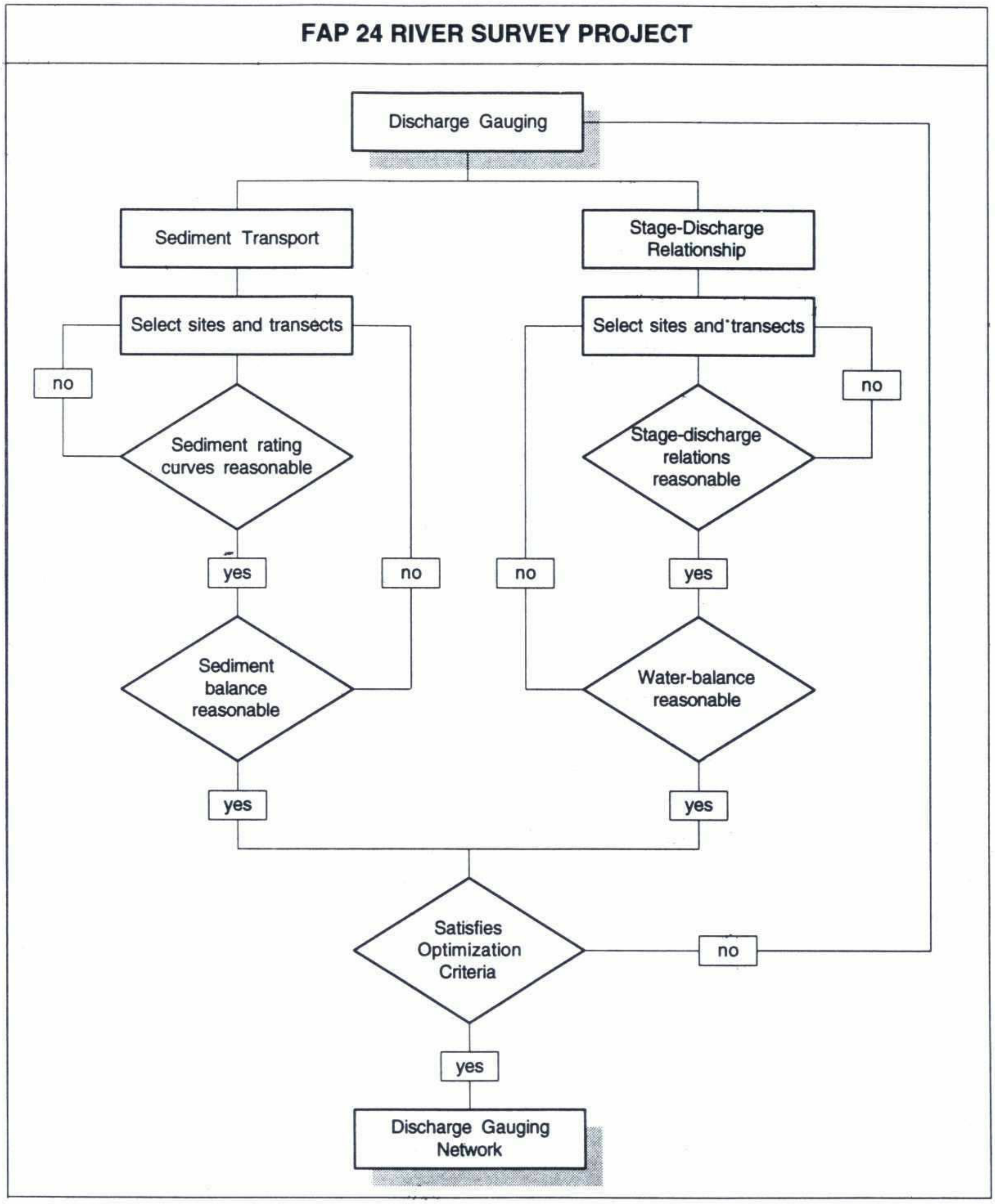

Figure 8.1: Optimization principle of a discharge gauging network

Before a general optimization criterion can be applied, the measurements have to yield some satisfactory diagnostic relationships, such as stage-discharge relationship or sediment rating curves. Thereafter, the results of the network will yield reasonable water balance or sediment balance results.

Of the 300 water level gauging stations and 80 discharge measurement stations in Bangladesh, 25 also include sediment measurements (BWDB, 1982). Data have been collected at these stations systematically since 1965. Table 8.1 shows 10 measuring stations on the main rivers of Bangladesh that are used by FAP24. Of these, eight are primary stations and two are secondary stations. BWDB does not operate stations at Sirajganj and at Arial Khan.

As indicated in Figure 8.1, a network optimization requires three initial steps prior to a suitable selection. Depending on the purpose, the steps are

- initial selection of a measuring transect that avoids converging and diverging flow lines, as recommended by WMO (1994)
- thus chosen, the measurements from the various sites should yield acceptable stage-discharge relations or sediment rating curves. If the results are not acceptable, the site selection procedure is repeated until the desired results are obtained
- using the resulting data, a water balance or sediment balance for the gauging network is computed. If the balances are acceptable, then they are screened against optimization criteria. If they are not acceptable, the former steps are repeated

The 1987 flood year was used to evaluate the stations with respect to their different qualities according to Figure 8.1. Using BWDB observations, stage-discharge relationships were established at Bahadurabad in the Jamuna River, at Hardinge Bridge in the Ganges River, and at Baruria in the Padma River. The stage-discharge relationship for Bahadurabad is shown in Figure 8.2.

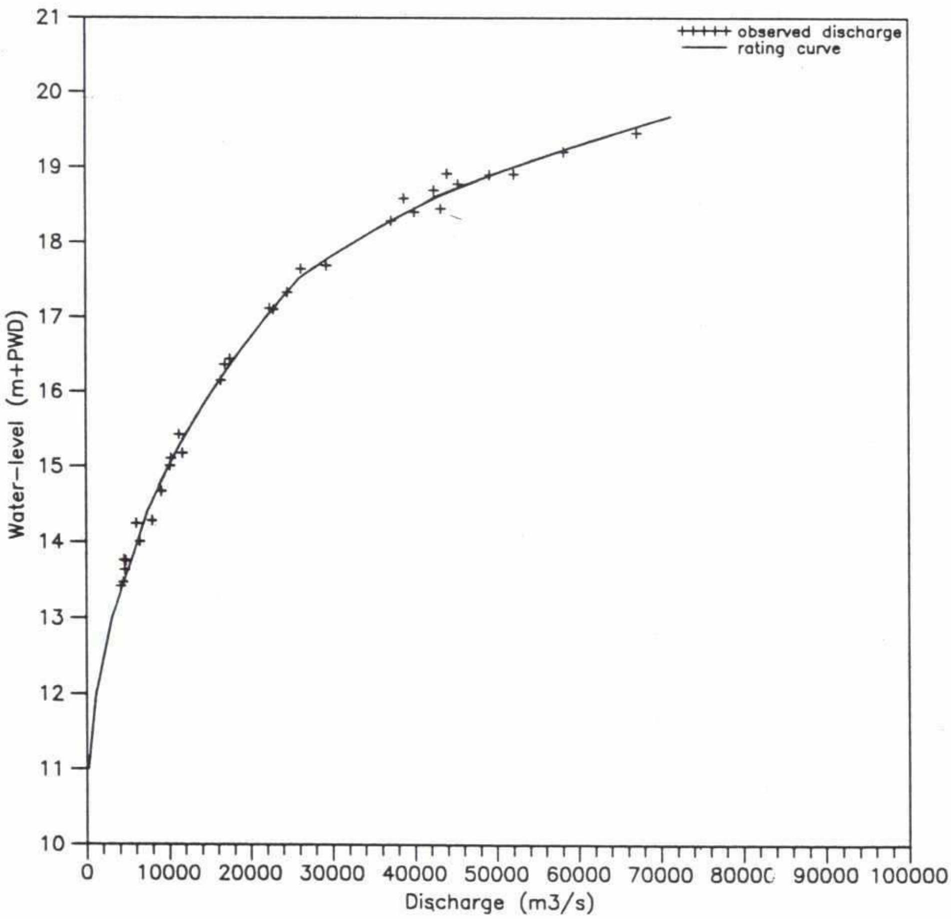

Figure 8.2: 1987 stage-discharge relationship of the Jamuna River at Bahadurabad

Accumulated volumes for 1987 were $387x10^9$ m^3 through the Ganges River at Hardinge Bridge, $688x10^9$ m^3 through the Jamuna River at Bahadurabad, and $966x10^9$ m^3 through the Padma River at Baruria. The water-balance indicated that 11 percent of the Padma discharge was shared by three distributaries: The Old Brahmaputra River, the Dhaleswari River, and the Gorai River. This exercise showed a reasonable water balance considering the unaccounted volumes for tributaries and distributaries, and the uncertainty ranges of these factors.

A similar exercise with BWDB suspended sand transport data showed some unrealistic results. In that case, sand transport rating curves were established with 1987 BWDB data. Twenty-four, 21, and 14 data points were established respectively for Bahadurabad, Hardinge Bridge, and Baruria stations. Using those rating curves, the sand volume was 55 million tons through the Jamuna River at Bahadurabad, 29 million tons through the Ganges River at Hardinge Bridge, and 95 million tons through the Padma River at Baruria. The total transport through the Ganges and the Jamuna was 84 million tons, a figure that was 11 million tons lower than the transport at Baruria. Such results indicated an unrealistic degradation of the system and led to the conclusion that, with respect to sediment gauging, the stations were not ideal.

Table 8.1 describes the status and importance of each station used by FAP24 as it relates to Bangladesh's overall water resources estimation.

Bahadurabad: Bahadurabad is a primary discharge and sediment transport measuring station in the Brahmaputra-Jamuna River. It is important for estimating water resources of the country, also in relation to cross-border flow. In the river's multiple channels, however, changes in planform occur rapidly, which makes it difficult to measure accurately. The station was covered both by FAP24 and BWDB.

Sirajganj: Sirajganj is a secondary network station for discharge and sediment measurements that was used to check the water and sediment balance of the Jamuna River. The current morphological condition of the river at Sirajganj makes it a suitable site for measurements. The station is not covered by BWDB.

Aricha: Aricha is a secondary network station for discharge, and sediment measurements. The station is not suitable for gauging due to its proximity to the Ganges-Jamuna Confluence.

Mymensingh: Mymensingh is a primary measurement network station for discharge and sediment transport measurements in the Old Brahmaputra River, one of the major distributaries of the Jamuna. The distributary occupies a course that the Jamuna abandoned two centuries ago and it holds an important position in the water resources of the northeast and north central regions. The transect near the Mymensingh Railway Bridge was an ideal measurement location. It was covered by both FAP24 and BWDB.

Tilly: Tilly is a discharge and sediment measuring station in the Dhaleswari River. It is a primary measurement network station. It is one of the Jamuna's major distributaries draining and supplying water to the north central region.

Hardinge Bridge: Hardinge Bridge is a primary discharge measuring station in the Ganges River used to monitor the cross-border flow through the Ganges River. The station is located in a constricted river bend and was found to be unacceptable for streamflow gauging. Relocation of the measuring site may be considered.

Kushtia Railway Bridge (Gorai Off-take): Kushtia Railway Bridge is a primary network station on the Gorai River — a right-bank distributary of the Ganges River. The river is important for drainage and for supplying fresh water to the southwest region.

Baruria: Baruria is a primary measurement station located in the Padma River. This station is not acceptable for stream gauging because it is affected by the confluence of the Ganges and the Jamuna, and by the river bend at the transect. Relocation of the measuring site may be considered.

Mawa: Mawa is a lower reach stream gauging station in the Padma River that experiences a seasonal tidal effect. This secondary station is important only to check Baruria's flow and the tidal effect on sedimentation and river morphology.

Arial Khan Off-take: The Arial Khan is a right bank distributary of the Padma River. This primary station located at the off-take is affected by seasonal tides. It is important for estimating water resources in the southwestern region and for monitoring of delta development.

Bhairab Bazar Railway Bridge: Bhairab Bazar is a primary discharge gauging station in the Upper Meghna River. The station is affected by seasonal tides. It is an important station for estimating water resources of the northeast region.

River System	River	Station	Network status	Remarks
Brahmaputra-Jamuna	Jamuna	Bahadurabad	Primary	Important for estimating water resources and cross-country flow through the river but difficult for gauging
		Sirajganj	Secondary	Present condition is good for gauging
		Aricha	Secondary	Too close to the Ganges-Jamuna confluence
	Old Brahmaputra	Mymensingh	Primary	Important for estimating water resources in NE and NC regions
	Dhaleswari	Tilly	Primary	Important for estimating water resources in the NC region
Ganges	Ganges	Hardinge Bridge	Primary	Important for estimating water resources and cross-country flow through the river
	Gorai	Kushtia Railway Bridge	Primary	Important for estimating water resources in the SW region and monitoring delta development
Padma	Padma	Baruria	Primary	Important for checking water-balance
		Mawa	Secondary	Seasonally tidal
	Arial Khan	Off-take	Primary	Seasonally tidal and important for estimating water resources in the SW region and monitoring delta development
Meghna	Upper Meghna	Bhairab Bazar Railway Bridge	Primary	Seasonally tidal and important for estimating water resources in the NE region

Table 8.1: Hydraulic measurements network in the main rivers of Bangladesh.
NE - northeastern region, NC - north-central region, SW - southwestern region

8.2 Optimization of frequency of measurements

When determining how often a measurement should be made, the variability of the physical parameters must be considered. In Bangladesh, the pronounced seasonality of the river stage and flow enhances the importance of the issue. Figure 8.3 shows a scheme in which the optimization process of measurement frequency is proposed.

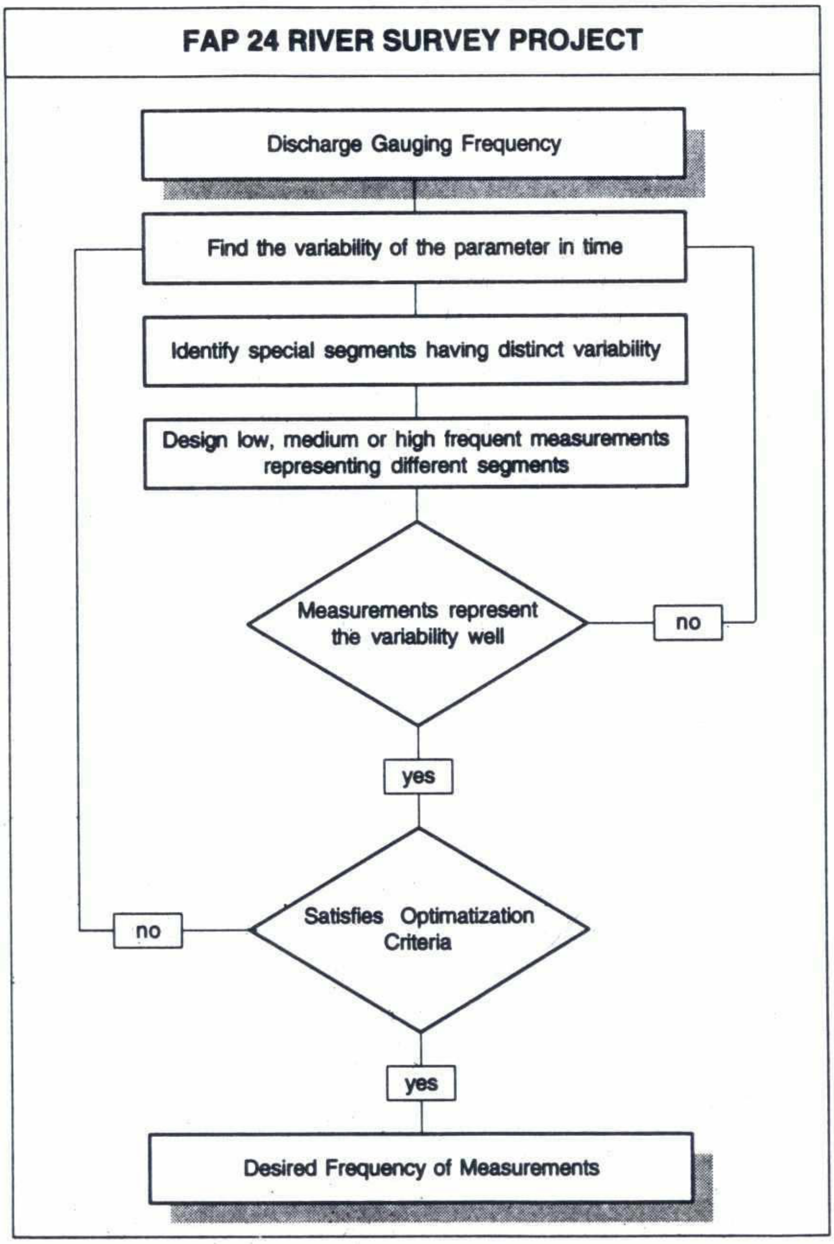

Figure 8.3: Optimization principle of the frequency of measurements

Essentially, the optimization process identifies the discontinuity and distinctness in the variability of the parameter being measured, and schematizes different segments so to avoid unnecessary measurements.

In this chapter, an attempt is made to identify distinct phases of the hydrograph that can be schematized for different measurement frequencies. This is necessary because stage-discharge relations and sediment rating curves have been found to depend on the phases of the hydrograph (Khan and Barua, 1995).

Figure 8.3 shows the steps to determine the optimization of frequency of measurements. The steps include examining the measurements' natural variability and screening them against optimization criteria.

Water-level and discharge hydrographs of major stations show some distinct segments representing the annual hydrograph. At first instance, a station can be characterised as tidal or non-tidal. Most of the RSP measuring stations are non-tidal except the Padma River station at Mawa, the Upper Meghna River station at Bhairab Bazar and the Arial Khan Offtake.

The variability of the different stations is summarized in Tables 8.2 and 8.3. Table 8.2 shows the variability status of non-tidal rivers where various phases of the hydrograph are identified. The rising limb of the hydrograph from March to June has been identified to consist of a slow rising part in March to May and a rapid rising part in June. The overall peak river stage from July to September has been identified as consisting of varying peaks in July-August to a very slow falling stage in September. Similarly, the falling river stage has been identified as consisting of a rapid falling limb in October and a slow falling limb in November-December. January and February represent a flat low river stage. Following these distinct phases of seasonal variability, measurement frequencies are suggested in Table 8.2. For flat low river stage, low-frequency (fortnightly) measurements are suggested, because little hydraulic or morphological action takes place during this stage. For slow rising and falling stages medium-frequency (weekly) measurements are suggested. For other river stages representing either rapid stages or peak stages a bi-weekly (every 4 days) measurements are suggested.

In this way, 60 to 70 measurements are indicated for each non-tidal station, enough to sufficiently develop or update a stage-discharge relationship or a sediment rating curve.

It should be noted that the measuring frequency schemes suggested in these tables are applicable only to routine measurements required for long-term data-base development. For any other purpose, such as special studies or research, a different scheme should be designed.

When many years of data indicate that a stage-discharge relation or a sediment rating curve is stable, a further optimization can be made by reducing the measurement frequency. However, episodic events, such as an unusual flood or an earthquake, should be given careful attention. The variability of rapid planform changes or bed-form developments in Bangladesh rivers indicate that rating relations should be continuously updated.

Phases	Variability Status	Months	Measuring Frequency
1	Slow rising	March-May	Medium (weekly)
2	Rapid rising	June	High (bi-weekly)
3	Varying peak	July-August	High (bi-weekly)
4	Very slow falling	September	High (bi-weekly)
5	Rapid falling	October	High (bi-weekly)
6	Slow falling	November-December	Medium (weekly)
7	Flat low	January-February	Low (fortnightly)

Table 8.2: Optimal routine hydraulic measurement frequency for non-tidal stations in the Bangladesh rivers obtained by considering the Jamuna River hydrograph at Bahadurabad.

For seasonally tidal stations, such as Mawa and Bhairab Bazar, a different scheme should be followed (Table 8.3). In these stations, a tidal variability is noticeable from December to April, so a different measurement scheme is shown in Table 8.3, incorporating weekly neap and spring tidal measurements from December to April. A tidal measurement should be made hourly during a full tidal cycle (preferably 26 hours). Establishing rating relations for such stations is difficult, but the residual flows should be related to both the river stage and the spring-neap tidal phases.

Phases	Variability Status	Months	Measuring Frequency
1	Nontidal slow rising	May	Medium (weekly)
2	Nontidal rapid rising	June	High (bi-weekly)
3	Nontidal varying peak	July-August	High (bi-weekly)
4	Nontidal very slow falling	September	High (bi-weekly)
5	Nontidal rapid falling	October	High (bi-weekly)
6	Nontidal slow falling	November	Medium (weekly)
7	Tidal	December-April	Spring-neap weekly tidal

Table 8.3: Optimal routine hydraulic measurements frequency for tidal stations at Mawa and. Bhairab Bazar and Arial Khan Off-take

8.3 Optimization of equipment and methods

A selected equipment and method should satisfy all the optimization criteria presented in Table 2.1. While it should have the lowest investment, operation and maintenance costs, the accuracy of the measurements should be at the desired level. It should also be operationally easy, have less maintenance requirements, time required for measurements should be least and the measuring parameters should be well-represented.

In the following analyses, some instruments have been included which were not applied by RSP, but which are used by different Bangladesh Organizations. This is done in order to extend the basis for fruitful and effective recommendations.

8.3.1 Instruments

A multi-criteria optimization analysis of different instruments is presented in Tables 8.4 to 8.7. Table 8.4 analyses positioning instruments. The results indicate that DGPS is optimal, the main advantages being accuracy, easy operation, short measurement duration, and low maintenance.

Table 8.5 presents a multi-criteria optimization of velocity measuring instruments; here, the ADCP is considered the optimal current measuring device. The main advantages of the ADCP are its accuracy, its expected representativity, and its resourcefulness in the complicated river systems of Bangladesh. Although this technology is new in Bangladesh, it is fast developing world-wide.

Table 8.6 analyses depth-measuring devices. As expected, the acoustic echosounder is the optimal solution.

Among water level gauging devices, the acoustic and pressure sensor systems are deemed optimal (Table 8.7). This is because of their advantages with respect to accuracy and operation, as compared with manual staff gauges.

Instrument	Cost x 2	Accuracy x 2	Operation x 1	Duration x 1	Main-tenance x 1	Represen-tativity x 1	Total
Sextant	6	2	1	1	3	n/a	13
Decca	2	4	2	2	2	n/a	12
DGPS	4	6	3	3	3	n/a	19

Table 8.4: Multi-criteria optimization analysis of positioning instruments

Instrument	Cost x 2	Accuracy x 2	Operation x 1	Duration x 1	Main-tenance x 1	Represen-tativity x 1	Total
ADCP	2	8	5	4	5	5	29
S4	4	8	2	3	4	4	25
EMF	6	8	2	3	4	3	26
Ott	8	4	4	2	3	2	23
Float	10	2	3	1	5	1	22

Table 8.5: Multi-criteria optimization analysis of velocity measuring instruments

Instrument	Cost x 2	Accuracy x 2	Operation x 1	Duration x 1	Main-tenance x 1	Represen-tativity x 1	Total
Rod-suspension	6	2	2	1	3	1	15
Cable suspension	6	2	2	1	3	1	15
Acoustic	2	6	3	3	2	3	19

Table 8.6: Multi-criteria optimization analysis of depth-measuring devices

Instrument	Cost x 2	Accuracy x 2	Operation x 1	Duration x 1	Main-tenance x 1	Represen-tativity x 1	Total
Auto-pressure	2	8	3	n/a	3	3	19
Auto-acoustic	2	8	4	n/a	3	3	20
Auto float-well	3	6	2	n/a	2	3	16
Manual staff gauge	8	2	1	n/a	1	1	13

Table 8.7: Multi-criteria optimization analysis of water level measuring devices

8.3.2 Measuring methods

Table 8.8 presents a multi-criteria optimization of discharge estimation methods. The ADCP-EMF moving boat method used by FAP24 proves optimal. This method is highly accurate, easy to operate, and has the shortest measurement duration. The traditional moving boat method (that samples only one point in the vertical) is less accurate and also more complicated to operate. The velocity-area method used by BWDB takes more time to complete and is complicated to operate.

Method	Cost x 2	Accuracy x 2	Operation x 1	Duration x 1	Main-tenance x 1	Represen-tativity x 1	Total
ADCP-EMF moving boat	2	6	3	3	n/a	n/a	14
Traditional moving boat	4	4	2	2	n/a	n/a	12
Velocity-area	4	4	1	1	n/a	n/a	10

Table 8.8: Multi-criteria optimization analysis of discharge estimation methods

9 Sustainability of hydraulic measurements

9.1 Evaluation basis

A survey technique is considered sustainable if it can be fully implemented for in-house application for its intended purpose by a certain institution in a certain context and a certain environment. A sustainable technique must satisfy the following six requirements: (see Table 9.1)

- the concerned institution can afford the investment
- the concerned institution has the capability to operate the technique and maintain the equipment
- technological compatibility for the technique exists in the country where it is implemented
- the technique provides optimal results
- the expected results and return justify the investment
- the technique is environmentally suitable

Among these criteria, the institutional capability and justification of results have been given double weight in the analysis. This is because equipment and methods cannot be sustained or even introduced until the institutional capability is developed. The capability includes training, human resource development, and capacity building. Also, the technique cannot be sustained unless the investment and operation and maintenance costs are in some way justified by the value of the results.

SUSTAINABILITY CRITERIA
1. Affordability of investment and O & M costs
2. Institutional capability in O & M
3. Technological compatibility
4. Optimal technique and survey results (see optimization criteria, chapter 2)
5. Justification of results against the incurred expenses
6. Suitability of the technique on environmental considerations

Table 9.1: Sustainability criteria for hydraulic measurements

9.2 Sustainability analysis

Tables 9.2 to 9.5 present multi-criteria sustainability scores of different categories of instruments, based on the evaluation criteria indicated in the previous section.

In this analysis, the sextant and the DGPS both emerge as sustainable positioning instruments (Table 9.2). The advantage of a sextant is its institutional capability requirements, while the advantage of DGPS is that it produces justifiable results. The propeller-type current meters were found to be the most sustainable velocity measuring devices, primarily because of their institutional capability requirements (Table 9.3). An acoustic system proved the most sustainable for depth measurements (Table 9.4). The acoustic system technology is already in use in Bangladesh and the institutional capability is adequate. The most sustainable water level gauge was the manual staff gauge, but other devices obtained an almost identical rank (Table 9.5). The velocity-area method for estimating discharge, as traditionally used by BWDB, was found sustainable. The method can be improved, however, by using sustainable DGPS and echosounders (Table 9.6).

Instrument	Afforda-bility x 1	Instit. capab. x 2	Techn. compat. x 1	Optimal technique x 1	Just. results x 2	Envir. suitable x 1	Total
Sextant	3	6	3	1	2	2	17
Decca	2	4	1	2	4	1	14
DGPS	1	4	2	3	6	1	17

Table 9.2: Multi-criteria sustainability scores of positioning instruments

Instrument	Afforda-bility x 1	Instit. capab. x 2	Techn. compat. x 1	Optimal technique x 1	Just. results x 2	Envir. suitable x 1	Total
ADCP	1	6	2	5	10	1	25
S4	3	6	2	3	8	1	23
EMF	2	6	2	4	8	1	23
Ott	4	10	5	2	6	3	30
Float	5	10	5	1	2	3	26

Table 9.3: Multi-criteria sustainability scores of velocity measuring instruments

Instrument	Afforda-bility x 1	Instit. capab. x 2	Techn. compat. x 1	Optimal technique x 1	Just. results x 2	Envir. suitable x 1	Total
Rod-suspension	3	6	3	1	2	3	18
Cable suspension	3	6	3	1	2	3	18
Acoustic	2	4	2	3	6	2	19

Table 9.4: Multi-criteria sustainability scores of depth measuring devices

Instrument	Afforda-bility x 1	Instit. capab. x 2	Techn. compat. x 1	Optimal technique x 1	Just. results x 2	Envir. suitable x 1	Total
Auto-pressure	1	4	2	3	8	1	19
Auto-acoustic	1	4	2	4	8	1	20
Auto float well	1	6	3	2	6	1	19
Manual staff gauge	3	8	4	1	2	2	20

Table 9.5: Multi-criteria sustainability scores of water level measuring devices

Method	Afforda-bility x 1	Instit. capab. x 2	Techn. compat. x 1	Optimal technique x 1	Just. results x 2	Envir. suitable x 1	Total
ADCP-EMF moving boat	1	2	1	3	2	1	10
Traditional moving boat	1	2	1	2	2	1	9
Velocity-area	3	6	3	1	4	2	19

Table 9.6: Multi-criteria sustainability scores of discharge measuring methods

10 Conclusions and recommendations

10.1 Optimal hydraulic measurements

The primary stations shown in Table 8.1 should get priority in data collection. Relocating some stations, however, such as Hardinge Bridge and Baruria, should be considered for hydrometric reasons. The Bahadurabad gauging station would be more suitably relocated upstream of the current site. Any relocation efforts should be considered against the changes that would occur with BWDB's long-term data-base.

The seasonal measurement frequency should reflect the discharge variability. Seven seasonal phases are recognized at nontidal stations, and bi-weekly, weekly, or fortnightly measurements are recommended (Table 8.2). Measurements taken at tidal stations should follow the recommendations presented in Table 8.3. No justification was found for measuring more frequently as is often done by BWDB at some stations. Once stable relations have been demonstrated, the measurement frequency can be further reduced.

The optimization analyses identified the DGPS as the optimal positioning system, the ADCP proved the best for velocity, echosounders were optimal for depth measurements, digital auto-acoustic and pressure-type AWLRs were optimal for water level measurements, and an ADCP-EMF moving boat method was the best for discharge gauging. (see Table 10.1)

Items	Optimal Instruments and Methods
Positioning	DGPS
Velocity measurements	ADCP
Depth-measurements	Acoustic (Echosounders)
Water level observation	Auto-acoustic/pressure type
Discharge estimation method	ADCP-EMF moving boat method

Table 10.1: Optimal instruments and methods - summary of optimization scores from Tables 9.2 to 9.6

10.2 Sustainable survey techniques

Table 10.2 gives a summary of the sustainability ranking made in section 9.2. This ranking is made on a wider basis than the optimization ranking, from which it is seen to differ. In accordance with the underlying evaluation criteria, the sustainability analysis favours technology that is already implemented in Bangladesh, or which is at least well compatible with such technology.

Items	Sustainable instruments and methods
Positioning	Sextant and DGPS
Velocity measurements	Propeller-type
Depth-measurements	Acoustic (echosounders)
Water level observation	Manual staff-gauge
Discharge estimation method	Velocity-area method

Table 10.2: Sustainable instruments and methods - summary of sustainability scores from Tables 20 to 24

10.3 Recommendations

The experience of FAP24 indicates the following recommendations on hydraulic measurements:

- The human factor is an important consideration of river surveying. A sophisticated and high-tech method can appear as auspicious, but can fail if the equipment and method are not applied correctly. Therefore, human resources development through training should be a fundamental component within any survey capability development
- A survey vessel, with its facilities, can be decisive to the failure or success of hydraulic measurements. Therefore, careful consideration should be given to vessel selection
- Accurate gauging of hydraulic parameters is critical at the primary gauging stations. If this is not possible, serious consideration should be given to relocating the station
- Discharge measurements should be made bi-weekly, weekly, or fortnightly, depending on the different phases of the hydrograph
- A DGPS positioning system should be pursued. This technique is developing quickly and provides a better accuracy and easier operation as compared with sextant or Decca positioning
- Although propeller-type current meters are found to be sustainable, other instruments are developing quickly and should be considered for future implementation
- The traditional acoustic-type echo sounder should be maintained for depth measurements
- Although manual staff gauges were found to be sustainable, other devices that provide a better accuracy should be considered
- The velocity-area discharge estimation method although was found generally suitable, it needs improved instrumentation, and a potential for optimization of the procedure has been identified. Also, a cost-effective application of the ADCP-EMF moving boat method can be sustainable under similar circumstances

References

Bangladesh Water Development Board (BWDB), 1982. Water Supply paper 1

Carter, R.W. and Anderson, I.E., 1963. Accuracy of current meter measurements. Jr. Hydr. Divn., HY4 (1), 105-115

Chen, Cheng-Lung, 1991. Unified theory on power laws for flow resistance. Jr. Hydraul. Divn., 117(3), 371-389

Delft Hydraulics, 1990. Network Optimization, part I and II. The Mekong Secretariat

Delft Hydraulics, 1992. User's manual for four quadrant electro-magnetic liquid velocity meter.

El-Haddi, K., 1990. Velocity measurements by floats and float diffusion. M.Sc. Thesis, University of Ottawa

Food And Agricultural Organization (FAO), 1969. Second hydrological survey in East Pakistan, sediment investigations

Fletcher, R., 1987. Practical methods of optimization. Wiley, Chichester, 436 pp

Gordon, L. and Bornhoft, J., 1991. Broadband ADCP discharge demonstration tests. RD Instruments

Hayes, F. Ch., 1978. Guidance for hydrographic and hydrometric surveys. Delft Hydraulics Publ. 200

International Standard Organization (ISO), 1983. Measurement of liquid flow in open channels. ISO standard handbook 16, Switzerland

InterOcean Systems, 1990. S4 current meter user's manual

INTERCONSULT, 1991. Determination of standard low water and standard high water levels in Bangladesh, vol. II of II: Technical Report, Bangladesh Inland Water Transport Authority

Jepsen, P., 1967. Current meter errors under pulsating flow conditions. Jr. Mechanical Engg. Science, 9, 45-54

Khan, Z.H. and Barua, D.K., 1995. Seasonal variation of certain hydraulic parameters of the Ganges River. Annul. Cov. Inst. Engg., 39th, Chittagong

Liu, H., and Martin, L.D., 1968. Analysis of integrating-float measurements at low velocities. Jr. Hydraulic Divn, ASCE, 94(HY5), 1245-1260

Mueller, A., 1989. Levels of velocity data collection in open channel flows. Proc. HYDROCOMP '89, Dubrovnik, Yugoslavia

Peters, J.J., 1993a. Morphological studies and data needs. Proc. International workshop on morphological behaviour of the major rivers in Bangladesh, Dhaka, Bangladesh

Peters, J.J., 1993b. Comments on FAP24 Phase 1 Hydrology Report

Peters, J.J., 1994. Report on mission Project Advisor. Seventh mission report. May 09 to June 03.

Peters, J.J., 1995. Report on mission Project Advisor. Tenth Mission report, March 8 to April 8.

Peters, J.J. and Goldberg, A., 1989. Flow data in large alluvial rivers. Proc. Conf. on Computational modelling and experimental methods in hydraulics, Dubrovnik, Yogoslavia

RD Instruments, 1989. Acoustic Doppler Current Profilers - principles of operation: a practical primer. RD Instruments, San Diego, California

River Survey Project (RSP), 1991a. Technical Speceifications and Bill of Quantities (ALA/90/04).

River Survey Project (RSP), 1991b. Technical Proposal. vol. I Text, vol. II Annexes

River Survey Project (RSP), 1993a. 1° Interim Report, vol. II, Annexures on survey work

River Survey Project (RSP), 1993b. Hydrological Study, phase 1

River Survey Project (RSP), 1993c. Test Ganging Report

River Survey Project (RSP), 1993d. Selection of Survey Techiques

River Survey Project (RSP), 1994. Morphological studies phase 1, available data and characteristics, RSP study report 3

River Survey Project (RSP), 1995. Water level gauging stations. RSP Special Report 2

River Survey Project (RSP), 1996a. Stage-discharge relationship at Bahadurabad RSP Special Report 4.

River Survey Project (RSP), 1996b. Bathymetric surveys. RSP Special Report 3

River Survey Project (RSP), 1996c. Joint BWDB-FAP24 measurements. RSP Special Report 19.

Sauer, V.B. and Meyer, R.W., 1992. Determination of error in individual discharge measurements. USGS open-file report 92-144

Tajeda-Guibent, J.A, 1994. Tidal discharge quantification in rivers of Bangladesh: station 273 Bhairab Bazar at Surma-Meghna River, BWDB.

Urik, R.J., 1975. Principles of underwater sound. McGraw-Hill, New York, 384 pp

World Meteorological Organization (WMO), 1994. Guide to hydrological practices - data collection and processing, analysis, forecasting and other practices, WMO No. 168, 5th Ed., Geneva, Switzerland

Special Report 11, Annexure A

Turbulent Flow Structure and Optimal Measuring Time

October 1996

Contents

69

Figures

Tables

88

1 Introduction

Turbulence is a usual characteristic of natural flows. Turbulence is caused by flow instabilities, generated by the shear action between fluid layers moving at different speeds and by bottom and wind friction. A multitude of eddies is formed having various sizes, l. In rivers, the sizes of the eddies range from the Kolmogorov scale (ν/v_*) to a flow thickness equal to the water depth, h.

$$\frac{\nu}{v_*} \leq l \leq h \qquad \ldots\ldots\ldots\ldots (1)$$

where
ν = kinematic viscosity
v_* = bed-friction velocity

Since the fluctuating velocities of all eddies have comparable magnitudes, their typical times or periods are different (Yalin, 1992). Therefore, the periods of different eddies can have the following ranges:

$$\frac{\alpha\,[\frac{\nu}{v_*}]}{v_f} \leq T \leq \frac{\beta h}{v_f} \qquad \ldots\ldots\ldots\ldots (2)$$

where
v_f = free stream velocity
α and β = constants; β varies between 3 to 7 with a mean of about 6

This time-scale was originally proposed by Rao et al. (1971) for representing vertical turbulent eddies which move across the horizontal x (stream wise), y (span wise) plane. The higher ranges represent macro time-scale vortices.

In open channel flows eddies also form whose axes are perpendicular to the x, z (vertical) plane (Yokosi, 1967). The time-scales of these horizontal turbulences are calculated as follows (Yalin, 1992):

$$T = \frac{6B}{v_f} \qquad \ldots\ldots\ldots\ldots (3)$$

Where B = flow width

Yokosi (1967) found a coefficient of 9 based on measurements in the Uji River. In sampling a flow-velocity, it is required that the exposure time of the current meter covers the dominant time-scales so that a representative mean-flow field can be sampled. The purpose of this is to reduce the pulsation error resulting from the turbulent flow field (Sauer and Meyer, 1992). This error is known as *Type I Error* (ISO, 1983). Studies by Carter and Anderson (1963) confirm that the standard pulsation error is reduced as the exposure time is increased. Their studies indicate that at 60% water depth, the standard error (ϵ) is related to the exposure time (τ) as,

$$\epsilon = 16.6\tau^{-0.28} \qquad \ldots\ldots\ldots\ldots (4)$$

The standard error is defined as a percentage and the exposure time is measured in seconds. This relation indicates that with a 50 s exposure time, the standard error is 5.6%. For the same exposure time, the standard error increases as the water-depth increases. The reason is attributed to the variable magnitudes of turbulence intensity which is usually higher near the bed than the surface (the turbulence intensity is defined as the root mean square value of the fluctuation about the mean). Different international bodies on standardization have suggested different exposure times. ISO (1983) recommended a measurement period of about 60 s. According to World Meteorological Organization (WMO, 1980), flow velocities should cover a "short time period;" 50 - 100 s is usually the time period suggested.

The objectives of this Annexure are

- to investigate the spectrum of flow frequencies existing at different water depths based on measurements in the Ganges and Jamuna Rivers (Figure A.1)
- to indicate the pulsation errors that can occur at different exposure times

This study used flow data collected by electronic sensors, the Acoustic Doppler Current Profiler (ADCP), and the Electro-magnetic Flow (EMF) meter. These sensors were assembled by the River Survey Project for surveying in Bangladesh rivers.

In order to see the deterministic periodic component from the spectra of turbulence, time-series analyses were done in the frequency domain. The result gives a multitude of eddy time-scales. Computed time-scales were grouped to show the frequency of occurrence. Standard pulsation errors were calculated for different exposure times of the sensor. Based on such analyses, an optimum averaging time was suggested. The information derived in this way was used for the optimization of hydraulic measurements, specifically in the selection of equipment and method.

In Annexure B, different turbulent parameters, especially using the longstream velocity components, are discussed in detail.

2 Instruments and field measurements

2.1 Acoustic Doppler Current Profiler

An Acoustic Doppler Current profiler (ADCP) measures the flow velocity utilizing the Doppler effect principle (Urik, 1975). Mathematically, each ADCP beam is measured as follows (RD Instruments, 1989),

$$F_D = 2F_s\left(\frac{V}{C}\right)\cos A \qquad \ldots\ldots\ldots\ldots(5)$$

where
F_D = Doppler frequency shift
F_s = frequency of the sound when everything is still (transmitted frequency)
V = relative velocity between the sound source and the sound receiver
C = speed of the sound wave
A = angle between the relative velocity vector and the acoustic beam

The relative velocity V is computed from the measured F_D, angle A, and the known F and C. If the velocity of the vessel is known either from bottom track or from DGPS positioning, the velocity of the scatterers can be computed. The backscatterers are suspended sediments, zooplankton, and detritus. In this way, one velocity component is measured with each beam. With 3-beam ADCP, three velocity components, u, v, and w, are measured. However, the set-up implemented in FAP24 vessels utilizes 4-beams to measure velocity and to compensate for errors.

The ADCP sends pulses along each of its four beams which are positioned 90° apart horizontally and directed downward into the water column at an angle of 20° from the vertical (Figure A.2). Part of the transmitted acoustic energy is reflected back toward the transducers by particulate matter (scatterers) moving with the water. The ADCP samples reflected signals from each beam at discrete time intervals during the progress of the advancing acoustic wave front; this allows velocities to be determined at each of the depth-intervals or bins. The ADCP can transmit and acquire acoustic data and calculate water velocity for each depth bin at a rate of up to 10 profile measurements (pings) per second.

The 300 kHz ADCP installed on board DHA was used for the measurements. In this ADCP, the bin height is 0.5 m, and 10 pings (profiles) were taken in a period of 5 to 6 s. The first bin is located approximately 2.8 m below the surface, and the last bin is located at 94% of the total depth. The average of 10 pings was calculated at about 5 to 6 s intervals. The standard deviation of the acquired velocity was 30 cm/s per ping; it was reduced to 9.5 cm/s for the time-averaged situation of 10 pings. The data obtained, therefore, were vertically averaged over 0.5 m and time-averaged over 5-6 s.

Rotation and translation of the ADCP were measured by different devices. Heading rotation was measured by a gyro compass, and pitch and roll rotation were measured inside the ADCP electronically. The movement of the instrument over the river bed was measured on-line by bottom tracking. In high sediment transports during the monsoon, bottom tracking results in underestimating the flow velocities. In those case, data were corrected off-line using Differential Global Positioning System (DGPS).

22

2.2 Electro-magnetic flow meter

The electro-magnetic flow meter, designed by Delft Hydraulics (Delft Hydraulics, 1990), is a small (~40 mm dia), light-weight electronic sensor employing Faraday's Induction Law. According to this law, the electro-magnetic induction voltage is directly proportional to the current velocity of the conductor:

$$E = \psi I v \qquad \text{..........} (6)$$

where

E = electromotive force
I = magnetic field intensity
v = flow velocity
ψ = a factor

A magnetic field is generated by a pulsed current meter through a small coil inside the body of the sensor. Two pairs of diametrically opposed platinum electrodes sense the voltage produced by the flow past the sensor. The sensors have been designed so that the voltages are proportional to the horizontal orthogonal components of the velocity vector at the plane of the electrode. The accuracy of the instrument is ± 0.5 cm/s. The device has been used in various field and laboratory applications. For example, Uittenbogaard (1995) used the instrument to determine the importance of internal waves for mixing in estuarine flow.

The sensor is deployed 0.5 m below the surface with a registration interval of 10 s.

2.3 Data collection

The measurements were taken by the FAP24 survey vessel, DHA, in Jamuna River near Bahadurabad and in the Ganges-Jamuna confluence near Aricha. The measurement locations are shown in Figures A.3 and A.4. At stations B1 and B2 (Figure A.3), measurements were taken on 1 April 1994; the durations of the records were 54 minutes and 33 minutes respectively (Table A.1). On 13 August 1994, another measurement was taken at station B3. Measurements at station B3 were taken near a dune field during a period of approximately 2 hours and 7 minutes. At the Ganges-Jamuna confluence near Aricha, the measurements were taken at stations G1, G2, and G3 on 13 April 1994. At station G1, measurements were taken for about 45 minutes. Figure A.5 shows the river stage during which the measurements were executed. The April measurements were taken during a seasonal rising river stage which occurred just after a small and short-duration peak. In contrast, the August measurements were taken when the river was at a higher stage during the rising limb of a short peak.

The measurements were taken from a vessel that was moored by one bow anchor. Therefore, oscillation of the vessel occurred during the recordings. The position of the vessel was determined by DGPS. In its stationary mode, the system has a standard oscillation of about ± 3 m. However, spurious signals are often observed. The ADCP and the DGPS antennas are located at the middle of the 20 m long DHA vessel. The EMF is located at the bow, approximately 7 m away from the DGPS antenna.

Trackplotting of the time-series of vessel positions are shown in Figures A.6 to A.11 for various stations. During the measurements at station B1, the oscillation of the vessel (Figure A.6) was within a region of about 32 m^2 (8 m in the Easting direction and 4 m in the Northing direction). Similarly, measurements at station B (Figure A.7) oscillated in a 60 m^2 area (10 m in the Easting direction and 6 m in the Northing direction). At station G1, the oscillation of the vessel (Figure A.8) was in an area of about 10 m^2 (5 m in the Easting direction and 2 m in the Northing direction). At stations G2, G3, and B3, the oscillations were much more erratic and extensive (Figures A.9, A.10, and A.11). Station G3 is located in a confluence scour hole location. Of these measurements, data collected from stations G2 and G3 were discontinuous and could not be used for analyses because of frequent ferry traffic which disturbed the turbulent flow field.

Figures A.6 through A.11 show the plotted vessel position oscillations which reflect both the actual oscillation of the vessel around the bow anchor and the oscillation of the DGPS signal. The implication of using these data for time-series analyses is that it assumes the flow field to be homogenous within the zone of oscillation. Another important consideration is that the ADCP beams spread downward (Figure A.2) at an angle of 20°. This implies that at 10 m water depth the horizontal spread is about 7 m and the flow is sampled from a zone of 7 X 7 m. The ADCP implicitly assumes that the flow is homogeneous within that region.

Station	River	Date	Sensor	Total depth	Duration
B1	Jamuna River at Bahadurabad	1 APR 1994	ADCP	9.6 m	54 min
B2			ADCP	8.3 m	33 min
B3		13 AUG 1994	ADCP	10.0 m	127 min
B3			EMF	10.0 m	127 min
G1	Jamuna River at the confluence	13 APR 1994	ADCP	4.1 m	45 min

Table A.1: Dates, total depths and durations of turbulence measurements at different stations in the Jamuna River

3 Analyses and results

3.1 Time-series analyses

Autocorrelation and spectral analysis techniques were used to perform time-series analyses on the collected data. In auto-correlation, the entire sequence of data is compared to itself at all possible positions. This is done by computing the auto-correlation function, which is defined as the linear correlation between a time-series and the same time-series at a later time. The offset between the two series being compared is called the time-lag. A diagram showing the relation between the autocorrelation function and time-lag is known as a correlogram.

In order to examine the turbulence structure of measured flow velocity, the HYMOS data-base software package (Delft Hydraulics, 1992) was used to obtain auto-correlation function and spectral density. This program is able to handle 400 equidistant time-series data. For the time-series data, x_i (i = 1, N), the auto-covariance function at time-lag k is given by,

$$c_{xx}(k) = \frac{1}{N}\sum_{i=1}^{N-k} (x_i - m_x)(x_{i+k} - m_x) \qquad \text{..........}(7)$$

where
m_x = average of x_i, i = 1, N
k = time-lag in time units equal to the time interval maximum up to L_{max}
L_{max} = maximum time-lag < N/2 (limited to 100 in HYMOS)
N = number of data

The auto-correlation function is defined as:

$$r_{xx}(k) = c_{xx}(k)/c_{xx}(0) \qquad \text{.........}(8)$$

The smoothed auto-spectral estimate for f = 0 to 1/2 is defined as:

$$C_{xx}(f) = 2\left[c_{xx}(0) + 2\sum_{k=1}^{M-1} c_{xx}(k)\, w(k) \cos(2\pi f k)\right] \qquad \text{..........}(9)$$

The spectral density function is defined as:

$$S_{xx}(f) = C_{xx}(f)/c_{xx}(0) \qquad \text{..........}(10)$$

where

f = frequency in cycles per unit time interval (computed at spacings $1/2N_f$, where N_f is 2 to 3 times M)
N_f = number of frequency points
M = truncation point or maximum lag of the autocovariance function. M ¾ L_{max}

Since the time-interval is approximately 5.5 s, the Nyquist frequency is 1/2*6 = 0.09. A resolution below this frequency representing a time-scale of 11 s is not possible.

The recorded bins and pings collected at the different stations add up to a large amount of digital data. The data selected for the analyses included one set from near the surface and one from near the bottom. The near-surface data were taken from the first bin which occurred at 2.8 m water-depth. The near-bottom data were taken at different depths, usually between 88 and 93% of the total depth (Table A.2). With reference to Figure A.2, the velocity record is not available in the near bed zone below about 94% of the total depth.

Due to a limitation of the HYMOS software, only 40 minutes of the data that were recorded were analyzed.

3.2 Results

3.2.1 Velocity

Table A.2 shows time-mean velocities at different stations; some velocity profiles are shown with the effect of averaging. The time-mean components of two orthogonal velocities and their vector azimuths are shown at different depths. Time-mean values were obtained by averaging the time-series data for the entire recorded period. Easting and Northing velocities recorded at these stations are shown in Figures A.12 to A.20. Near-surface time-mean velocities are about 1.3 m/s at all three stations, B1, B2, and G1, during the April 1994 measurements. During the August measurements, the velocity was about 2 m/s at station B3. In the Jamuna River stations near Bahadurabad, the flow was almost southward; at station G1, however, the flow was southeastward.

Figures A.21 through A.24 show the nature of ADCP pings and the effect of averaging. The square data points in these figures represent 10-ping ADCP averages at specified times and the triangular points represent averages of 11 sets of 10 pings. Averaging irregular data can result in overestimates or underestimates of the velocity. A deformity of the velocity profile is noticeable at station B1. At other stations, the profiles are fairly smooth.

Station	Meas. depth (m)	Percent of depth	*Easting velocity (m/s)	*Northing velocity (m/s)	*Velocity vector (m/s)	Vector azimuth (°)
B1	2.8	29	0.29	-1.30	1.33	167
B1	8.8	92	0.07	-0.76	0.76	175
B2	2.8	34	-0.06	-1.25	1.25	183
B2	7.3	88	-0.05	-0.84	0.84	183
G1	2.8	68	0.73	-0.73	1.03	135
G1	3.8	93	0.62	-0.64	0.89	136
B3	2.8	28	-0.30	-1.76	1.79	190
B3	8.8	88	-0.22	-1.36	1.38	189
B3	0.5	5	-0.30	-2.00	2.02	189

* indicates time-mean values

Table A.2: Time-mean Easting, Northing and vector velocities and directions at different depths in the Jamuna River measuring stations

2a

3.2.2 Frequency spectrum

Figures A.12 to A.20 show the spectral densities of Northing and Easting velocities for different depths at different stations. Figure A.12 shows the spectral densities at station B1 at a water depth of 2.8 m. The spectral density indicating the power of the signal has a maximum of about 5 for both the Easting and the Northing. Figure A.13 shows the densities for the same station at a water depth of 8.8 m. Here, the maximum spectral power was about 3 for Easting and 5.5 for Northing. In both cases, the low frequency events have a higher spectral power than the high frequency events.

Figures A.14 and A.15 show the spectral densities of Easting and Northing velocity at B2 at water depths of 2.8 m and 7.3 m respectively. At a water depth of 2.8 m, the maximum spectral power is about 5, but at a depth of 7.3 m, the spectral power is more than 13 in the Northing. In the Easting at a depth of 2.8 m, the spectral power is higher for high frequency events.

Similarly, Figures A.16 and A.17 show the spectral densities for Easting and Northing velocities at station G1 at depths of 2.8 m and 3.8 m, respectively. In all cases, spectral densities of various events are of comparable magnitudes. Both high and low frequency events have similar power distributions. The similarity is probably due to the closeness of the two bins. This profile also indicates the limitation of ADCP application in shallow water.

Figure A.18 shows the EMF velocity time series data at a water depth of 0.5 m together with the spectral densities. Maximum spectral power of the Northing velocity is about 16; this is nearly twice that of the Easting. The Northing spectral density shows almost a line spectrum. The dominant low frequency event has a time-scale of about 1000 s (16 minutes and 40 seconds).

Similar ADCP time-series of velocities and spectral densities are shown in Figures A.19 and A.20. In all cases, the spectral powers of low frequency events are dominant.

Figures A.21 through A.24 show the ADCP profiles (with an average of 10 pings) at specific times. The profiles were modified by averaging 11 such profiles.

Figure A.25 shows the summary of occurrence of different time-scale eddies in the Easting direction. Approximately 42% of turbulent events have a time-scale of less than about 30 s. The minimum period observed was about 12.5 s. 13% of the events had a time-scale greater than about 2 minutes. The maximum time-scale observed was about 5 minutes and 33 seconds. Figure A.26 shows the summary of these occurrences for the Northing. In this case, 43% of the events were less than about 30 s. The minimum period observed was about 12.2 s, and the maximum period observed was about 16 minutes and 40 seconds. Yokosi (1967) measured a maximum time-period of 14 minutes in the Uji River. The frequency distributions are almost identical in both orthogonal directions. Figure A.27 combines the Northing and Easting events.

3.2.3 Turbulence intensity

Figures A.28 through A.32 show the turbulence intensities at different depths for different stations as a function of data used for averaging.

Three things are noticeable from the graphs. First, the averaging time applied for minimizing instrumental errors can not be applied for obtaining turbulence intensity. In most cases, the turbulence intensities stabilize at 100 or more (~ 10 minutes) data averages. Averaging of turbulence intensities using a longer time does not change the value appreciably. Second, the turbulence intensities are higher near the bed than near the surface. Table A.3 indicates that while the near surface intensities vary within about 0.07 and 0.16 m/s, the near bottom turbulence intensities vary within 0.11 and 0.19 m/s. Third, the turbulence intensity can be compared with the overall bed shear velocity. Assuming a river-bed slope of about 7×10^{-5} and a depth of 10 m for the Jamuna River, the mean bed shear velocity is about 0.08 m/s. It can be seen that the turbulence intensity is 1 to 2.5 times the bed-shear velocity.

Station	Date	Depth (m)	Turbulence intensity, Easting (m/s)	Turbulence intensity, Northing (m/s)
B1	1 APR 94	2.8	0.13	0.13
B1	1 APR 94	8.8	0.18	0.14
B2	1 APR 94	2.8	0.13	0.13
B2	1 APR 94	8.8	0.14	0.18
G1	13 APR 94	2.8	0.11	0.11
G1	13 APR 94	3.8	0.12	0.11
B3	13 AUG 94	0.5	0.07	0.10
B3	13 AUG 94	2.8	0.13	0.16
B3	13 AUG 94	8.8	0.15	0.19

Table A.3: Turbulence intensities of Easting and Northing velocities for different stations at different depths

3.2.4 Standard pulsation errors

Standard pulsation errors are computed as the relative standard deviation in percentage. These errors represent an error within a confidence level of 67%.

Figure A.33 shows the standard errors as a function of exposure time for station B1. This was done for the orthogonal velocity components (Easting and Northing), and for the velocity vector. For a given exposure time, there is a higher error near the bottom than near the surface, particularly for Northings and vectors. The following equations can be fitted:

At 2.8m $\epsilon_e = 761\tau^{-0.92}$ ....(11)

At 8.8m $\epsilon_e = 954\tau^{-0.68}$ ....(12)

At 2.8m $\epsilon_n = 172\tau^{-0.77}$ ....(13)

At 8.8m $\epsilon_n = 422\tau^{-0.92}$ ....(14)

At 2.8m $\epsilon_v = 180\tau^{-0.79}$ ....(15)

At 8.8m $\epsilon_v = 645\tau^{-1.0}$ ....(16)

ঐ

Figure A.34 shows the errors for station B2. In all cases at this station there is a greater error near the bottom than near the surface. The following equations can be fitted to the curves:

At 2.8m $\epsilon_e = 11414\tau^{-1.17}$ ....(17)

At 7.3m $\epsilon_e = 684\tau^{-0.52}$ ....(18)

At 2.8m $\epsilon_n = 64\tau^{-0.65}$ ....(19)

At 7.3m $\epsilon_n = 19\tau^{-0.17}$ ....(20)

At 2.8m $\epsilon_v = 77\tau^{-0.96}$ ....(21)

At 7.3m $\epsilon_v = 19\tau^{-0.17}$ ....(22)

Figure A.35 shows the turbulence intensity at station G1. Here, the depths of measurements are closer, and therefore, hardly any difference in error occurs. The following equations can be fitted:

At 2.8m $\epsilon_e = 139\tau^{-0.69}$ ....(23)

At 3.8m $\epsilon_e = 290\tau^{-1.32}$ ....(24)

At 2.8m $\epsilon_n = 81\tau^{-0.69}$ ....(25)

At 3.8m $\epsilon_n = 1959\tau^{-1.29}$ ....(26)

At 2.8m $\epsilon_v = 41\tau^{-0.55}$ ....(27)

At 3.8m $\epsilon_v = 2538\tau^{-1.37}$ ....(28)

Figure A.36 shows the errors at station B3 at a water depth of 0.5. The following equations can be fitted:

At 0.5m $\epsilon_e = 958\tau^{-0.81}$ ....(29)

At 0.5m $\epsilon_n = 27\tau^{-0.44}$ ....(30)

At 0.5m $\epsilon_v = 26\tau^{-0.44}$ ....(31)

Figure A.37 shows the errors at station B3. Here, in all the cases, the standard error is higher for situations near the bottom. The following equations can be fitted:

At 2.8m $\epsilon_e = 108\tau^{-0.25}$ ....(32)

At 8.8m $\epsilon_e = 214\tau^{-0.35}$ ....(33)

At 2.8m $\epsilon_n = 31\tau^{-0.37}$ ....(34)

At 8.8m $\epsilon_n = 191\tau^{-0.52}$ ....(35)

At 2.8m $\epsilon_v = 21\tau^{-0.30}$ ....(36)

At 8.8m $\epsilon_v = 158\tau^{-0.48}$ ....(37)

In all cases, the symbols represent the following:

ϵ = standard error
τ = exposure time
subscript e = Easting
subscript n = Northing
subscript v = vector

The above standard error equations for velocity vectors can be summarized giving an average picture of the situation. At a water depth of 2.8 m, which represents 28 to 68% of the total depths, the error for velocity vectors is:

$\epsilon_v = 80\tau^{-0.65}$ ....(38)

Near the bottom, which represents about 88 to 93% of the total water depths, the error for velocity vectors is:

$\epsilon_v = 269\tau^{-0.76}$ ....(39)

3.2.5 Optimum averaging time

The standard error analyses indicate that as exposure times are increased, the errors decrease. Table A.4 shows the errors at different exposure times. With 50 s averaging time, there can be 5 to 14% error. As the exposure time is increased to 100 s, errors are reduced to 3 to 8%.

Fraction of depth, h	Standard error at 50 s exposure time	Standard error at 100 s exposure time
5% h	± 4.7%	± 3.4%
[$]28% - 68% h	± 6.3%	± 4.0%
[&]88% - 93% h	± 13.8%	± 8.1%

Equation 31 is used
[$]Equation 38 is used
[&]Equation 39 is used

Table A.4: Standard errors at 50 s and 100 s exposure times at different water depths

An optimum averaging time should have an exposure time several times longer than the dominant turbulence time-scales. These are about 20 to 30 s. Two of these time-scales are covered at a 50 s exposure time; four are covered at 100 s averaging. In general, an optimum averaging time should be set at an acceptable level of accuracy. The accuracy is increased as the exposure time is increased. Using a longer exposure time, however, will increase the required time for doing the measurements, or the number of vessels required for making a full transect in a reasonably short time as compared with the fluctuations of the cross-section average flow. This, in turn, means higher measurement costs.

4 Discussion

The pulsation error equation derived from this study's measurements is different from Carter and Anderson's equation 4 (1963). For a given exposure time, equation 4 results in a lower estimate of the error.

Errors in discharge estimates depend on the velocity estimates. On a river of width b, a mean depth h, and a depth-mean velocity u perpendicular to a transect, the discharge is given as

$$q=uhb \qquad \ldots\ldots\ldots\ldots (40)$$

The error analyses of this relation is given as

$$\left(\frac{\sigma_q}{q}\right)^2 = \left(\frac{\sigma_u}{u}\right)^2+\left(\frac{\sigma_h}{h}\right)^2+\left(\frac{\sigma_b}{b}\right)^2 \qquad \ldots\ldots\ldots\ldots (41)$$

Errors in velocity estimation at a single point comprise errors from several sources, such as

- systematic errors of the instrument
- random sampling errors
- pulsation errors

In addition, depth-mean velocity estimation is influenced by computational errors.

With typical depth and width estimation errors of 0.05 (Van Rijn and Schaafsma, 1986), Figure A.38 is constructed using equation 41. It shows that even with no error in the velocity estimation, there can be a 7% error in discharge estimation. A 10% error in the velocity gives a discharge estimation error of about 14%. Similarly, for a 5% pulsation error, the discharge error is about 9%.

Equation 2 indicates that the maximum vertical turbulence time-scale can be in the order of 30 to 60 s for a water depth of 10 m and a free-stream velocity range of 1 to 2 m/s. Figures A.25 and A.26 indicate that events at this time-scale occur for about 70% of the cases. Events having time-scales higher than that must belong to the horizontal turbulence spectra. With the observed maximum time-scale of 1000 s, use of equation 3 would indicate that the channel width can be approximately 167 to 333 meters. This is the width-scale of a third order channel in the Jamuna River (Bristow, 1987). It is important to note, however, that time-scales larger than that can occur.

202

5 Conclusions

ADCP and EMF velocity measured at different stations in the Jamuna River during rising and peak river stages reveal various interesting aspects of the turbulent flow field. Analyses of the collected data were conducted to suggest an optimum averaging time and related accuracy. The analyses and results support the following conclusions:

1 Fourier analysis of time-series data indicates that in most cases, the spectral density of the low frequency eddies are higher than the high frequency eddies. Approximately 42% of the turbulence frequencies have time-scales less than about 30 s. Approximately 13% of turbulent frequencies have time-scales more than about 2 minutes. In the range of water-depths and free-stream velocities during which the measurements were taken, the vertical turbulent eddies can have a maximum period of about 30 to 60 s. These eddies occupy 70% of the turbulent frequencies. The rest of the frequencies belong to the horizontal turbulent eddies

2 The turbulence intensity almost stabilizes to a constant value as the averaging time is increased. The stabilizing time was found to be about 10 minutes. The turbulence intensity is higher near the bed than near the surface. The near-surface values vary between 0.07 and 0.16 m/s, while the near-bottom values vary between 0.11 to 0.19 m/s. These turbulence intensities are higher than the bed-shear velocity (0.08 m/s) by about 1 to 2.5 times.

3 Standard pulsation error analysis for orthogonal velocities, Easting and Northing, and vector velocities, indicates that this error decreases as the exposure time is increased. For the same exposure time, there is a larger error near the bottom. The following relations are derived for the velocity vectors:

At 5% of total depth, $\epsilon_v = 26\tau^{-0.44}$.
At 26 to 68% of total depth, $\epsilon_v = 80\tau^{-0.65}$.
At 88 to 93% of total depth, $\epsilon_v = 269\tau^{-0.76}$.

Use of these relations indicates that at 50 s exposure time, the average error is about 8.3%. At 100 s exposure time, the error is reduced to 5.2%

4 An exposure time of 100 s or less is suggested for one- or two-point methods of depth-mean velocity estimation, while an exposure time of 50 s or more is suggested for the multi-point method

202

References

Bristow, C.S., 1987. Brahmaputra River: Channel migration and deposition. The Society of Economic Paleontologists and Mineralogists, pp. 63-74

Carter, R.W. and Anderson, I.E., 1963. Accuracy of current meter measurements. Jr. Hydr. Divn., Proc. ASCE, HY 4, part 1, 105-115

Delft Hydraulics, 1990. Electromagnetic Flow Meter. User's Manual

Delft Hydraulics, 1992. Introduction to HYMOS, version 3.00

International Organization for Standardization (ISO), 1983. Measurement of liquid flow in open channels. ISO standard handbook 16, Switzerland

Rao, K.N., Narashima, R., and Narayanam, M.A.B., 1971. The bursting phenomenon in a turbulent boundary layer. J. Fluid Mech., 48:339-352

RD Instruments, 1989. Acoustic Doppler Current Profilers - principle of operation: A practical primer. RD Instruments, San Diego, California

Sauer, V.B. and Meyer, R.W., 1992. Determination of error in individual discharge measurements. USGS open file report no. 92-144

Soulsby, R.L., 1983. The bottom boundary layer of shelf seas. In: Johns, B., (ed.), Physical oceanography of coastal and shelf seas. Elsevier Science, Amsterdam

Uittenbogaard, R. E., 1995. The importance of internal waves for mixing in a stratified estuarine tidal flow. Ph. D. Thesis, Technical University, Delft.

Urick, R.J., 1975. Principles of underwater sound. McGraw-Hill, New York, 384 pp

World Meteorological Organization (WMO), 1980. Manual on stream gauging (vol.1), field work, WMO No. 519

Van Rijn, L.C. and Schaafsma, A.S., 1986. Evaluation of measuring instruments for suspended sediments. Delft Hydraulics Communication no. 368

Yalin, M.S., 1992. River Mechanics. Pergamon Press, Oxford, 219 pp

Yokosi, S., 1967. The structure of river turbulence. Bull. Disaster Prevention Res. Inst., Kyoto Univ., vol. 17, part 2, No. 121

206

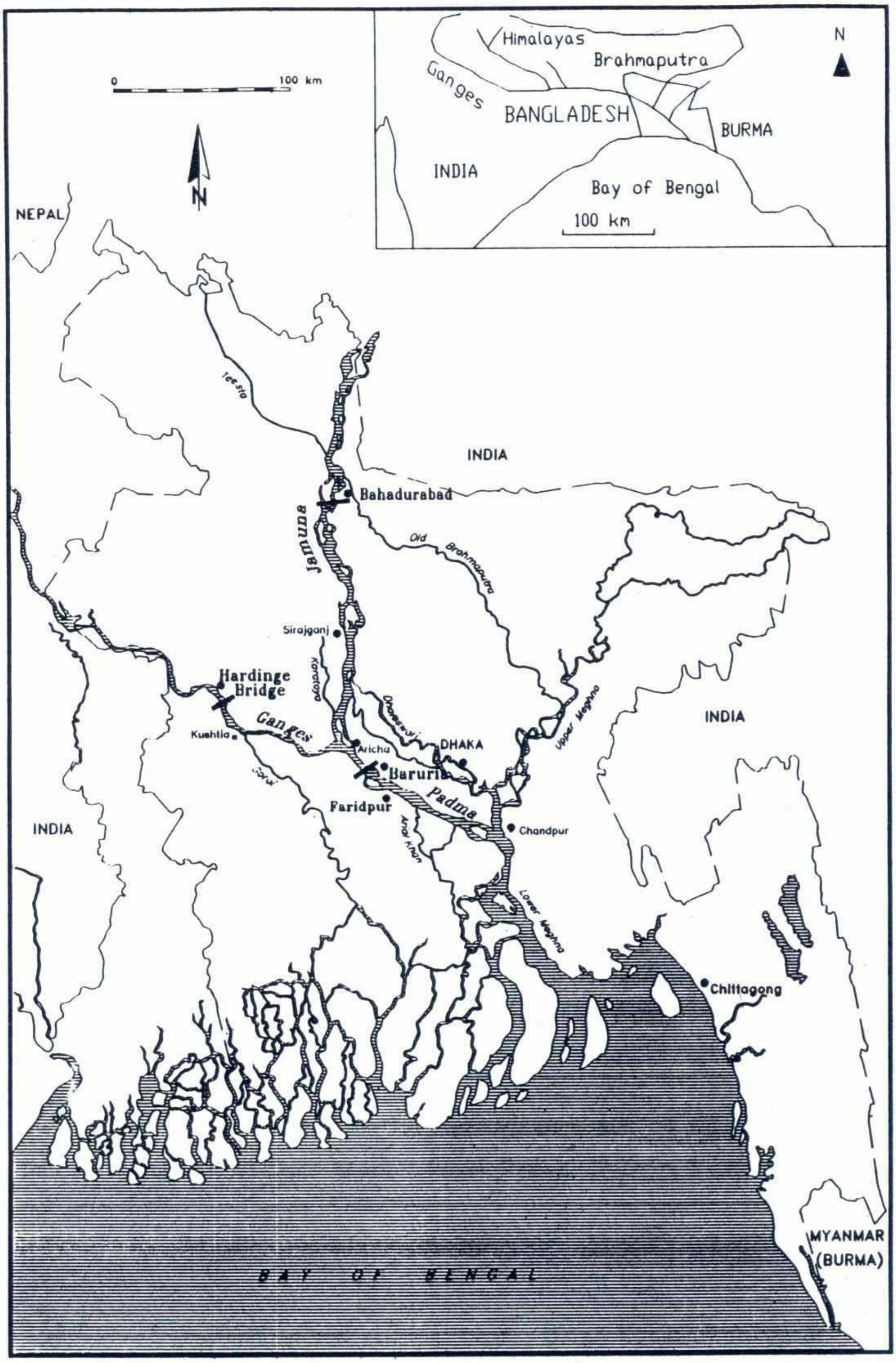

Figure A.1 Rivers of Bangladesh

208

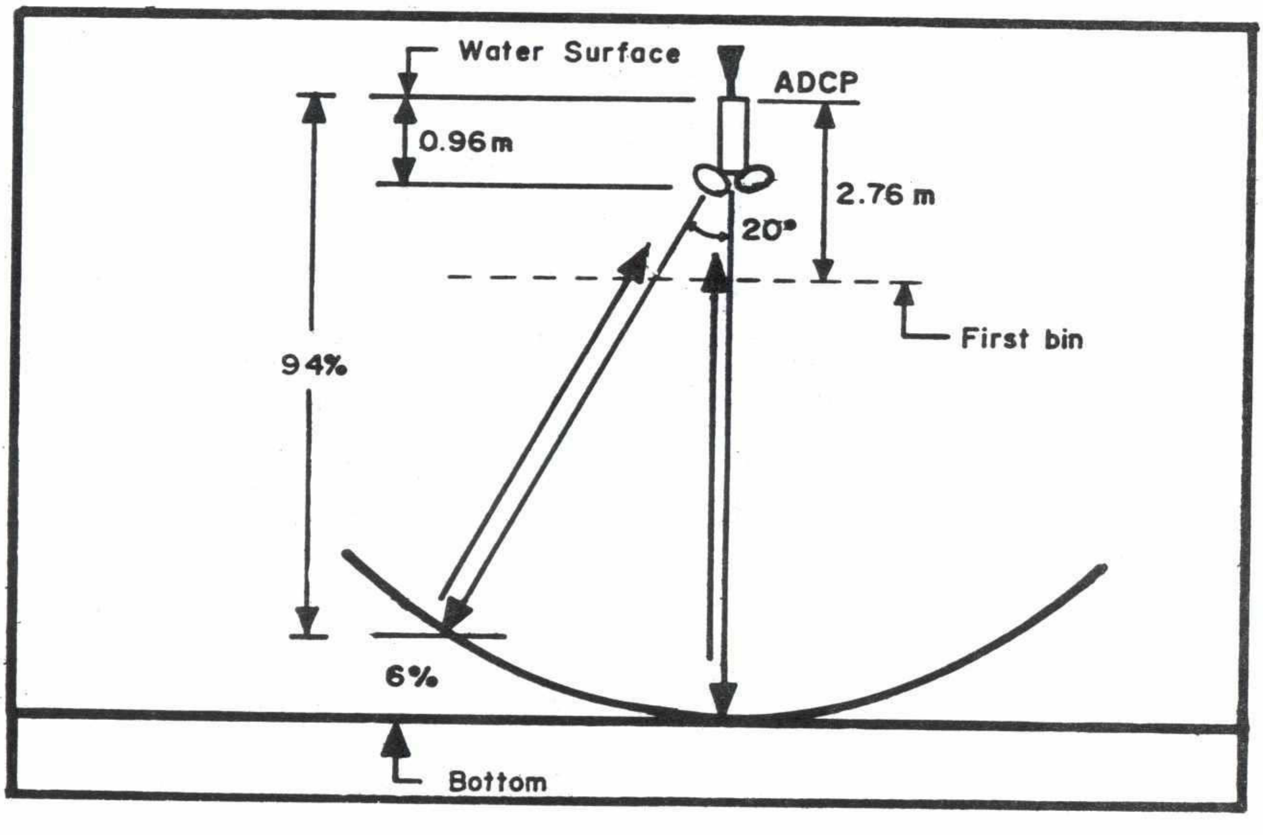

Figure A.2 ADCP flow measurement principles as implemented by FAP24

204

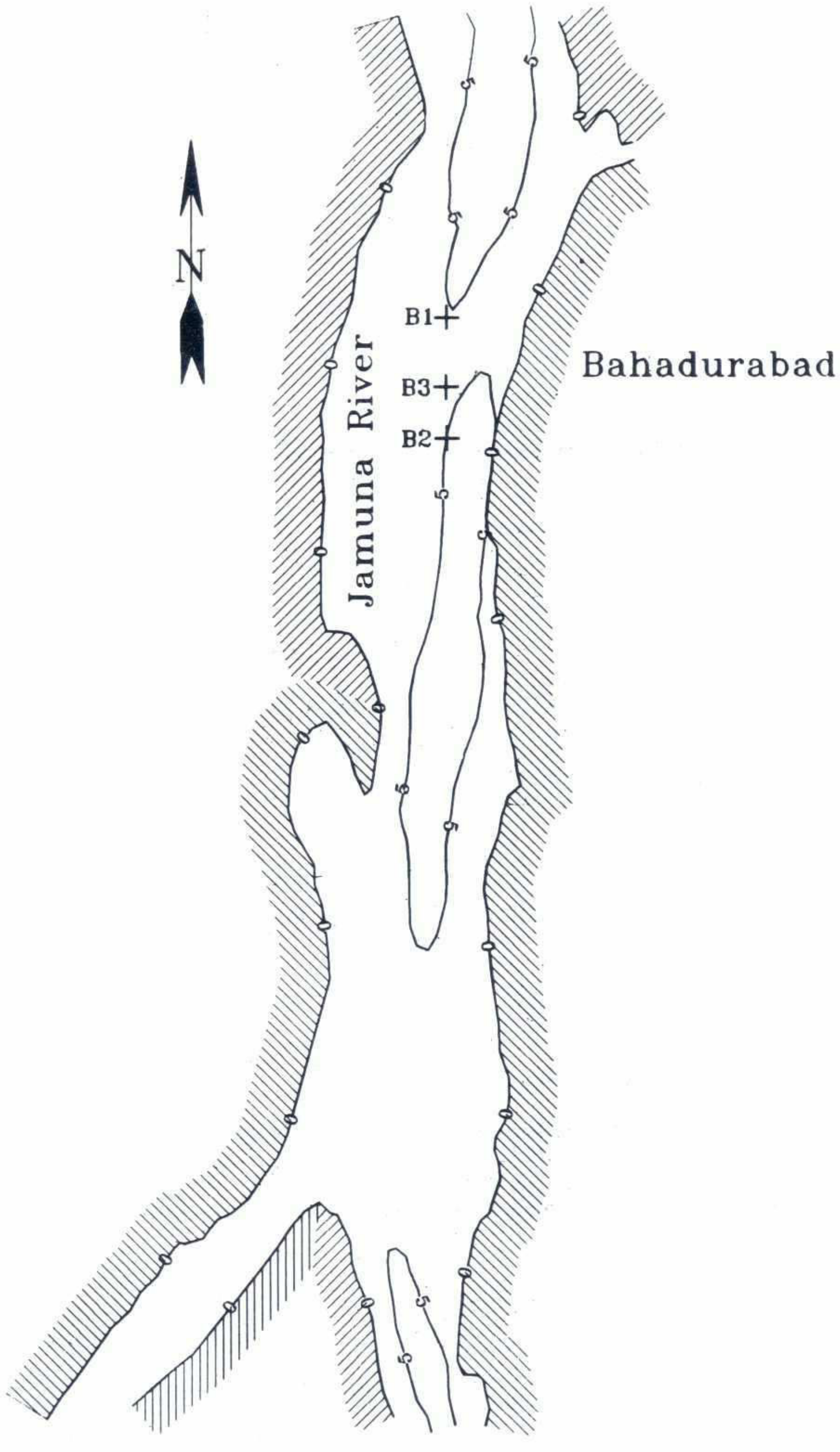

Figure A.3 Part of the Jamuna River near Bahadurabad showing measurement locations B1 and B2

209

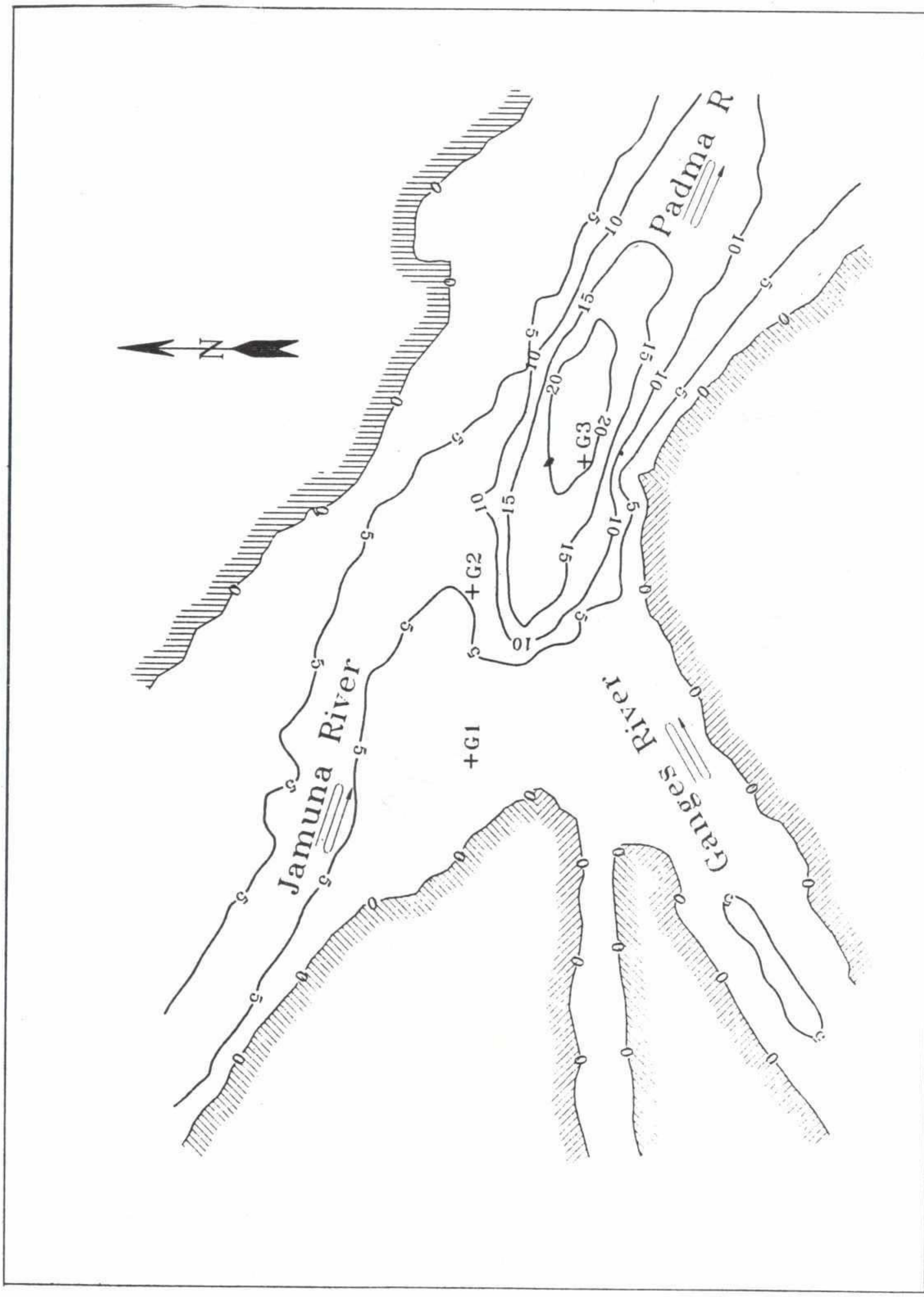

Figure A.4 Ganges-Jamuna Confluence near Aricha showing measurement locations G1, G2 and G3

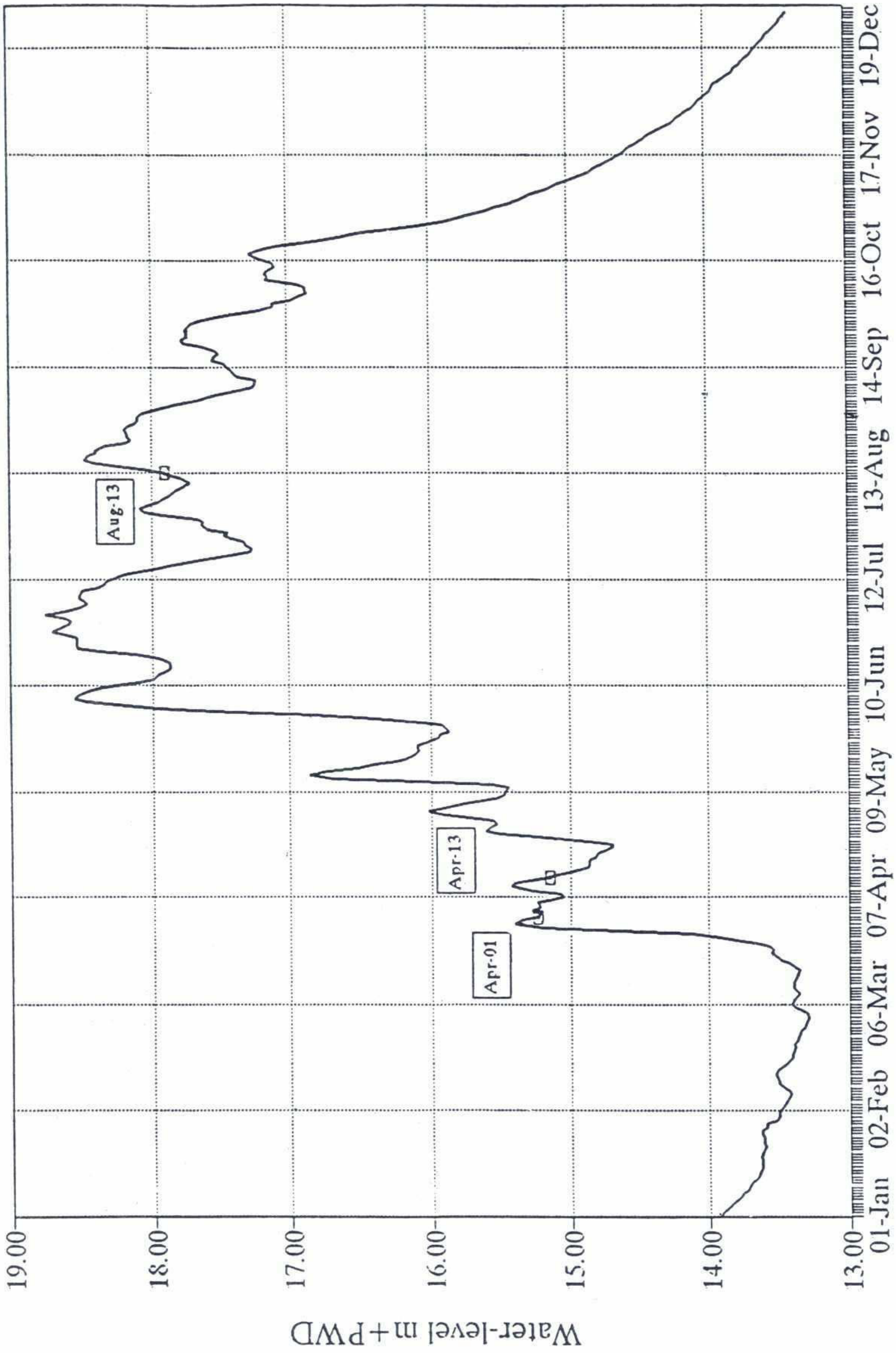

Figure A.5 Hydrograph of the Jamuna River at Bahadurabad showing the dates of the measurements

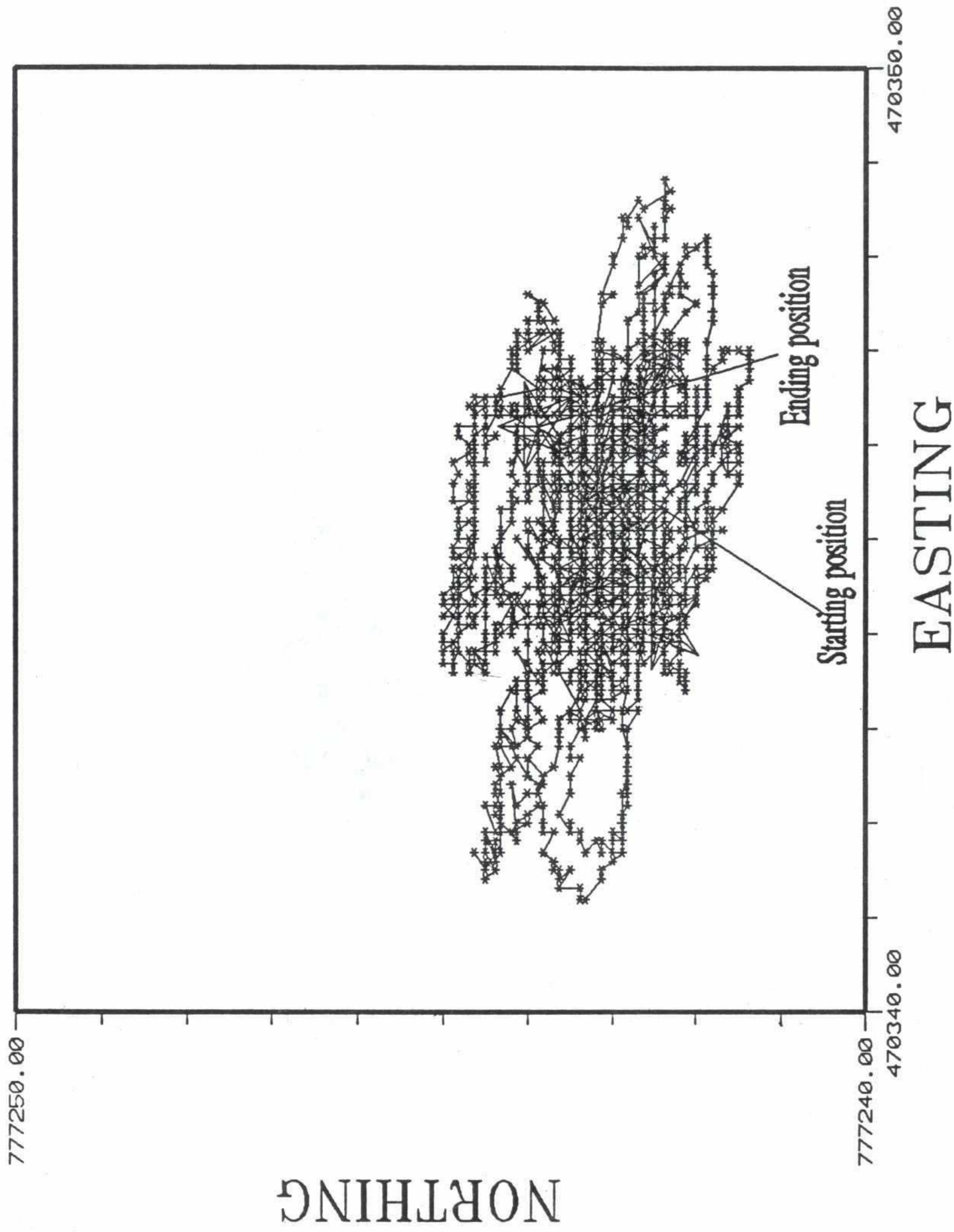

Figure A.6   Ship-track of DHA at location B1 for a measurement duration of about 54 minutes on 1 April 1994.

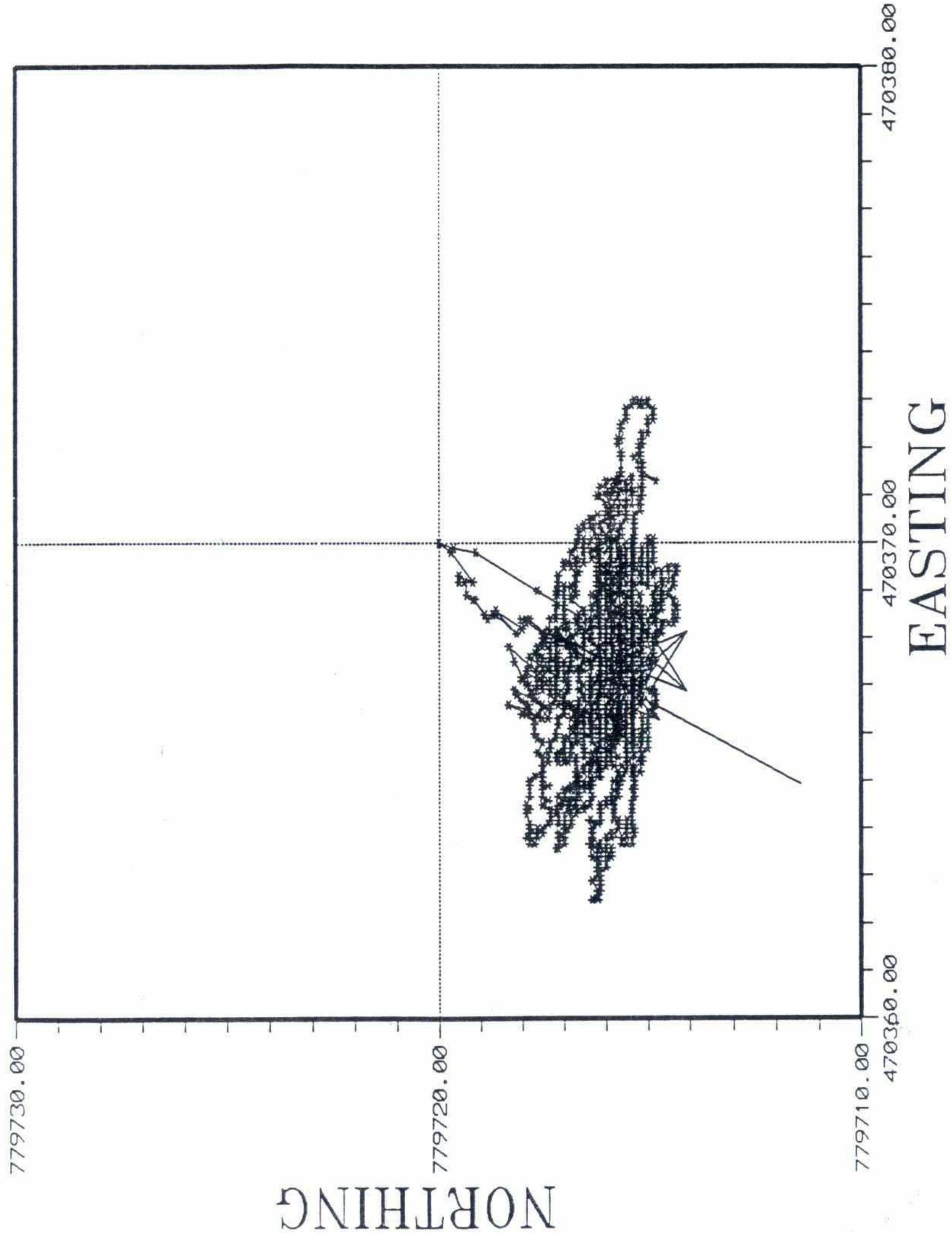

Figure A.7 Ship-track of DHA at location B2 for a measurement duration of about 33 minutes on 1 April 1994.

220

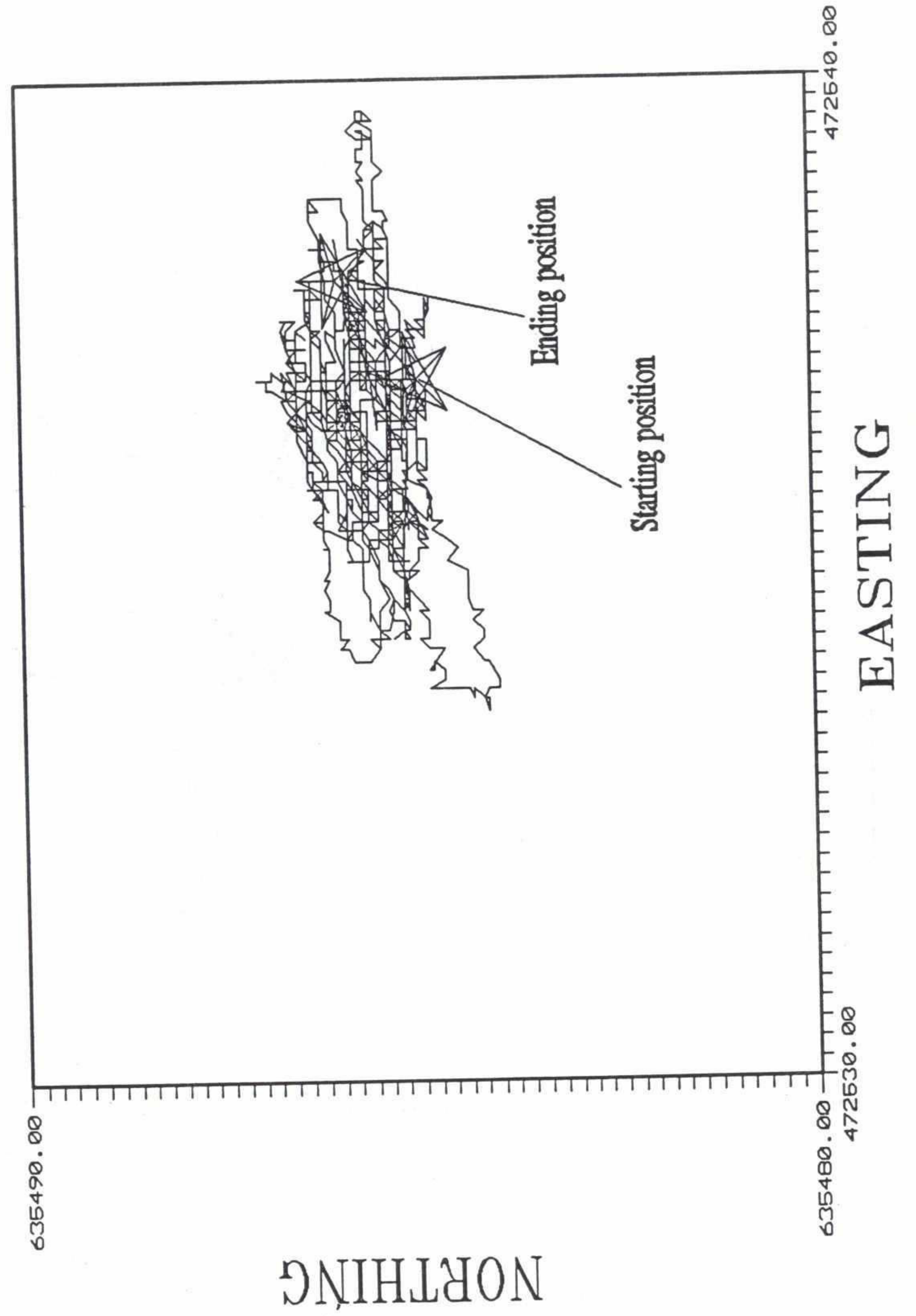

Figure A.8 Ship-track of DHA at location G1 for a measurement duration of about 45 minutes on 13 April 1994.

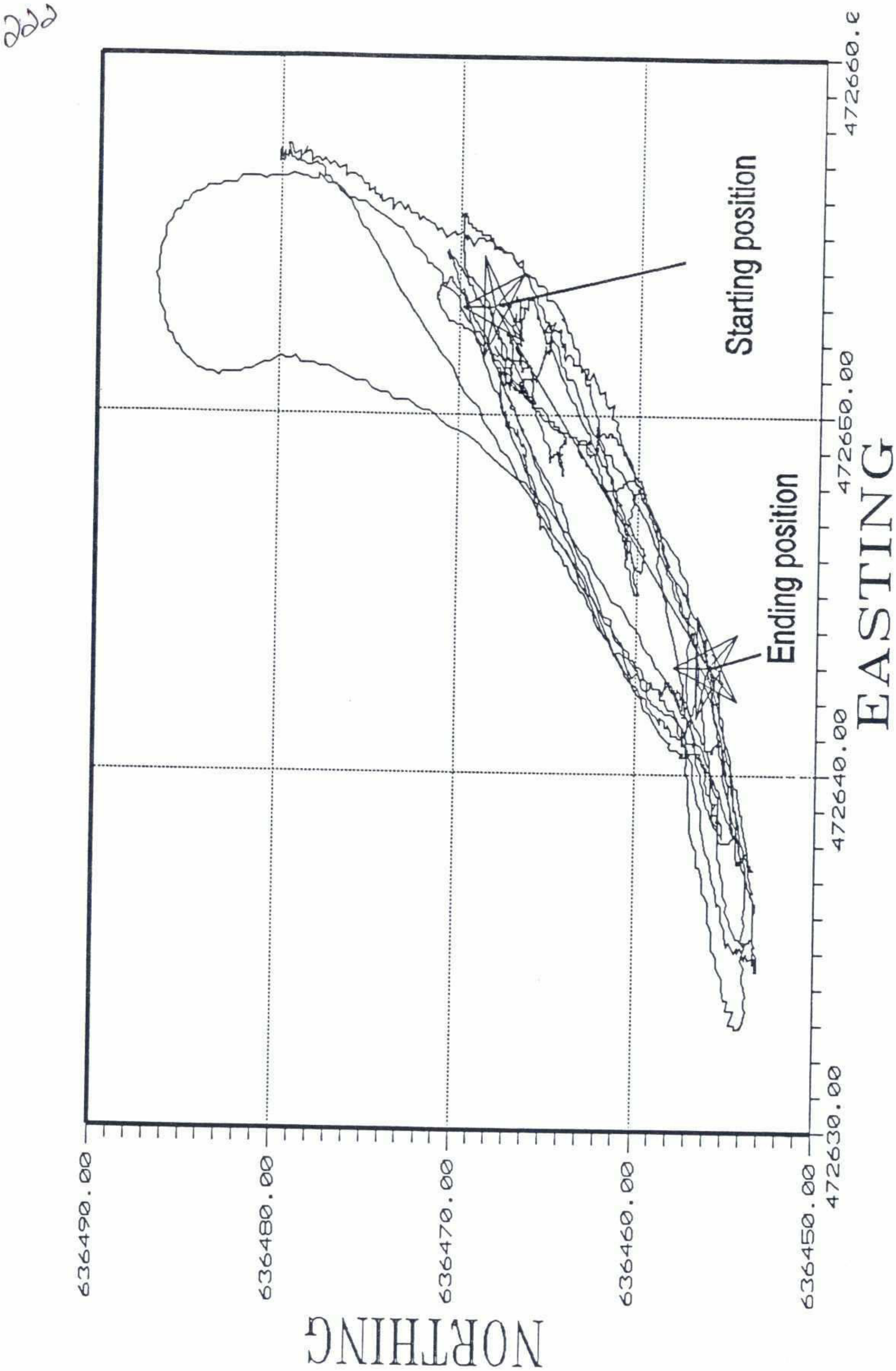

Figure A.9 Ship-track of DHA at location G2 for a measurement duration of about 45 minutes on 13 April 1994.

221

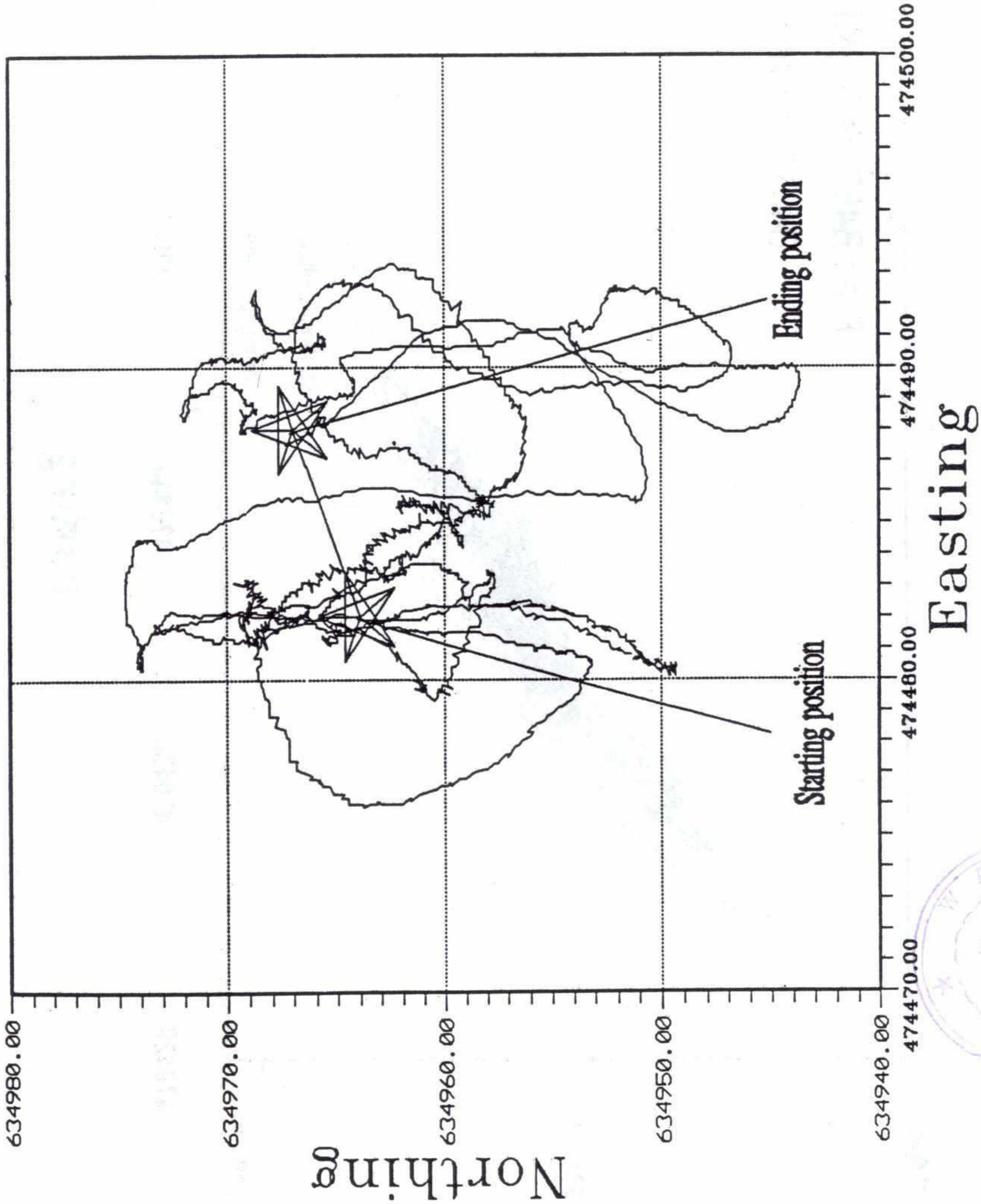

Figure A.10 Ship-track of DHA at location G3 for a measurement duration of about 45 minutes on 13 April 1994.

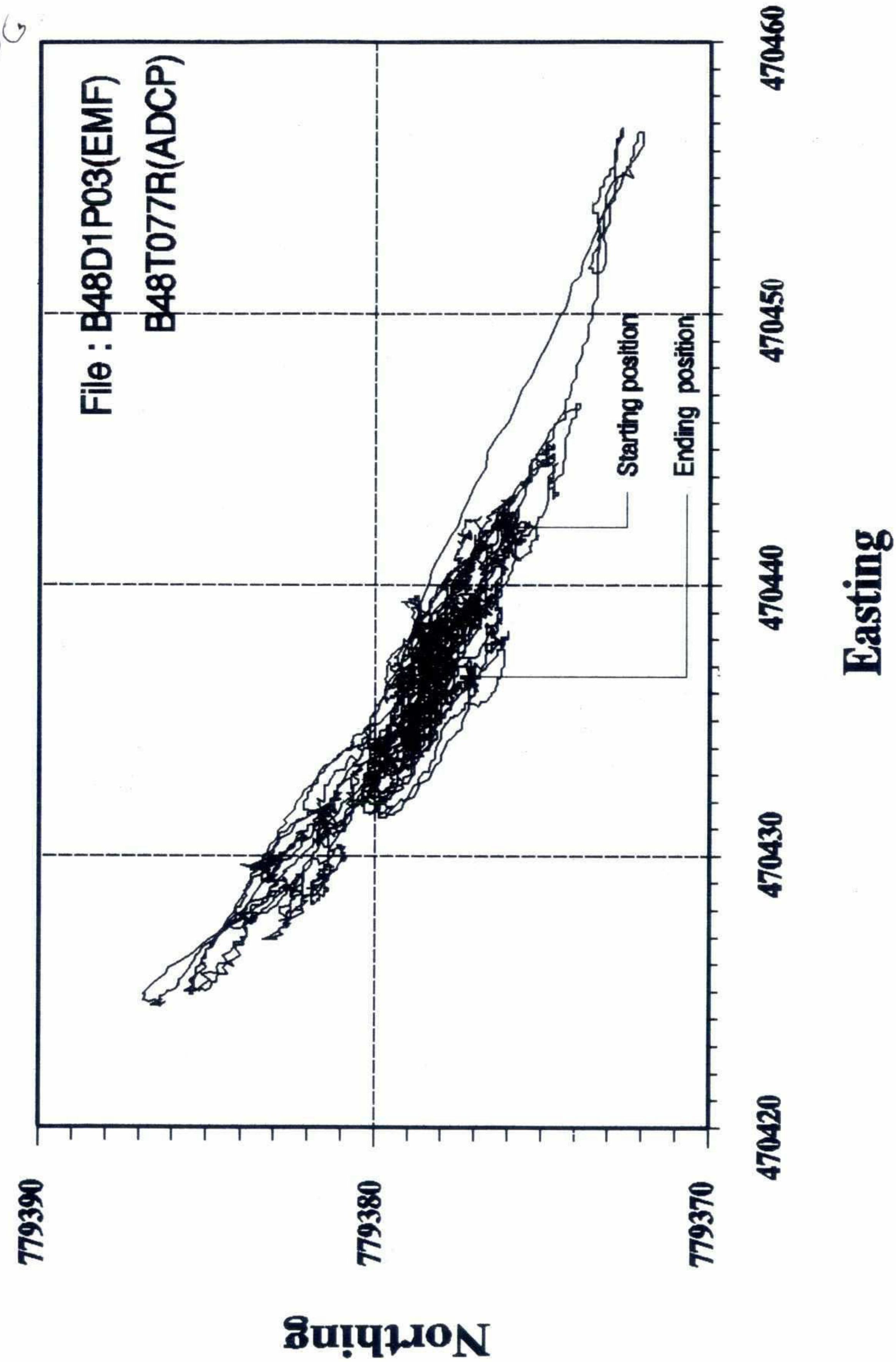

Figure A.11 Ship-track of DHA at location B3 for a duration of about 2 hours and 7 minutes on 13 August 1994.

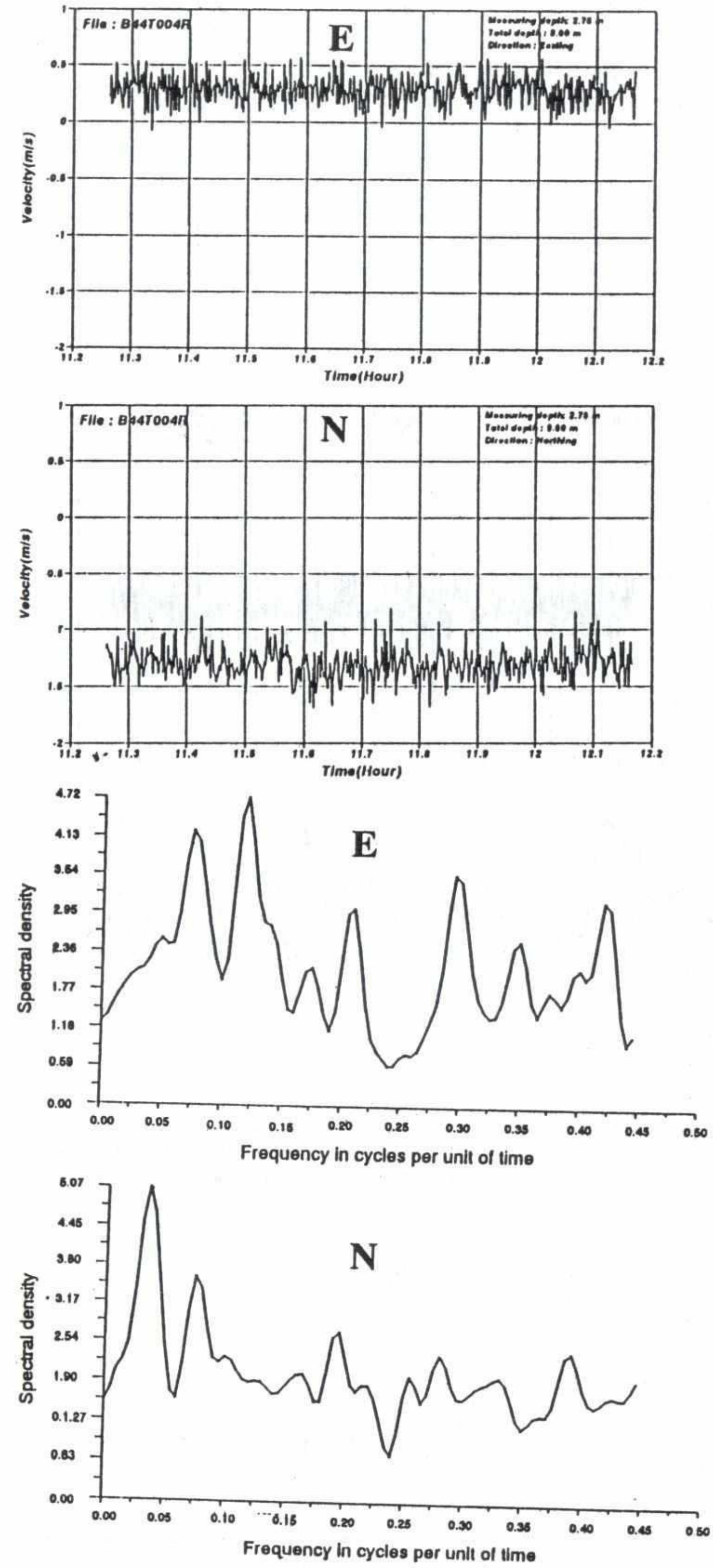

Figure A.12 ADCP velocities and their spectral densities at 2.8 m depth measured at B1 in the Jamuna River left anabranch measured on 1 April 1994

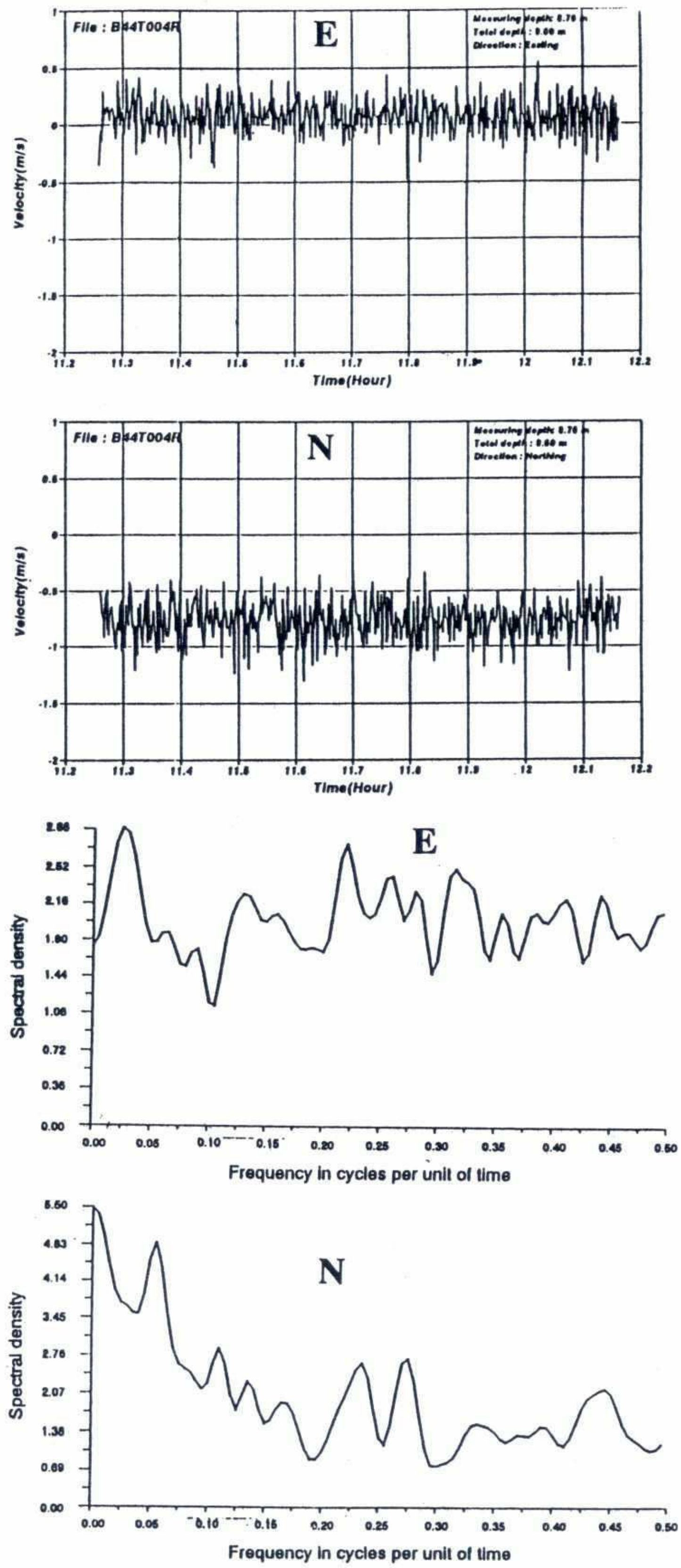

Figure A.13 ADCP velocities and their spectral densities at 8.8 m depth measured at B1 in the Jamuna River left anabranch measured on 1 April 1994

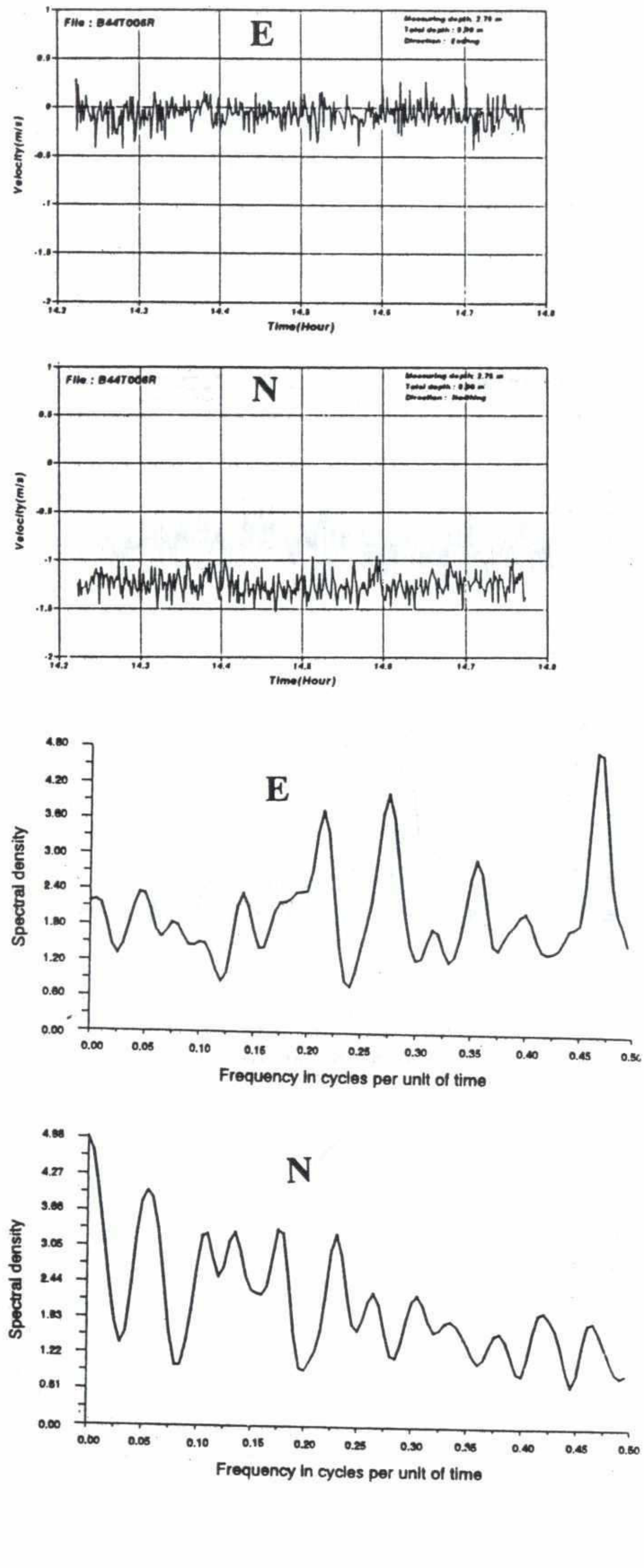

Figure A.14 ADCP velocities and their spectral densities at 2.8 m depth measured at B2 in the Jamuna River left anabranch measured on 1 April 1994.

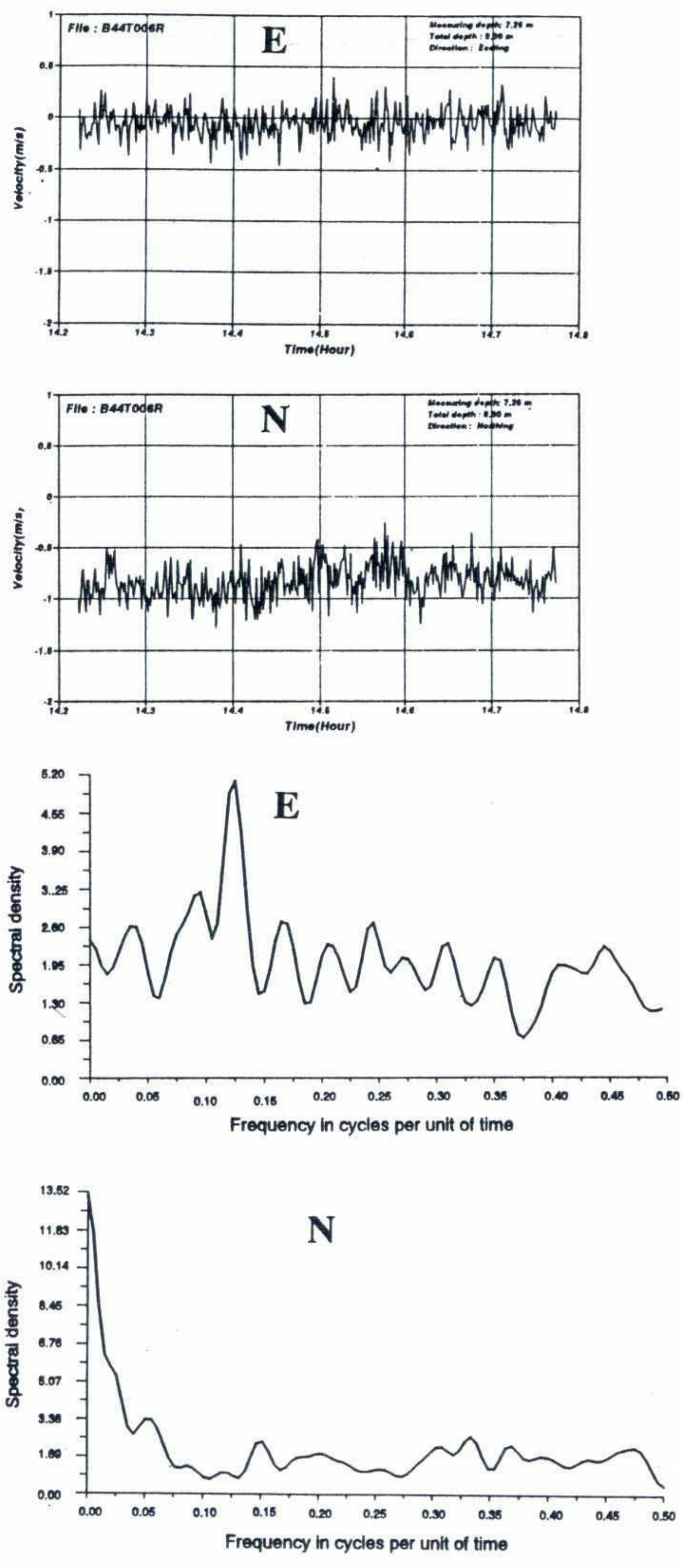

Figure A.15   ADCP velocities and their spectral densities at 7.3 m depth measured at B2 in the Jamuna River left anabranch measured on 1 April 1994.

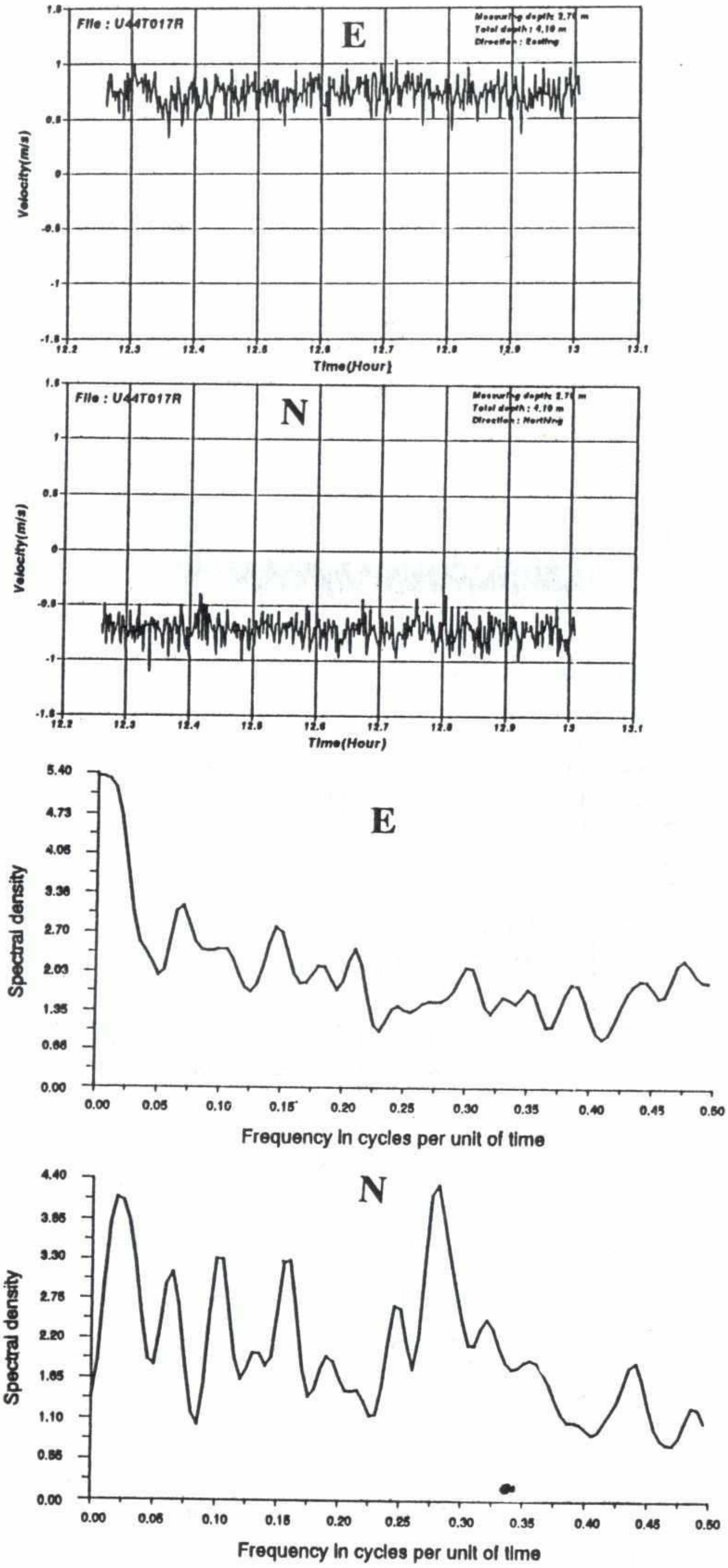

Figure A.16   ADCP velocities and their spectral densities at 2.8 m depth measured at G1 in the Ganges-Jamuna confluence measured on 13 April 1994

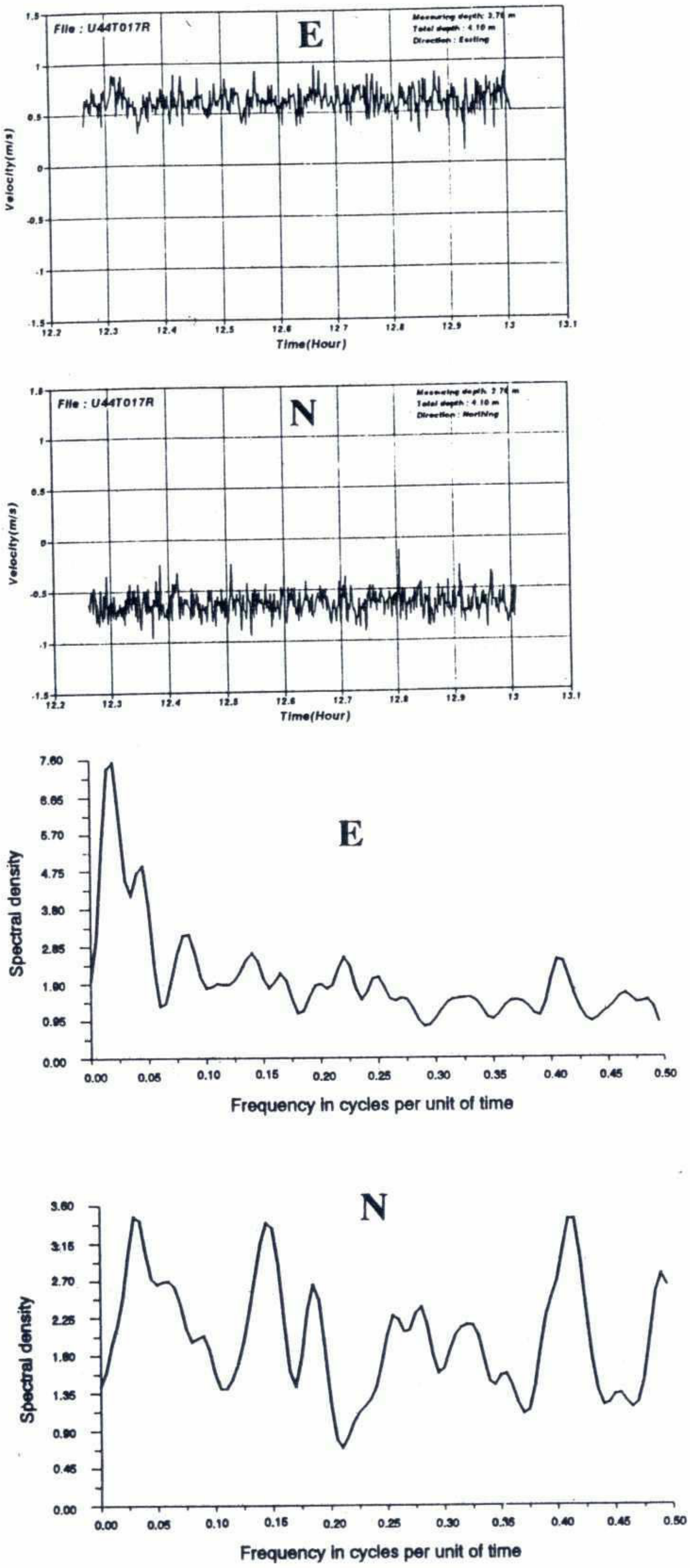

Figure A.17 ADCP velocities and their spectral densities at 3.8 m depth measured at G1 in the Gage-Jamuna confluence measured on 13 April 1994

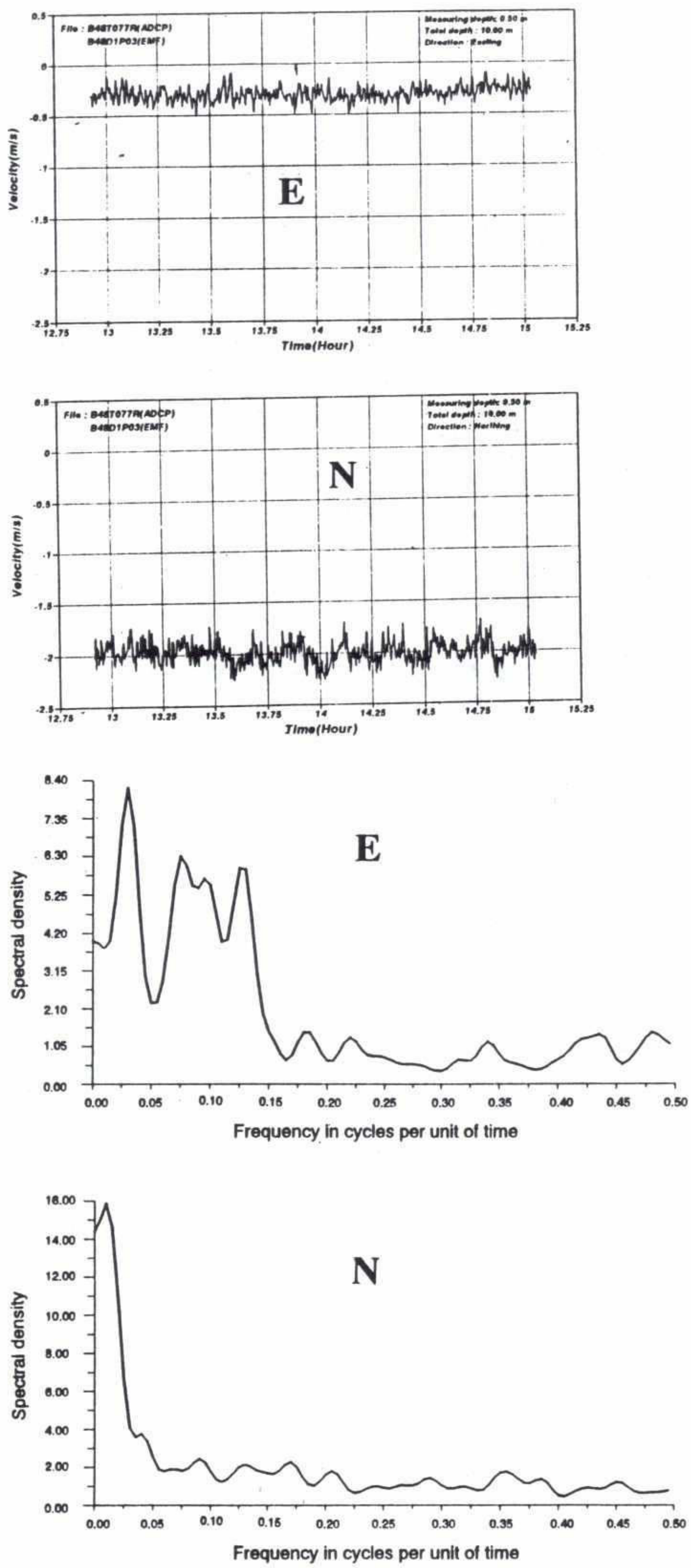

Figure A.18 EMF velocities and their spectral densities at 0.5 m depth measured at B3 in the Jamuna River left anabranch measured on 13 August 1994.

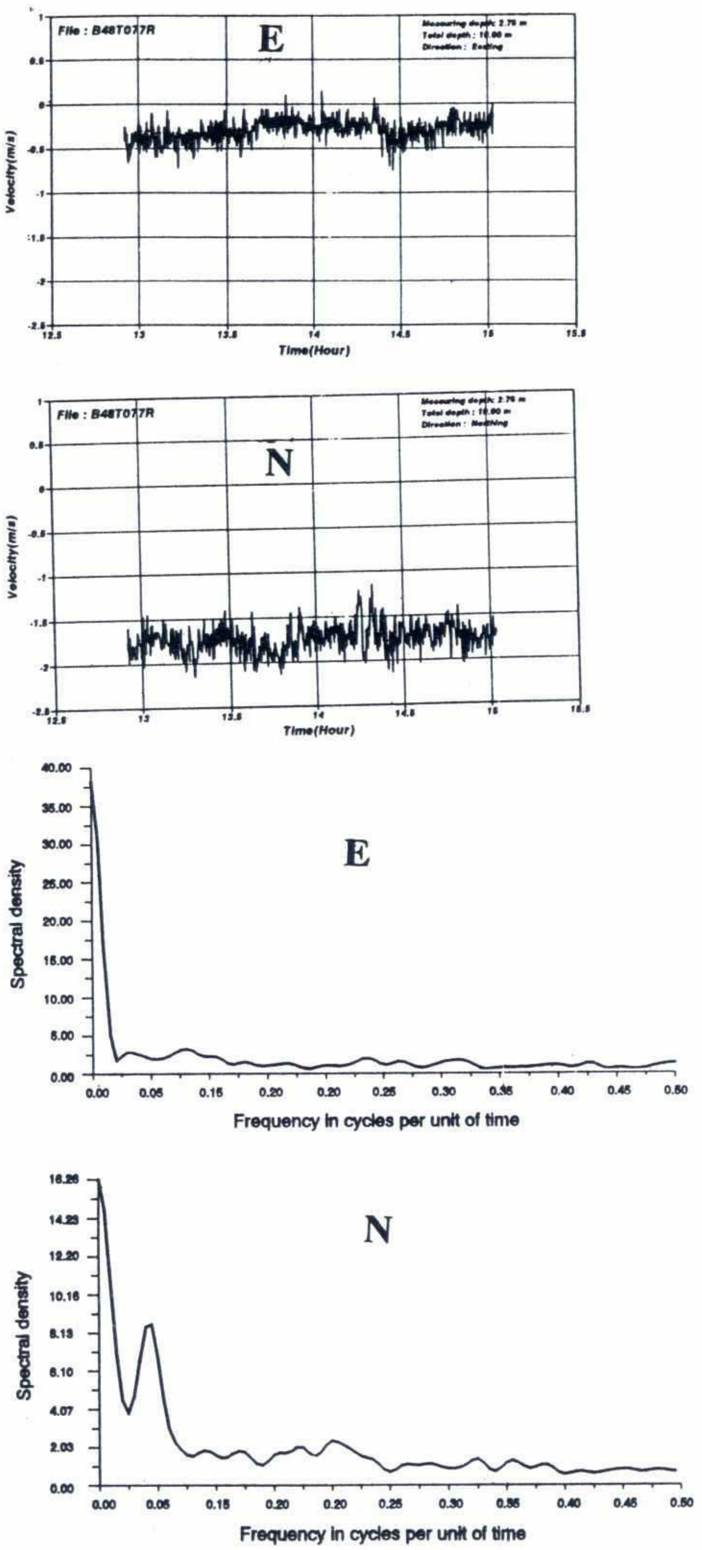

Figure A.19 ADCP velocities and their spectral densities at 2.8 m depth measured at B3 in the Jamuna River left anabranch measured on 13 August 1994.

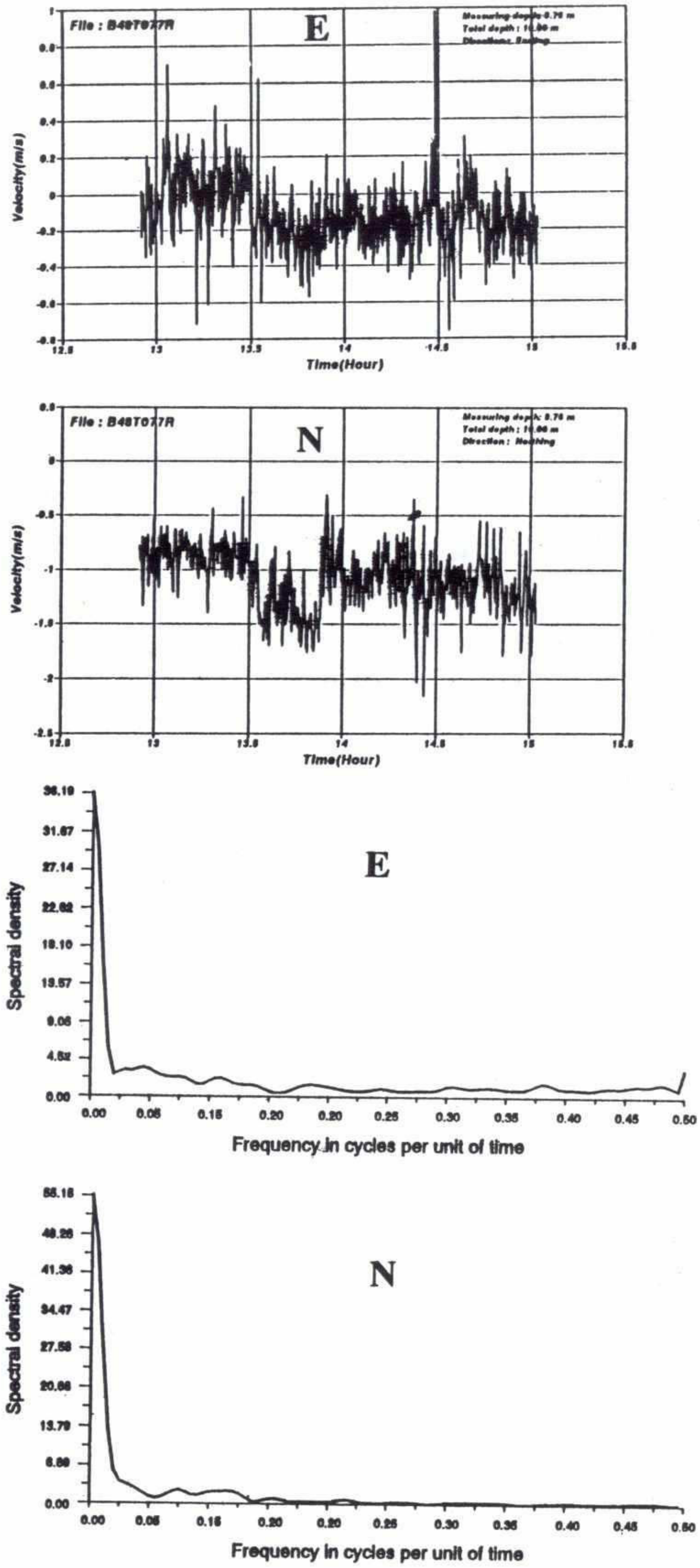

Figure A.20   ADCP velocities and their spectral densities at 8.8 m depth measured at B3 in the Jamuna River left anabranch measured on 13 August 1994.

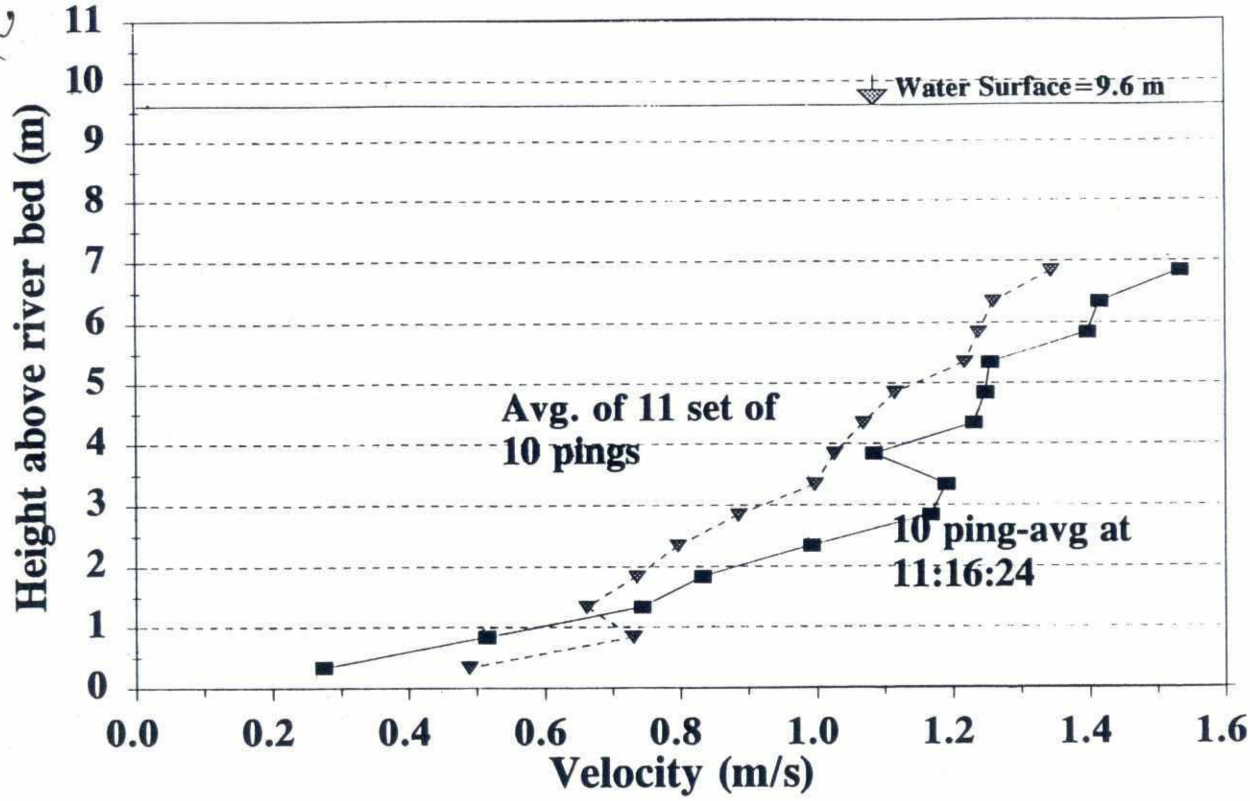

Figure A.21 ADCP velocity profile measured at B1

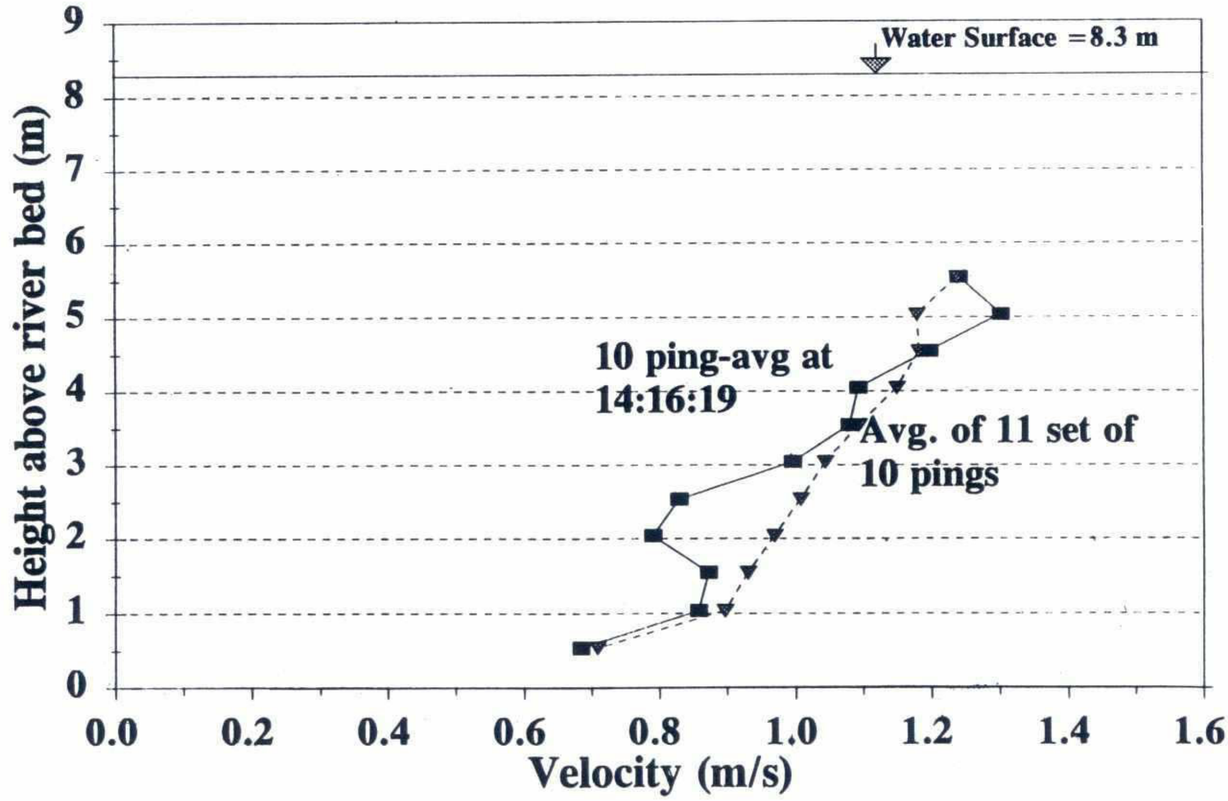

Figure A.22 ADCP velocity profile measured at B2 in the Jamuna River left anabranch on 13 August 1994.

28

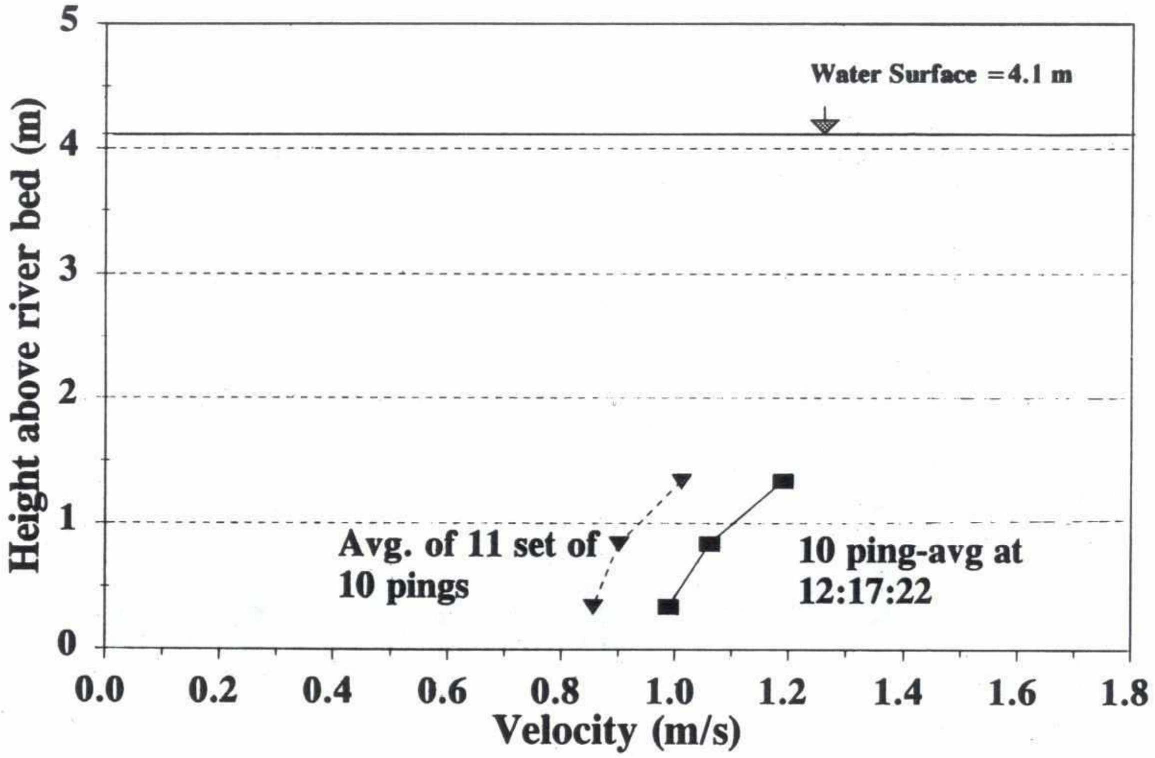

Figure A.23 ADCP velocity profile measured at G2

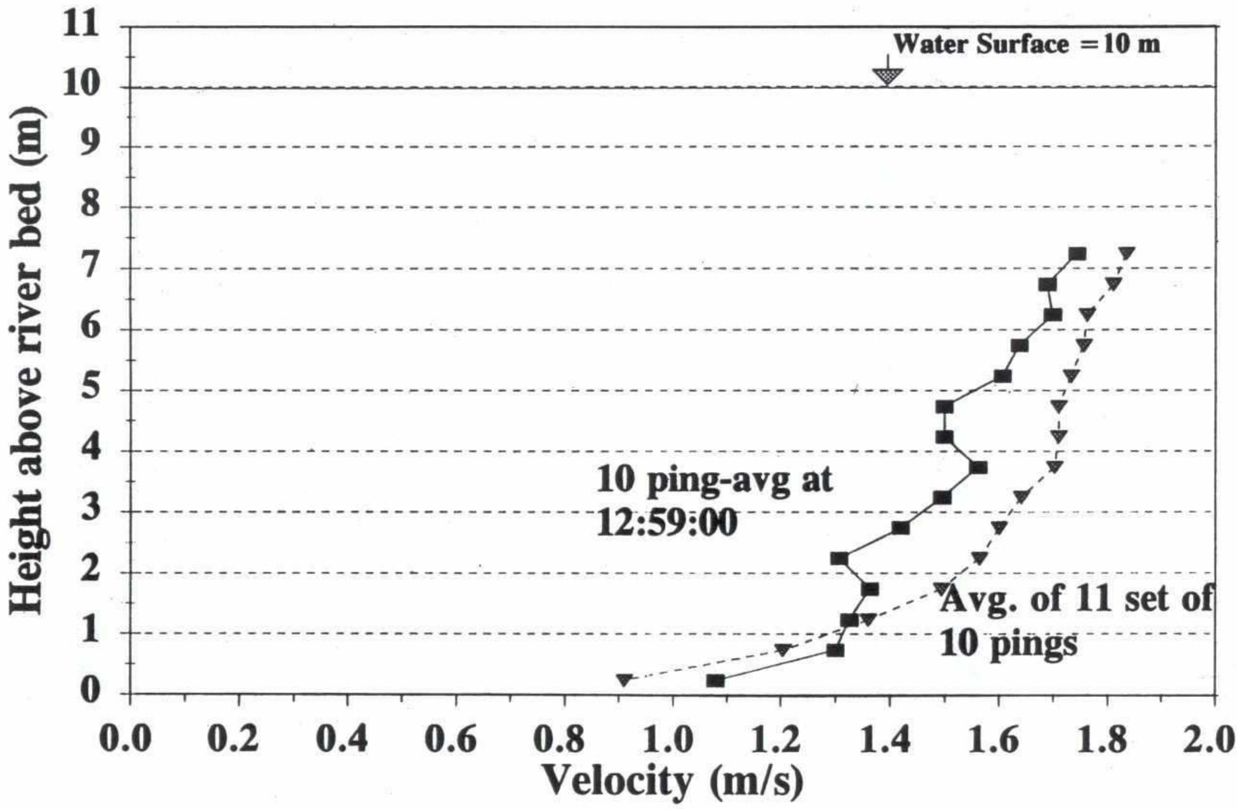

Figure A.24 ADCP velocity profile measured at B3 in the Jamuna River left anabranch on 13 August 1994.

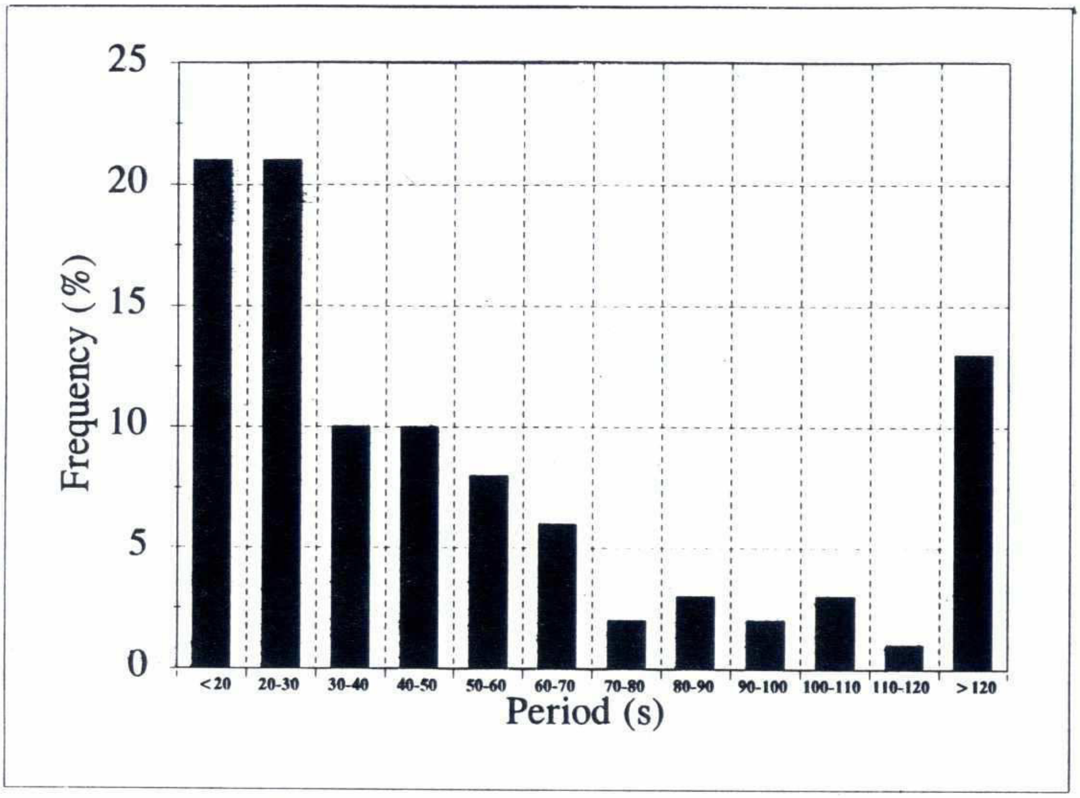

Figure A.25 Frequency of occurrence of time-scale turbulence events in the direction towards east

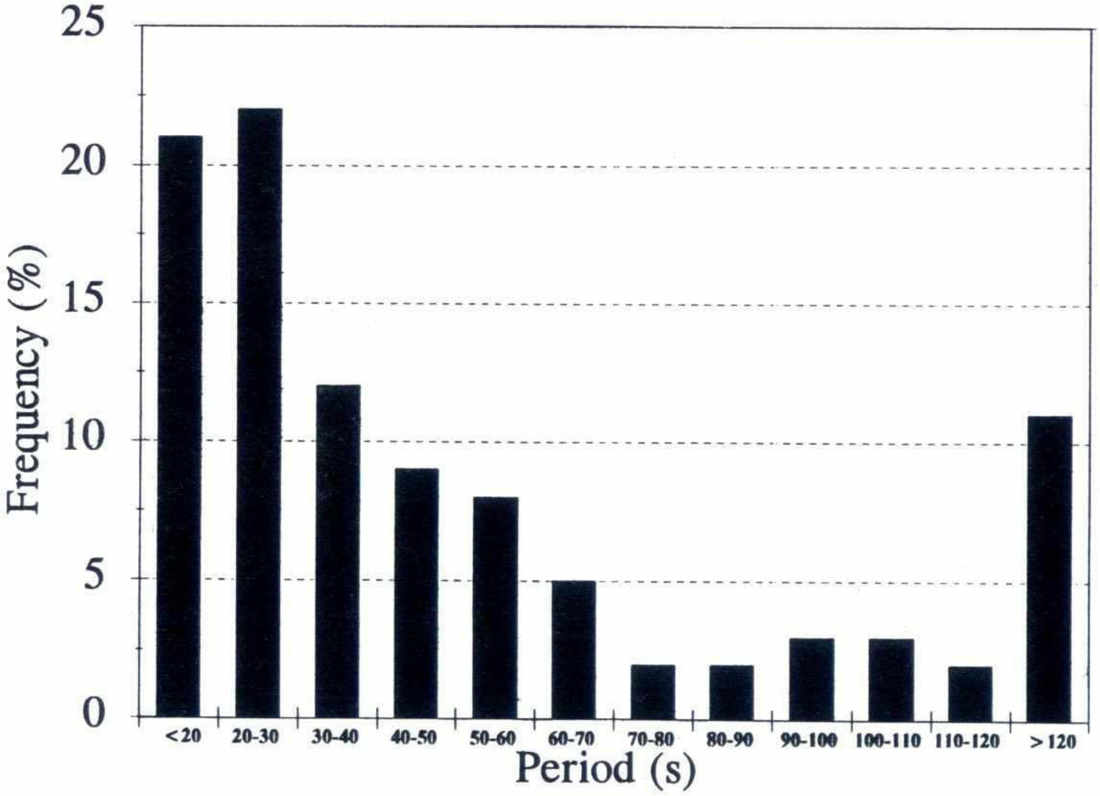

Figure A.26 Frequency of occurrence of different time-scale turbulence events of the northing component considering all the four stations.

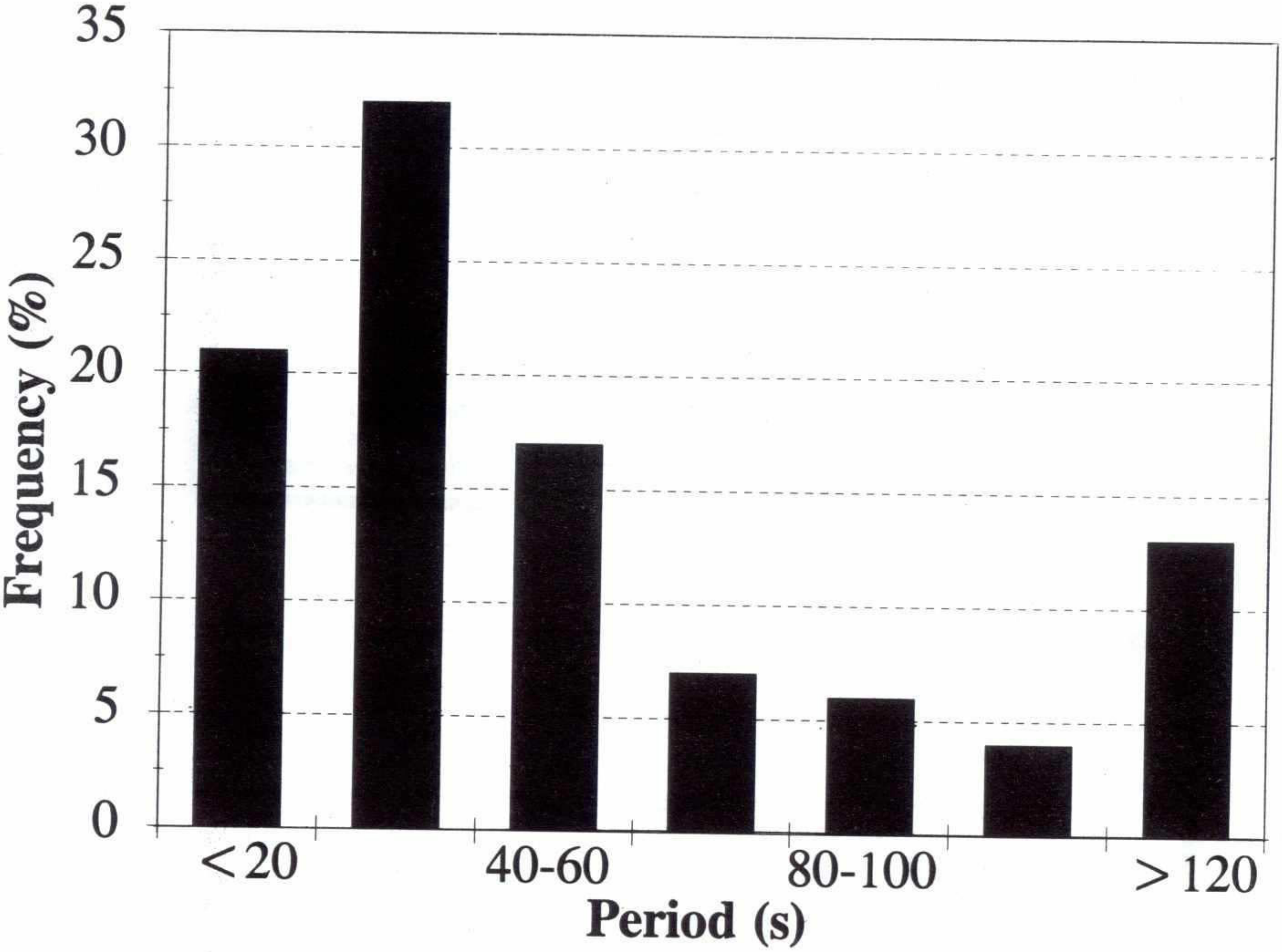

Figure A.27 Frequency of occurrence of different time-scale turbulence events of the velocity vectors considering all the four stations

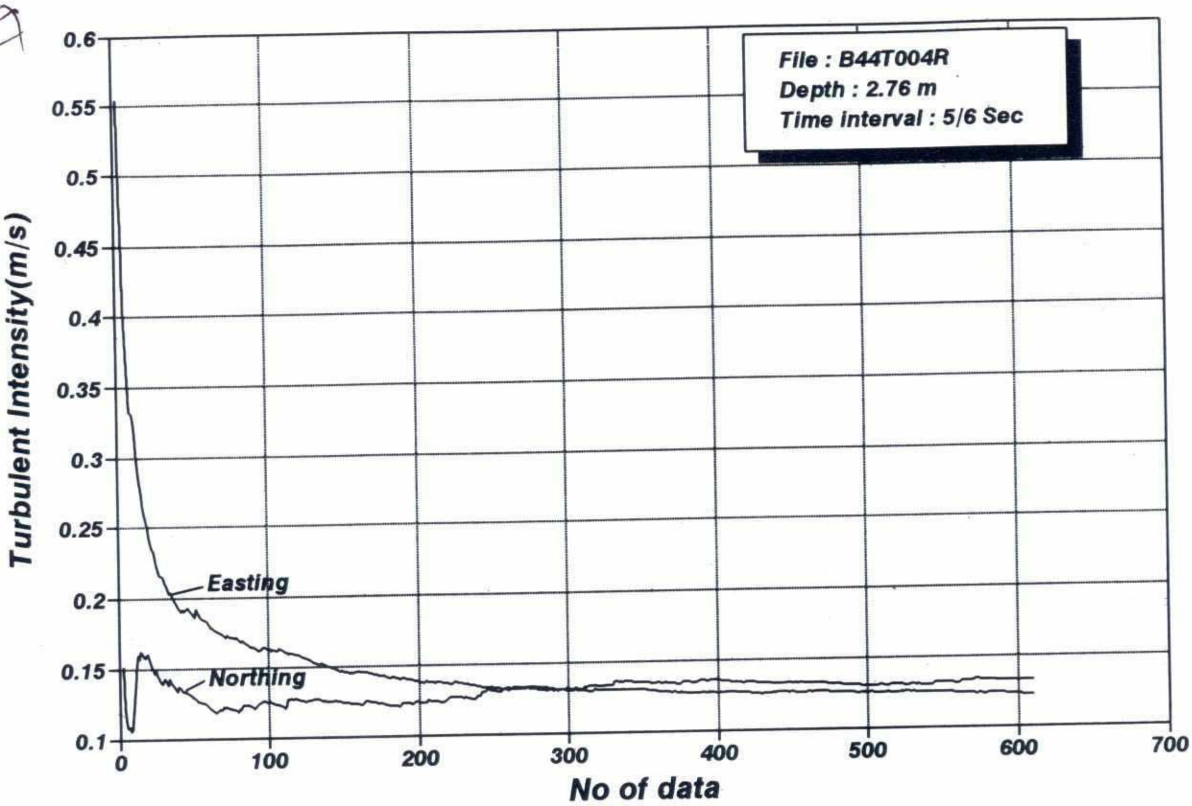

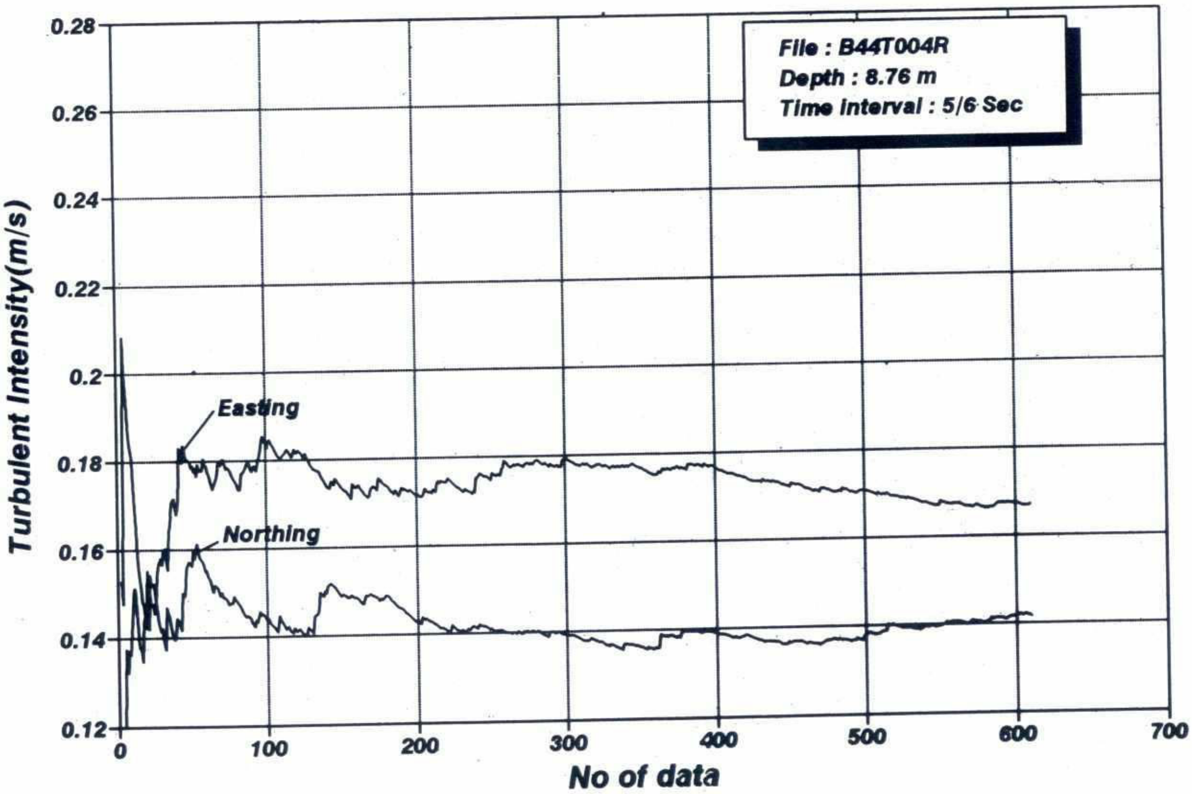

Figure A.28 Turbulence intensities as a function of the numbers of data used for averaging considering the data measured at station B1 on 1 April 1994.

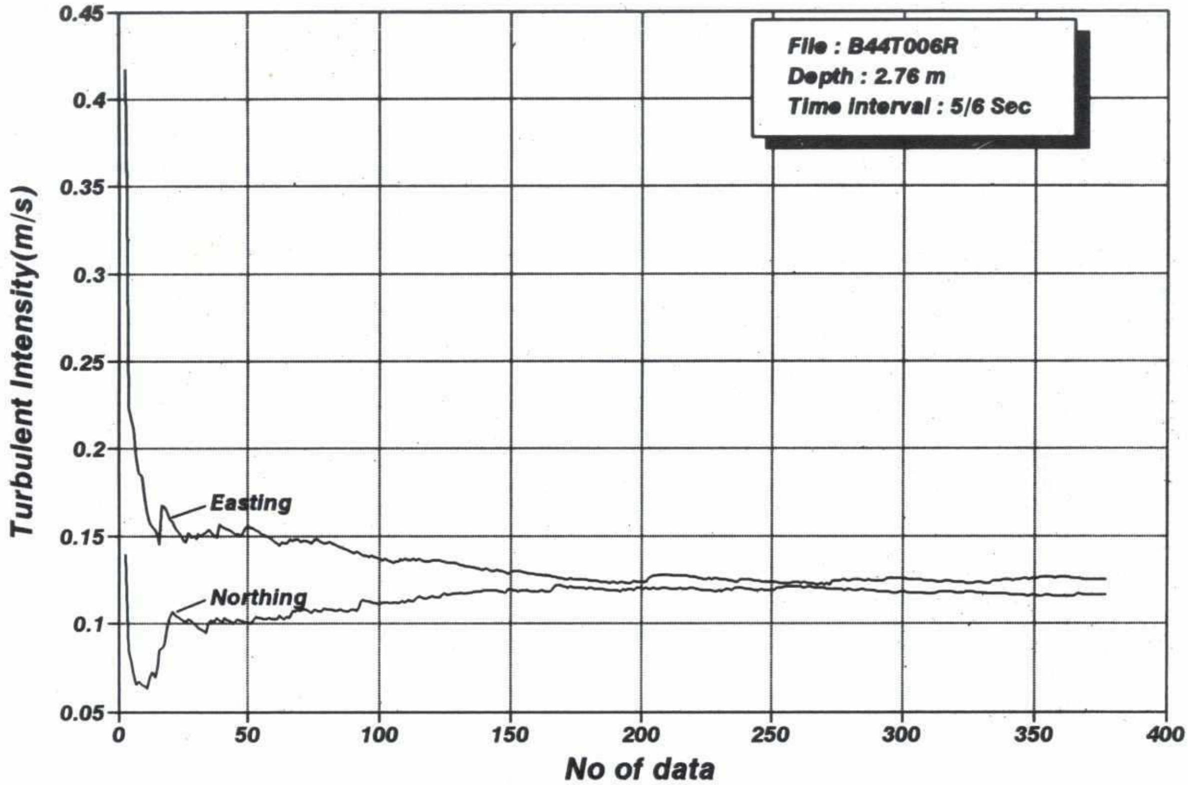

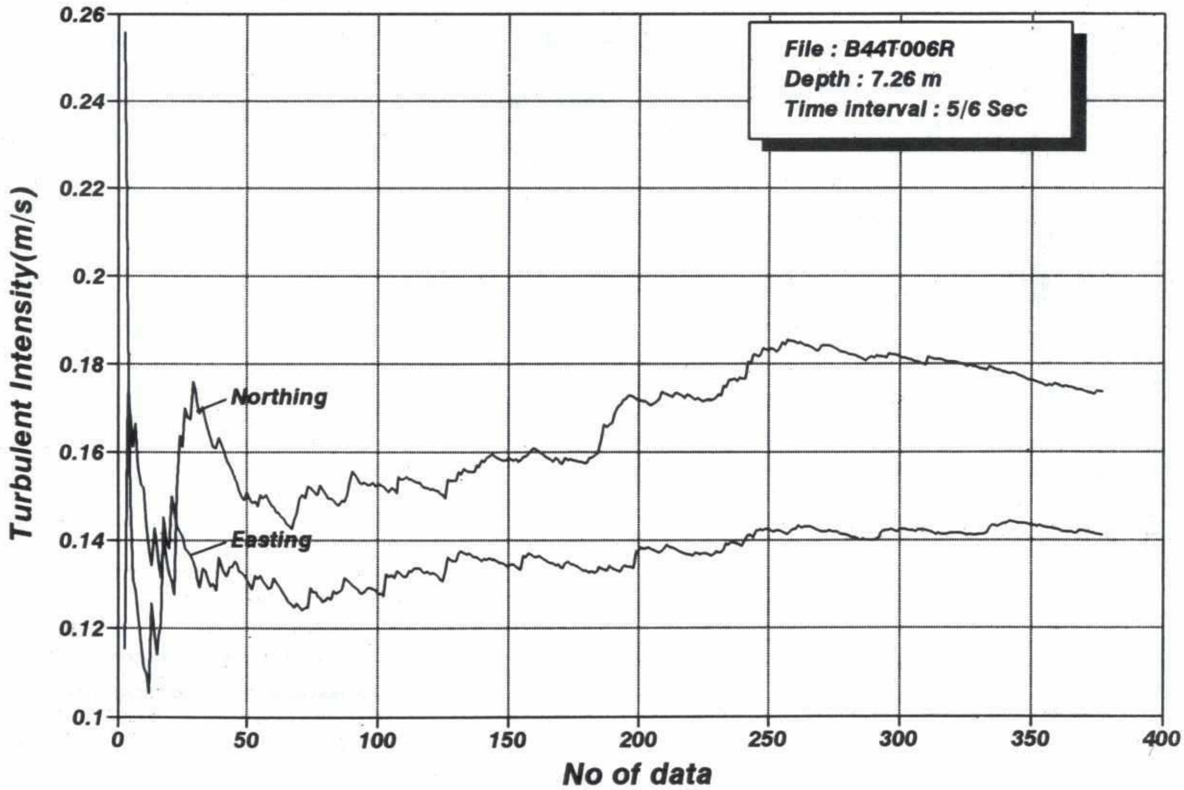

Figure A.29 Turbulence intensities as a function of the numbers of data used for averaging cansidering the data measured at station B2 1 April 1994.

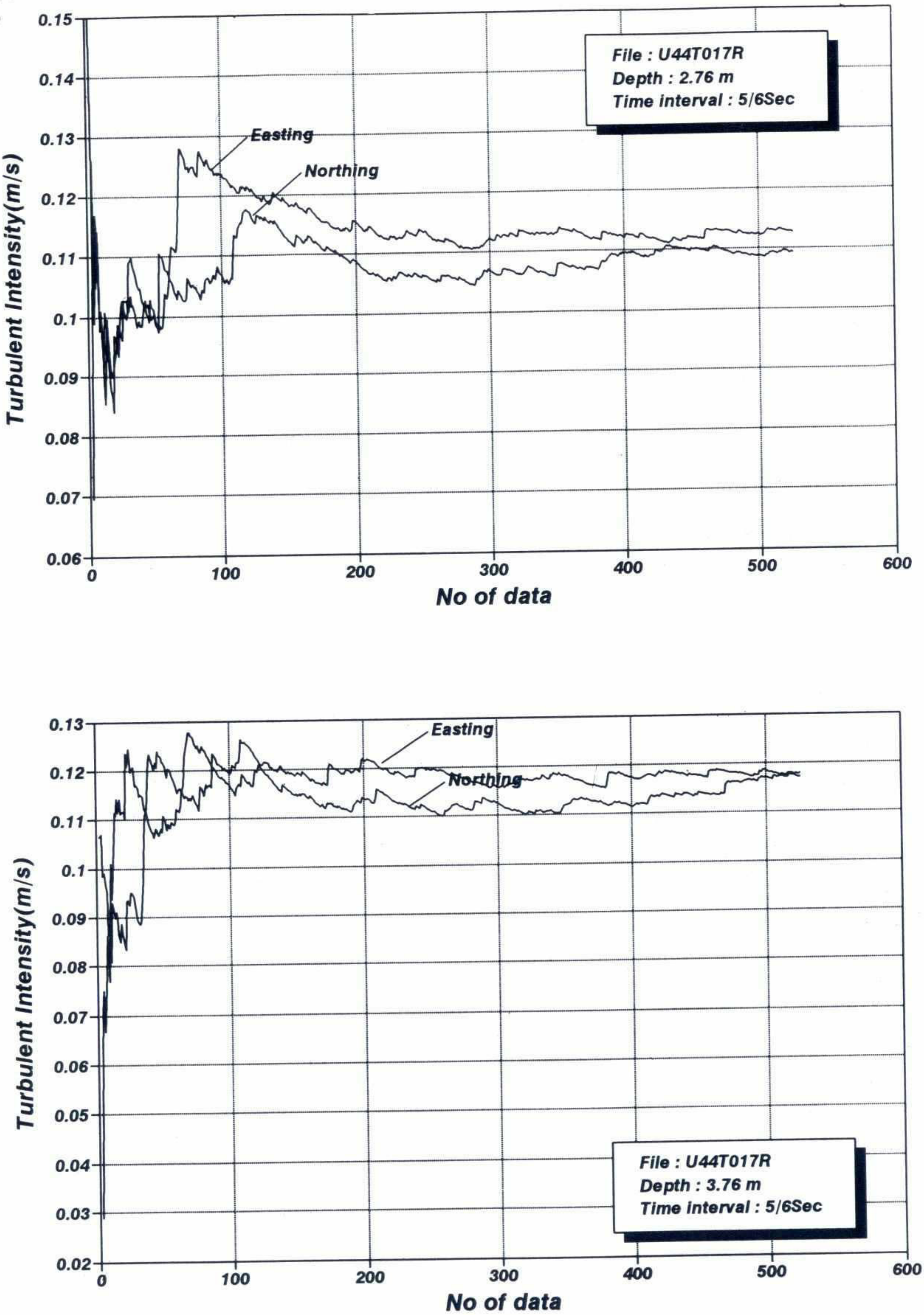

Figure A.30 Turbulence intensities as a function of the numbers of data used for averaging considering the data measured at station G1 on 13 April 1994.

262

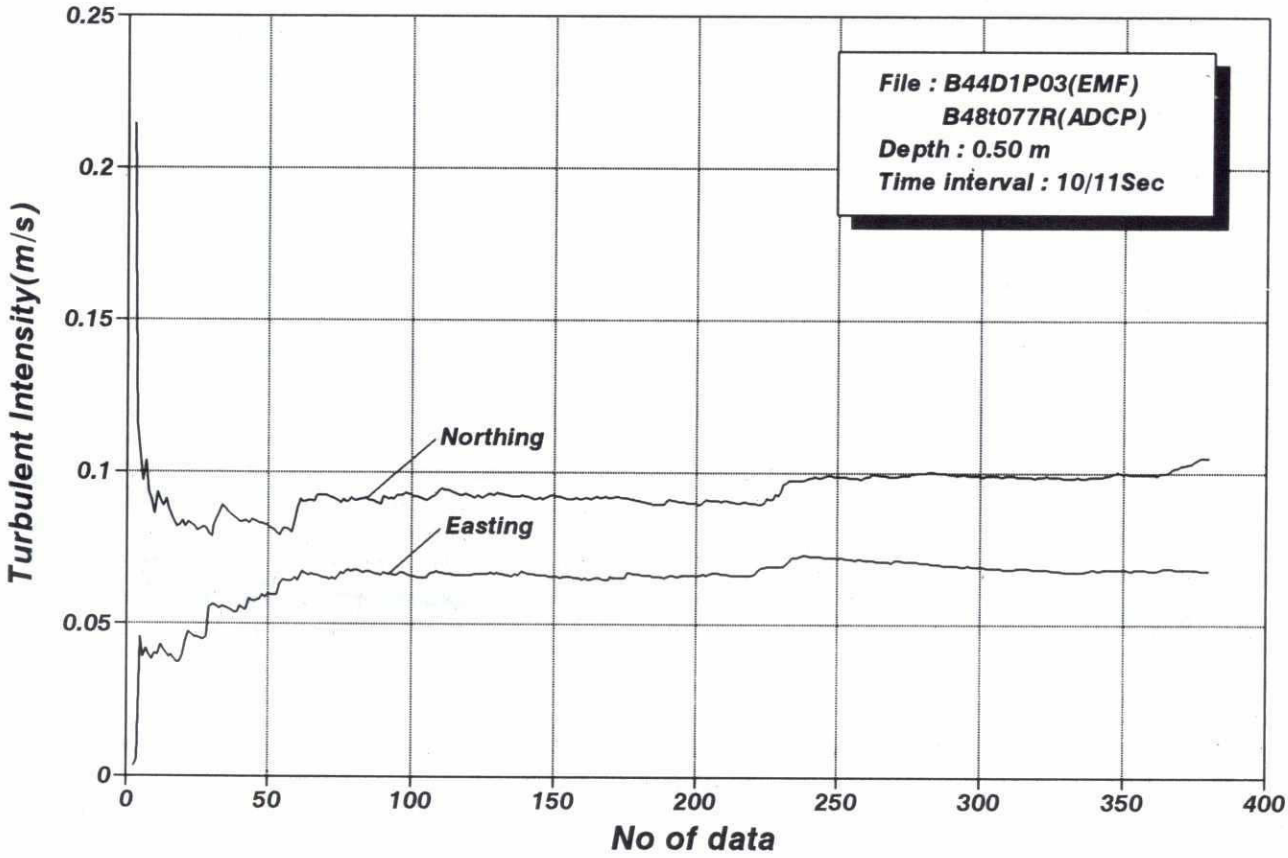

Figure A.31 Turbulence intensities as a function of the numbers of data used for averaging considering the data measured at station B3 on 13 August 1994.

262

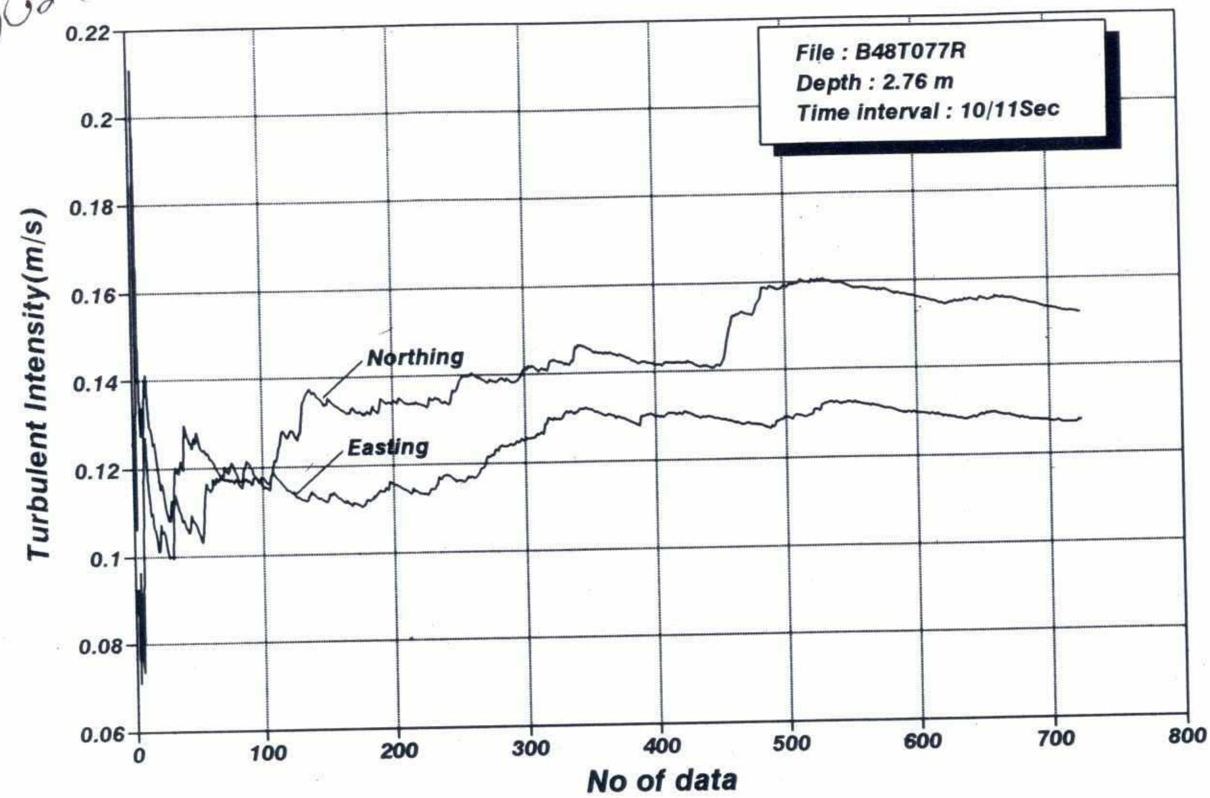

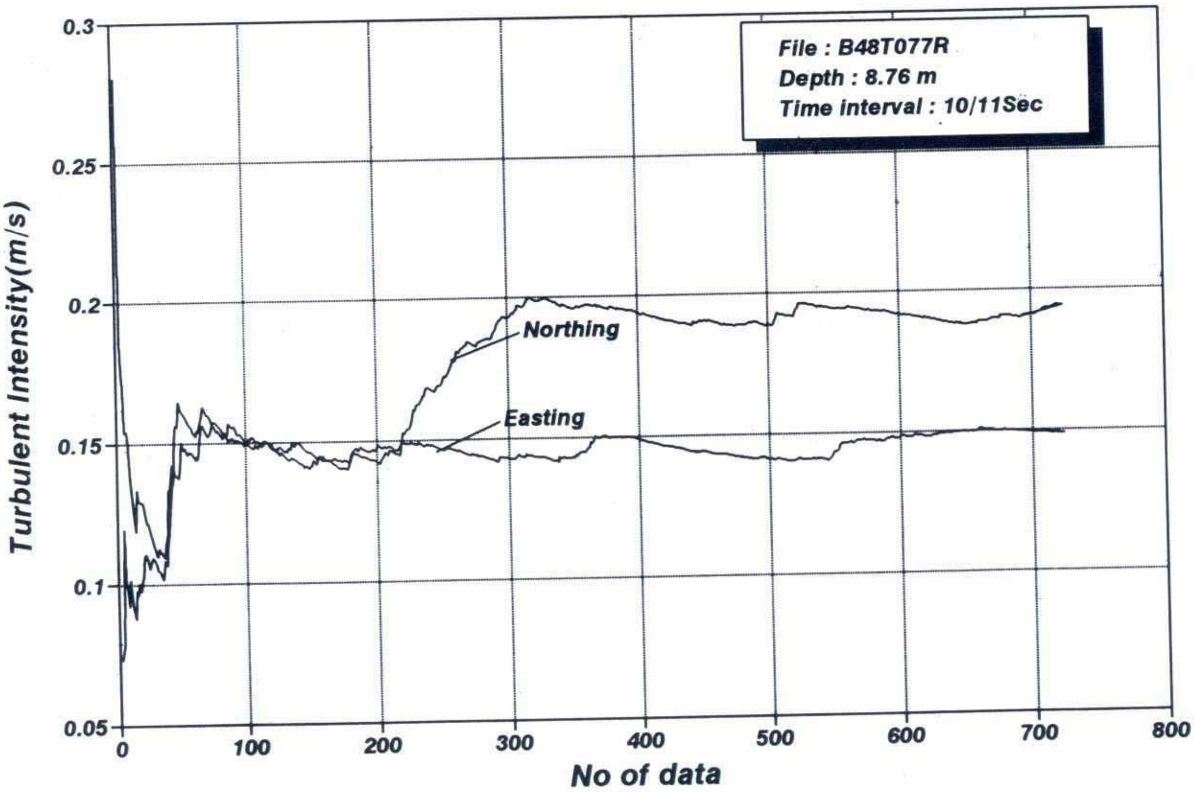

Days

Figure A.32 Turbulence intensities as a function of numbers of data used for averaging considering the data measured at station B3 on 13 August 1994.

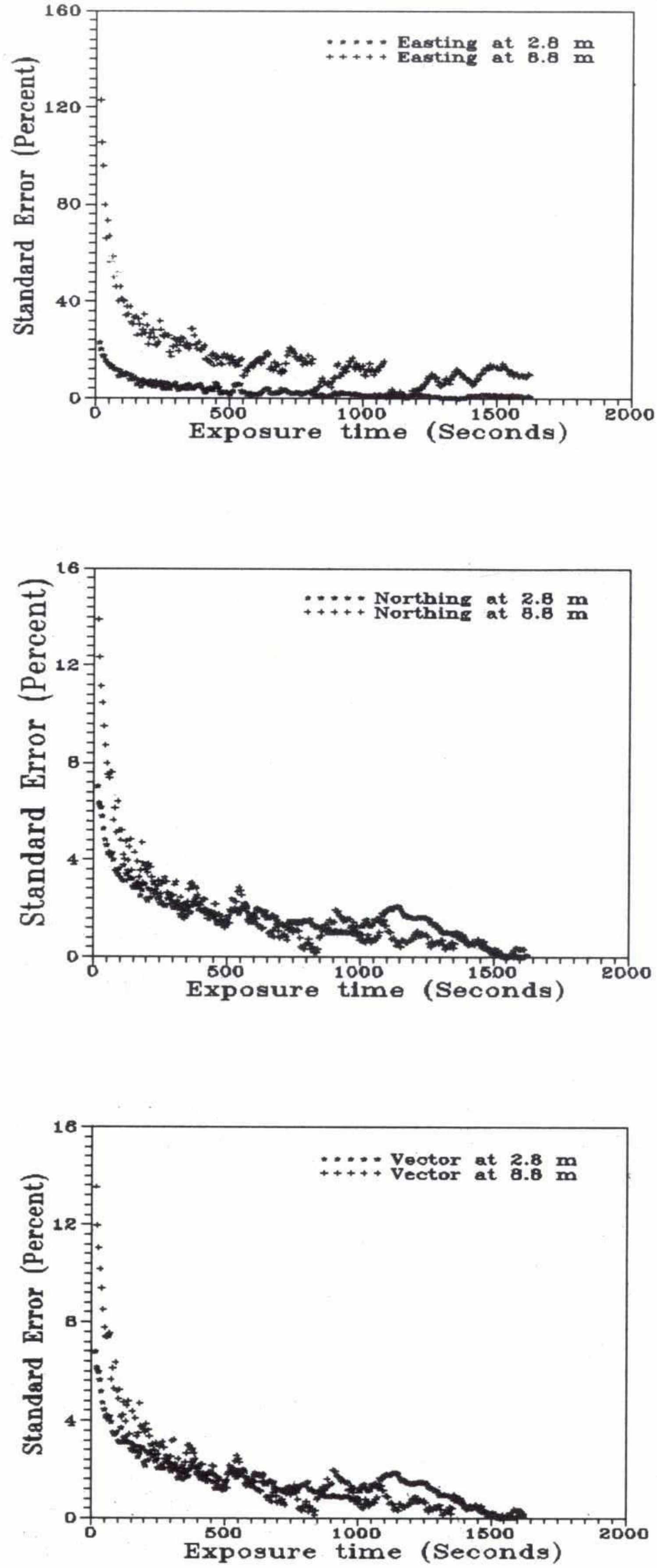

Figure A.33 Standard errors as a function of the exposure time for ADCP velocities measured at station B1 on 1 April 1994.

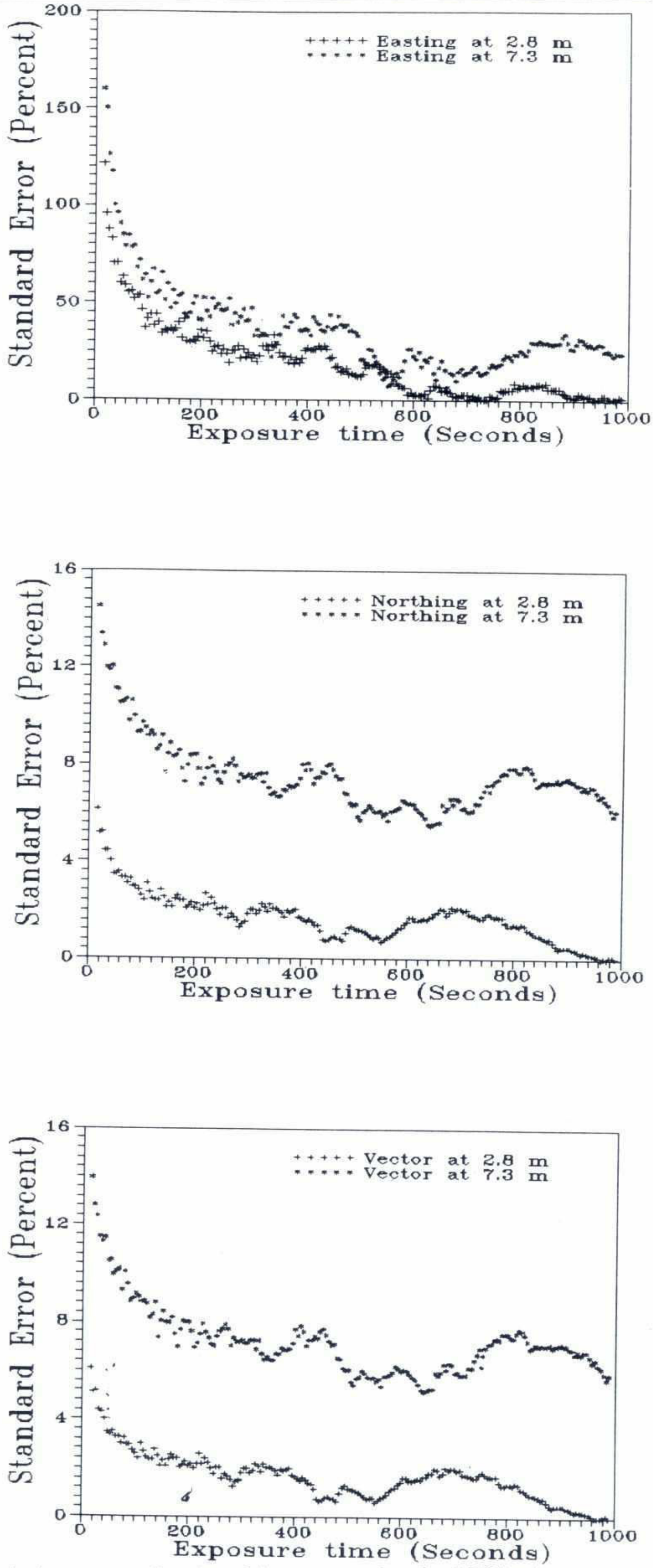

Figure A.34 Standard errors as a function of the exposure time for ADCP velocities measured at station B2 on 1 April 1994.

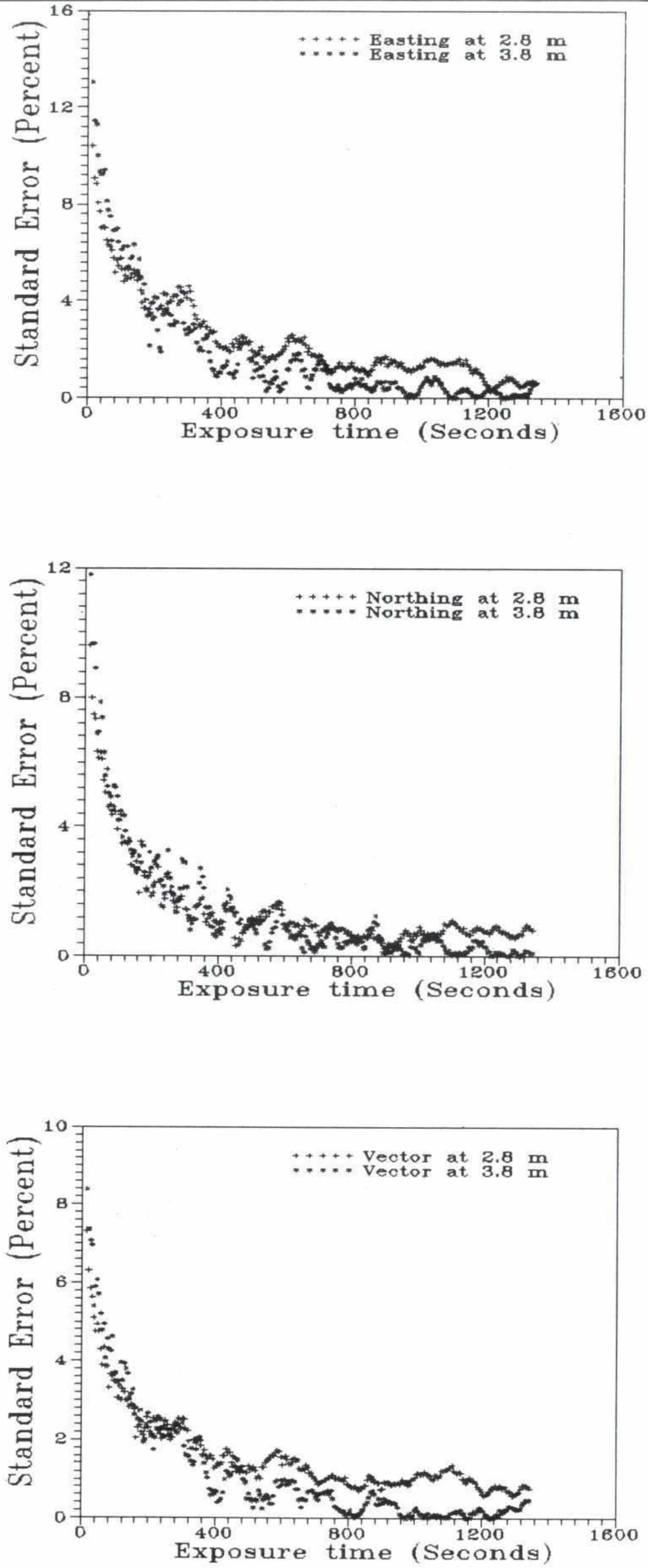

Figure A.35 Standard errors as a function of the exposure time for ADCP velocities measured at station G1 on 13 April 1994.

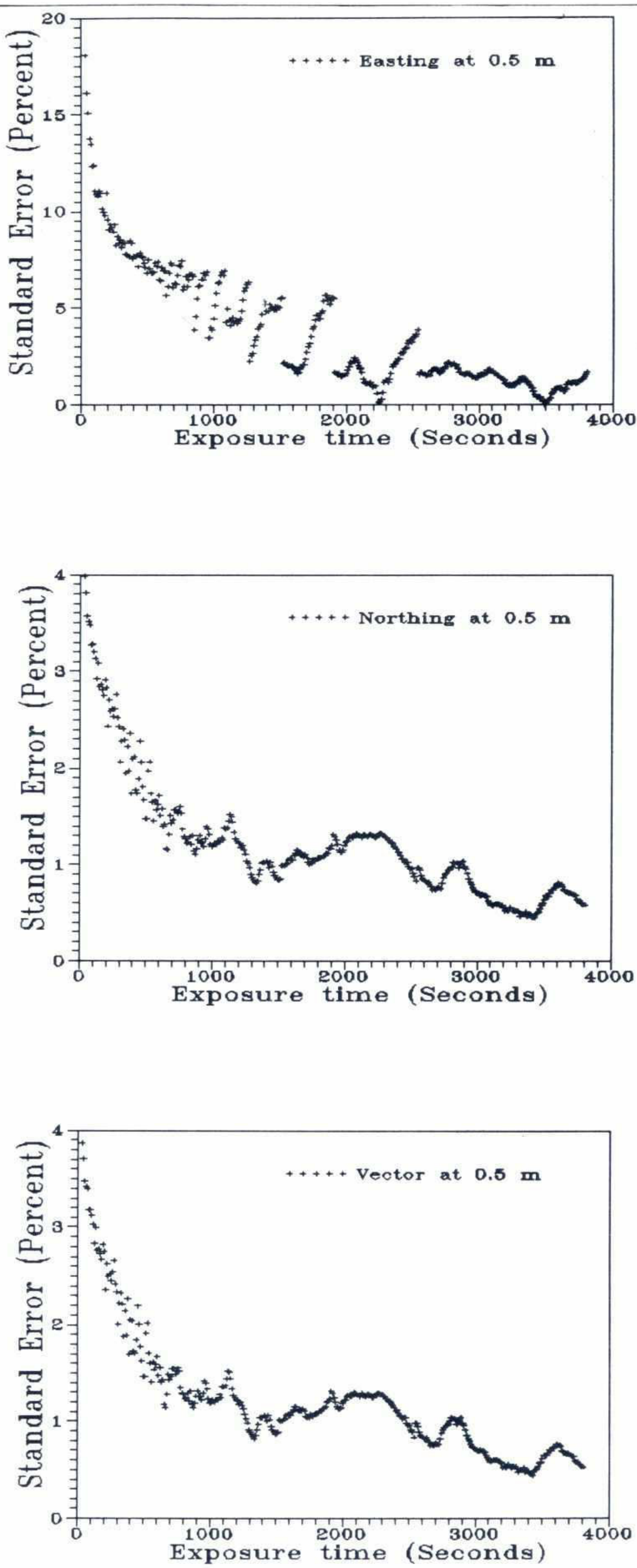

Figure A.36 Standard errors as a function of the exposure time for EMF velocities measured at station B3 on 13 August 1994.

263

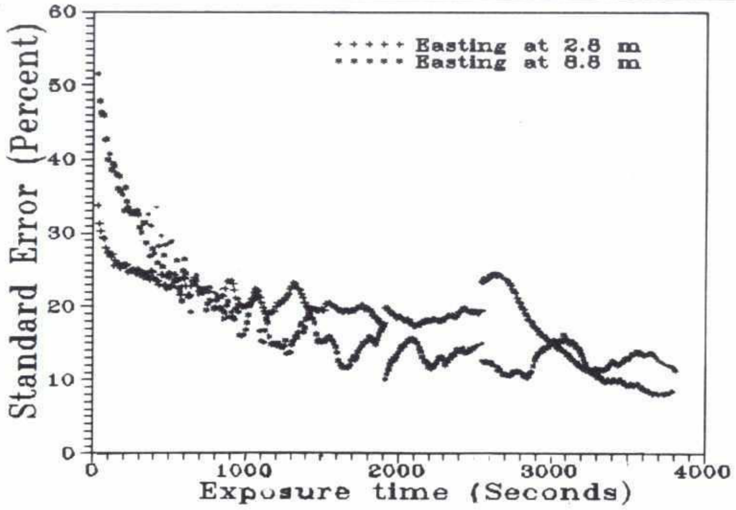

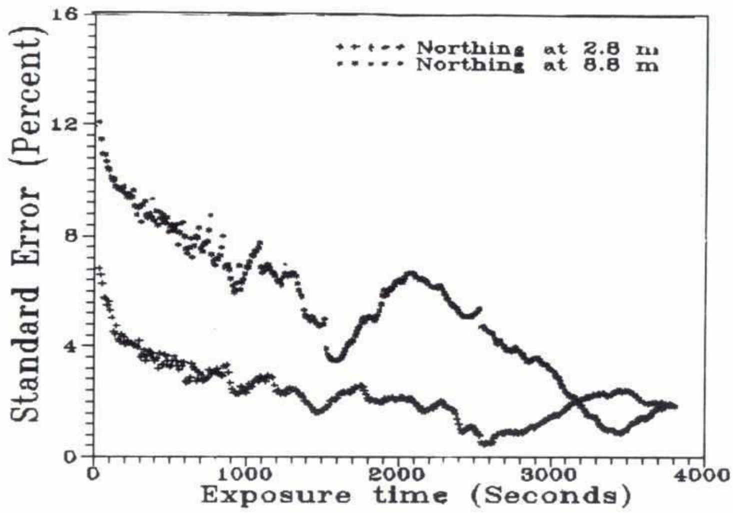

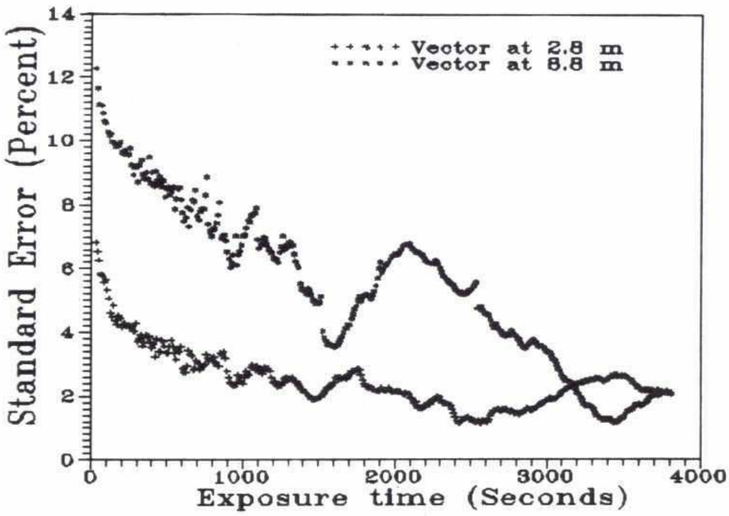

Figure A.37 Standard errors as a function of the exposure time for ADCP velocities measured at station B3 on 13 August 1994.

209

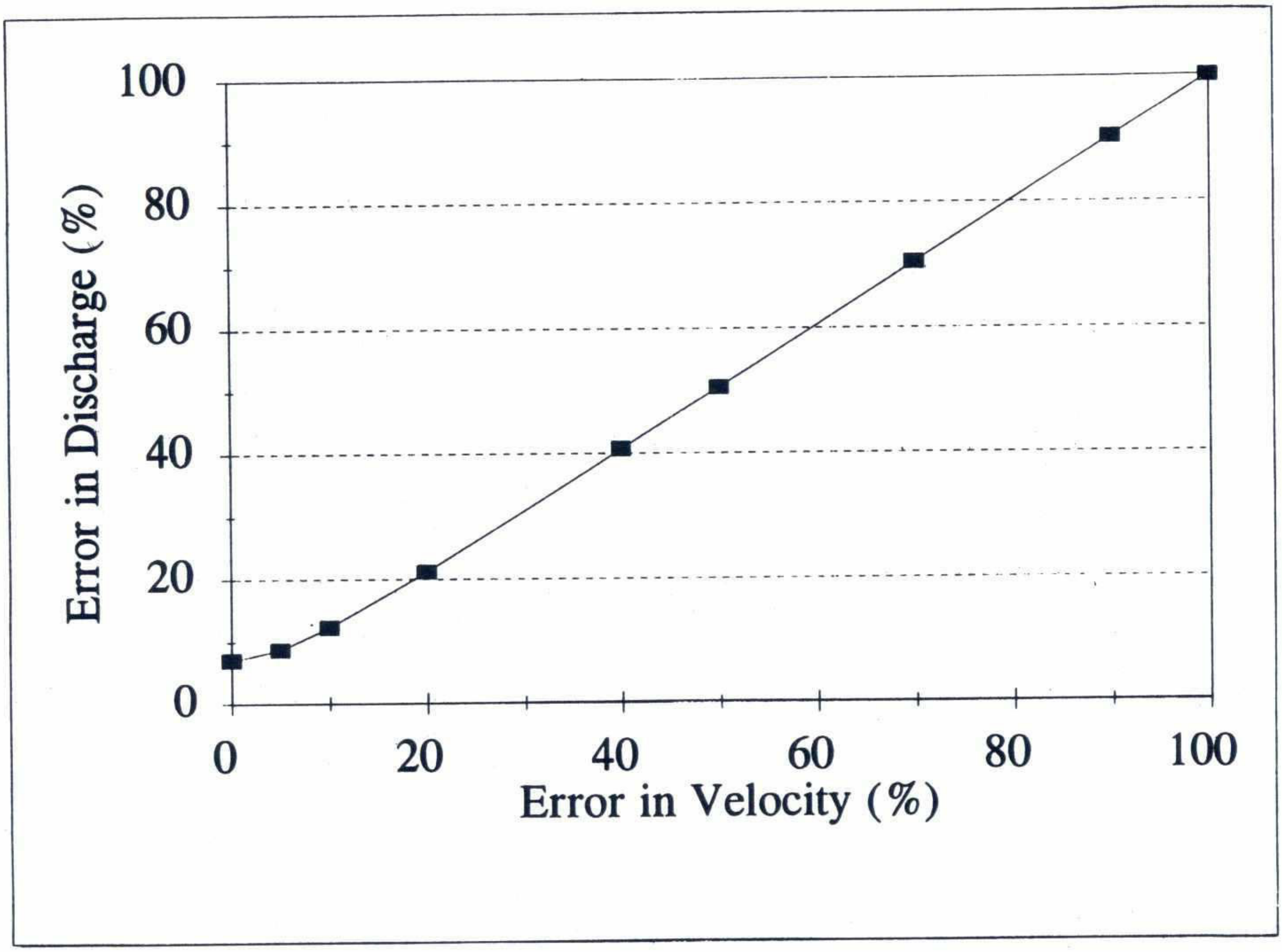

Figure A.38 Theoretical standard errors in estimating discharge as a function of error made in estimating velocity.

26f

Special Report 11, Annexure B

Some Aspects of Turbulent Flow Structure in Large Alluvial Rivers

October 1996

207

Contents

280

Figures

Table

Notation

B	channel width
h	water depth
T_h	horizontal turbulence time-scale
T_v	vertical turbulence time-scale
U	downstream mean flow velocity
U_f	downstream free-stream velocity
U_*	downstream bed-friction velocity
u	downstream instantaneous flow velocity
u'	downstream velocity fluctuation
W	cross-stream mean flow velocity
w	cross-stream instantaneous flow velocity
w'	cross-stream velocity fluctuation
X	downstream axis
Y	vertical axis
Z	cross-stream axis
ν	kinematic viscosity
α, β	coefficients
λ	eddy size

382

Abstract

This paper reports different aspects of turbulent flow structure using the ship-board time-series velocity data collected by an Acoustic Doppler Current Profiler (ADCP) in the multi-thread Jamuna River in Bangladesh. The measurements were made in the mega-ripple environment during the rising river stage and in the large-dune environment during the peak river stage. Based on analyses of the downstream flow velocity obtained from the three subdivisions of the boundary layer, different turbulence parameters such as frequency spectra and related periodicities, and turbulence intensity were found. Spectral analyses of the velocity data indicate that periodicity is obvious in the lower frequency events but obscure in the higher frequencies. The maximum period observed was 18 min and the minimum was about 11.5 s. Resolution of the minimum period to the lowest possible extent is limited by the fact that the resolvable period was 11 s. Analyses of the frequency of occurrence of different periodic events show that about 70% of the turbulence have their origin in the river-bed, the rest are horizontal turbulence having their origin at the river-bank discontinuity. The maximum frequency of occurrence of different turbulent events is in the 11-20 s periodic band. Variability of turbulence intensity in time indicates that 15 min averaging time is required to estimate the turbulence intensity. Over-the-water-column variation indicates a higher turbulence intensity in the wall region than in the free-stream region. Their magnitudes are about 7 to 10% of the local downstream velocity in the free-stream region but increases to about 11 to 23% in the wall region.

1 Introduction

The structure of turbulence in open-channel flows has been the subject of considerable research in recent years. Various aspects of these studies are reviewed and synthesized by Nezu and Nakagawa (1993). One of the aspects deals with the statistical description of turbulence. The description includes different turbulence parameters such as its spectrum and time-scales, and higher-order moments. Among the higher-order moments the second-order moment is known as the turbulence intensity. Investigations of these parameters in large alluvial rivers are important for various reasons. Firstly, the periodicities of turbulence whose time-scales related either to water-depth or to channel width indicate the sources of their origins (Yokosi, 1967; Yalin, 1992). Their origins indicates the river morphology and sediment transport processes (Leeder,1983; Yalin, 1992; Best, 1993). Secondly, a dominant periodicity having a higher spectral power would indicate the length of the averaging which would be necessary to estimate higher order moments (Soulsby, 1980).

Turbulent flow structure comprise a broad spectrum of turbulence frequencies caused by a multitude of eddies having various sizes. The eddies are formed from instability in flow known as Kelvin-Helmholtz instability which is the result of the shear between fluid layers moving at different speeds and/or by friction at the fluid-solid boundary. The sizes of the eddies, *l*, may range from Kolmogorov scale (ν/U_*) to the flow thickness equal to water depth, h.

$$\frac{\nu}{U_*} \leq \lambda \leq h \qquad (1)$$

Where ν is kinematic viscosity and U_* is downstream bed friction velocity. The spatial scales of eddies as shown in equation 1 can be transformed to temporal scales by applying Taylor's hypothesis, $T = \lambda/U$, in which T is period and U is local mean downstream velocity. In terms of free-stream velocity (U_f), the periods of vertical turbulent eddies (T_v) can, therefore, have the following ranges (Yalin, 1992):

$$\frac{\alpha\,[\frac{\nu}{U_*}]}{U_f} \le T_v \le \frac{\beta h}{U_f} \qquad (2)$$

where ν and β are coefficients. β varies between 3 and 7 with a mean of about 6 (Yalin, 1992). The higher ranges represent macro time-scale turbulence which was originally proposed by Rao *et al.* (1971). Levi (1983) proposed that the higher ranges follow the Strouhal Law and that $\beta = 2\pi$. They represent vertical turbulent eddies whose axes of rotation are perpendicular to the vertical X, Y plane. In open channel flows eddies also form with their axes of rotation perpendicular to the horizontal X, Z plane (Yokosi, 1967). The time-scale (T_h) of this horizontal turbulence is about (Yalin, 1992),

$$T_h = \frac{\beta B}{U_f} \qquad (3)$$

where B is channel width. Yokosi (1967) found β coefficient as 9 based on his measurements in the Uji River.

We investigated various aspects of turbulent flow structure which include different parameters such as frequency spectrum, turbulence time-scales and intensity based on ship-board time-series velocity measurements in the Brahmaputra River (Jamuna River in Bangladesh). The objectives are to show their magnitudes and variability in space and time which can be used to study sediment transport mechanism and river morphology. Data used for this study were collected for optimization of hydraulic measurements by the River Survey Project (FAP24). This project was launched in 1992 by the Flood Plan Coordination Organisation, Government of Bangladesh and funded by the European Union.

The Brahmaputra-Jamuna River draining the northern slope of the Himalayas is a top ranking river in the world both in terms of its discharge and sediment flux (Milliman and Meade, 1983). The 290-km long river-reach (Figure B.1) in Bangladesh traversing over the deltaic alluvial plain is a highly mobile multi-thread fine sand-bed river. Various characteristic features and morphological aspects of the river are described by Coleman (1969), Bristow (1987), Klaassen and Vermeer (1988), Thorne *et al.* (1993), Barua (1994), Barua *et al.*(1995). The river has an average width of about 11 km and a mean depth of about 5 m. With an annual average discharge of about 19,600 m^3/s, it carries an annual sediment load of some 500 million tons. The river has an average bed-slope of 7×10^{-5}. It is a fine sand-bed river with an average median diameter of about 220 μm.

2 Field measurements

Time-series field measurements were made by FAP24 survey vessels in the Jamuna River left channel near Bahadurabad (Figure B.1). This channel is currently the active channel of the multi-thread Jamuna River. Figure B.2 shows the bed-profiles at the measuring stations. The total water-depths at the three stations B1, B2 and B3 were 9.6, 8.3 and 10.0 m, respectively. Different dune-scale bed-forms were present during the measurements representing the images from mega-ripples to dunes. While mostly mega-ripples were present during April 1 measurements (Fig B.2a, B.2b), large dunes were present during August 13 measurement (Figure B.2c). Measurements at station B1 represent an accelerating flow condition (flow approaching a lower-depth region) while the measurements at station B2 represent a decelerating flow condition (flow leaving a lower depth region). Measurements on 13 August represent a dune crest location. Figure B.3 shows the 1994 hydrograph of the river stage observed at Bahadurabad. The April 1 measurements made at stations B1 and B2 represent typical conditions during a seasonal rising river stage which occurred just after a small and short-duration peak. The August measurements executed at station B3, on the other hand, are on the high river stage which occurred during the rising limb of a short peak.

The measurements at stations B1, B2 and B3 were made by a 300 kHz ADCP from a vessel moored by one bow anchor. Measurement durations were 54 min at B1 and 33 min at B2; on August 13 the duration of measurements was 127 min. A Differential Global Positioning System (DGPS) was used for positioning of the vessel which in stationary mode has an accuracy of about ± 3m. Various aspect of the measurement are presented in Table B.1.

The principle of acoustic measurements under water is described by Urick (1975). The ADCP implemented by FAP24 uses four beams which are positioned 90° apart horizontally and directed downward into the water column at an angle of 20° from the vertical. The ADCP sends pulses along each of its beams and part of the transmitted acoustic energy is reflected back toward the transducers by particulate matter (scatter) moving with the water (RD Instruments, 1989). The ADCP detects the reflected signals from each beam at discrete time intervals during the progress of the advancing acoustic wave front which allows velocities to be determined at depth-intervals or bins. The ADCP can transmit and acquire acoustic data and can calculate water velocity for each depth bin at a rate of up to 10 profile measurements (pings) per second (RD Instruments, 1989). The ADCP used for the measurements has a bin-length of 0.5 m. In the 300 kHz ADCP 10 pings (profiles) are made in a period of 5 to 6 s. The first bin is located at about 2.8 m below surface and the last bin is located at 6% of the water depth above the river bed. The average of these 10 pings are stored at about 5.5 s interval for 300 kHz ADCP. The standard deviation of the acquired velocity is 30 cm/s which reduces to 9.5 cm/s for the time-averaged situation of 10 pings. Rotation and translation of the ADCP are measured by different devices. Heading rotation is measured by gyrocompass, and pitch and roll rotation are measured inside the ADCP electronically. The translation is measured on-line by bottom tracking.

Station	Date	Total depth, h (m)	Measurement duration (minutes)	Measurement elevation, Y (m)	Y/h	Time-mean downstream velocity (m/s)	Turbulence intensity (m/s)	Turbulence intensity as percent of velocity (%)
B1	1 Apr 94	9.6	54	6.8	0.71	1.36	0.13	9.6
				4.8	0.50	1.19	0.15	12.6
				0.8	0.08	0.78	0.18	23.1
B2	1 Apr 94	8.3	33	5.5	0.66	1.25	0.12	9.6
				4.0	0.48	1.12	0.13	11.6
				1.0	0.12	0.82	0.18	22.0
B3	13 Aug 94	10.0	127	7.2	0.72	1.79	0.12	6.7
				5.2	0.52	1.68	0.14	8.3
				1.2	0.12	1.39	0.16	11.5

Table B.1: Summary of measurement characteristics and other turbulence parameters at stations B1, B2 and B3

3 Analyses and results

3.1 Data reduction and analyses

Proprietary logging software allows ADCP velocity at recorded intervals are given in Easting, Northing and Vertical directions. In addition, vector magnitudes and directions are given simultaneously. These records are given at 0.5 m bin-lengths. The vertical velocity component lying mostly within the accuracy range of ADCP, precluded its use for further analyses. We used the other velocity components to obtain the downstream and the cross-stream velocity components. The Bathurst *et al.* (1977) method was used for velocity reduction which has also been used among others by Bridge and Gabel(1992) to compute the downstream and the cross-stream components. The method essentially assumes the depth-mean cross-stream component to be zero. At these stations the cross-stream component was found to be negligibly small and within the accuracy range of ADCP, therefore, we did not use the data for further analyses.

We subjected the downstream velocity component to auto-correlation and spectral analysis techniques. Such techniques are commonly used to determine the frequency spectrum of turbulence flow structure (for example, by McLean and Smith, 1979). We used HYMOS data-base programme (Delft Hydraulics, 1992) to analyze the time-series data. In this programme smoothed auto-spectral density function is computed as a function of frequency. The smoothed power spectrum is ensured by including the Tukey window function. A smoothed power spectrum is a better technique of showing the true periodic structure compared to a raw power spectrum (Davies, 1973). The spectral density obtained by the analyses is normalised against autocovariance function at 0 time-lag, therefore, the output is given as coefficient or function of auto-spectral density. To get a better representation of the data used, the maximum truncation lag is taken as 15% of the total data points (Haan, 1977). The programme is able to handle 400 equidistant time-series data with a record-length of about 40 to 70 min. 5.5 s recording intervals by ADCP imply that the Nyquist frequencies for the 300 kHz ADCP data is $1/2*5.5=0.09$ representing resolvable recurrence intervals of 11 s. The unresolvable high frequencies get aliased to the resolved frequencies.

The total duration of records from the different stations at the recorded ADCP bins and pings comprise huge quantities of digital data. We had to make a choice in the selection of the data in order to limit the number of analyses but without loosing the interesting variability over the water column. Obviously, we made a choice based on the three sub-divisions of open channel flow field (Nezu and Nakagawa, 1993). In this sub-division, the free-stream region occurs in the water column between Y/h = 60% and 100%, and the wall region between 0% and 15%, with the intermediate region covering the in-between location. Our final choice was made on the basis of ADCP bin-configurations and trying to avoid corrupt data. The free-stream velocity was taken from the first bin which occurred at Y/h =71% to 72 %. The wall region was chosen at 8% to 12% and the intermediate region was chosen at 50% above the bed.

3.2 Turbulence frequency spectra

A maximum 40 to 70 min of downstream velocity data from the selected bins representing different regions of the boundary layer were subjected to time-series analyses. The results from the three stations are shown in Figures B.4, B.5 and B.6. Figure B.4 shows the downstream velocity data from station B1 and their spectral density functions at different frequency points. The time-mean velocity U, at the three levels were 1.36 m/s (Figure B.4a), 1.19 m/s (Figure B.4b) and 0.78 m/s (Figure B.4c). Figure B.4d shows the spectral density function at different frequency points. Overall, the spectral densities are higher for low frequent events. The spectral powers of highly frequent eddies are negligible and close to about 2 in all the cases. Maximum periods of the analyzed series were 550 s at Y/h = 0.7, 1100 s at Y/h = 0.5 and 157 s at Y/h = 0.1. Similarly, the minimum periods observed were 12 s, 12 s and 11.5 s. at these elevations. The periods representing the highest spectral densities in the three regions were, 100 s at Y/h = 0.7, 157 s at Y/h = 0.5 and 157 s at Y/h = 0.1. The close correspondence of frequency events at the three levels are noticeable in the low frequent events.

Similar data and results are shown for station B2 in Figure B.5. The time-mean velocities at this station were 1.25 m/s at Y/h = 0.7 (Figure B.5a), 1.12 m/s at Y/h = 0.5 (Figure B.5b) and 0.82 m/s at Y/h = 0.1 (Figure B.5c). Figure B.5d shows the spectral density as a function of frequency points. The highest periods observed was 100 s in free stream region, 367 s in the intermediate region and 109 s in the wall region. The lowest period in all the cases was about 12 s.

The results of high river stage measurement at station B3 are shown in Figure B.6. The time-mean velocities at this station were 1.79 m/s at Y/h = 0.7 (Figure B.6a), 1.68 m/s at Y/h = 0.5 (Figure B.6b) and 1.39 m/s at Y/h = 0.1 (Figure B.6c). A long period of about 30 min is obvious in the velocity record. Figure B.6d shows the spectral densities at different frequency points. The highest periods observed were 350 s in the wall region and 263 s above. The lowest periods observed were 21.9 s at Y/h = 0.1 and 23.6 above. The long periodicity in the data (about 30 min) obviously could not be resolved by our programme which can handle only 40 minutes of digital data. Figure B.7 shows a typical boil observed near the vessel on the measurement day.

At all the stations a broad spectrum of frequencies existed representing different periods. However, the higher frequency events appear to be more stochastic than periodic, as the spectral power of them are very low (around 2), although few periodicities are discernable. The distribution of spectral density at different frequency points is not identical at the three stations. Nevertheless some overall similarities can be noticed. The periodicities of low frequent events are obvious and spectral densities of them in the wall region are higher than above. Comparison of Figures B.4d, B.5d and B.6d shows that in the low frequent events, the August measurements show a higher spectral power than the others. Also, the spectral power at station B2 is higher than B1. This may be related to the accelerating and the decelerating flow conditions.

The occurrence of different frequency events are further synthesised in Figure B.8. It shows a summary of frequency of occurrence of different periodic events (irrespective of their spectral density) at the three analyzed elevations of the water column. At stations B1 and B2 the highest occurrence is in the period 11 to 20 s. This periodic event is not available for B3, because the resolvable period here is 21 s. The frequency of occurrence gradually decreases as the periods are increased. Although the period at B3 could not resolved below 21 s, it appears logical to suggest that the dominant events have a period between 11 and 20 s. A smaller-scale period is also possible, but we do not have any idea of them due to the practical limitation of the data.

3.3 Turbulence intensity

We attempted to show the variability of turbulence intensity defined as,

$$\sqrt{\overline{(u-U)^2}}$$

in time and Y dimensions. Time-dimension is important because it indicates the influence of averaging time which should be used for obtaining turbulence intensity. Figure B.9 shows the turbulence intensity as a function of the averaging time for stations B1, B2 and B3. They show that a wrong turbulence intensity can be estimated by choosing a 'too short' or 'too long' averaging time. At station B1 (Figure B.9a), the turbulence intensity stabilise to a nearly constant value at an averaging time of about 300 s. Using an averaging time longer than that does not change intensity value. Similar time applies for station B2 (Figure B.9b). However. here, at Y/h, the intensity increases as the averaging time is increased. Station B3 gives a longer record (Figure B.9c). Here, the choice of an averaging time appears to be very crucial. Turbulence intensity appears to be varying and getting larger as the averaging time is increased. This is probably related to be periodicity in the data as well as non-stationality in flow. We chose a 900 s averaging time to estimate the turbulence intensity. They are shown in Table B.1. As expected the variation of the intensity over the water column can also be noticed. It is higher in the wall region and lower above. Such vertical variation is common and has been observed by other investigators (Grass, 1971). Turbulence intensity at all the stations are of the same order of magnitudes and varies from about 0.12 m/s in the free-stream region to 0.18 m/s in the wall region.

We further showed the vertical distribution of turbulence intensity by making it dimensionless (Figure 10). Using an averaging time of 900 s, turbulence intensity was determined at each depth cell (bin). The bed friction velocity U_* was determined from the velocity profile. In order to reduce the pulsation error (River Survey Project, 1995), we averaged 11 profiles (representing a 50 s exposure time) to derive a single profile. From each station, one such profile was chosen and a log-linear Karman-Prandtl profile was fitted. The values obtained for the three stations ranged from 0.07 to 0.12 m/s. They are comparable to the mean bed-friction velocity obtained by using the river-slope. Assuming a slope of about $7x10^{-5}$ for Jamuna River and a depth of 10 m, the mean bed-friction velocity obtained was about 0.08 m/s. We used a bed friction velocity of 0.1 m/s to obtain the dimensionless turbulence intensity. These values are plotted in Figure B.10. It shows that the peak turbulence intensity occurs at about Y/h = 0.05. After that it gradually diminishes.

4 Discussion

Although the analyses of time-series velocity data observed by using a 300 kHz ADCP indicate some interesting turbulence parameters in the Jamuna River in Bangladesh, it is necessary that we are aware of the certain limitations in the data. First is related to the dynamic position of the vessel which contains actual oscillation of the vessel and the DGPS positioning. In addition, ADCP beams spreading at 20° from the vertical averages a larger area near to the bed. The implication of this is that we assume the velocity to be homogenous within the covered area. Second is the inability of ADCP to record instantaneous velocity data to an acceptable accuracy level. With the time-averaged data (5.5 s or 10.5 s) which we used, frequencies smaller than 11 and 21 s could not be resolved.

Using the frequency spectra, some idea could be formed of turbulence time-scales. Assuming h to be the eddy size scale, use of equation 2 indicates that the vertical turbulence time-scale can be in the order of 33 to 46 s for a water-depth of 10 m and a free-stream velocity range of 1.3 to 1.8 m/s. Examination of Figure B.8 shows that this time-scale event and lower than them occur for about 60% to 80% of the time. Events having periods higher than that must belong to the horizontal turbulence spectra. With the observed maximum period of 1100 s, use of equation 3 indicates that the channel width can be in the order of 240 to 330 m. This width-scale is obviously the scale of a third order channel in the Jamuna River (Bristow, 1987). However, it should be noted that time-scales larger than that can also occur. For example, at station B3, a long period of about 30 min is obvious (Figure B.6c) providing a width-scale of about 500 m. The observed highest periods 18.3 or 30 min can be compared with the 14 min observed in the Uji River by Yokosi (1967).

With the dominant period of 11-20 s, a 900 s averaging time means that some 45 to 80 burst forming events are sampled to estimate turbulence parameters. This can be compared with the observations by Soulsby (1980). Based on the considerations that at least 30 bursts should be included to determine turbulence intensity, he suggested that at least 10 to 15 min should be used for averaging.

It is interesting to see how the turbulence intensity scales with the local velocity. Bowden and Fairbrin (1956) observed that the turbulence intensity is about 8-10% of the velocity. Our comparisons summarised in B.1 show that they can range from 6.7% to 23.1% of the local downstream flow velocity. In all the cases, the higher percentages occurred in the wall region.

5 Conclusions

ADCP time-series velocity data measured at different stations in the Jamuna River during rising and peak river stages reveal various interesting aspects of turbulent flow field. Analyses of the downstream velocity component were made over the water column covering three sub-divisions of open-channel flow - the free-stream region, the intermediate region and the wall region. The measurements were made in the mega-ripple to dune-size bed-form environment.

Auto-correlation and Fourier analyses of the downstream time-series velocity data indicate that a broad spectrum of turbulence frequencies exist. However, while the periodicity is obvious in the low frequency events, they are obscure in the higher frequencies.

It appears that an averaging time of about 15 min. should be used to estimate various turbulence parameters. Turbulence intensity was found to be 7 to 23% of the local flow velocity. Over-the-water-column analyses of turbulence intensity indicates that it is higher in the wall region and lower above.

Acknowledgements

The authors would like to thank several of their office colleagues at the River Survey Project for their help during this study. Particularly, we like to thank Messrs. H. Hoyer, P. van Groen, M. van der Wal, G. J. Klaassen and J. J. Peters. Drs. J. Best and P. Ashworth at the University of Leeds made valuable suggestions at an early stage of drawing up of this manuscript. DELFT-DHI consortium and the University of Leeds kindly supported the conference participation. This study, carried out as an optimization of hydraulic measurements was supported by the Flood Plan Coordination Organisation, Government of Bangladesh and the European Union.

References

Barua, D.K., 1994. 'On the environmental controls of Bangladesh river systems', *Asia Pacific J. on Env. and Dev., Bangladesh Unnayan Parishad,* **1(1),** 81-98

Barua, D.K., Klaassen, G.J. and Mahmood, S., 1995. 'On the adaptation and equilibrium of Bangladesh rivers, *Proc. 6th International Symposium on River Sedimentation,* New Delhi, India

Bathurst, J.C., Thorne, C.R. and Hey, R.D., 1977. 'Direct measurements of secondary currents in river bends', *Nature,* **269,** 504-506

Best, J.L., 1993. 'On the interactions between turbulent flow structure, sediment transport and bedform development : some considerations from recent experimental research', in Clifford N.J., French, J.R. and Hardisty, J. (Eds.), *Turbulence: Perspectives on Flow and Sediment Transport,* Wiley, Chichester

Bowden, K.F., and Fairbrin, L.A., 1956. 'Measurements of turbulent fluctuations and Reynolds stress in a tidal current', *Proc. Roy. Soc. London,* **A237**, 422-438

Bridge, J.S. and Gabel, S.L., 1992. 'Flow and sediment dynamics in a low sinuosity braided river: Calamus River, Nebraska Sandhills', *Sedimentology*, **39**, 125-142

Bristow, C.S., 1987. 'Brahmaputra River: channel migration and deposition', in Ethbridge, F.G., Flores, R.M, and Harvey, M.D. (Eds), *Recent Developments in Fluvial Sedimentology*, Society of Economic Paleontologists and Mineralogists Special Publications, **39**, 63-74

Coleman, J.M. 1969. 'Brahmaputra River : channel processes and sedimentation', *Sediment Geol.*, **3**, 129-239

Davies, J.C., 1973. *Statistics and data analysis in Geology*, Wiley, Chichester, 550 pp

Delft Hydraulics, 1992. *Introduction to HYMOS, version 3.00,* Delft Hydraulics, Delft, the Netherlands

Grass, A.J., 1971. 'Structural features of turbulence over smooth and rough boundaries', *J. Fluid Mech.,* **50,** 233-255

Haan, C.T., 1977. *Statistical methods in hydrology*. The Iowa State University Press, Iowa, 378 pp

Klaassen, G.J., and Vermeer, K., 1988. 'Channel characteristics of the braiding Jamuna River, Bangladesh', *Proc. int. conf. fluvial, Hydraul, Budapest, Hungary,* 395-408

Leeder, M.R., 1983. 'On the interactions between turbulent flow, sediment transport and the bedform mechanics in channelized flows', *Spec. publ. int. Assoc. Sediment,* **6,** 5-18

Levi, E., 1983. 'A universal Strouhal law', *J. Eng. Mech. ASCE,* **109 (3),** 718-728

McLean, S.R. and Smith, J.D., 1979. 'Turbulence measurements in the boundary layer over a sand wave-field', *J. Geophys. Res.,* **84(C12),** 7791-7808

Milliman, J.D. and Meade, R.H., 1983. 'World-wide delivery of river sediment to the oceans', *J. Geol.*, **91**, 1-21

Nezu, I. and Nakagawa, H., 1993. *Turbulence in open-channel flows,* A. A. Balkema, Rotterdam, 281 pp

Rao, K.N., Narashima, R. and Narayanam, M.A.B., 1971. 'The bursting phenomenon in a turbulent boundary layer', *J. Fluid Mech.,* **48,** 339-352

RD Instruments, 1989. *Acoustic Doppler Current Profilers - principle of operation: a practical primer,* RD Instruments, San Diego, California

River Survey Project, 1995. 'Optimization of hydraulic instruments: turbulent flow structure and an optimum averaging time', *River Survey Project working paper,* Flood Plan Coordination Organization, Government of the People's Republic of Bangladesh

Soulsby, R.L., 1980. 'Selecting record length and digitization rate for near-bed turbulence measurements', *J. Phys. Ocean.,* **10,** 208-219

Thorne, C.R., Russel, A.P.G. and Alam, M.K., 1993. 'Planform pattern and channel evolution of the Brahmaputra River, Bangladesh', in Best J.L. and Bristow, C.S. (Eds), *Braided rivers,* Geological Society Special Publication, **75,** 257-276

2870

Urick, R.J., 1975. *Principles of underwater sound,* McGraw-Hill, New York, 384 pp

Yalin, M.S., 1992. *River Mechanics,* Pergamon Press, Oxford, 219 pp

Yokosi, S., 1967. 'The structure of river turbulence', *Bull. Disaster Prevention Res. Inst., Kyoto Univ.,* **17**, 2-121

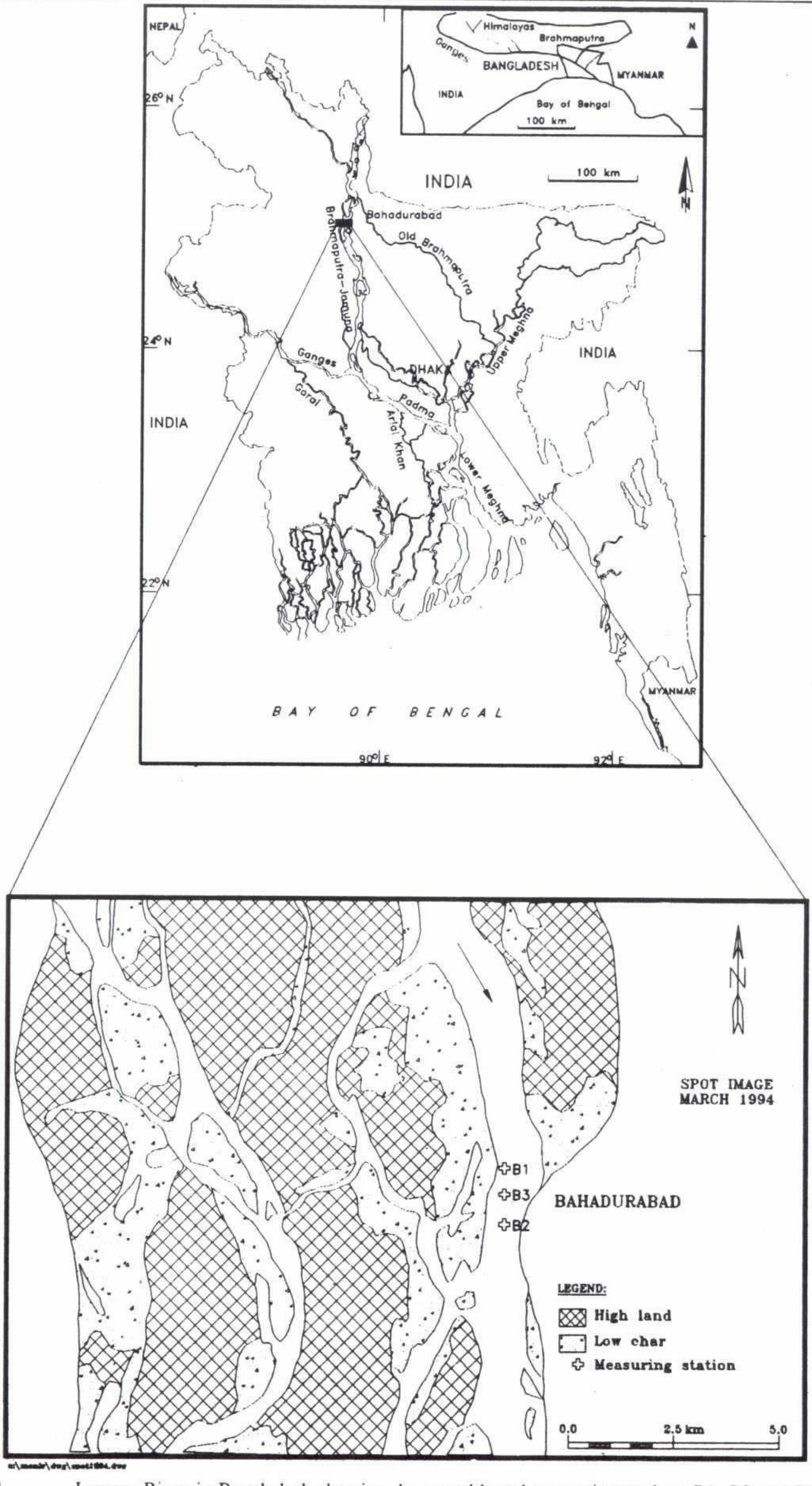

Figure B.1 Jamuna River in Bangladesh showing the vessel-based measuring stations B1, B2 and B3 on the left anabranch near Bahadurabad

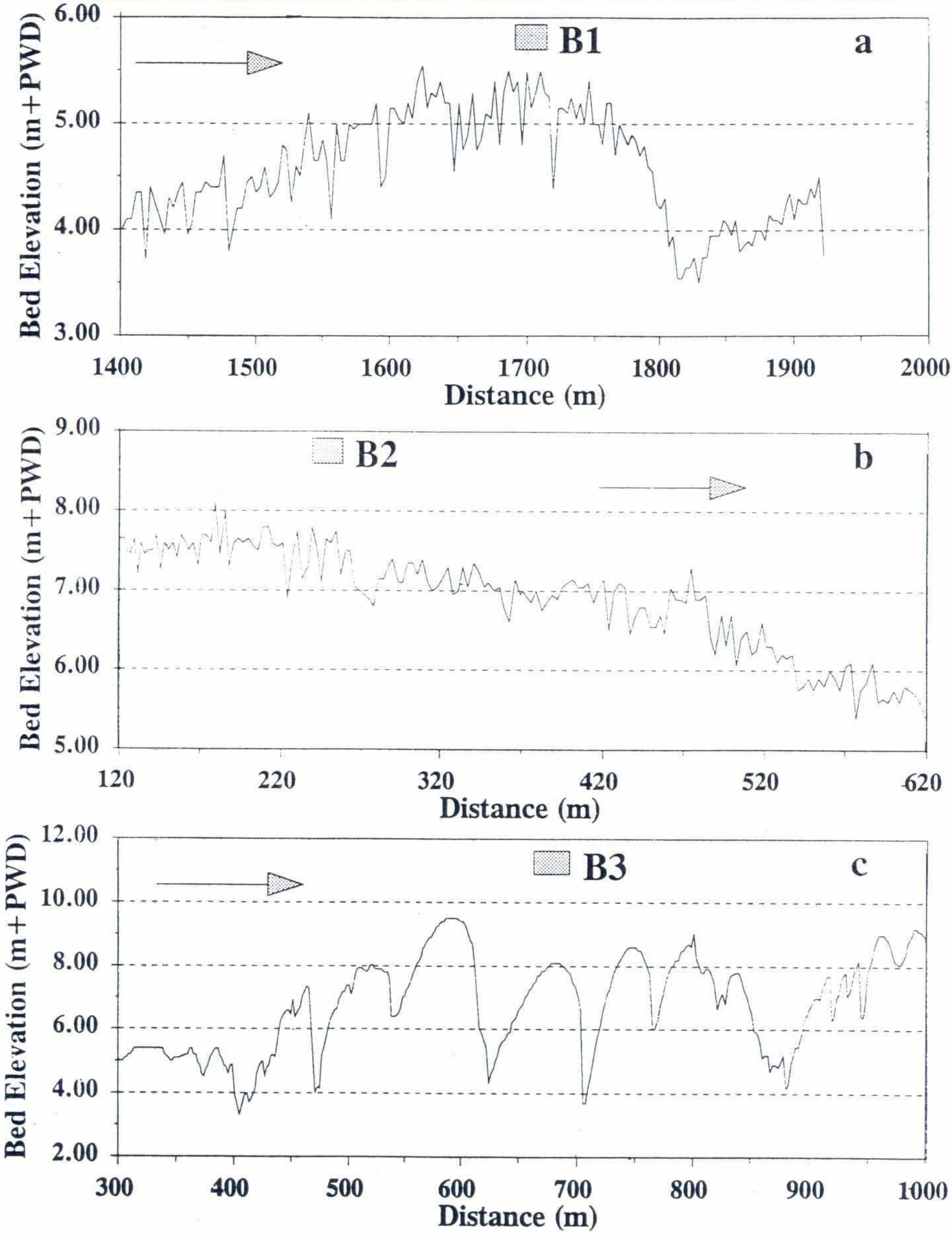

Figure B.2 Bed-profile covering part of the long-stream sounding lines. a. across station B1. b. across station B2. c. across station B3. PWD refers to Public Works Datum - a national datum of Bangladesh

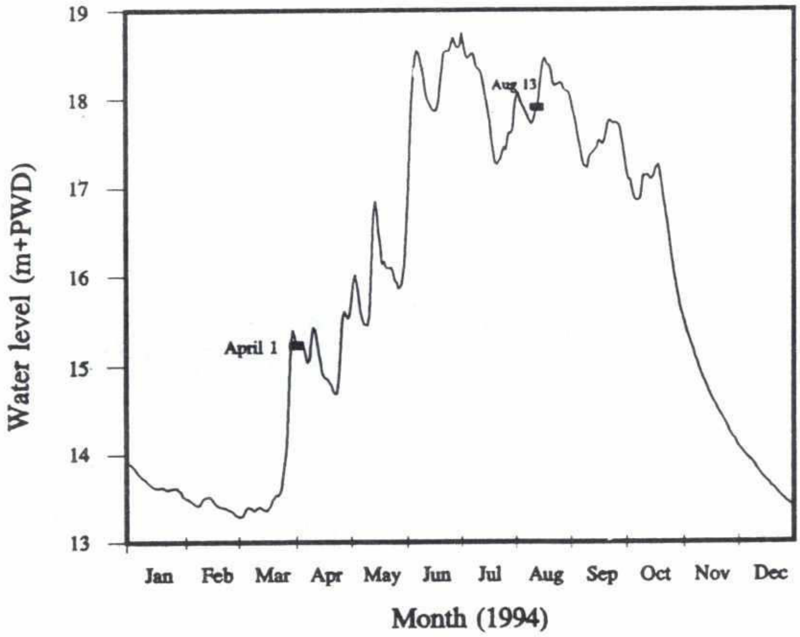

Figure B.3 Water level hydrograph of the Jamuna River at Bahadurabad in 1994 showing river stages during which the measurements were executed. PWD refers to Public Works Datum - a national datum of Bangladesh

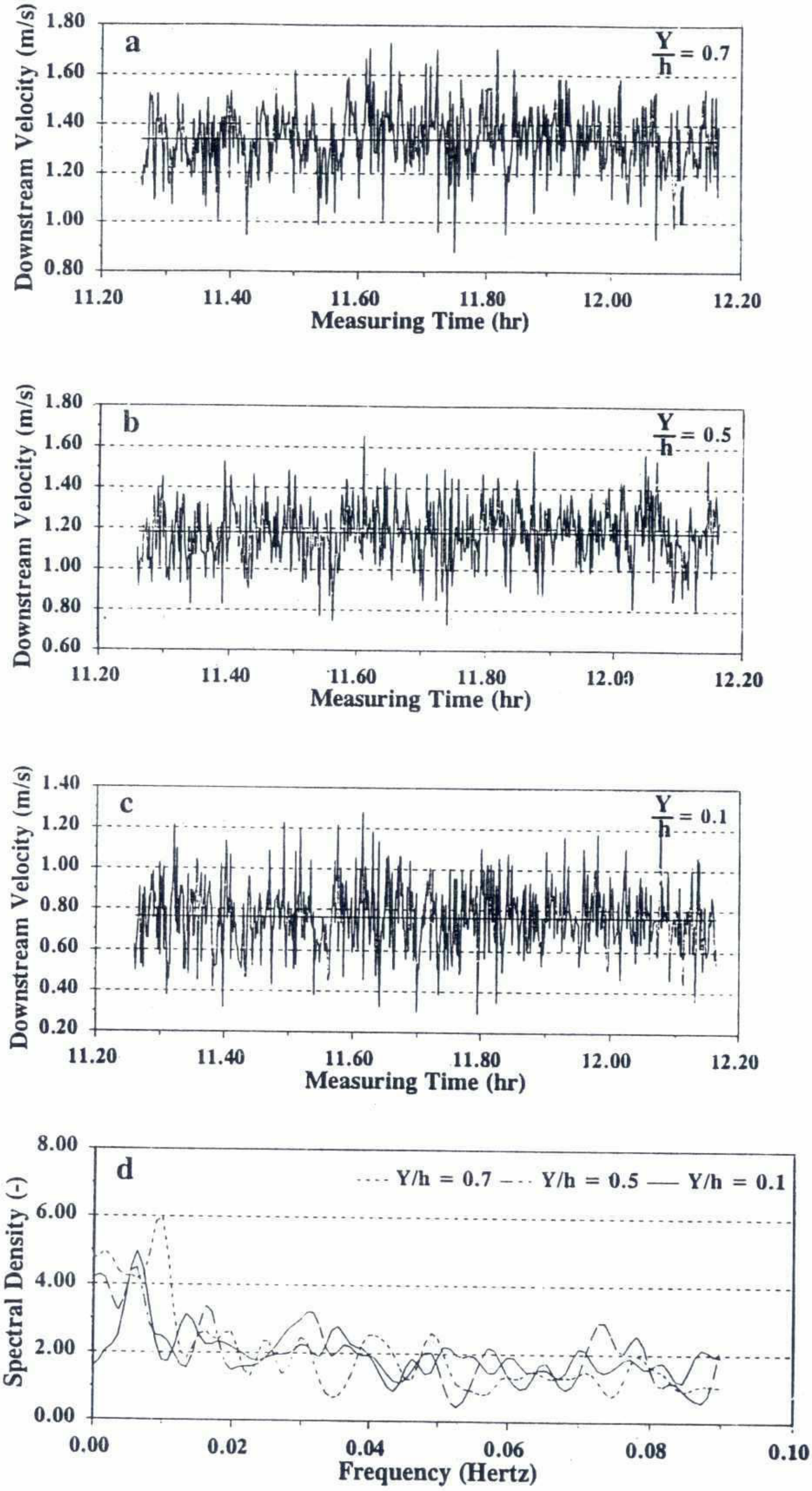

Figure B.4 Downstream velocities and spectral densities at different elevations above river bed at station B1. a. Downstream velocity in the free-stream region at Y/h = 0.7. b. Downstream velocity in the intermediate region at Y/h = 0.5. c. Downstream velocity in the wall region at Y/h = 0.1. d. Spectral density as functions of frequency points for the three regions of the boundary layer

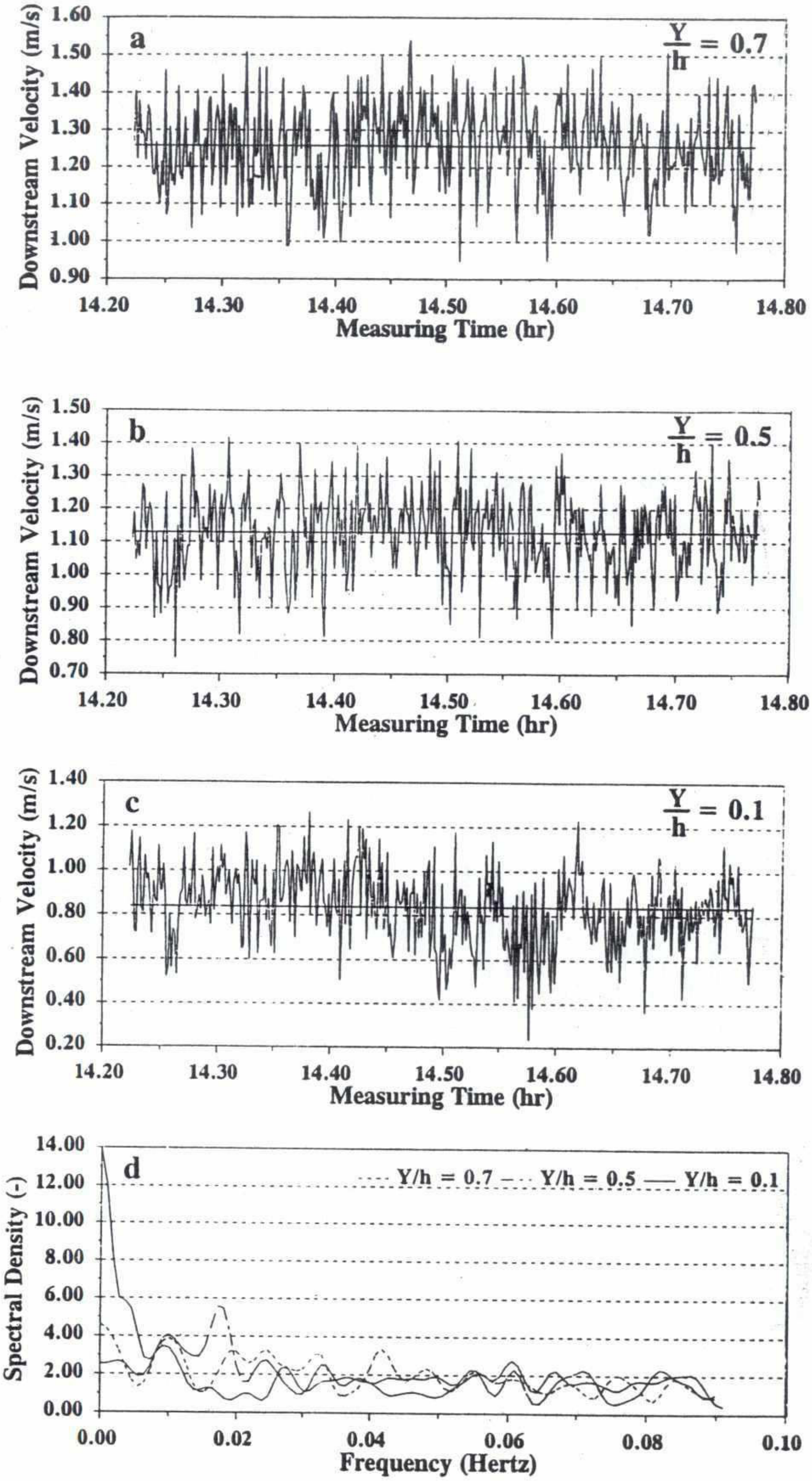

Figure B.5 Downstream velocities and spectral densities at different elevations above river bed at station B2. a. Downstream velocity in the free-stream region at Y/h = 0.7. b. Downstream velocity in the intermediate region at Y/h = 0.5. c. Downstream velocity in the wall region at Y/h = 0.1. d. Spectral density as functions of frequency points for the three regions of the boundary layer

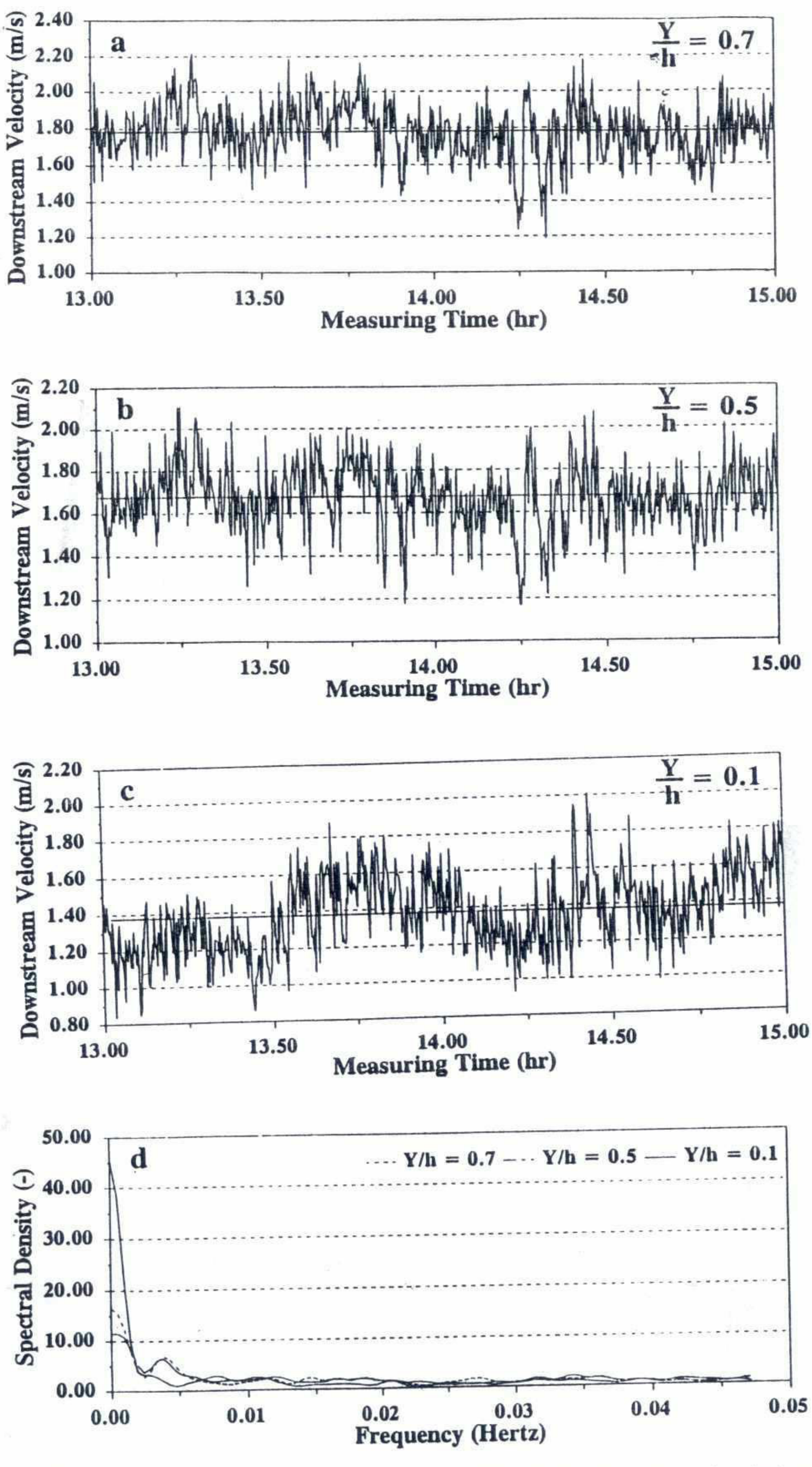

Figure B.6 Downstream velocities and spectral densities at different elevations above river bed at station B3. a. Downstream velocity in the free-stream region at Y/h = 0.7. b. Downstream velocity in the intermediate region at Y/h = 0.5. c. Downstream velocity in the wall region at Y/h = 0.1. d. Spectral density as functions of frequency points for the three regions of the boundary layer

Figure B.7 A typical boil observed near the survey vessel on 13 August 1994

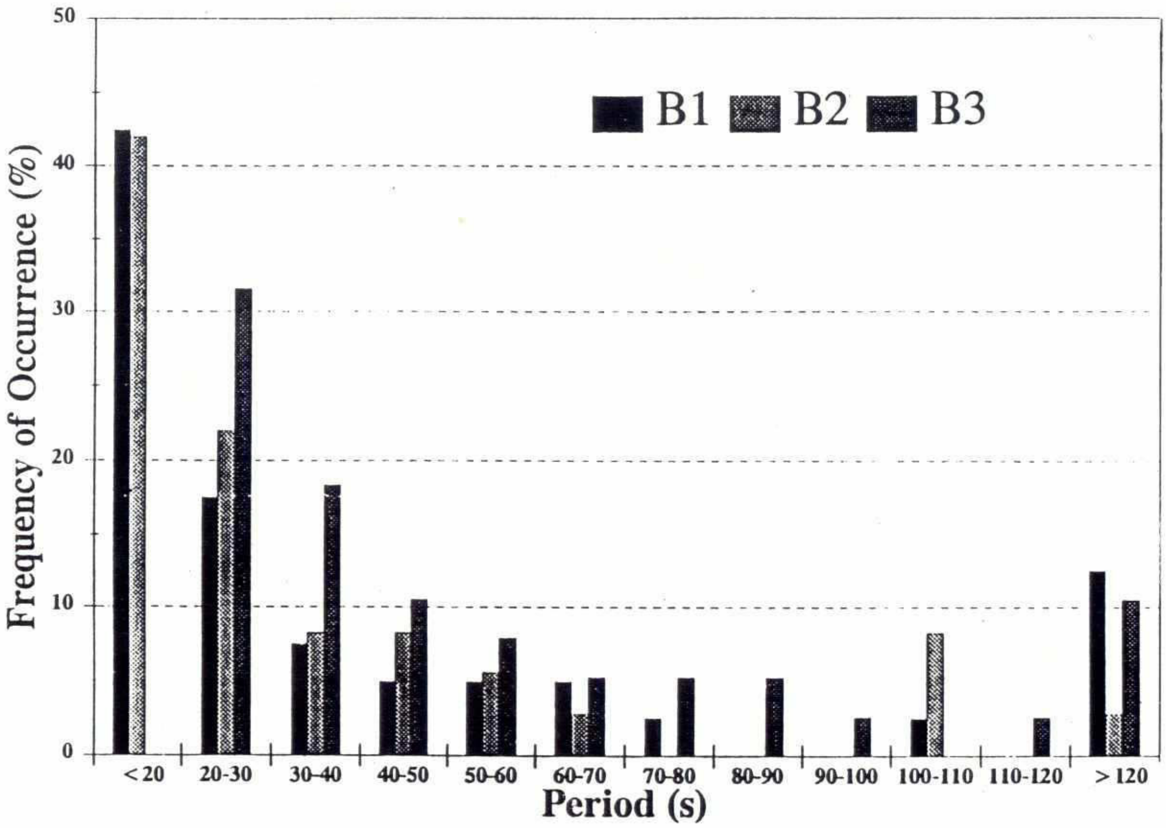

Figure B.8 Frequency of occurrence of different periodic events at stations B1, B2 and B3

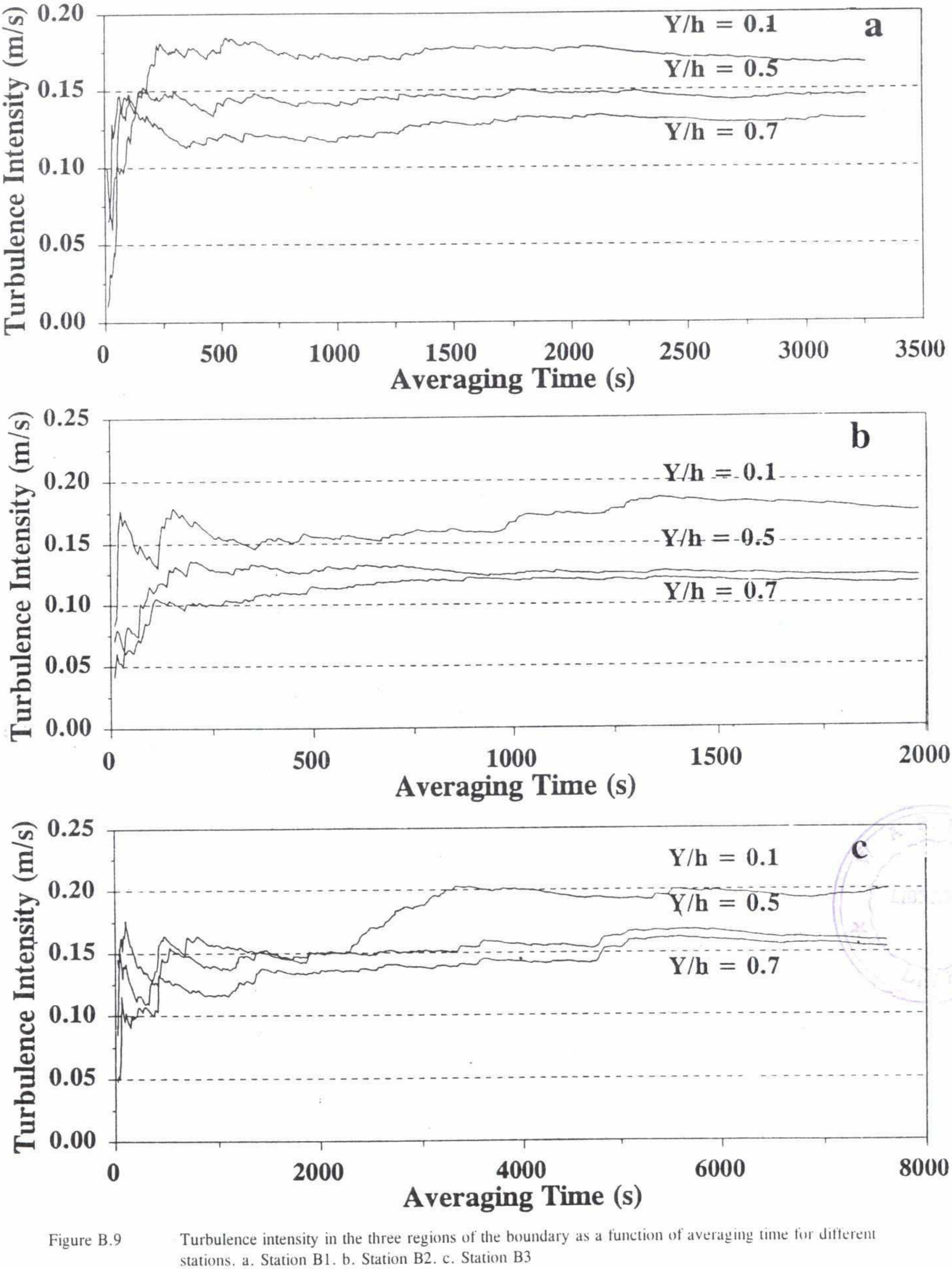

Figure B.9 Turbulence intensity in the three regions of the boundary as a function of averaging time for different stations. a. Station B1. b. Station B2. c. Station B3

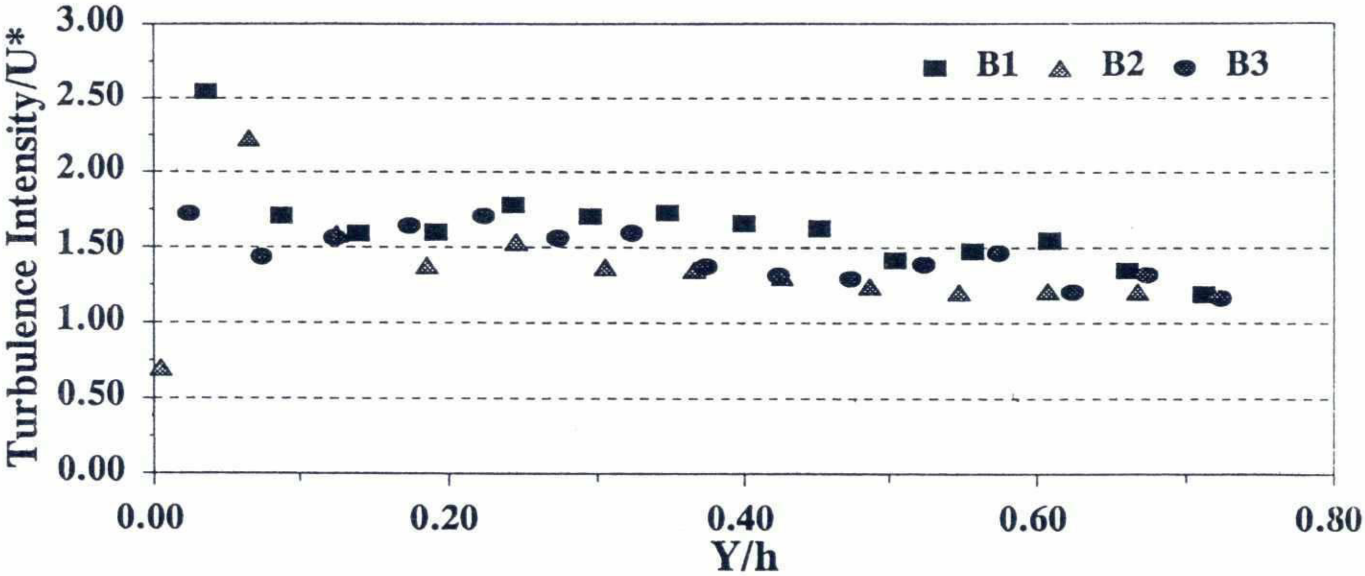

Figure B.10 Dimensionless turbulence intensity as a function of dimensionless water-depth observed at stations B1, B2 and B3

"Y4D"

Special Report 11, Annexure C.

Optimal Vertical and Horizontal Distribution of Velocity Measurements in Discharge Estimation

October 1996

Contents

272

Figures

Tables

1 Introduction

Estimating discharge of large natural alluvial rivers is not easy. The main rivers of Bangladesh are especially challenging because they are highly mobile, complex, and have large water-flows. Anastomosing multi-channels of some rivers such as the Jamuna make the task even more difficult. The challenges include finding an ideal and a suitable measuring transect, as prescribed by WMO (1981), and actually executing the data collection.

The Bangladesh Water Development Board has been collecting discharge data since 1964 using the velocity-area method. Two-point velocity data (at 20% and 80% of water-depth) are collected at each vertical. The verticals are located such that the discharge between two verticals does not exceed 10% of the total discharge. The River Survey Project (RSP, or FAP24) introduced the ADCP-EMF moving boat method which uses advanced techniques such as the Acoustic Doppler Current Profiler (ADCP) and Differential Global Positioning System (DGPS). The details of FAP24 application are described in the 1st Interim Report of the project (RSP, 1993). It should be noted that the ADCP-EMF moving boat method is different from the traditional moving boat method, where data are obtained from only one point in the water column. The ADCP-EMF moving boat method by FAP24 measures nearly the complete vertical velocity profile.

The accuracy of each method regarding the optimal number of points in a vertical and the optimal number of verticals in a transect is a matter of interest. The objective of this report is to examine the accuracy of flow measurements based on the results of a special survey in the Jamuna River near Bahadurabad (Figure 1).

2 Principles of discharge measurements

Estimates of discharge in natural alluvial rivers can be made in two principal ways, either directly based on actual measurements, or indirectly based on estimated parameters. Slope-area is one example of an indirect method. The direct method involves measuring the discharge components directly.

The direct method is based on the following principle:

$$Q = \sum_{i=1}^{m} \bar{u}_i \; b_i \; h_i \; \sin\theta_i \qquad (1)$$

where

Q = discharge
$\bar{u}$ = depth-averaged velocity
b = spacing or width between two verticals
h = depth at the vertical
i = number of verticals which can vary from 1 to m
Θ = angle between the transect and the velocity vector.

The depth-averaged velocity is computed using the following formula:

√38

$$\bar{u} = \frac{1}{h} \sum_{j=1}^{n} u_j \, d_j \qquad (2)$$

where

j = number of points in a vertical from 1 to n
u_j = velocity at the measuring point, j
h = total depth
d_j = depth at j

Width and depth are the two basic components determining the cross-sectional area of a discharge measurement transect. Besides uncertainty in the measurement of velocity, any uncertainty occurring in discharge estimation occurs due to uncertainty in measurement of width and depth. A brief discussion of the measurement of width and depth follows.

2.1 Measurements of basic components

2.1.1 Width

Measurement of the width of a channel in large alluvial rivers is not easy. This is because the width measurements are usually taken by a moving platform sailing from one bank of the channel to the other. With the help of electronic positioning or sextant sighting, distance is measured. The usual sources of errors are as follows:

- The shallow part of the channel usually can not be measured due to the limitation in the draft of the vessel. Thus the width is usually approximated by the field worker. Figure 2 illustrates the problem in estimating the shallow channel width
- For estimating discharge, the width must be perpendicular to the stream-flow direction. This is often difficult to achieve. An oblique width estimation always results in a higher estimation
- The third source of error is the instrument itself. With DGPS in stationary mode, the positioning error is usually ± 3 m. In sextant positioning, the uncertainty is very dependent on the efficiency of the surveyor

Although such uncertainties are clear, the available literature on the subject underplays the role of the width measurement error. For example, Sauer and Meyer (1992) report an error of less than 1%. ISO (1983) recommends that the width error be less than ± 1%. These estimates are obviously based on measurements in a single regular channel.

In the estimation of discharge, however, the effect of the error in width-estimation is not significant. This is because the shallow part of the section usually does not form a conveying section, rather it stores water. Therefore, a large shallow channel width with low flow velocities can increase the discharge very little.

2.1.2 Depth

The other source of uncertainty is the depth measurements. Here, errors can arise from the following sources:

- One source of error is instrumental. Different depth measuring devices can measure the same depths differently. Sauer and Meyer (1992) reported a 10% error in mobile streambed using different devices such as rod suspension, cable suspension, and acoustic system. The resolution of an acoustic depth measurement is dependent on the angle of the acoustic beam. The 200 kHz echosounders used by FAP24 have opening angles between 7°-10°. The 30 kHz echosounder has an opening angle of 24°

- The second source of error is related to the spatial density of the depth-measuring verticals. If the depth-measuring verticals are too sparsely located some details may be overlooked

2.1.3 Velocity

Velocity can be estimated by either a mechanical current meter or an electronic sensor. The following four types of measuring errors are possible when estimating velocity:

- Instrumental error
- Error due to limited exposure time of the sensor (Type I error)
- Error due to limited numbers of sampling points in a vertical (Type II error)
- Error due to limited numbers of verticals in a cross-section (Type III error)

The *Type I error* is discussed in Annexure A. The purpose of this Annexure C is to discuss Type II and III Errors.

Type II error:

ISO-Neth (1971) found the following standard error on vertical distribution of flow measurements:.

$$\epsilon_v = 7.4\ M^{-0.61}$$

where

ϵ_v = standard error in percentage
M = number of points in a vertical

Carter and Anderson (1963) showed that an error of 11.2% occur in 1-point measurement (at 60% water-depth) and 4.3% occur in 2-point measurement (20% and 80% water-depth). The errors were computed by assuming a 11-point velocity profile.

Type III error:

ISO-Neth (1971) found the following standard error:

$$\epsilon_h = 46.8\ N^{-1.05}$$

ISO (1979) recommended using a relation such as the following:

$$\epsilon_h = 32\ N^{-0.88}$$

for estimating errors due to the limited numbers of verticals. The errors found in this way are based on the assumption that the verticals are located equidistant. Here, ϵ_h is the standard error and N is the number of verticals. WMO (1981) suggested two ways of locating a vertical:

- The verticals can be located on the principle that discharge between two verticals is less than or equal to 10% of the total discharge. This means that at least 9 verticals should be sampled

- or, the spacing between two verticals is less than about 5% of the total width. This means that at least 19 verticals should be sampled

Figure 3 indicates the principles of locating a vertical.

2.2 Discharge estimation methods

The direct method involves two basic approaches: The velocity-area method, utilizing multi-point and multi-vertical velocity observations, and the moving boat method. A brief description is given of each of these methods.

2.2.1 Velocity-area method

Equation 1 explains the principles of discharge estimation by the velocity-area method. There are two basic ways of estimating discharge as outlined in the ISO (1979) report. Using a mean-section method, the average of the depth-mean velocity is multiplied by both the average depth at the two verticals and the spacing between the two verticals.

$$q = [\frac{v_i+v_{i+1}}{2}][\frac{d_i+d_{i+1}}{2}][b_{i+1}-b_i]$$

where

q	= discharge between the verticals i and i+1
v_i	= depth-averaged velocity at vertical i
d_i	= depth at vertical i
b_i	= distance of the vertical i from a certain reference location

In a mid-section method, the depth-averaged velocity of a vertical is multiplied by both the depth of that vertical and a width comprising the mid-points between the reference vertical and the two adjacent verticals. Figure 4 illustrates the principle of computation.

$$q_i = v_i d_i[(\frac{b_{i+1}-b_i}{2})-(\frac{b_i-b_{i-1}}{2})]$$

where

q_i	= discharge surrounding vertical i
v_i	= depth-averaged velocity at vertical i
d_i	= depth at vertical i
b_i	= distance of the vertical i from a certain reference location

2.2.2 Moving boat method

This method measures the discharge by sampling the water column as the boat sails across the channel. The RSP applied the so-called ADCP-EMF moving boat method, which measures the vertical current profile by ADCP and EMF while transversing the river. The application is discussed in the River Survey Project Interim Report (RSP, 1992). Figure 5 illustrates the principles of the method. The unmeasured bottom portion is estimated by fitting a power curve (Chen, 1991). The algorithm of discharge estimation is provided by Gordon (1989) and Simpson and Oltman (1990).

239

3 Field measurements

Special field measurements were made in Jamuna River near the Bahadurabad discharge measurement transect from 26 to 30 July 1995. Transects T1 and T2 and the verticals are shown in Figure 1. Figure 6 is a water level hydrograph near Bahadurabad which shows the river stage during the measurements. Figure 7 shows the transect T1 with 12 measurement verticals, and two additional measurement verticals 3A and 10A. Similarly, 19 verticals and some additional verticals are shown in Figure 8. In vertical V5, which represents RA in Figure 1, detailed measurements along the vertical were taken.

The purpose of the survey was to optimize the number of points in a vertical and the number of verticals in a transect. The measurements were executed together with sediment measurements. Basically, the scope of the survey was to obtain the following:

- Velocity measurements by S4 at several points along the vertical at different fractions of water-depth
- Velocity profile measurements by ADCP at several verticals along a transect. This was done using the equally spaced vertical method and vertical spacing with discharge around 10% of the total discharge

In the following tables, the measurement details are shown. Table 1 presents the multi-point velocity observations at several verticals. Table 2 provides the details of the multi-vertical observations along transects T1 and T2. Transect T1 comprises a channel-width of about 700 m and 14 verticals were sampled in this transect (Fig. 7). Transect T2 comprises a channel-width of about 1500 m and 23 verticals were sampled in this transect.

Location General	Location Coordinates	Date	Time	Total depth	Remarks
RA	463175 m (E) 781806 m (N)	27 July 1995	15:50 to 17:43	9.2 m	ADCP velocity profile for the entire measuring period
LB	470532 m (E) 778630 m (N)	29 July 1995	11:30 to 13:35	13.8 m	-do-
LC	470308 m (E) 779051 m (N)	29 July 1995	14:25 to 16:31	11.3 m	-do-
LD	470202 m (E) 776560 m (N)	30 July 1995	08:03 to 10:27	10.5 m	-do-
LE	470179 m (E) 776504 m (N)	30 July 1995	11:12 to 15:02	9.2 m	-do-

Table C.1: Schedule of multi-point velocity measurements in the right and left channels of the Jamuna River near Bahadurabad (see Figure 1 for locations)

Transect	Date	Time	Total number of verticals	Remarks
T1	27 July 1995	12:37 to 15:02	15 verticals	Measurements taken together with sediment sampling
T2	28 July 1995	11:26 to 17:24	23 verticals	-do-

Table C.2: Schedule of multi-vertical discharge measurements in the right channel of the Jamuna River near Bahadurabad (see Figure 1 for locations)

Tables C.3 to C.7 show the multi-point measurement details at 5 verticals. A 50 s exposure time was used for integration of S4 velocities presented in Tables C.3 to C.7.

Time	Measuring depth (m)	Percent of total depth (%)	S4 velocity (m/s)
16:05	1.84	20	1.80
16:12	2.76	30	1.92
16:24	3.68	40	1.80
16:34	4.60	50	1.70
16:45	5.52	60	1.60
16:55	6.44	70	1.44
17:06	7.36	80	1.22
17:16	7.82	85	1.28
17:27	8.28	90	1.27
17:36	8.74	95	1.10

Table C.4: 10-point velocity measurements at RA on 27 July 1995 (see Figure 1 for locations)

Time	Measuring depth (m)	Percent of total depth (%)	S4 velocity (m/s)
12:00	2.76	20	2.70
12:09	4.14	30	2.70
12:19	5.52	40	2.80
12:29	6.90	50	2.70
12:52	8.28	60	2.70
13:00	9.66	70	2.70
13:09	10.35	75	2.50
13:19	11.04	80	2.50
13:25	11.73	85	2.40

Table C.4: 9-point velocity measurements at LB on 29 July 1995 (see Figure 1 for locations)

Time	Measuring depth (m)	Percent of total depth (%)	S4 velocity (m/s)
15:06	2.26	20	1.65
15:15	3.39	30	1.62
15:25	4.52	40	1.61
15:32	5.65	50	1.52
15:42	6.78	60	1.63
15:48	7.91	70	1.52
15:57	8.48	75	1.60
16:08	9.04	80	1.52
16:20	9.41	85	1.26

Table C.5: 9-point velocity measurements at LC on 29 July 1995 (see Figure 1 for locations)

Time	Measuring depth (m)	Percent of total depth (%)	S4 velocity (m/s)
08:37	2.10	20	2.24
08:47	3.15	30	2.10
08:56	4.20	40	2.17
09:05	5.25	50	2.13
09:14	6.30	60	2.01
09:24	7.35	70	1.97
09:36	7.88	75	2.02
09:46	8.40	80	1.94
09:57	8.93	85	1.95
10:06	9.50	90	1.89
10:16	9.80	95	1.47

Table C.6: 11-point velocity measurements at LD on 30 July 1995 (see Figure 1 for locations)

Time	Measuring depth (m)	Percent of total depth (%)	S4 velocity (m/s)
12:06	1.84	20	2.40
12:15	2.76	30	2.20
12:21	3.68	40	2.27
13:27	4.6	50	2.13
13:38	5.52	60	2.09
13:47	6.44	70	1.96
13:56	6.9	75	2.03
14:22	7.36	80	1.98
14:31	7.82	85	2.02
14:38	8.28	90	2.06
14:47	8.74	95	1.88

Table C.7: 11-point velocity measurements at LE on 30 July 1995 (see Figure 1 for locations)

Figures C.9 to C.13 give the velocity profiles measured at multi-points along the vertical by S4 current meter.

4 Analyses and results

4.1 Optimal vertical distribution in a multi-point method

Utilizing the S4 velocities measured at different points along the vertical, the depth-averaged velocities are computed using different distributions. The distribution used is as shown in Table 8.

1 point	=	0.5h
2 points	=	0.2h, 0.8h
3 points	=	0.2h, 0.6h, 0.8h
4 points	=	0.2h, 0.4h, 0.6h, 0.8h
5 points	=	0.2h, 0.4h, 0.5h, 0.6h, 0.8h
6 points	=	0.2h, 0.3h, 0.4h, 0.6h, 0.7h, 0.8h
7 points	=	0.2h, 0.3h, 0.4h, 0.5h, 0.6h, 0.7h, 0.8h
8 points	=	0.2h, 0.3h, 0.4h, 0.5h, 0.6h, 0.7h, 0.8h, 0.9h
9 points	=	0.2h, 0.3h, 0.4h, 0.5h, 0.6h, 0.7h, 0.75h, 0.8h, 0.9h
10 points	=	0.2h, 0.3h, 0.4h, 0.5h, 0.6h, 0.7h, 0.75h, 0.8h, 0.85h, 0.9h
11 points	=	0.2h, 0.3h, 0.4h, 0.5h, 0.6h, 0.7h, 0.75h, 0.8h, 0.85h, 0.9h, 0.95h

Table C.8: Distribution followed for computation of depth-averaged velocity

Figures C.14 through C.18 compare the computed depth-velocities with 11-point depth-averaged velocities (which are assumed to be correct). The percent deviation in depth-averaged velocity is computed as follows:

$$\delta = \frac{\bar{u}_i - \bar{u}_m}{\bar{u}_m} x\ 100$$

where,
$\bar{u}_i$ = depth-averaged velocity using i points in the vertical
$\bar{u}_m$ = depth-averaged velocity using maximum numbers of observed velocities in the vertical

In Figure C.14, the percentage deviation is shown at station RA with respect to 10-point velocity. It can be seen that depth-averaged velocities estimated with 5 to 10 points have hardly any variation. However, when the vertical number is less than that, the underestimation can be up to 22%. At station LB (Figure C.15), the variation between different methods are negligible. While little overestimation occurred, velocity using 2-point is underestimated by 1.5%. At station LC (Figure 16), overestimation occurred in most cases. The maximum (some 4.5%) occurred with the 3-point method. Figure 17 shows the variation at station LD. Here, the maximum underestimation occurred by approximately 7%. At station LE (Figure 18), the variation is negligible. The percentages of variation in 5 verticals are summarized in Table 9.

The average of the 5 verticals indicates that the maximum underestimation occurs by about 5.3%.

Measuring point numbers	Percent variation at RA	Percent variation at LB	Percent variation at LC	Percent variation at LD	Percent variation at LE	Average variation at 5 verticals
1	-12.8	02.3	-01.3	03.9	-01.4	-01.9
2	-22.6	-01.5	03.3	-07.3	01.4	-05.3
3	-19.5	00.0	04.6	-07.8	01.0	-04.3
4	-18.5	00.8	03.9	-07.3	01.4	-03.9
5	-00.5	01.1	03.3	-07.3	01.4	-00.4
6	00.5	01.1	03.3	-07.8	00.5	-00.5
7	00.5	00.8	02.6	-07.3	00.0	-00.7
8	00.5	00.0	0.00	02.0	00.5	00.6
9	01.0	00.0	0.00	02.0	00.9	00.8
10	00.0	-	-	06.8	00.9	-
11	-	-	-	00.0	00.0	-

Table C.9: Summary of the percentage of variation of depth-averaged velocity at 5 verticals in the Jamuna River near Bahadurabad

In summary, it is indicated that to minimize the relative deviation to ±1.0%, the numbers of points in a vertical should be 5 or more; the distribution outlined above can be followed.

Therefore, the effect of uncertainty in depth-averaged velocity estimation (type II error) is not large. The finding is supported by ISO-neth (1971) and Carter and Anderson (1963).

4.2 Optimal horizontal distribution in a multi-vertical method

As can be seen in Figures 7 and 8, the right channel of the Jamuna River near Fulchari contains two primary sub-channels. The measurements at transects T1 and T2 were utilized to compute the discharge for a varying number of verticals. Figures 19 and 20 show the percent deviation in discharge which is computed as follows:

$$\Delta = \frac{q_j - q_n}{q_n} x\ 100$$

where,

q_j = discharge using j verticals

q_n = discharge using the maximum numbers of verticals, n

Figure 19 shows the discharge deviation obtained by using data from two to 12 verticals. An overestimation occurs if the number of verticals is reduced. The relation can be described by a linear best-fit line Y = 22 - 2.1 X, where Y is the discharge deviation in percentage and X is the number of verticals.

In Figure 20, the discharge deviation is indicated for transect T2. Here, a larger overestimation is shown than transect T1. The linear best-fit line in this case is Y = 34 - 2.7 X.

The overestimation for fewer verticals in the two cases is due to starting with 2 verticals at the deep channels. A different deviation-relation is possible if another distribution would have been followed. These two examples show the significance of type III errors. Although these indications do not give the uncertainty ranges, as have been derived by ISO-Neth (1971) or ISO (1979), they show that a large error in discharge estimation can occur as a result of choosing too few verticals.

Table 10 compares the total discharge of three methods, the ADCP-EMF moving boat method and two velocity-area methods. The discharge does not vary appreciably using these different methods. The discharge determined by the ADCP-EMF moving boat method is approximately 2% higher than the one determined by the velocity-area methods.

1	2	3	4	5	6
Transect	ADCP-EMF moving boat discharge (m^3/s)	Velocity-area (Equidistant verticals) discharge (m^3/s)	Velocity-area (10% distribution) discharge (m^3/s)	Percent var. of 3 from 2	Percent var. of 4 from 2
T1	5260	5151	5182	-2.0%	-1.5%
T2	5929	5874	5923	-0.9%	-0.1%

Table C.10: Discharge across transects T1 and T2 along the right channel of the Jamuna River near Fulchari

5 Conclusions

The analyses of the effects of limited numbers of measuring points in a vertical and limited numbers of verticals in a transect in Jamuna River near Bahadurabad support the following tentative conclusions:

- To limit the relative deviation of the depth-averaged velocity estimation to $\pm$ 1 percent, the minimum numbers of points in a vertical should be at least five. The maximum deviation is well within five percent, however. On average, an underestimation occurs when fewer points are measured. The current analyses indicated that when only two points are measured (20 percent and 80 percent water-depth) it is no better than when one point is measured (50 percent water-depth). This is contrary to the observations by Carter and Anderson (1963).

- Estimating the total discharge using the mid-section method appeared to be dependent on choosing the vertical numbers. In the two cases compared, overestimation occurred when the number of verticals were reduced. The dependence on the vertical numbers is described in the following linear equations:

  At transect T1: $Y = 22 - 2.1\ X$
  At transect T2: $Y = 34 - 2.7\ X$

  where Y is the percentage discharge deviation from the discharge using 12 verticals, and X is the number of verticals. Figures C.19 and C.20 show the discharge deviation as a function of the numbers of verticals

- The total discharge estimates made using the ADCP-EMF moving boat method and the two velocity-area methods were comparable in magnitude. However, the velocity-area method appeared to slightly underestimate the flow

References

Carter, R.W. and Anderson, I.E., 1963. Accuracy of current meter measurements. Jr. of Hydraulics Divn., American Society of Civil Engineers, HY 4, part 1, pp. 105-115

Chen, Cheng-Lung, 1991. Unified theory on power laws for flow resistance. Jr. Hydraul. Divn., 117(3), 371-389

Gordon, R.L., 1989. Acoustic measurement of river discharge. Jr. Hydraul. Divn., 115(7), 925-936
3
International Standard Organization, 1979. Liquid flow measurements in open channels - velocity area methods. ISO 748, 23 pp

International Standard Organization, 1983. Liquid flow measurements in open channels - velocity area methods - investigation of total error. In: Measurement of liquid flow in open channels, ISO Standard Handbook 16, ISO, Switzerland, 518 pp

Mueller, A., 1989. Levels of velocity data collection in open channel flows. Proc. HYDROCOMP '89, Dubrovnik, Elsevier Applied Science Publisher, Essex

Netherlands Working Group TC 113 (ISO-Neth), 1971. Investigation of the total error in measurement of flow by velocity-area methods

RD Instruments, 1992. User's manual for the RD instruments transect program. RD Instruments, San Diego, California

River Survey Project (RSP), 1993. 1^0 Interim Report (Vol. II) - Annexures on survey work

Sauer, V.B. and Meyer, R.W., 1992. Determination of error in individual discharge measurements. USGS open-file report 92-144

Simpson, M.R. and Oltmann, R.N., 1990. An Acoustic Doppler Discharge Measuring system. Proc. 1990 National Conference on Hydraul. Engg., 2, 903-908

Smoot, G.F. and Novak, C.E., 1969. Measurement of discharge by the moving-boat method. In: Techniques of water-resources investigations of the United States Geological Survey, Chapter A11

Task Committee on Hydrographic Investigations, 1983. Measurements of hydrographic parameters in large sand-bed streams from boats. American Society of Civil Engineers, New York, 81 pp

World Meteorological Organization (WMO), 1981. Guide to hydrological practices, vol. 1, WMO No. 168, Geneva, Switzerland

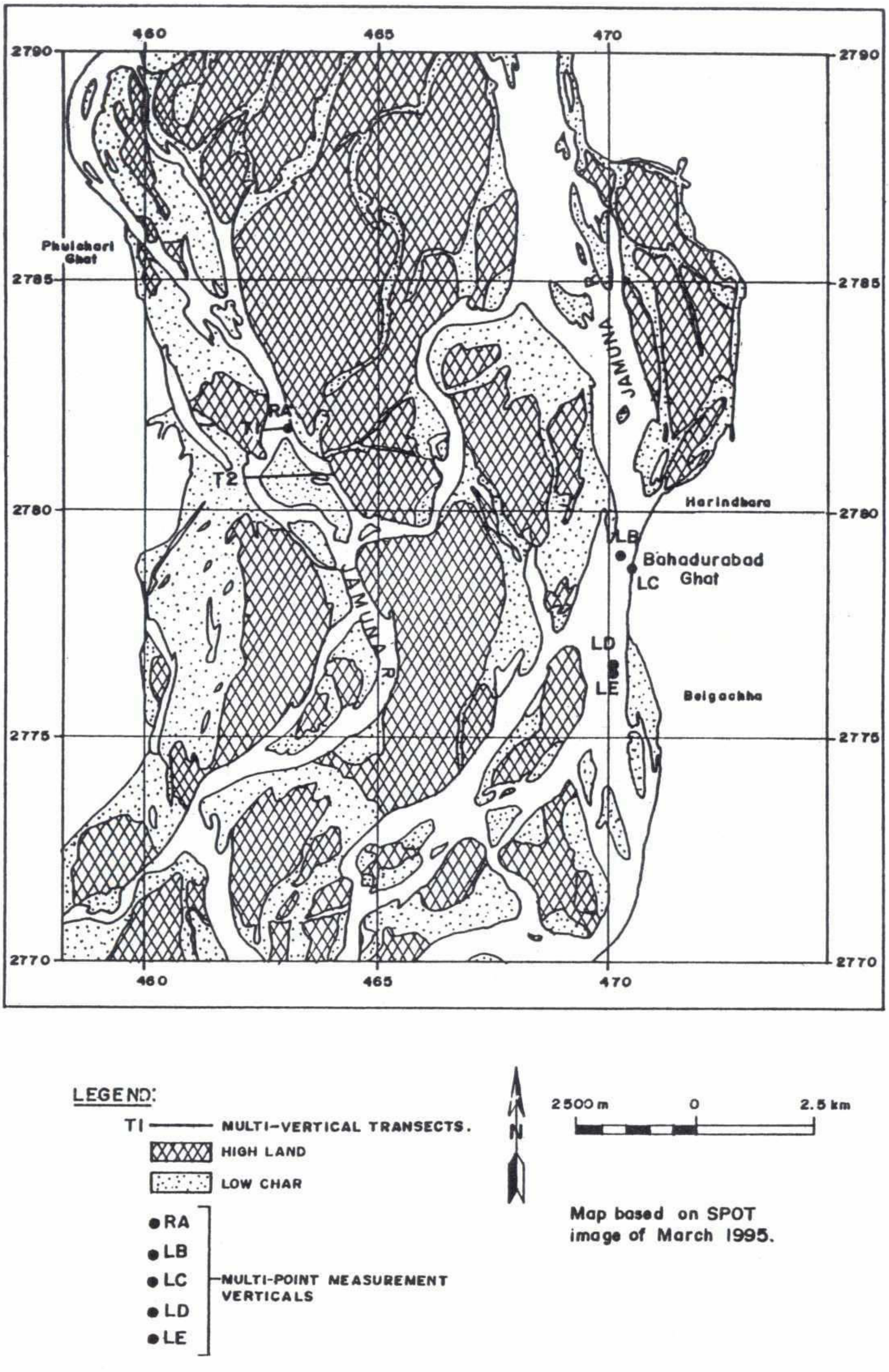

Figure C.1: Locations in the Jamuna River near Bahadurabad where measurements were made on 27-30 July 1995.

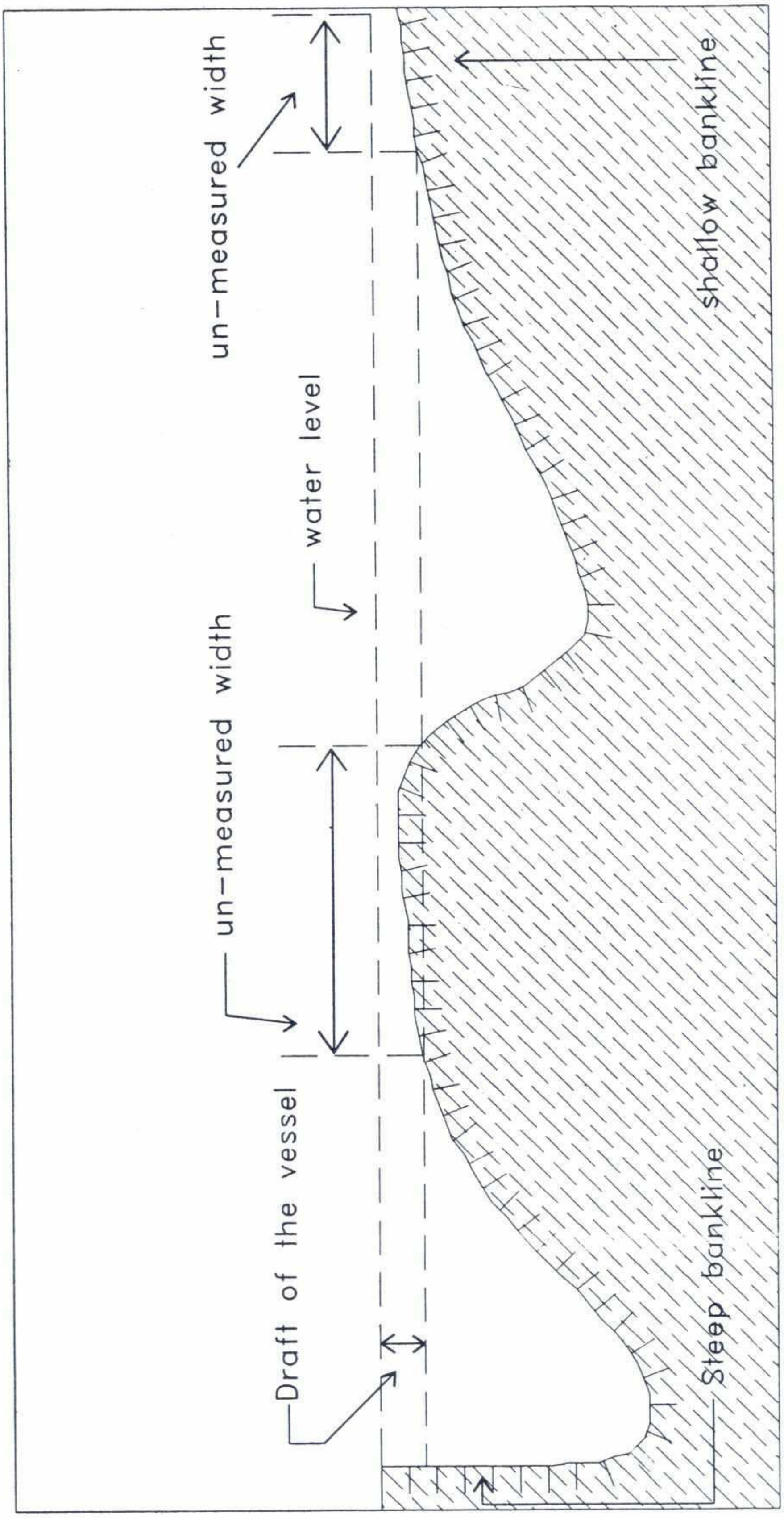

Figure C.2: Schematic diagram showing the difficulty in measuring at shallow-depths

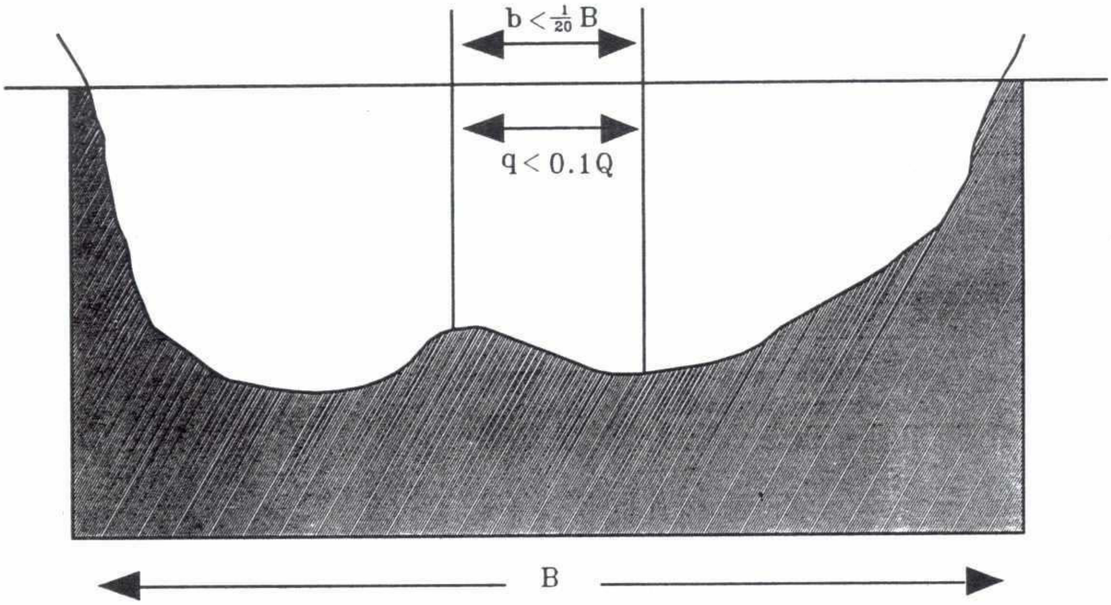

Figure C.3: Schematic diagram showing the principles of locating a vertical according to WMO (1981)

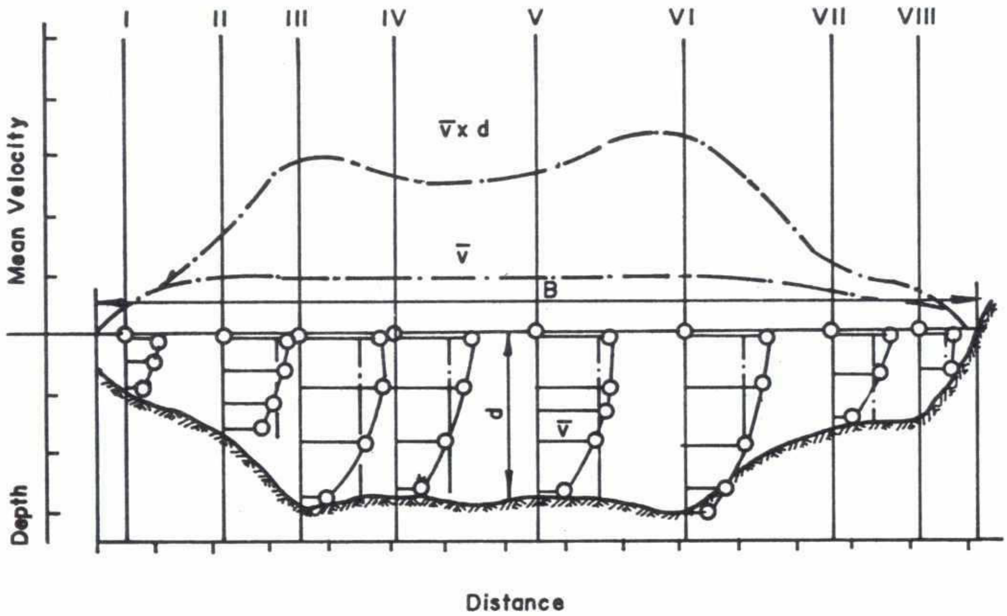

Figure C.4: Schematic diagram showing discharge computation principle by the velocity-area method

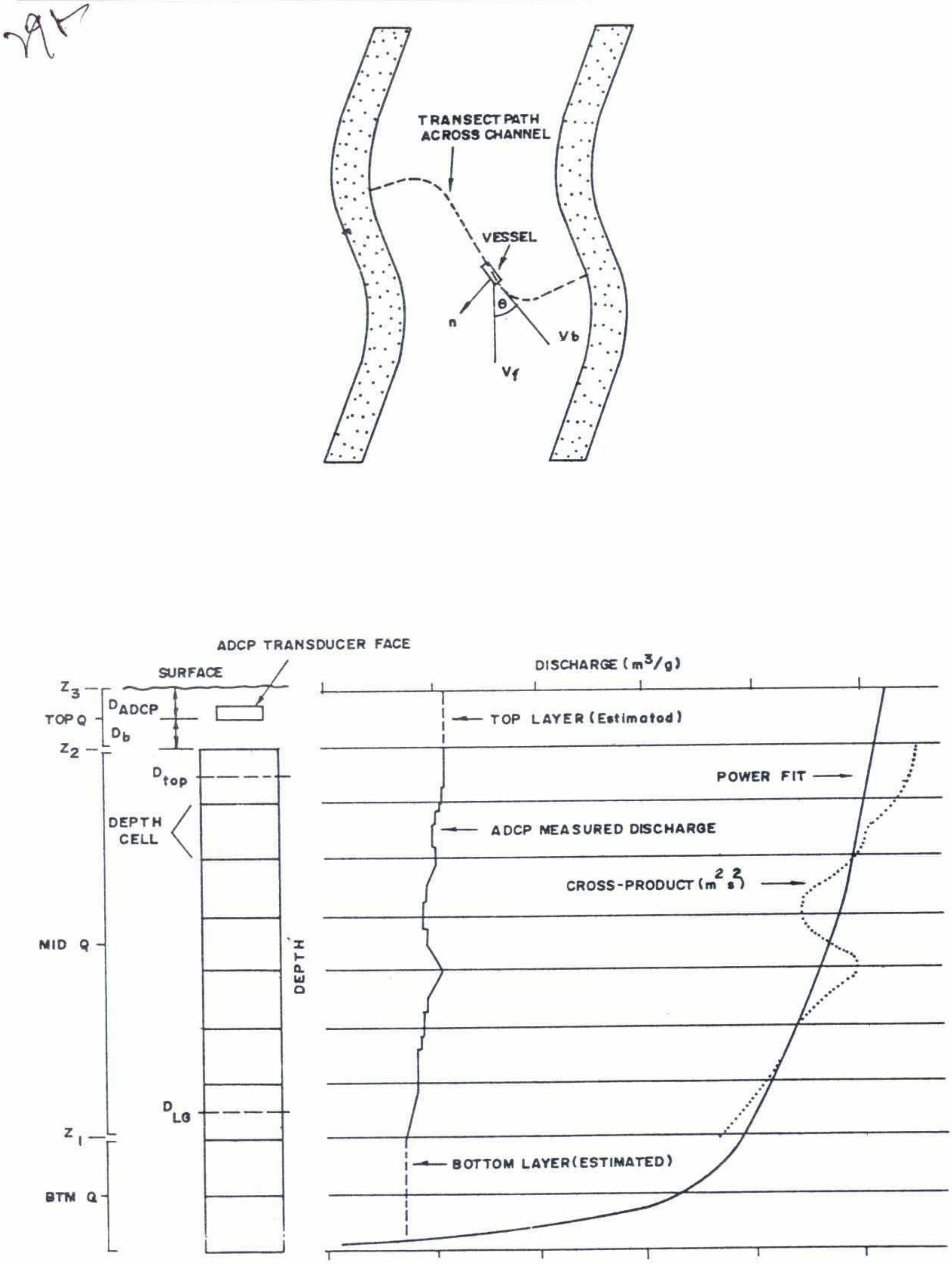

Figure C.5: ADCP-EMF moving boat principle employed by FAP24 (RD Instruments, 1992). v_b = mean vessel velocity vector, v_f = mean water velocity vector, n = unit vector normal to transect path at a general point, D_{ADCP} = depth of the ADCP transducer face from the water surface, D_b = blank beyond transmit, D_{top} = depth of the centre of the first bin, D_{LG} = depth of the last good bin, TOP Q = estimated discharge for the unmeasured data at the top of the profile, BTM Q = estimated discharge for the unmeasured data at the bottom of the profile

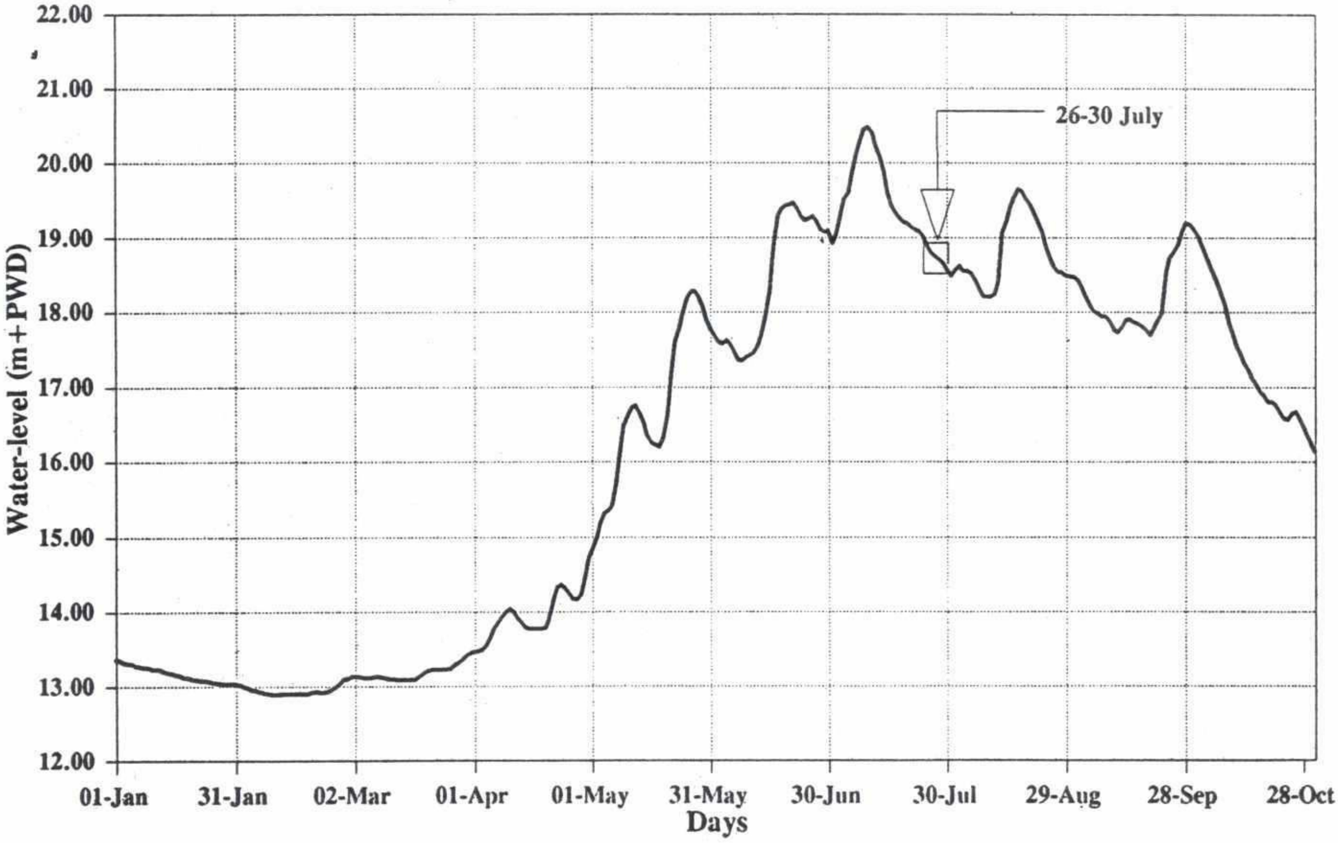

Figure C.6: Daily water level hydrograph of the Jamuna River at Bahadurabad for 1995

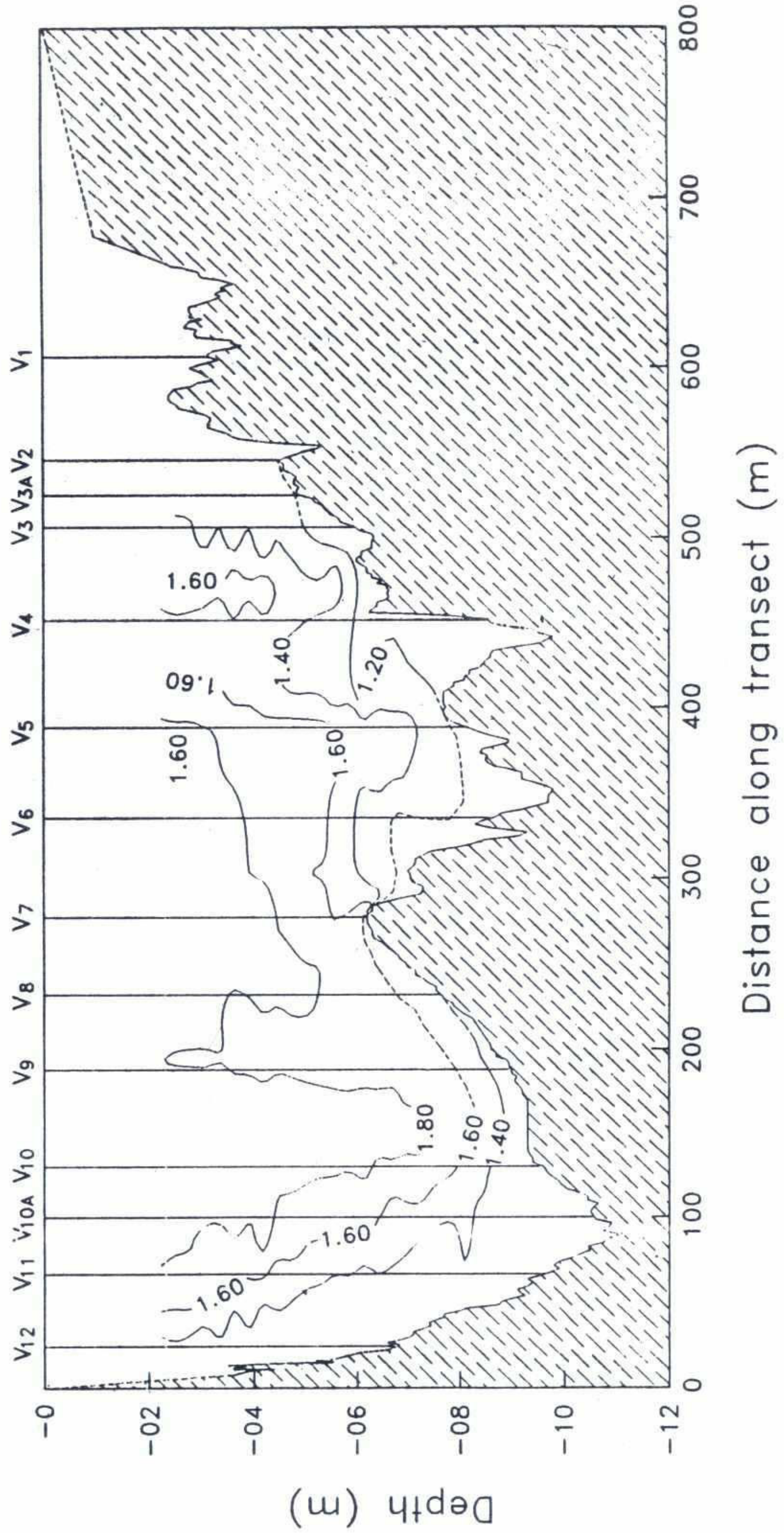

Figure C.7: Cross-sectional profile with isovels and measurement vertical locations along transect T1. V_{3A} and V_{10A} represent additional verticals. Isovels are shown in m/s

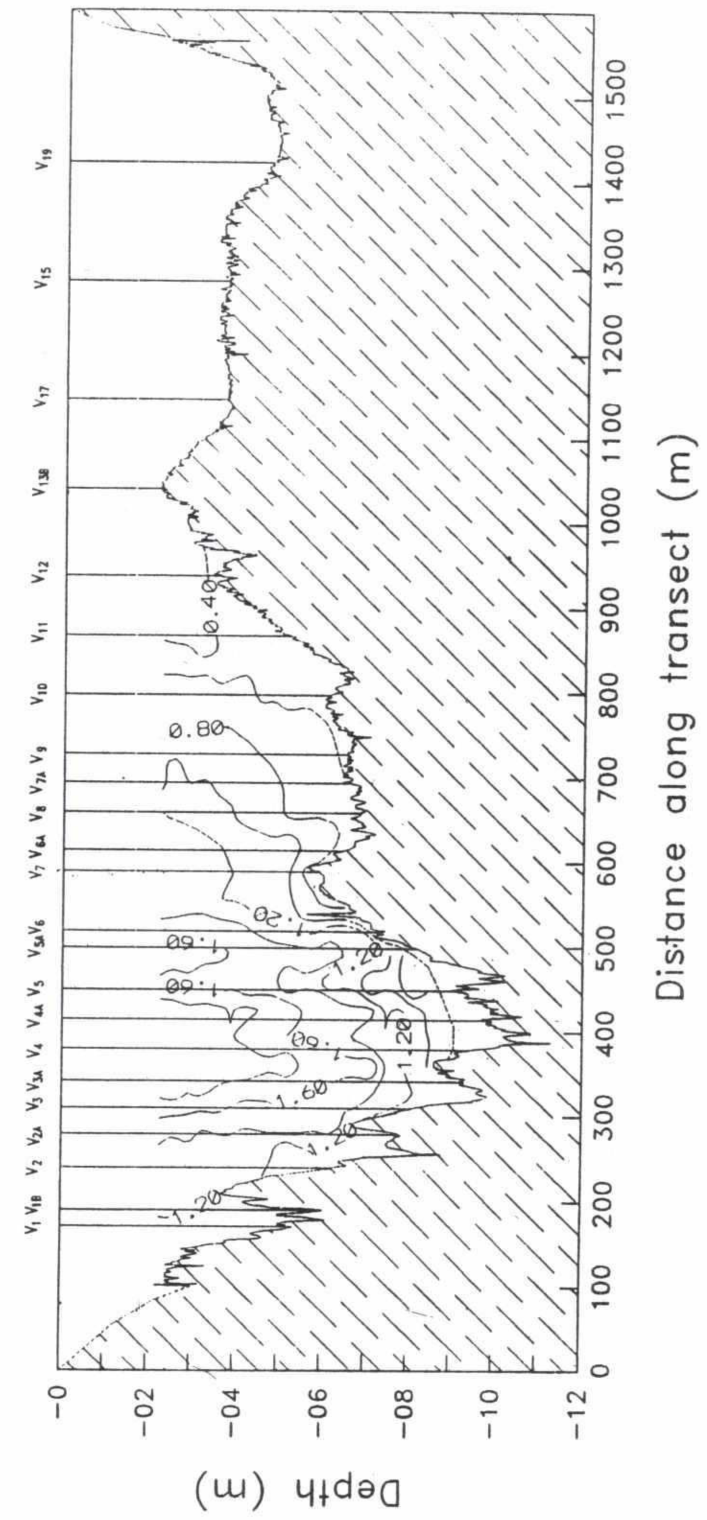

Figure C.8: Cross-sectional profile with isovels and measurement vertical locations along transect T2. Subscripts A and B represent additional verticals. Isovels are shown in m/s

182

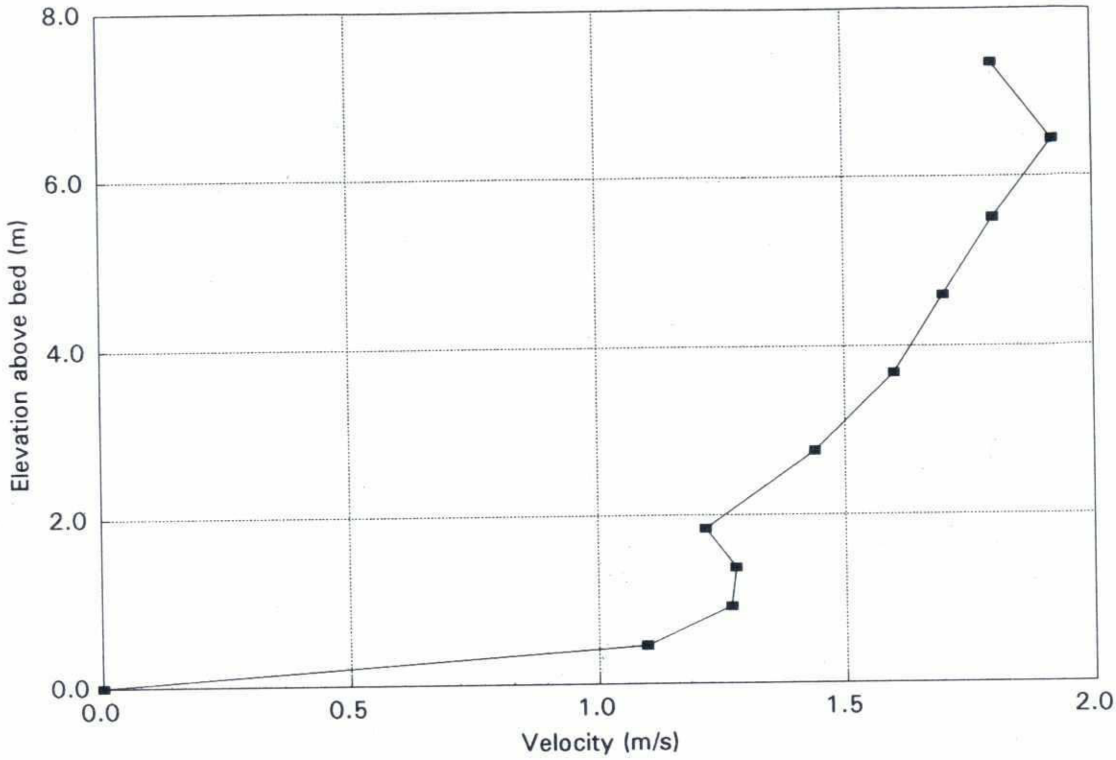

Figure C.9: Velocity profile at RA obtained from multi-point velocity observations by S4 current meter on 27 July 1995

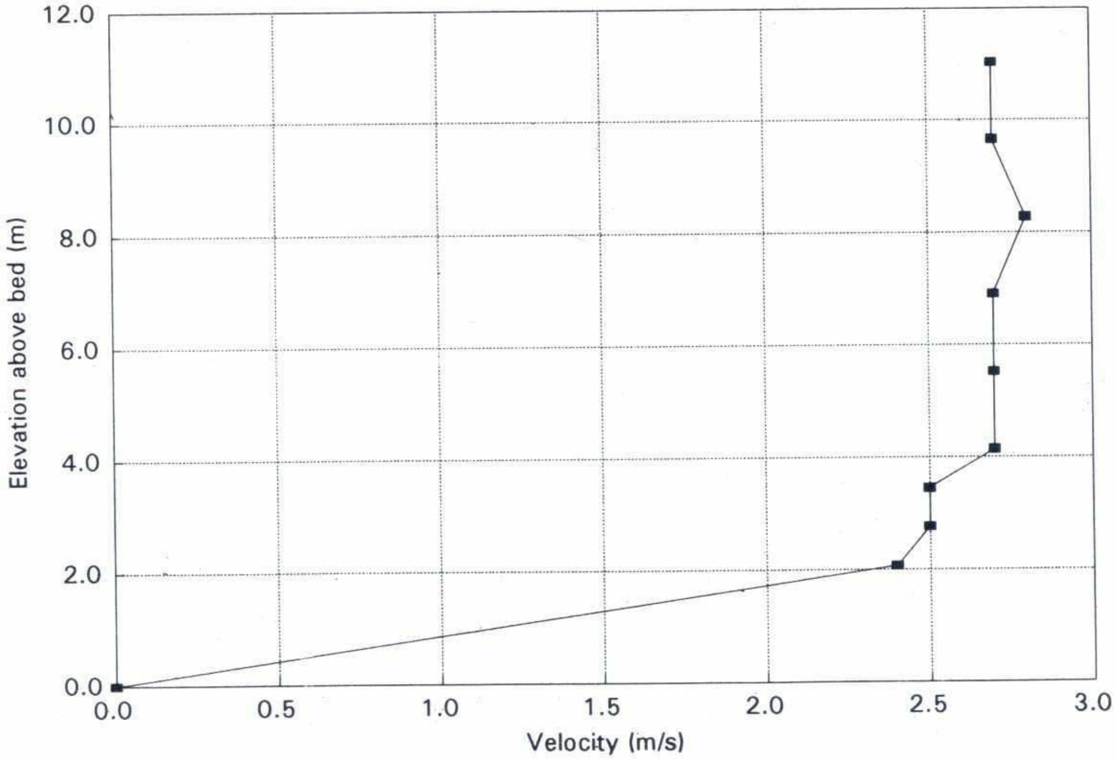

Figure C.10: Velocity profile at LB obtained from multi-point velocity observations by S4 current meter on 29 July 1995

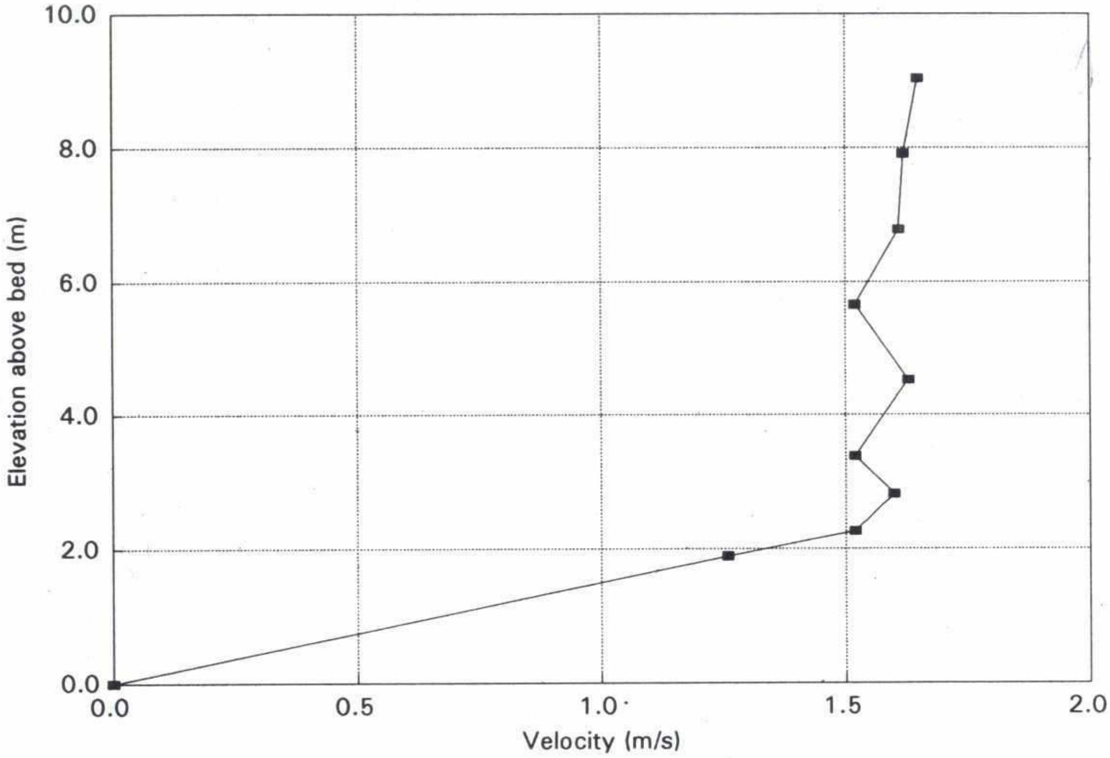

Figure C.11: Velocity profile at LC obtained from multi-point velocity observations by S4 current meter on 29 July 1995

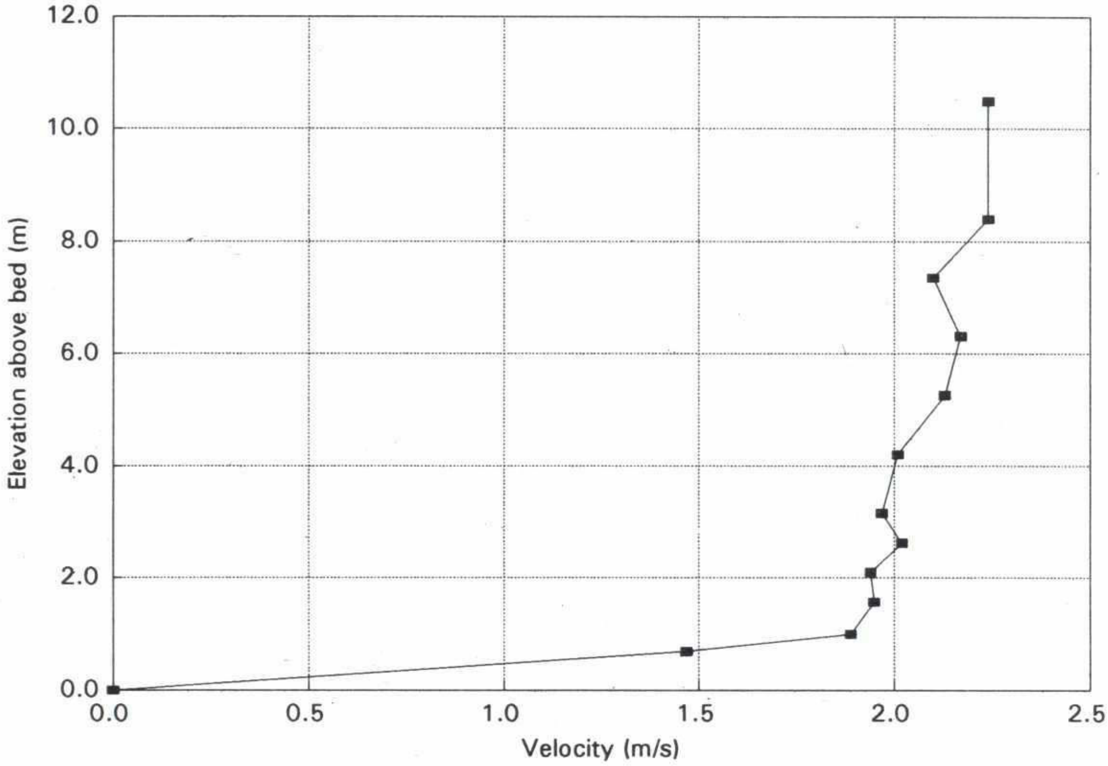

Figure C.12: Velocity profile at LD obtained from multi-point velocity observations by S4 current meter on 30 July 1995

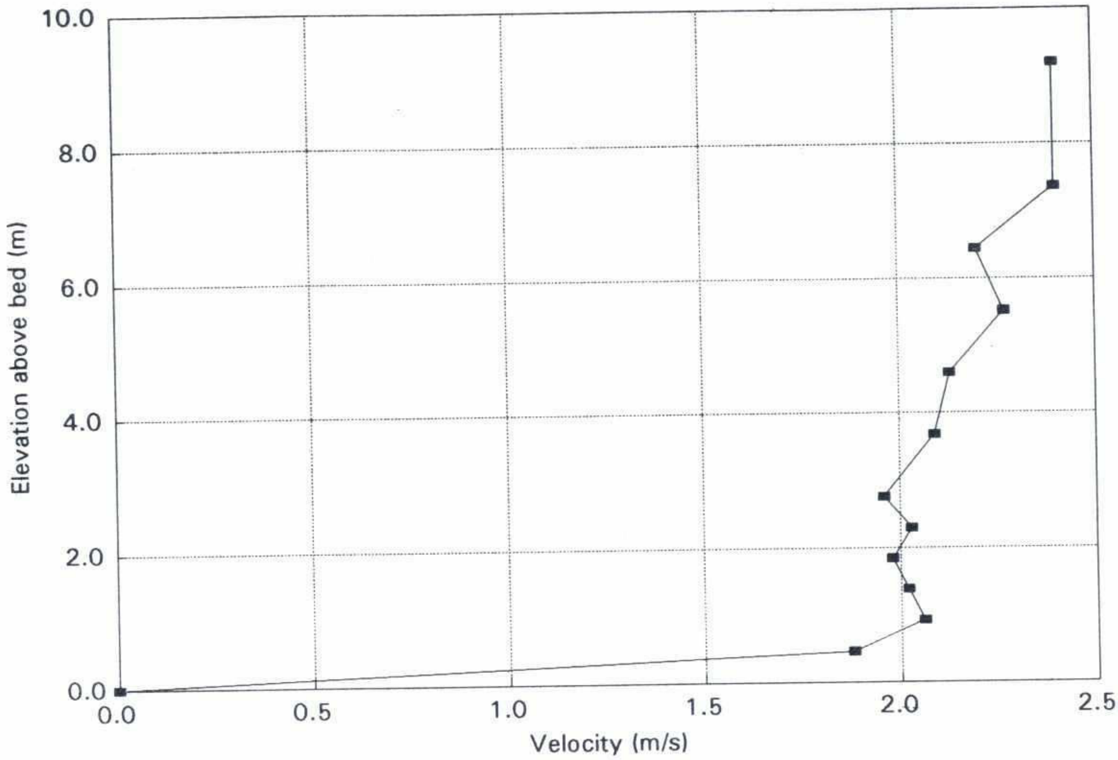

Figure C.13: Velocity profile at LE obtained from multi-point velocity observations by S4 current meter on 30 July 1995

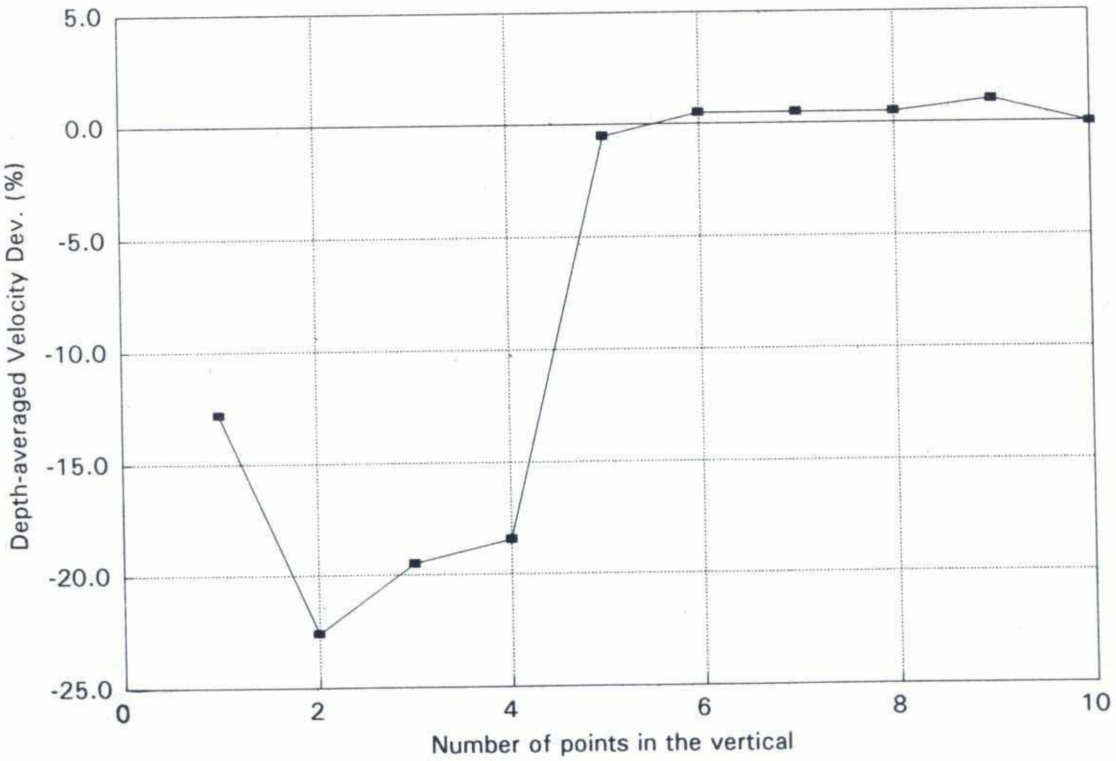

Figure C.14: Percentage deviation of the depth-averaged velocities obtained by using different points in the vertical from the depth-averaged velocity using all 10-points in the vertical at station RA. Positive deviation indicates overestimation and negative deviation indicates underestimation. The 10-point depth-averaged velocity is 1.95 m/s

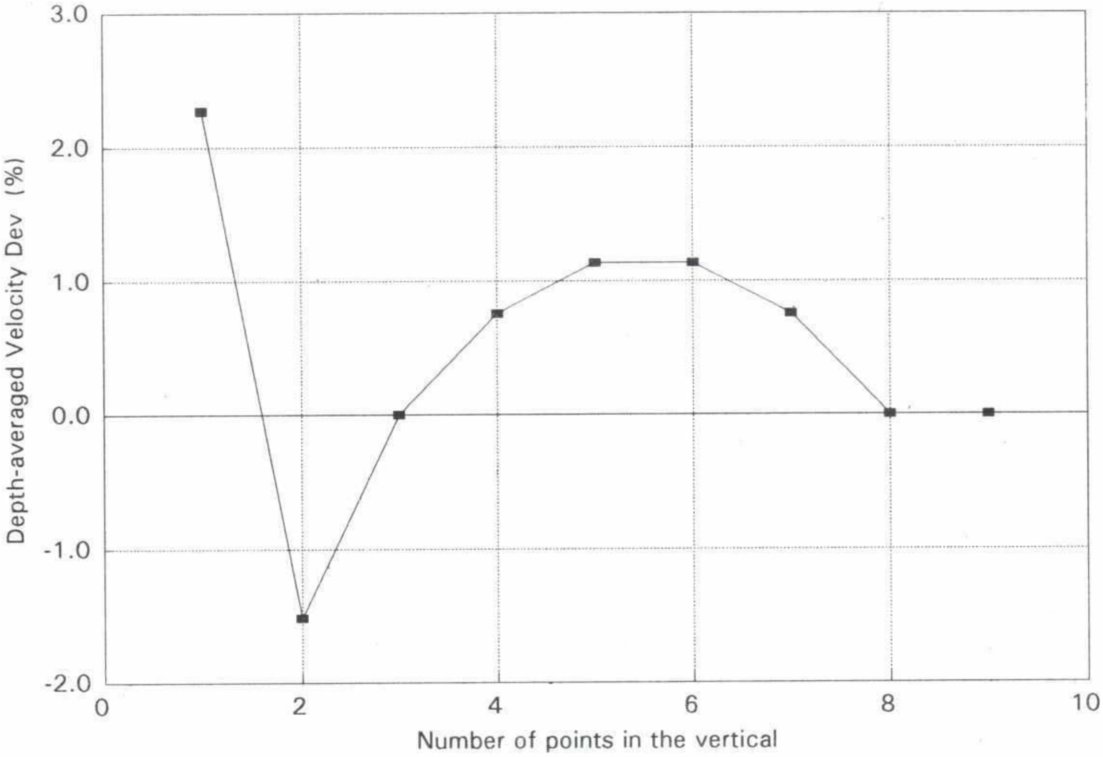

Figure C.15: Percentage deviation of the depth-averaged velocities obtained by using different points in the vertical from the depth-averaged velocity using all 9 points in the vertical at station LB. Positive deviation indicates overestimation and negative deviation indicates underestimation. The 9-point depth-averaged velocity is 2.64 m/s

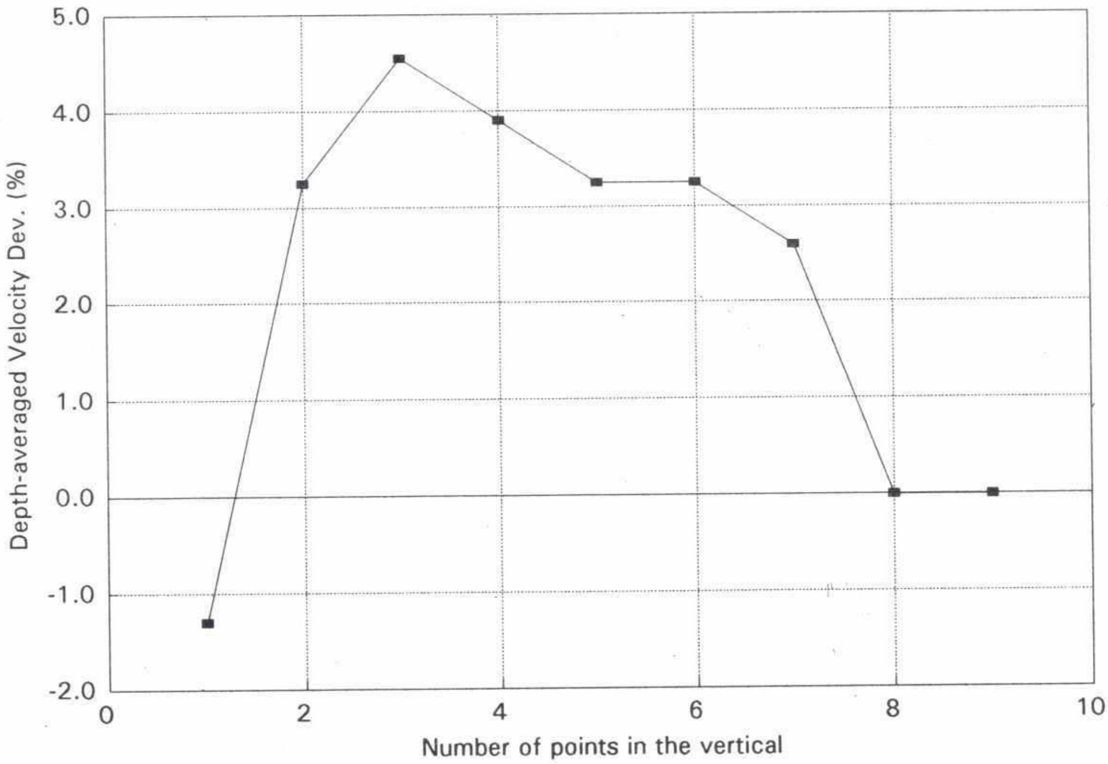

Figure C.16: Percentage deviation of the depth-averaged velocities obtained by using different points in the vertical from the depth-averaged velocity using all 9 points in the vertical at station LC. Positive deviation indicates overestimation and negative deviation indicates underestimation. The 9-point depth-averaged velocity is 1.54 m/s

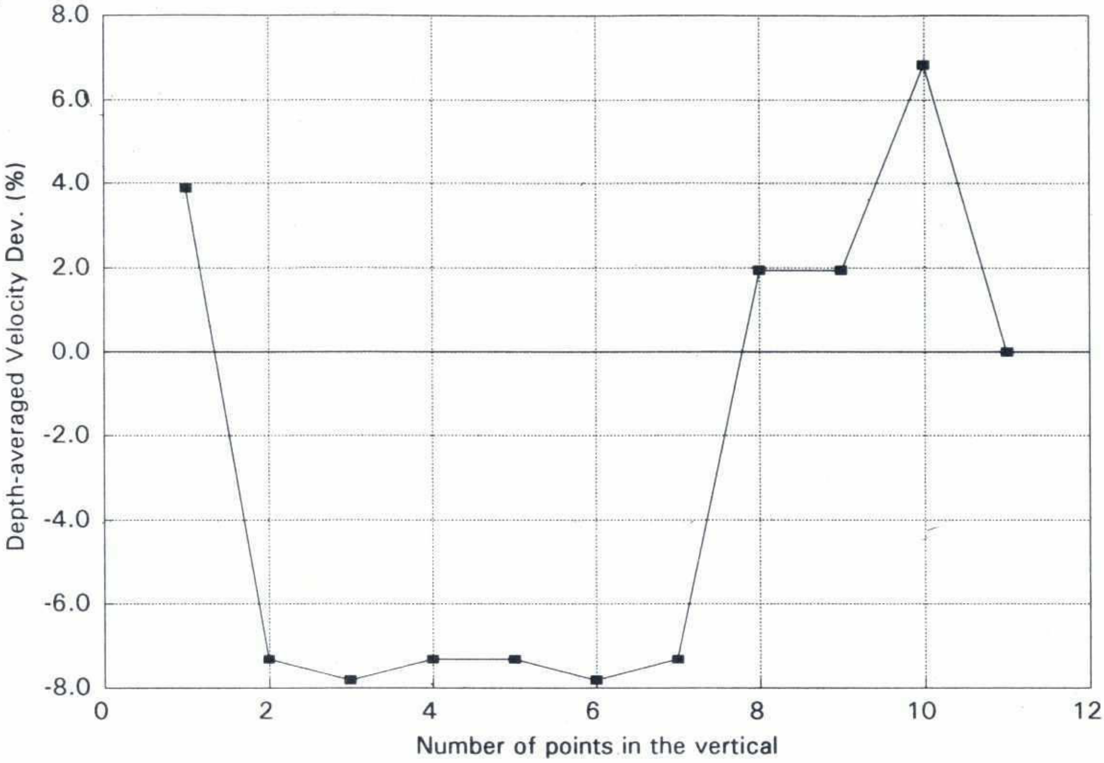

Figure C.17: Percentage deviation of the depth-averaged velocities obtained by using different points in the vertical from the depth-averaged velocity using all 11 points in the vertical at station LD. Positive deviation indicates overestimation and negative deviation indicates underestimation. The 11-point depth-averaged velocity is 2.05 m/s

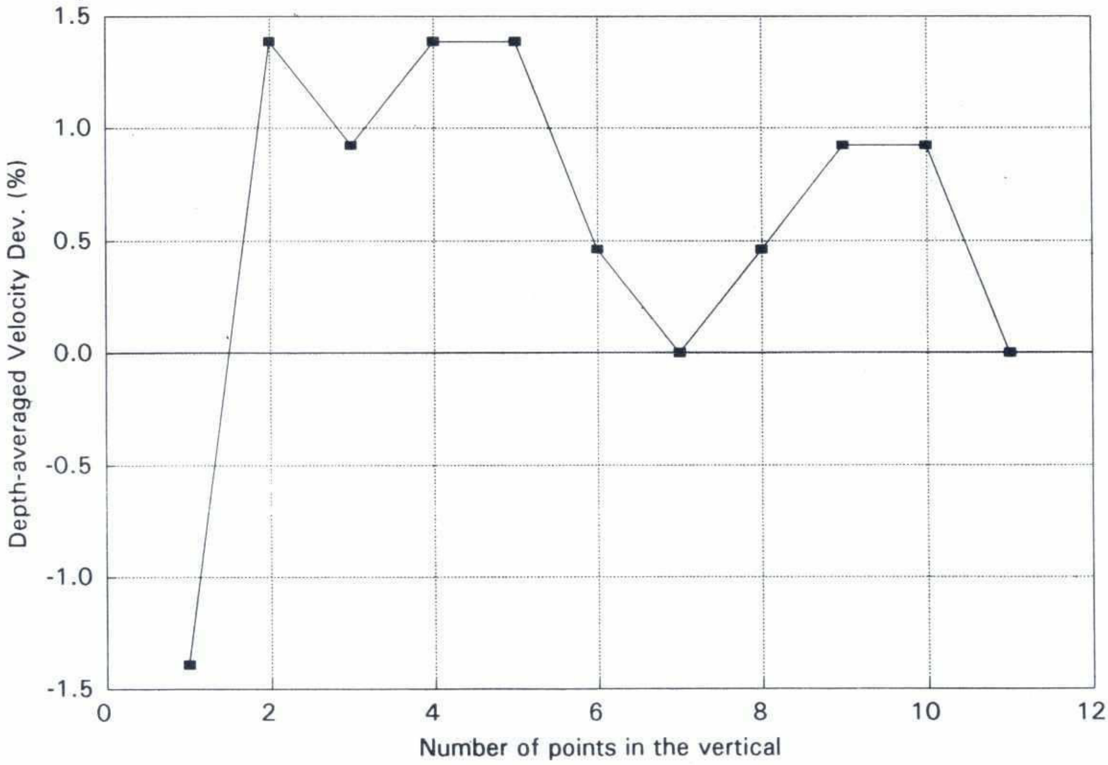

Figure C.18: Percentage deviation of the depth-averaged velocities obtained by using different points in the vertical from the depth-averaged velocity using all 11 points in the vertical at station LE. Positive deviation indicates overestimation and negative deviation indicates underestimation. The 11-point depth-averaged velocity is 2.16 m/s

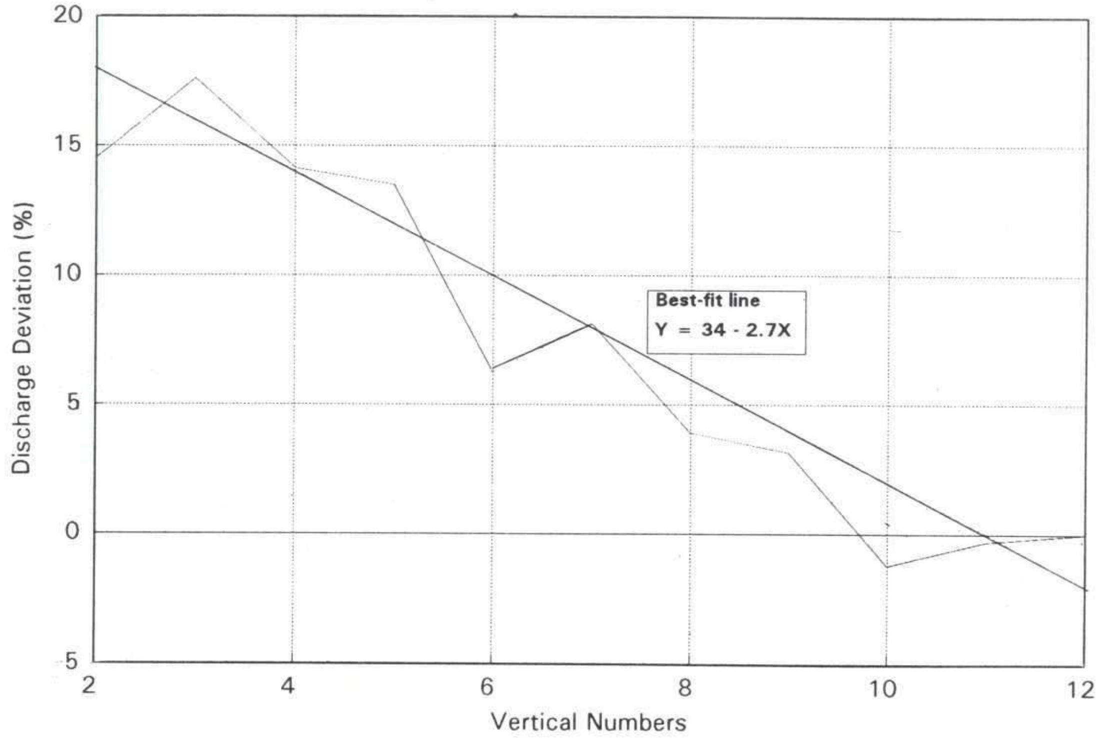

Figure C.19: Percentage deviation of discharge estimates using different verticals at transect T1 from the discharge estimate using all the verticals based on measurements in the Jamuna River near Bahadurabad on 27 July 1995. Positive deviation indicates overestimation and negative deviation indicates underestimation

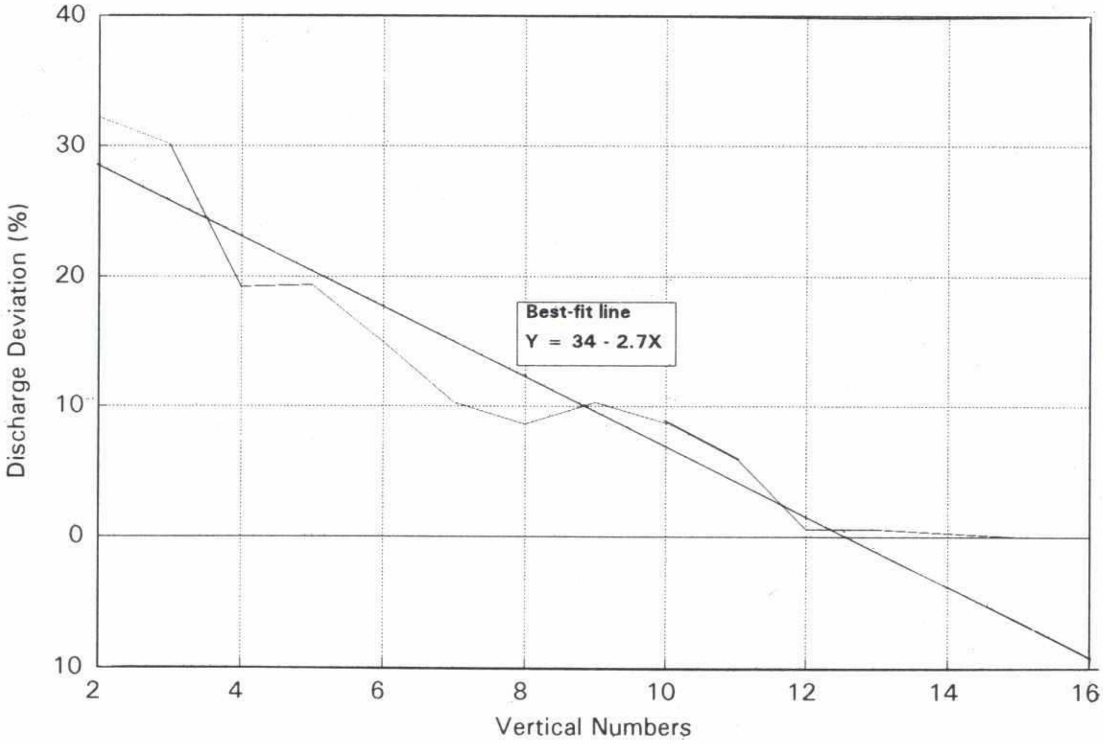

Figure C.20: Percentage deviation of discharge estimates using different verticals at transect T2 from the discharge estimate using all the verticals based on measurements in the Jamuna River near Bahadurabad on 28 July 1995. Positive deviation indicates overestimation and negative deviation indicates underestimation

Special Report 11, Annexure D

Analysis of Tidal Survey Data

October 1996

Contents

m2D

Figures

Mawa (Phase 2), Water levels and flow conditions

Mawa (Phase 2), Sediment grain sizes

Mawa (Phase 2), Sediment concentrations and transport

Mawa (Phase 2) , Bed profiles

Table

1 Introduction

To establish a good set of data at a station which is strongly influenced by tidal flow requires far more extensive measurements and resources than would be required at a station without tidal influence. Such detailed data may be needed for various purposes, which are in principle the same as for non-tidal locations:

Information about the transport of sediment as well as about the flow may be required to:

- assess the tidal volume and the tide generated flow velocities
- assess the net discharge and the runoff related discharge
- estimate the volume of sediment 'available' for future deposition (wash load as well as bed material load)
- assess the sediment balance of part of a river system
- assess the relation between flow and bed material transport including any phase lag
- assess the net inflow or outflow of sediment to and from a certain area (wash load as well as bed material load)

It is assumed that there is no or insignificant salinity intrusion (as it is the case at the measuring stations of RSP).

In case the above assessments are carried out with 1D or 2D modelling as a tool, the data collection may be planned so that they can form the input and calibration/verification data for the model.

The tidal surveys of the RSP have been carried out at selected stations during the dry season because during this period the tidal effects are most pronounced. Three phases of measurements were carried out. The early measurements (Phase 1) in 1993-94 at Bhairab Bazar, Baruria and at Arial Khan offtake are the least extensive and do not cover entire tidal periods. These 'pilot surveys' were used to select locations and survey strategy for the more extensive surveys at Bhairab Bazar and Mawa in 1995 (Phase 2). The last tidal surveys carried out in January-February 1996 (Phase 3) focused on Mawa, after taking into account the findings from Phase 2.

The BWDB makes biweekly 15-hour tidal discharge measurements at Mawa and at Bhairab Bazar stations during the January-April period. These data are collected for developing rating curves. BWDB carried out their tidal measurements simultaneously with the RSP at Bhairab Bazar and Mawa in 1995 and 1996 (spring tide). This gives the opportunity to make comparisons between the two sets of data.

2 Objectives

Tidal measurements are carried out to provide a 'sufficient' picture of the variation of flow and sediments in time as well as in space.

Along the river: Bathymetric information upstream and downstream of the transect line is useful for understanding measurement results.

Across the river: Frequent transects provide all necessary information on the flow.

For sediment transport, the number of verticals required depends on the width and channel characteristics of the river.

Vertically: Verticals with ADCP, S4, Helley Smith, Delft Bottle, bed samples, pump samples and bulk samples provide good coverage.

In time: short term, i. e. for one tidal cycle, the repeated measurements are quite sufficient, but not long-term (for balances).

Main objectives of FAP24 tidal measurements are to enable:

1. Assessment of errors made using traditional methods.

2. Assessment of the need for detailed measurements to improve balances.

3. Assessment of the net flow and sediment transport rates in different tidal situations.

The first objective is met through comparisons with BWDB data. Regarding the second objective, the repeated ADCP transects are well suited for establishing the water balance over a short period of time (the duration of the tidal measurements). Sediment balances, however, require very dense measurements across the river covering the entire measuring period. When it comes to long term balances and evaluation of long-term tidal storage (split of net flow in tide related and drainage/runoff related), the present measurement campaign does not provide the necessary long term data.

228

3 Tidal Surveys

The term 'tidal survey' is used about a survey which, as a minimum, includes a number of discharge measurements, covering a substantial part of one tidal period. With this definition the following tidal surveys have been carried out by the RSP, see also Main Report, Annex 1:

Station	Period	Survey Bulletin no.	Remarks
Bhairab Bazar	27-28 April 1993	5	Phase 1
Bhairab Bazar	10 February 1994	34	Phase 1
Baruria	21-22 March 1994	43	Phase 1
Arial Khan Offtake	18-19 April 1994	53	Phase 1
Baruria	3-5 May 1994	56	Phase 1
Mawa	17-18 February 1995	134	Phase 2
Arial Khan Offtake	23 February 1995	136	Phase 2
Bhairab Bazar	17-20 March 1995	139	Phase 2
Mawa	30-31 January 1996	254	Phase 3
Mawa	7-8 February 1996	256	Phase 3

Table D.1: Tidal surveys in the Padma River at Mawa and in the upper Meghna River at Bhairab Bazer from 1993 to 1996.

The Survey Bulletins provide overviews of the results of each survey and selected data files are kept in the PSD24.

The Phase 1 surveys have been processed largely in the same way as routine gaugings. The layout of the Survey Bulletins is similar, except that the bulletins for tidal surveys include time series of calculated discharges covering the period of the survey.

In the Phase 2 and 3 surveys more effort has been made to cover the flow and sediment transport in space and time. The Survey Bulletins are correspondingly more detailed.

Briefly described the Phase 2 and 3 include the following types of measurements:

- measurement of the flow distribution and discharge at short intervals for 26 hours using ADCP/EMF and DGPS. ADCP backscatter signal is used to select locations for stationary verticals.
- measurement of the vertical flow distribution at stationary verticals using ADCP/EMF and S4 current metre.
- measurement of sediment data at stationary verticals, including:
  - bed samples for bed sediment size

- Helley Smith and Delft Bottle samples for near bed transport and sediment size (measure sediment flux)
- pump bottle samples (measure sediment concentrations) for suspended sediment transport and vertical distribution
- bulk suspended sediment samples for determining size distribution of sediment (not in Phase 3 measurements)

- dune trackings (only Phase 2), including repeated surveys of selected lines along the flow direction using echosounder and DGPS

In the Phase 2 measurements DHA was anchored in the main channel doing one stationary profile and DHC was anchored in a secondary channel, also measuring one stationary profile. DHB was taking care of the moving boat discharge measurements and also the dune trackings.

In Phase 3 a main change to the survey programme was to leave out the dune trackings because they had proved less useful. This gave more time to DHB, which then in between discharge measurements lay by an anchored country boat at one of three preselected additional verticals for stationary profile measurements. The measurements at the three additional verticals are less frequent than the measurements at the two permanent stationary verticals. The intention behind this was to cover the relatively wide cross section at Mawa (more than 2 km wide) better with respect to lateral sediment transport distribution, and thereby make it possible to estimate the components of sediment transport for the entire cross section. Furthermore, to ease the interpretation of the Phase 3 measurement results the area of bathymetric survey in the Padma was extended approximately 5 kilometres downstream.

4 Data Analyses

Some analyses of the survey data are included in the presentations in the Survey Bulletins. For the more comprehensive Phase 2 and 3 surveys in Mawa and Bhairab Bazar some more detailed analyses have been carried out. The analyses of Phase 3 measurements were, however, limited to a minimum due to lack of time.

Of the two locations Mawa has the strongest tidal influence, with flow reversal during a short period of the flooding tide. Flow reversal does not take place at Bhairab Bazar. The Phase 2 measurements at Bhairab Bazar showed very little sediment transport with only weak correlation with the flow. The sediment transport at Mawa was higher and clearly correlated with the tide. Both measurement series were carried out during spring tide.

For these reasons, the third phase concentrated on Mawa, but included measurements at neap tide as well as during spring tide. The analyses below are, therefore, also more complete for the Mawa measurements than for the measurements at Bhairab Bazar.

In the following the results from the Phase 2 survey is first analysed and conclusions are drawn from these surveys. Then a few results from the Phase 3 survey is presented, but due to lack of time the analysis of Phase 3 survey results was never completed and no conclusions were drawn from these.

4.1 Mawa

Phase 2

Water levels

The AWLR of the RSP is situated near the ferry ghat on the left bank. Close to it is a staff gauge belonging to BWDB. The 3 months dry season time series of water levels from this AWLR and the staff gauge (Figure D.2) clearly shows the tidal influence. The tidal variation of water levels is composed of a daily variation of approximately 0.5 m and in addition a spring to neap variation of about the same magnitude. The spring to neap variation indicates the variation in storage created by the tidal cycle. The spring tide measurements 17-18 February 1995 are carried out around day 49 in the figure. Figures D.2 and D.3 also shows that the AWLR dries out during neap tide, but this did not limit the data coverage because the water level record is complemented by the staff gauge readings.

A temporary staff gauge was established on the right bank and read during the tidal measurements. Unfortunately, this staff gauge was never connected to PWD. Nevertheless, a comparison of the water level records from the two banks clearly shows a water level difference of up to 0.25 m which is clearly correlated with the discharge (highest at the highest discharge).

Figure D.4 shows the variation of the water level difference over a tidal cycle, together with the measured discharge (due to the missing connection of the right bank gauge only the variation, not absolute values of differences should be considered).

Discharge

The discharge was measured approximately half-hourly during 26 hours. The purpose was to cover a whole tidal cycle of 24.8 hours. In Figure D.6 the average (moving average) discharge is found, partly by integrating over 12.4 hours, partly by integrating over 24.8 hrs. In this case it does not seem to make much difference: The average discharge is 4000-4200 m^3/s. In Figure D.7 the total discharge is split into an average discharge and a time varying tidal component. The tidal component is seen to have a high flooding discharge of up to more than 5000 m^3/s of short duration and an ebbing discharge component of less than 2500 m^3/s, but with a longer duration.

Velocity

Velocity measurements 1 metre above the bed using the S4 current metre at the two permanent stationary profiles (DHA and DHC) were carried out together with sediment sampling (the records are shown in Survey Bulletins). The flow velocity records themselves show that:

- the magnitude of the flow velocities 1 m above bed is nearly the same at the two locations (between 0.1 m/s ingoing and 0.5 m/s outgoing)
- at the secondary channel (DHC) there is a small phase difference between the flow velocity near the bed and the discharge: The near bed flow velocity is 10-15 minutes ahead of the discharge. At the main channel the phase difference is insignificant.
- the net flow velocity is 0.2-0.3 m/s (outgoing).

Figure D.8 shows for the S4 record at the secondary channel (DHC), how this record may be split into a net flow component and a tidal component.

Sediment

The following characteristics are considered:

- grain sizes
- concentrations
- transport rates

Figure D.9 shows that grain sizes of the Delft Bottle samples are similar to the grain sizes of the bed sediment and fairly constant over the tidal cycle (not much dependent on the flow velocity). It also shows that the grain sizes of the Helley Smith samples are significantly higher than the grain sizes of bed samples and Delft Bottle samples. This agrees well with the findings of Special Report 12, that the Helley Smith catches only the coarser fractions of the sediment transport. Figure D.9 further indicates that the grain size of Helley Smith samples increases with flow velocity. It is, however, doubtful whether this indicates anything about the grain size of the near bed sediment transport.

Figures D.10 and D.11 shows that the grain sizes of the various fractions are independent of the flow velocity, except for the d_{90}, which varies distinctly with the variation in flow. This seems to indicate that the grain sizes of the suspended sediment increases when the flow velocity increases. It is interesting that this is not at all reflected in the variation of the median grain size, d_{50}, but only in the d_{90}, ie in the size of the coarsest 10 per cent of the suspended sediment.

Figures D.12 to D.15 show the variation with time of measured sediment concentrations at different levels. Both total concentrations and the concentrations of sand only, are considered. Figures D.11 and D.13 (main channel) clearly show that concentrations vary with the tide. Especially the sand fraction vary strongly with the tide near the bed (1 m above bed). The sand fraction generally contributes to the total concentrations by less than 10 per cent, except nearest to the bed (1 m above) where it reaches approximately 20 per cent near maximum ebb flow. Figures D.12 and D.13 indicate that there is a phase lag of the sediment concentrations behind the discharges of the order of a few hours. Figures D.14 and D.15 (secondary channel) show no distinct variation of concentrations with the tide. Concentrations are generally somewhat smaller in the secondary channel than in the main channel.

Figure D.16 shows the variation of the sediment flux as measured by Delft Bottle 5 and 15 cm above the bed. It also shows the corresponding variation in grain size of the samples. There is a significant variation of the measured fluxes with the tide, but no distinct difference between measurements at the two levels.

Finally, in Figure D.17, the product of measured concentrations and velocities has been integrated over the depth at the stationary vertical in the main channel (DHA) to give specific transport rates of suspended sediment at a vertical. The average sediment flux which can be derived from these measurements is of the same order of magnitude as the fluxes measured near the bed by Delft Bottle (Figure D.16).

The sediment transport over the entire cross section cannot be assessed with sediment measurements at only two verticals, as it was done in the Phase 2 measurements. In Phase 3 a small number of sediment measurements were carried out at 3 additional verticals in order to be able to estimate the integrated sediment transport for the whole river cross section.

Dune trackings

Repeated dune trackings were carried out along a predefined survey line in order to possibly detect migrations or modifications of bed form caused by the combined flow conditions.

A bed level survey was carried out 9 times of a predefined more than 1 kilometre long straight line nearly parallel to the direction of the flow. Figure D.18 shows the track lines of all 9 lines. Up to 10 metres spacing between the lines is not unusual; in some cases the spacing is more than 15 metres.

For a comparison between the bed levels at different times to be made, it is necessary to carry out a horizontal as well as a vertical correction.

Start and end points of the survey lines may deviate by up to 50 metres. The horizontal correction is carried out as follows: A typical 'average' line is defined. Then all the survey lines are projected onto this line. In principle this involves a length adjustment factor as well as a shift of the starting point. But, because the direction of the lines are almost the same, the length adjustment factor was found to be 1.00 for all lines.

The vertical correction is carried out by reducing the bed levels to PWD. The water level from the AWLR at the left bank is used. Effects of a tilting water level (up to 0.25 m across the river) will not be included.

Figure D.19 shows the results of all 9 surveys along the selected line. The lines are show from downstream to upstream. The first half of the survey shows no signs of any bed forms. The last half shows some asymmetrical bed forms with the steepest slope facing downstream, indicating that the main direction of sediment transport is in downstream direction. The bed forms are typically 90-110 metres long and up to 2 metres high. The are no clear signs of changes in dune shape during the measurements.

Figure D.20 shows the changes in bed level from the first survey to each of the subsequent surveys. The changes are generally within half a metre. Only 2-3 locations have larger changes; especially a reach between 800 and 850 metres from the start of the line has up to 1.5-2 metres changes. This could be due to migration of the dune at this location. Figure D.21 shows a detailed plot of the bed levels around this dune, which indeed indicate this dune may have migrated 10 metres downstream from the first to the last survey. The surveys in between these two surveys, however, indicate migrations in both directions of up to 5 metres. It is more likely that these are only apparent migrations, which in reality represent a high uncertainty on dune tracking over such a short time interval. At best we can, therefore, conclude that this particular dune has migrated 5-15 metres during 24 hours. From this we can make an estimate of the transport which must be 'trapped' by the dune

$$q_{s,trap} = c \cdot H \cdot (1-n)$$

where n is the porosity of the bed (0.4 assumed), H is the dune height (=2 m) and c is the migration rate (=5-15 metres per 24 hours). The trapped transport rate is thereby found to be $0.7\text{-}2 \cdot 10^{-4}$ m^2/s or 0.2-0.5 kg/m/s. Compared to measured transport rates even the lowest transport estimate from this dune tracking is higher than the total measured suspended transport. There are two possible explanations of this. Either:

- the dune migration is overestimated (the measured 'migration' is apparent only due to inaccuracies in the measurement).

- the measured transport rates by suspended sediment sampling underestimates the sediment transport significantly.

Since it seems most likely that the first explanation is the correct one, let us have a look at which inaccuracies are involved in the estimate of the dune migration:

- The discharge dependent lateral slope of the water level implies that the water level at the survey line may deviate from the water level taken at the AWLR by a variable amount: maximum vertical error, 0.25 m.

- The offset distance between the repeated surveys means that the lines are not describing exactly the same line. If the dune pattern is three-dimensional, or if it is two-dimensional with dune crest lines that are not perpendicular to the sailed line, this will cause an error. Since the offset distance is up to 10-15 metres, it is estimated that a 2-5 metres error on the horizontal location of the dunes can easily occur.

- Positioning errors. The DGPS works with a certain accuracy, which is estimated to be 6-10 metres in horizontal direction.

Considering these possible inaccuracies, it does not seem unlikely that most of the estimated dune migration of 5-15 metres could be mainly due to inaccuracies of the measurements.

It is concluded that dune trackings, to be successful should be carried out over a period where the dune can be expected to migrate a measurable distance. How long period is required, depends on sediment transport conditions.

Phase 3

The net flow in the Padma during the Phase 3 measurements was around 50 percent higher than during the Phase 2 measurements (approximately 6000 m^3/s). Flow reversal did not occur during the Phase 3 measurements in any of the verticals (minimum outward flow approximately 1000 m^3/s).

There was a gap in the discharge measurements of around 3 hours once during the measurements. This made a check of the averaging procedure (12.4 hours against 24.8 hours) less conclusive.

4.2 Bhairab Bazar

The maximum discharge of the Meghna during tidal flow measurements at Bhairab Bazar was found to be much smaller than for the Padma at Mawa (approx. 2000 m^3/s for the Meghna and 6000 m^3/s for the Padma). Contrary to Mawa, Bhairab Bazar has clearly reversing flow, with a higher discharge at during flooding than during ebbing (Figure D.27).

Grain sizes, both for the bed material and the near bed suspended material, seem to be lower during flood flow than during ebb flow (Figure D.28). The number of data is too few, however, to draw a firm conclusion.

As for Mawa, the D90 and no other fractions of the suspended material 1 metre above the bed show a variation with time. In the case of Bhairab Bazar, however, the variation does not seem to be related to the flow conditions (Figure D.29). Similarly near the surface, although here it seems that the coarser fractions tend to be coarser at high ebb flow than at other times (Figure D.30).

Suspended sediment concentrations are very low (<10 mg/l), clearly highest after flood flow. The sand fraction is less than 20 percent; lowest during flooding (5-10 percent). The measurements indicate (based on one vertical) that the direction of the net transport of suspended sediment is upstream. This is more pronounced for the fine material (wash load) than for the coarser material.

202

5 Conclusions and Recommendations

The following main conclusions and recommendations with respect to survey method have been drawn from a limited number of surveys and should therefore be regarded as indicative only:

1. With respect to **flow measurements**, the half-hourly measurements over 13 or 26 hours of discharges and water levels provides a good short-term description of flow conditions. For a long-term description the detailed tidal measurements should be combined with long-term flow velocity measurements, for instance by a self-recording current meter at a fixed location 1-2 metres below surface. A one-dimensional model will be a strong tool for long-term tidal flow analysis. Long-term water level data along the river will be required for setting up the model, see also Tajeda-Guibert (1994).

2. With respect to **sediment transport measurements**, measurements in two verticals is insufficient to establish the integrated transport rates over the entire cross section in a main river. Measuring at a large number of verticals requires large resources. As a compromise it may be possible to measure regularly at few verticals and less frequently at a number of additional verticals. This method requires scaling during analysis, and has not been tested.

3. A detailed **bathymetric survey** covering a reach of minimum 2 times the width of the river upstream and downstream is useful for interpreting the measurements of sediment transport.

4. The use of **dune tracking** to determine bed load and near bed transport proved less useful. The results will be dominated by measuring inaccuracies when the transport rate is relatively low and the measuring period is short.

The following detailed conclusions can be drawn from the measurements carried out at the two locations:

Phase 2, Mawa

- The flow in the minor channel seems to be ahead of the overall flow by 10-15 minutes.

- The average flow is 4000-4200 m^3/s and not much different with 24.8 hours averaging compared with 12.4 hours averaging. Reversed flow occurred under this condition (approximately 1000 m^3/s).

- The median grain sizes of the Delft Bottle samples are nearly the same as for the bed sediment. There is a tendency that it is lower at high flow rate.

- The median grain sizes for the Helley Smith samples are much higher than for the Delft Bottle samples. It tends to be highest at high flow rate/high Helley Smith catch.

- For the suspended sediment, the grain size of only the coarsest fraction varies with the flow. The d_{90} increases with the flow velocity with a phase lag which depends on the level above bed (1 and 9 metres above bed in main channel).

- The sediment flux measured by Helley Smith, Delft Bottle (kg/m2/s) and from pump samples (multiplied by velocities) are generally of the same magnitude. All three methods show clear dependence on flow rate, but there are no clear phase shifts.

- It is not possible accurately to estimate the total transport over a more than two kilometres cross section based on measurements at only two verticals.
- The sand fraction of concentrations is up to 20 per cent one metre above bed; up to 10 per cent at higher levels (in main channel).
- There is a clear phase lag of the concentrations compared to the discharge.
- In the secondary channel there is no distinct temporal variation of concentrations.

Phase 2, Bhairab Bazar

- Grain sizes of both bed material and near bed suspended material seem to be lower during flood flow than during ebb flow (only few data).
- The coarser fractions of suspended material tend to be coarser during ebb flow than at any other time.
- The measurements indicate that the sediment balance may be different for the wash load and for bed material load.

206

6 References

1. Tajeda-Guibert, J. A. : 'Tidal discharge quantification in rivers of Bangladesh: Station 273 Bhairab Bazar at Surma-Meghna river'.
Bangladesh Water Development Board. United Nations Development Program. UN Department for Development Support and Management Services. April 1994.

208

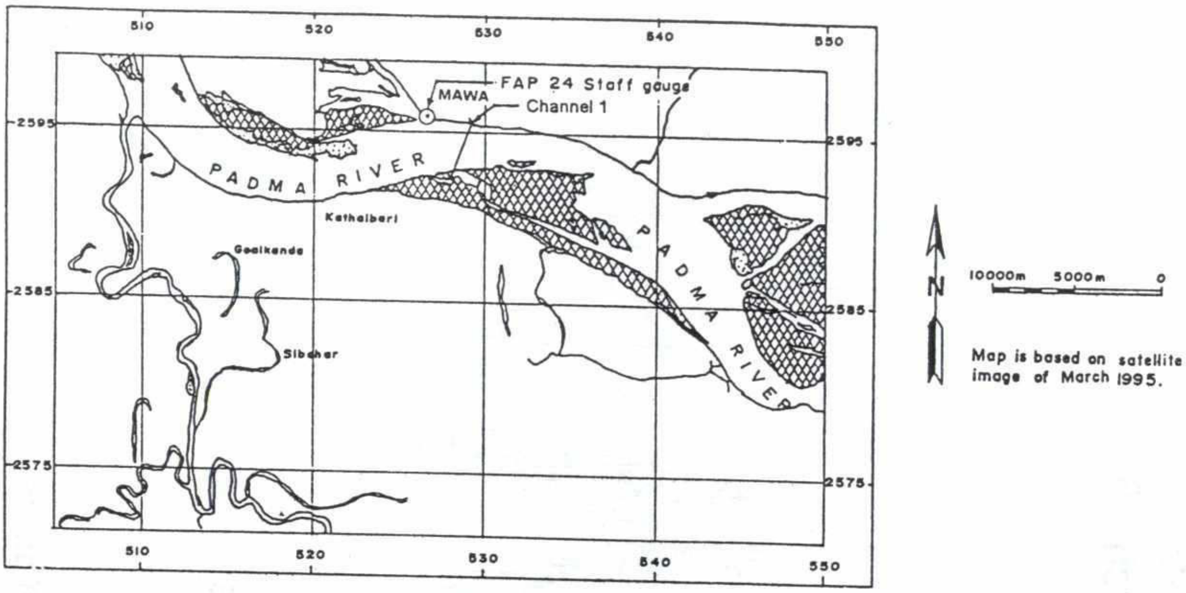

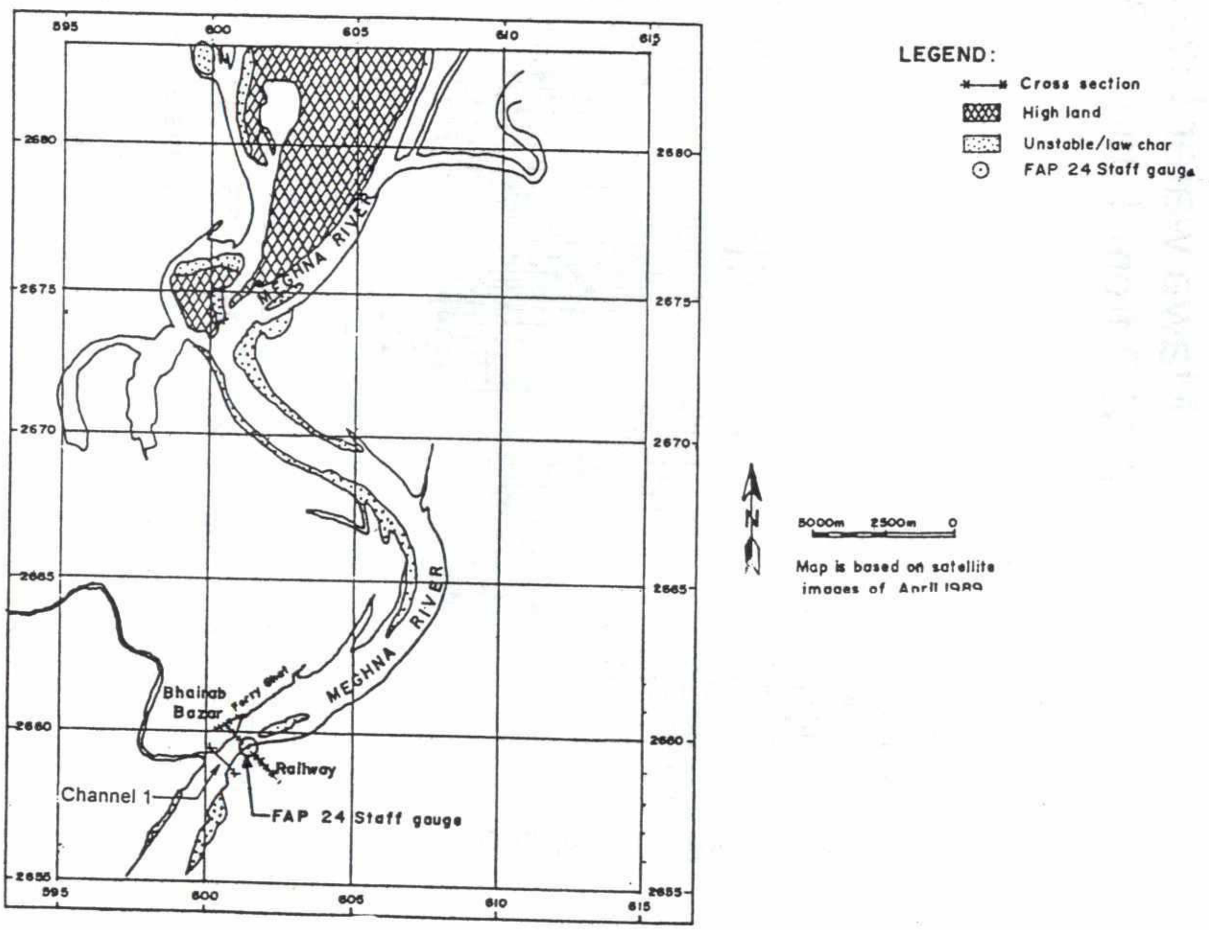

Figure D.1   Location maps. Tidal measurement locations at Mawa and Bhairab Bazar

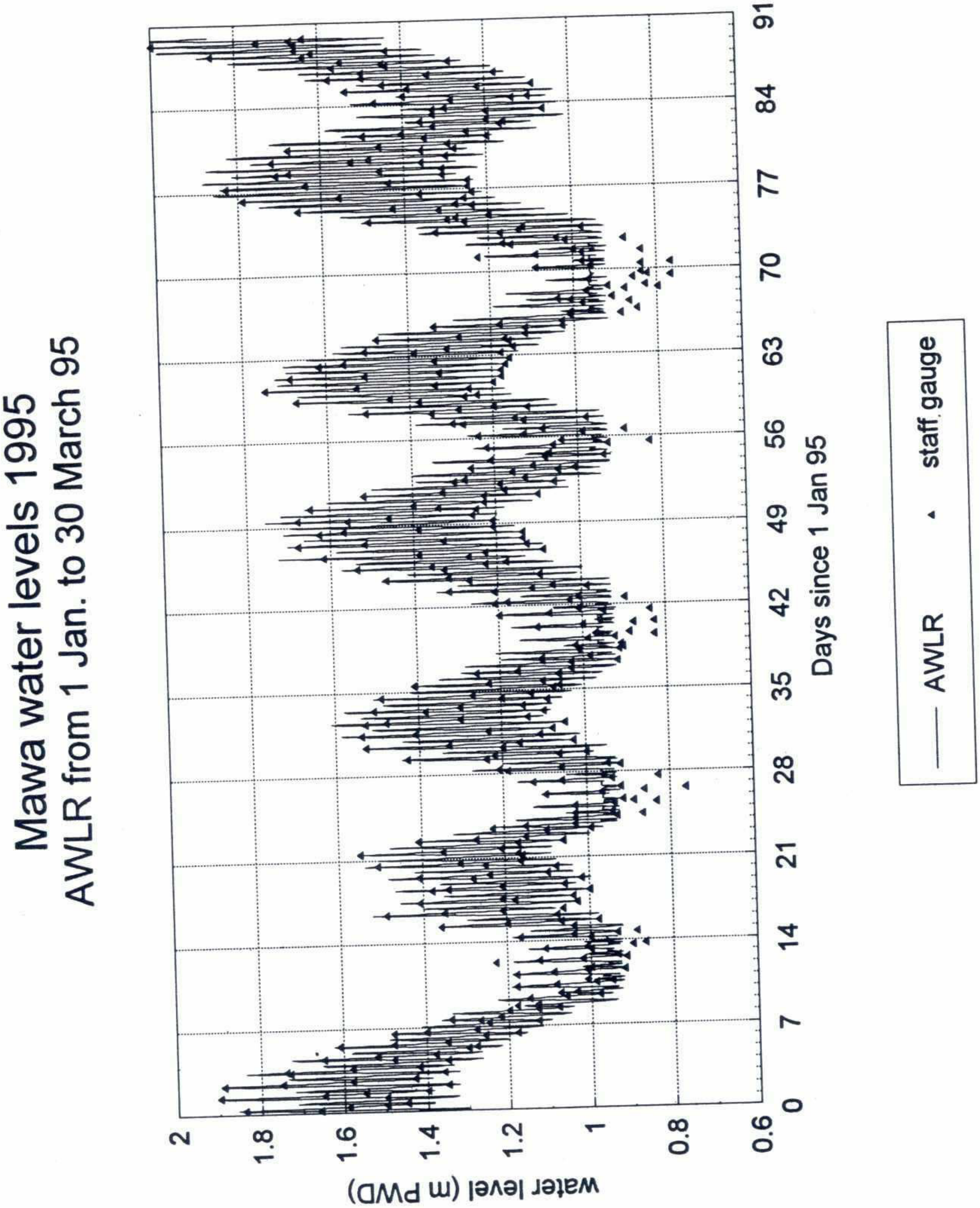

Figure D.2 Three months time series of water levels at Mawa. Automatic water level recorder and staff gauge (both left bank).

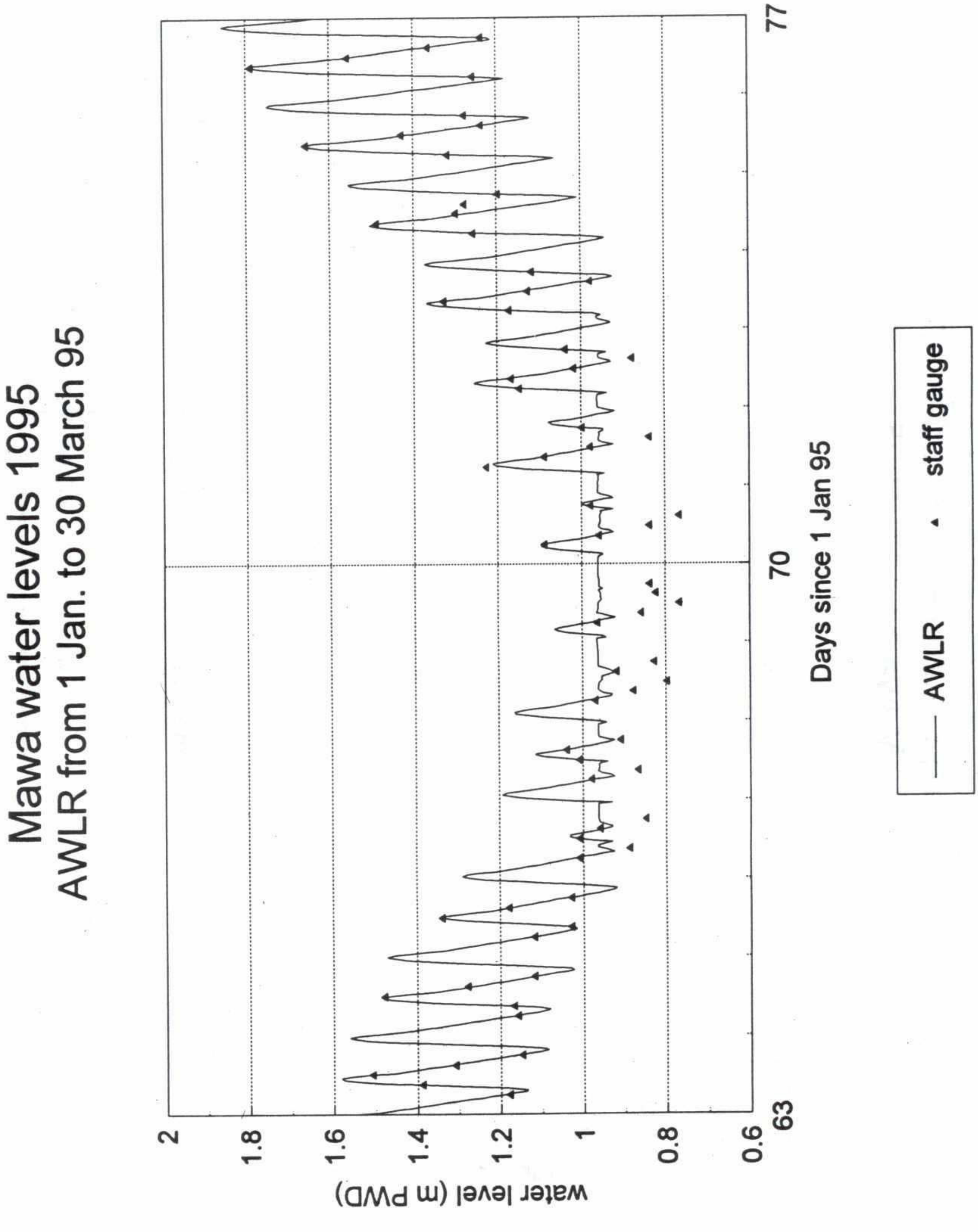

Figure D.3 Two weeks time series of water levels at Mawa. Automatic water level recorder and staff gauge (both left bank), showing the drying out of the AWLR.

207

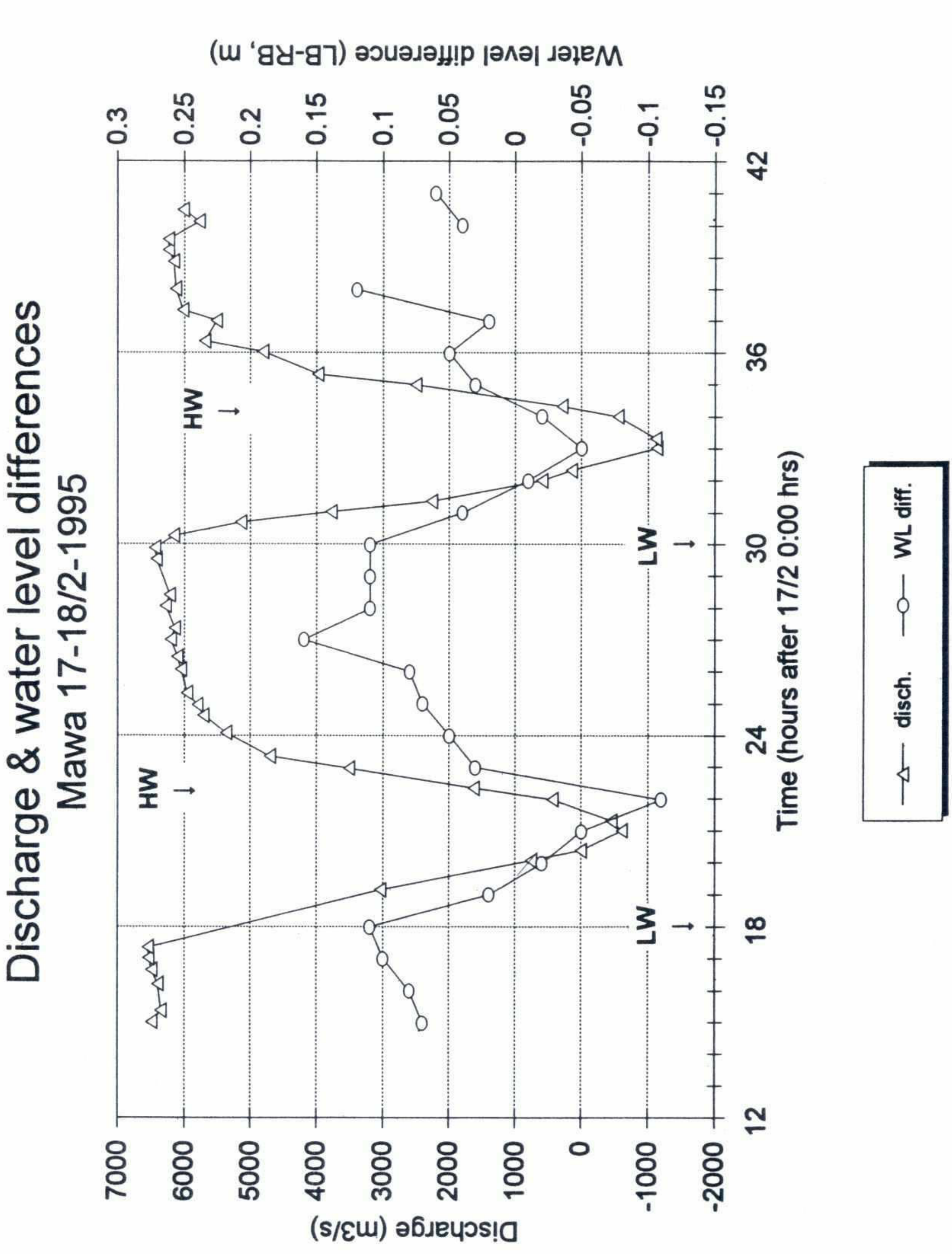

Figure D.4 Mawa. Time series of discharge and water level difference between left and right bank. Note: The left and right bank gauges were not connected to a common datum, so absolute differences should be disregarded.

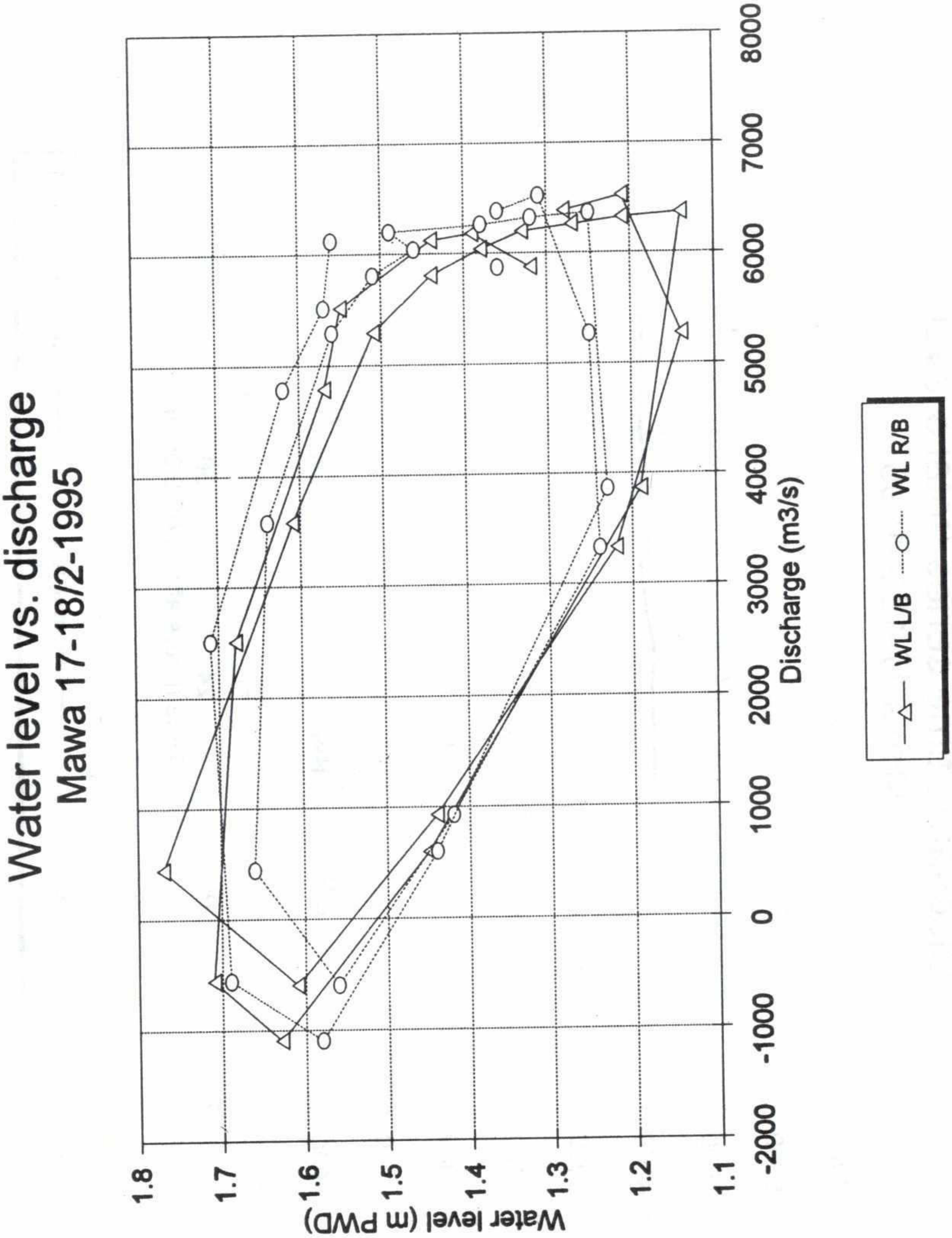

Figure D.5 Mawa. Measured water levels vs. discharges. Note: For right bank the absolute level is guessed.

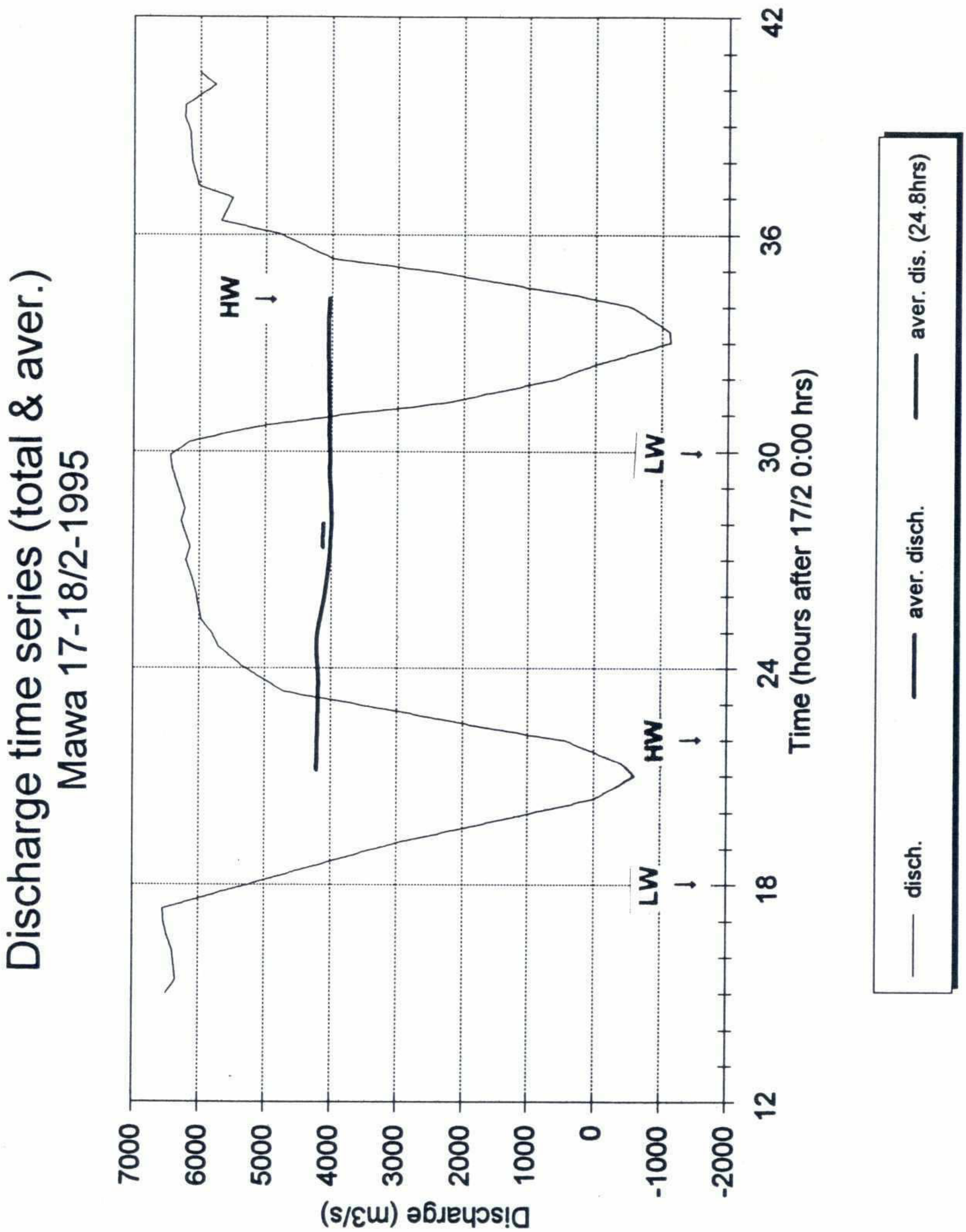

Figure D.6 Mawa. Discharge time series as measured and averaged over 12.4 and 24.8 hours.

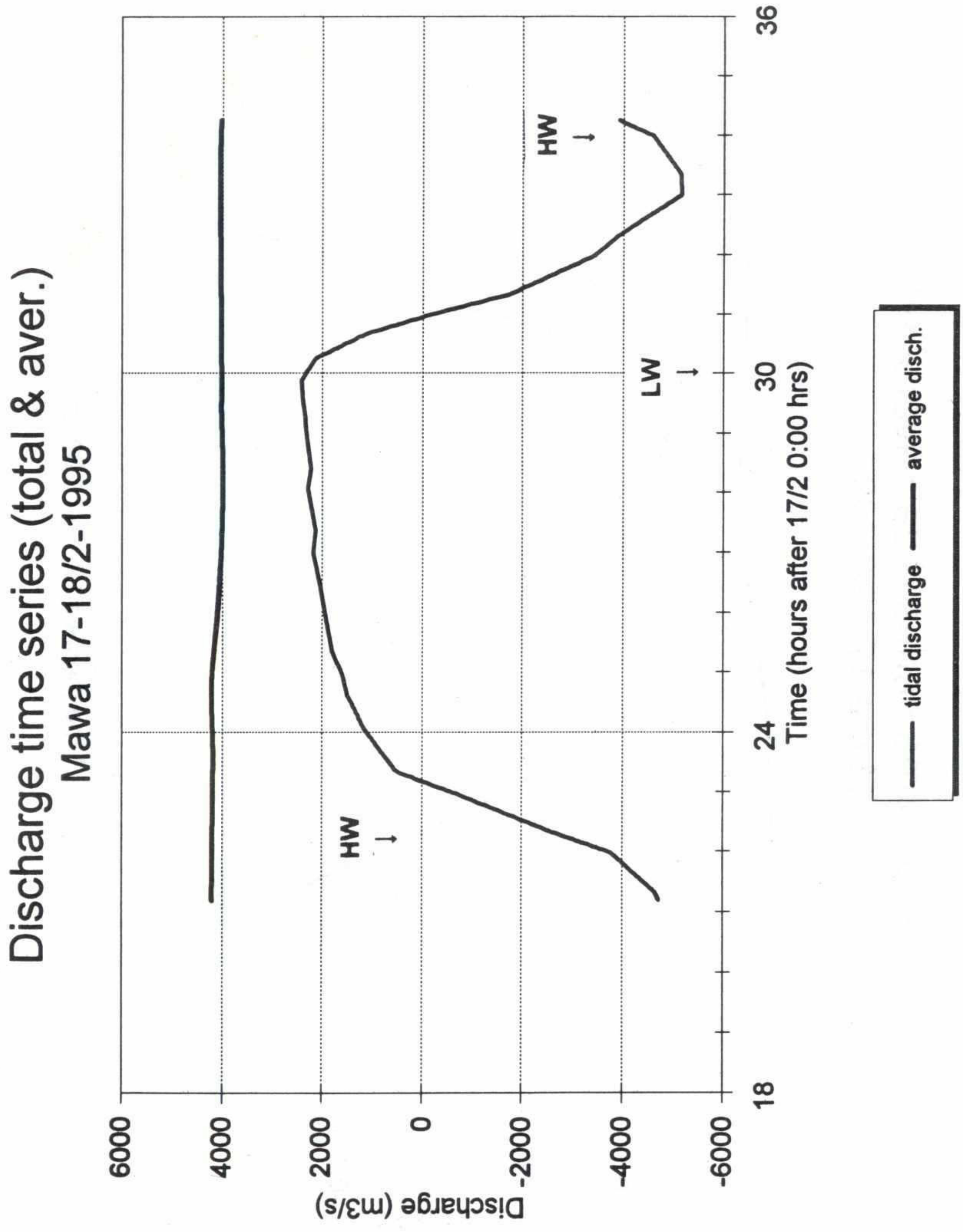

Figure D.7 Mawa. Average and tidal discharge.

222

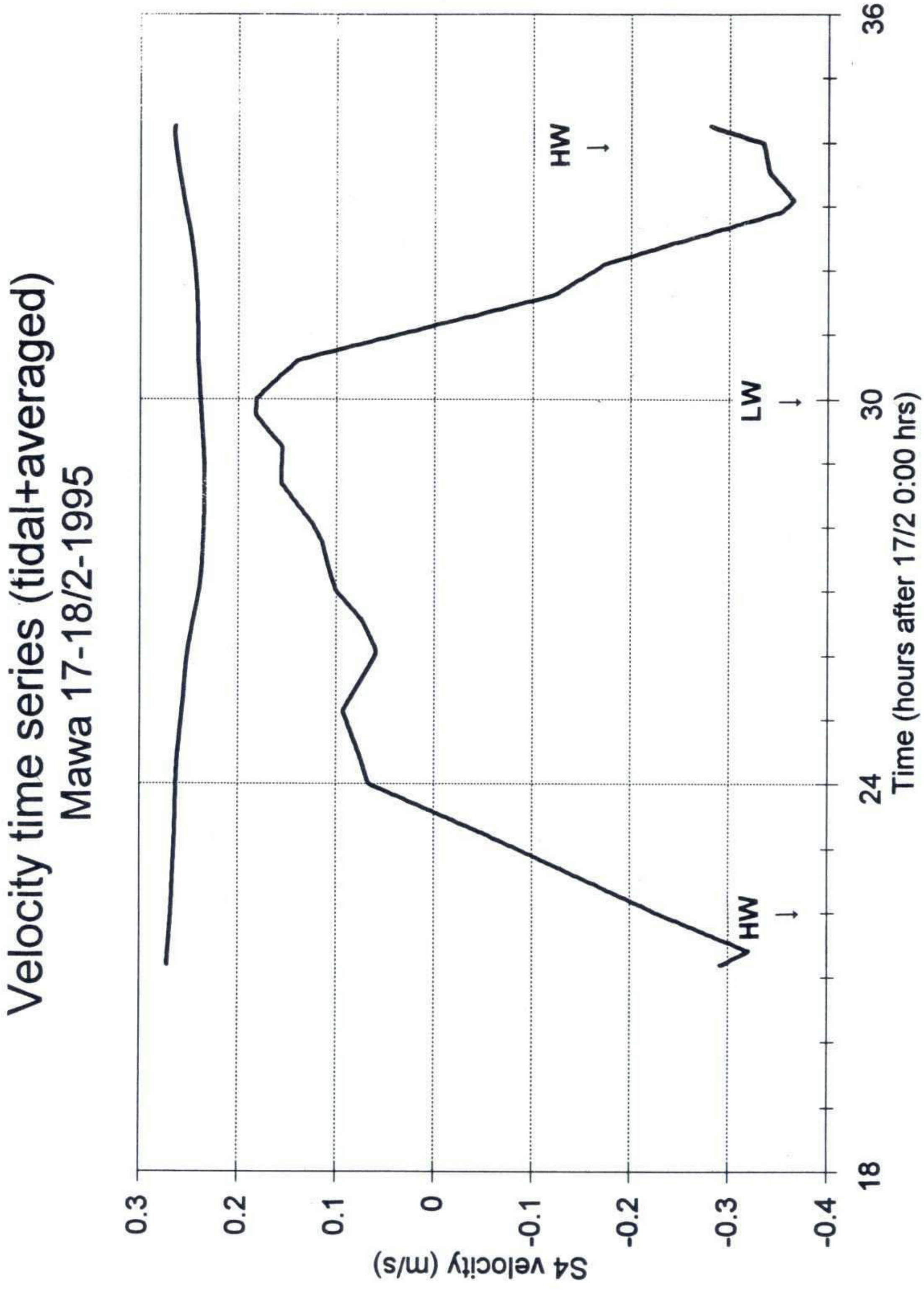

Figure D.8 Mawa. Average and tidal components of flow velocity 1 m above bed at secondary channel (DHC).

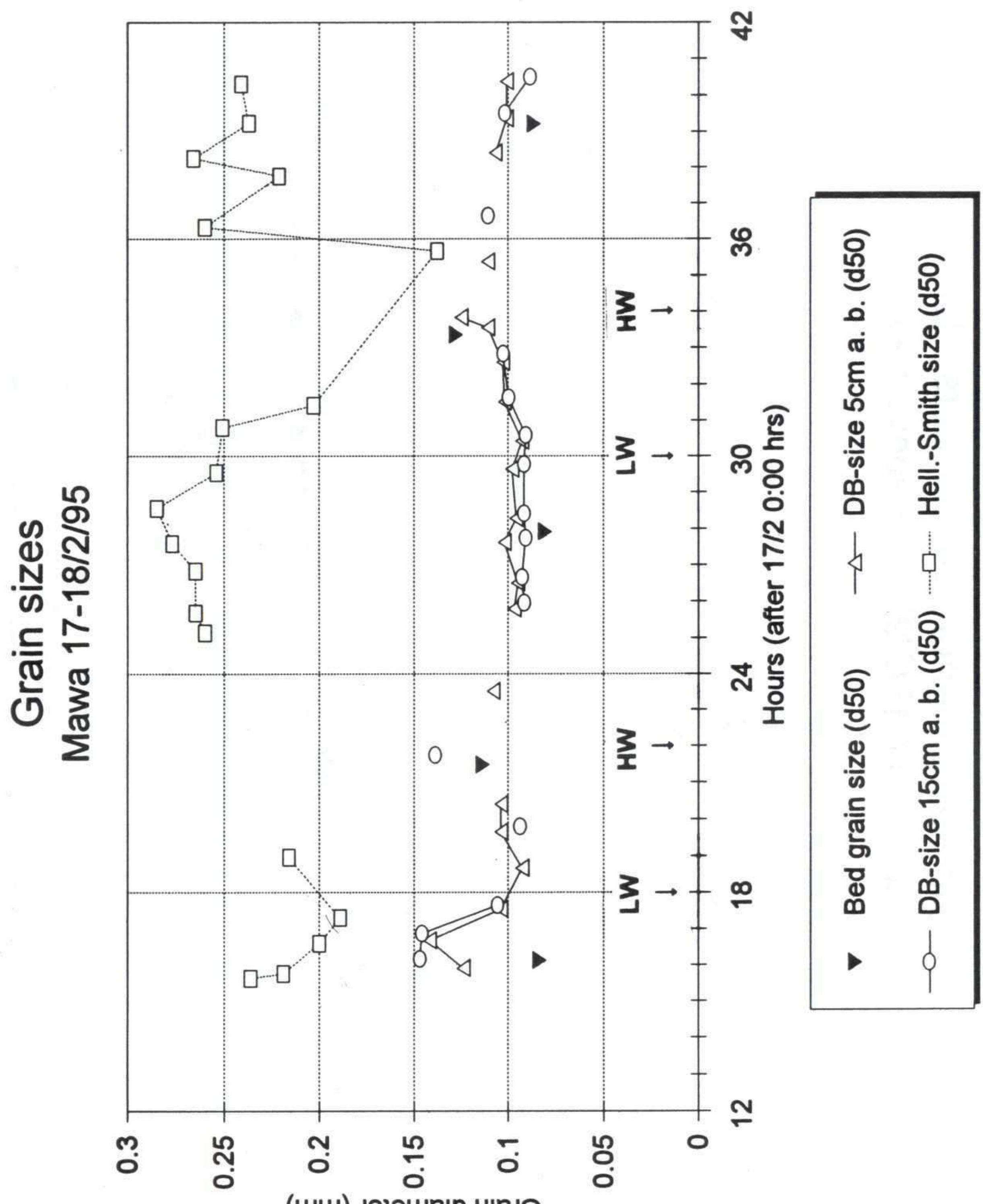

Figure D.9 Mawa. Median grain sizes of bed material samples, Helley Smith samples and Delft Bottle samples (Main channel, DHA).

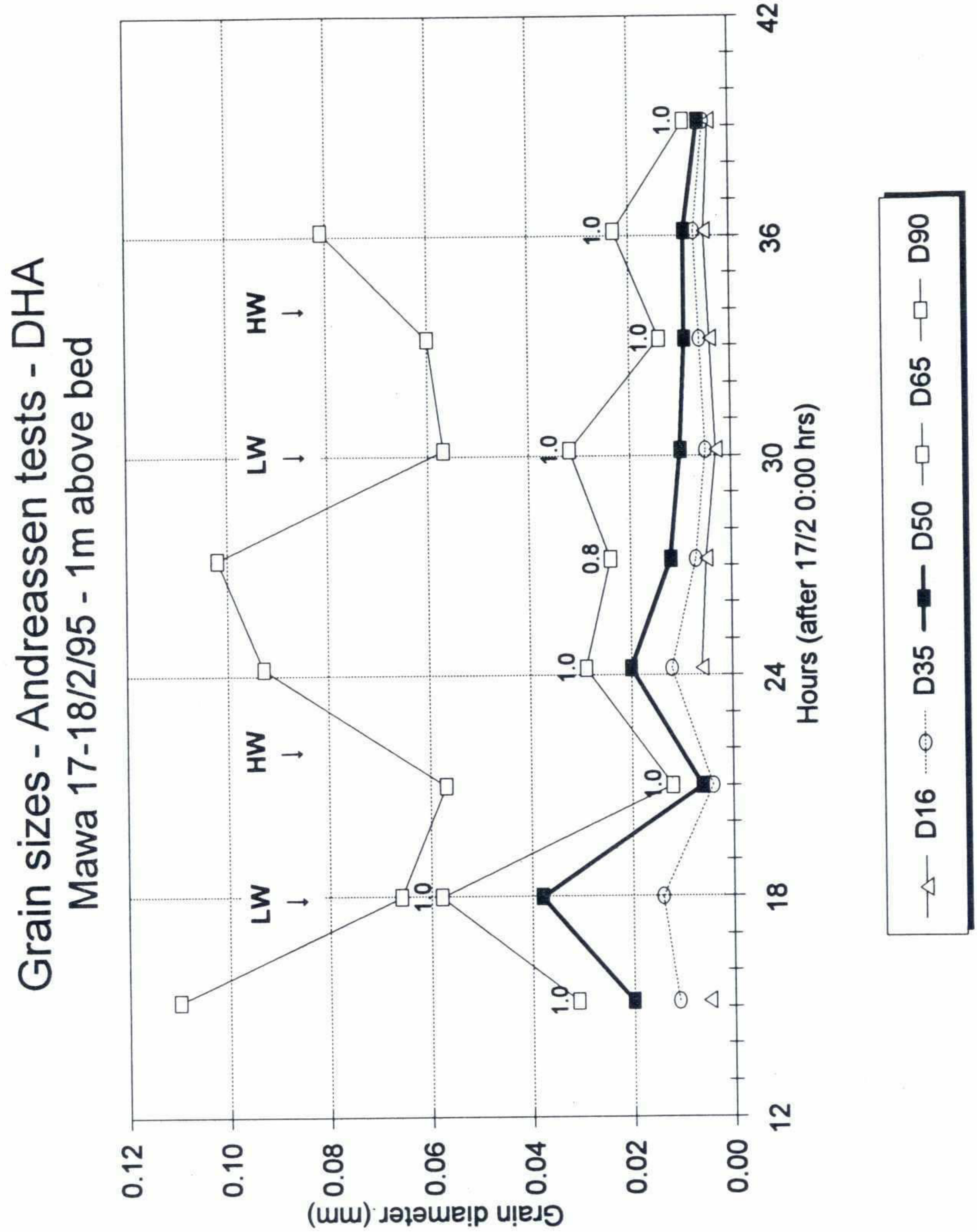

Figure D.10 Mawa. Grain sizes fractions determined by Andreassen tests for bulk sediment samples taken approximately 1 m above bed (Main channel, DHA). The labels indicate sampling level above bed (m).

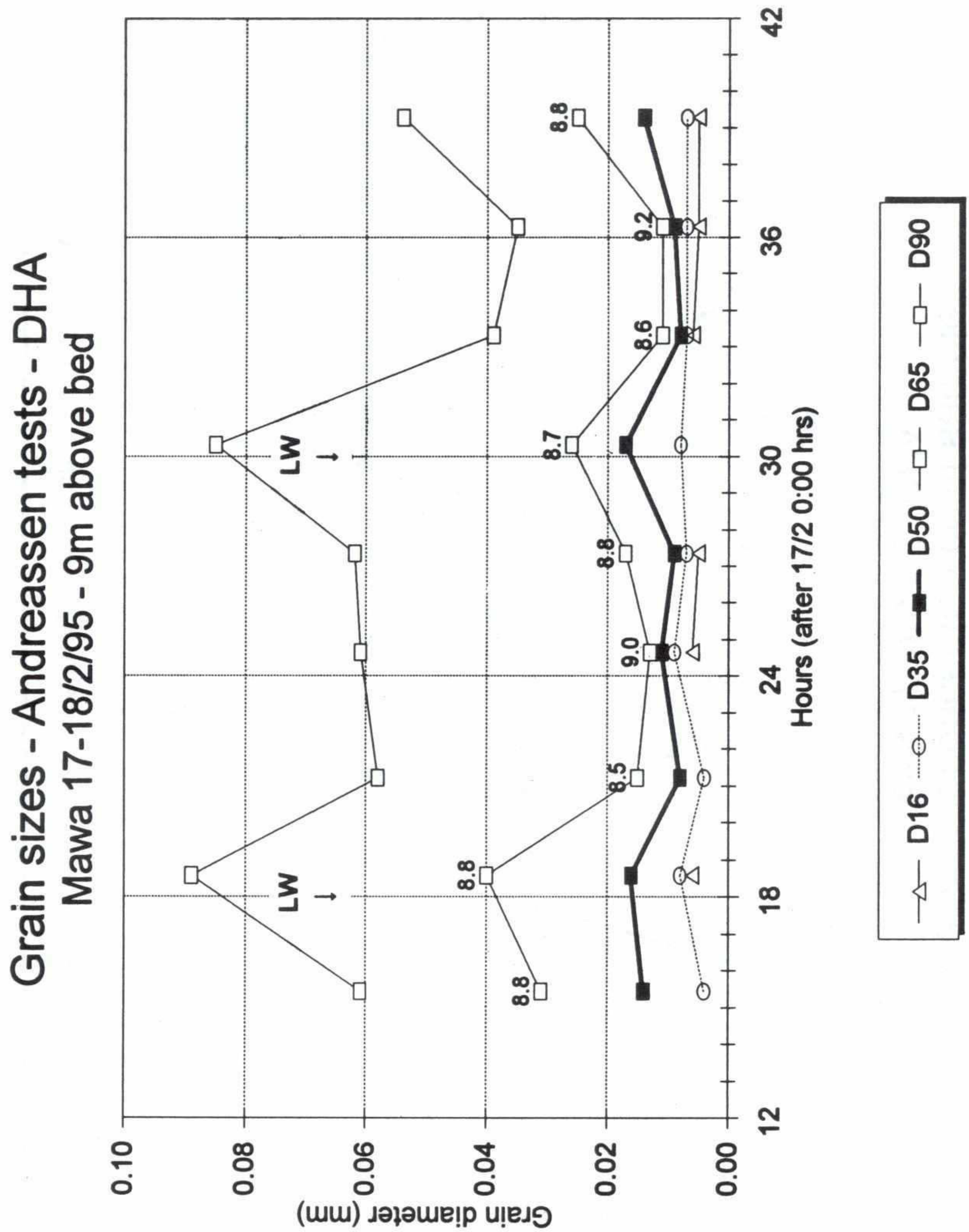

Figure D.11 Mawa. Grain sizes fractions determined by Andreassen tests for bulk sediment samples taken approximately 9 m above bed (Main channel, DHA). The labels indicate sampling level above bed (m).

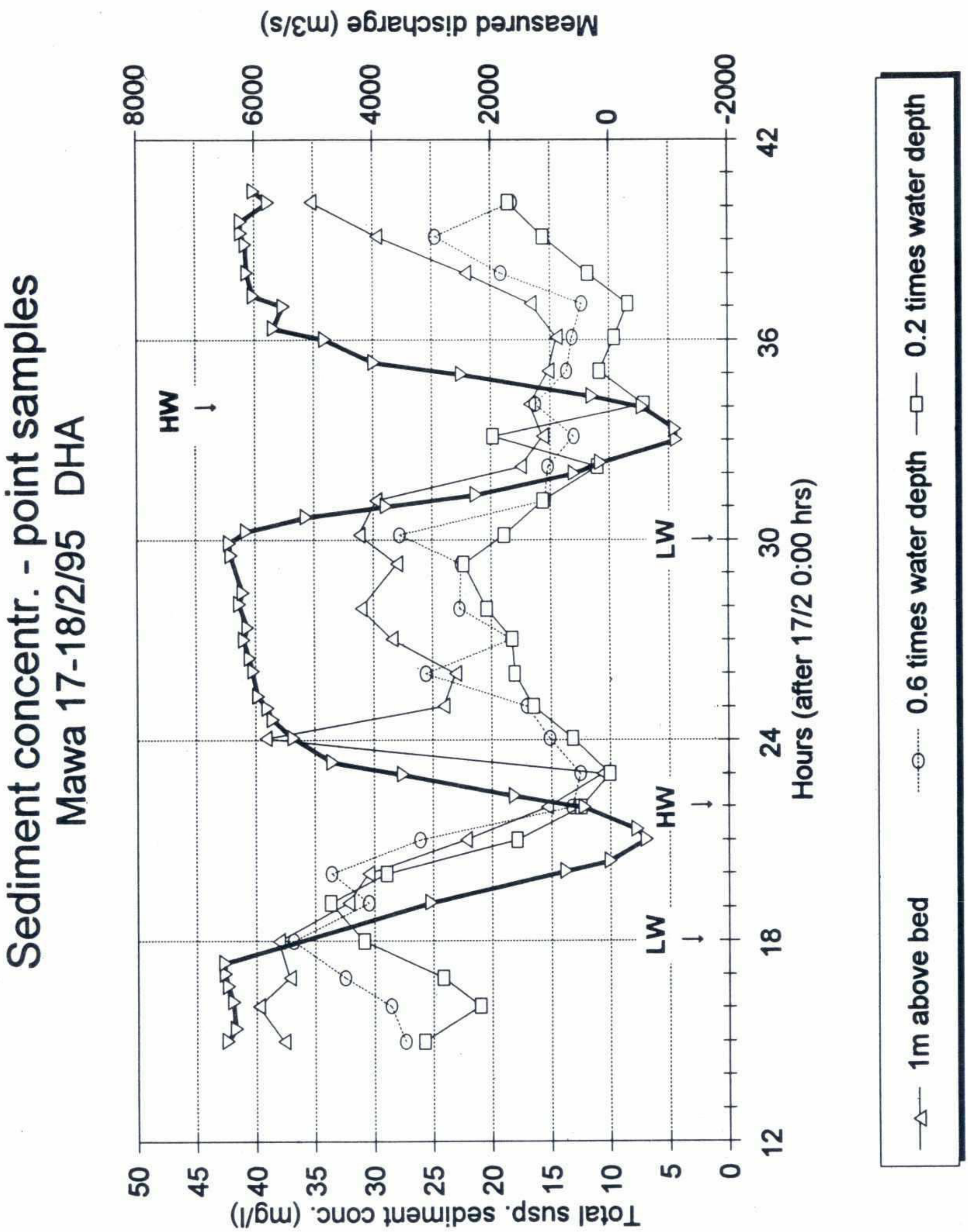

Figure D.12 Mawa. Measured sediment concentration time series (pump bottle samples) shown together with the discharge time series (Main channel, DHA).

224

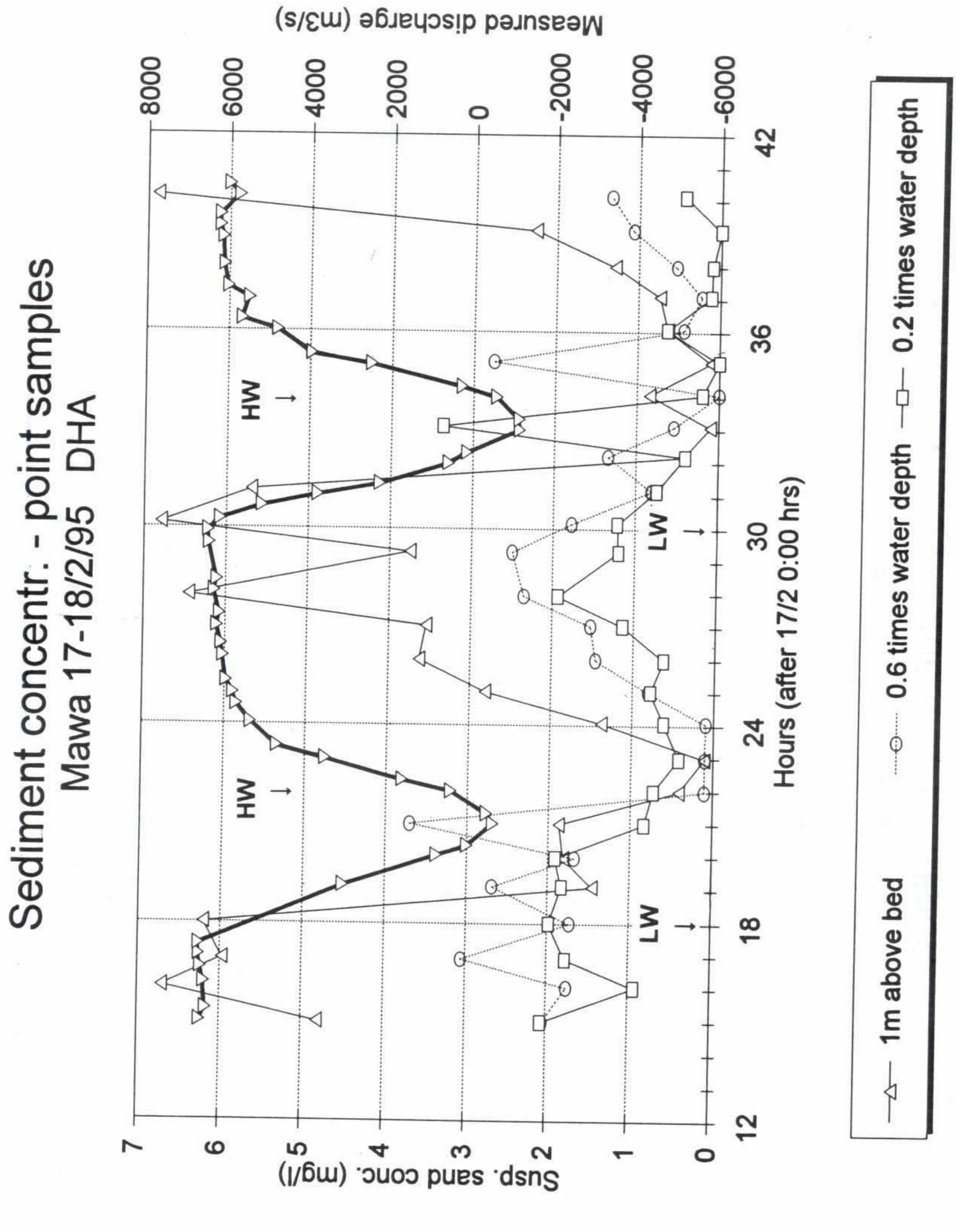

Figure D.13 Mawa. Measured time series of sand concentrations (pump bottle samples) shown together with the discharge time series (Main channel, DHA).

229

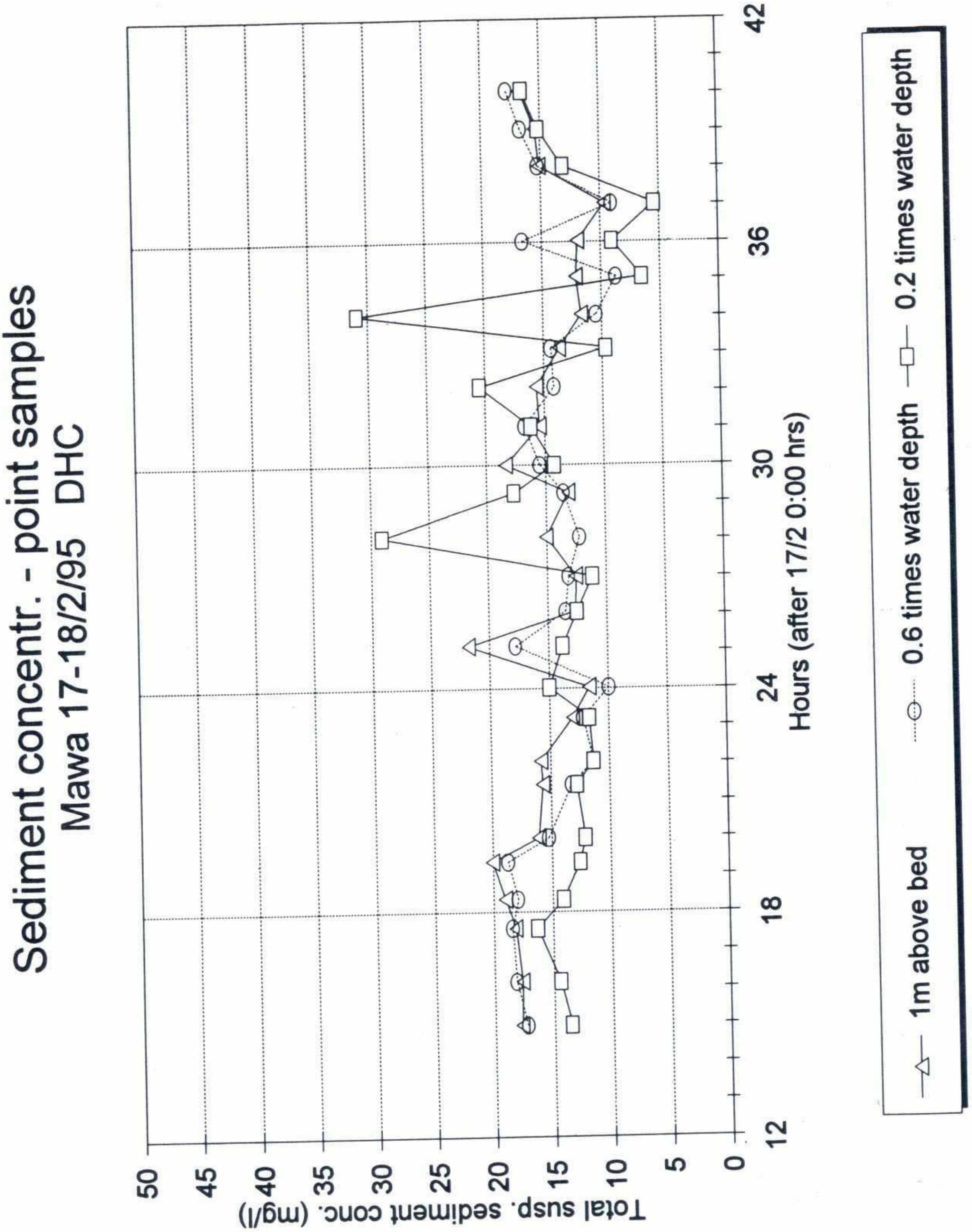

Figure D.14 Mawa. Measured sediment concentration time series from pump bottle samples (Secondary channel, DHC).

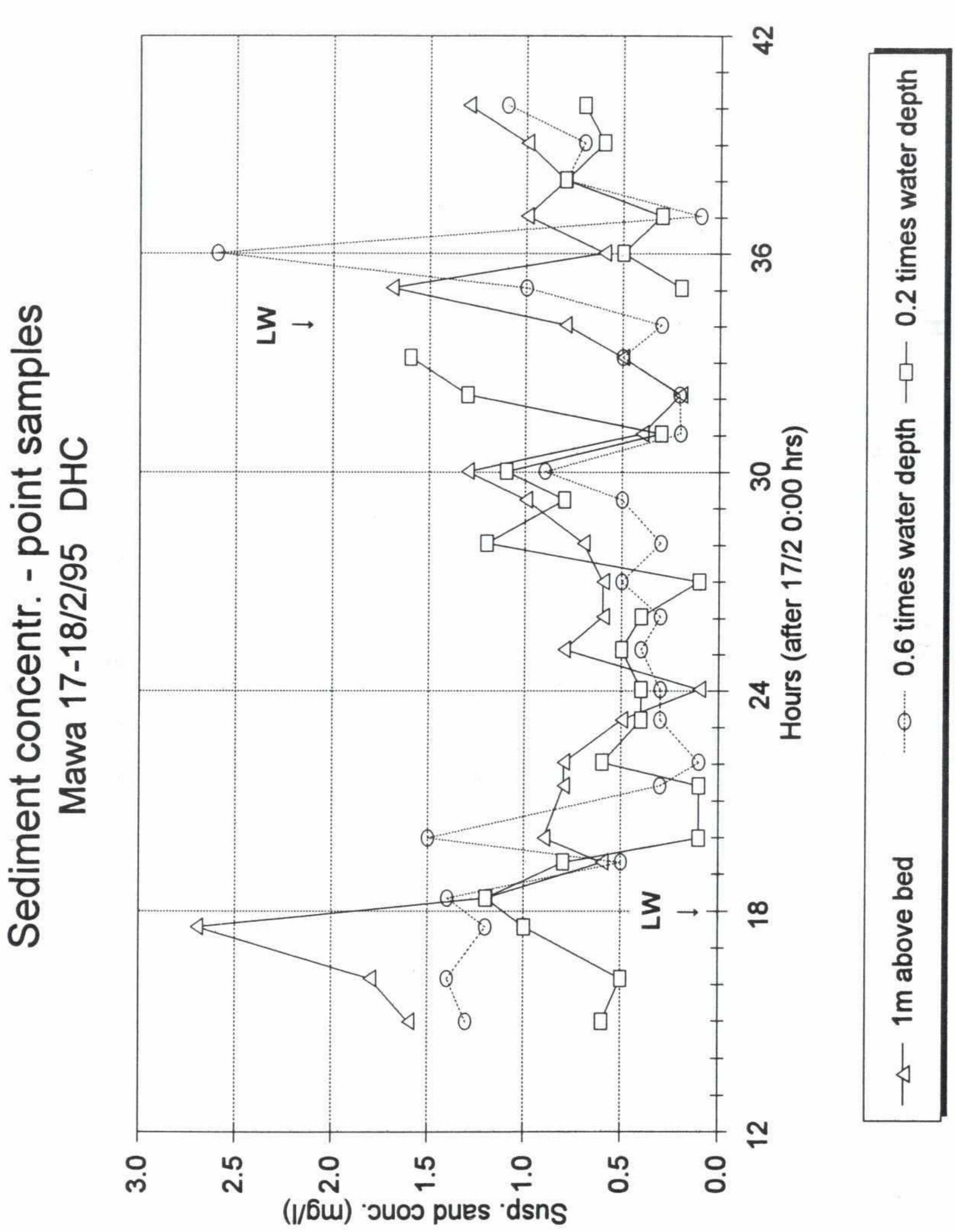

Figure D.15 Mawa. Measured time series of sand concentrations from pump bottle samples (Secondary channel, DHC).

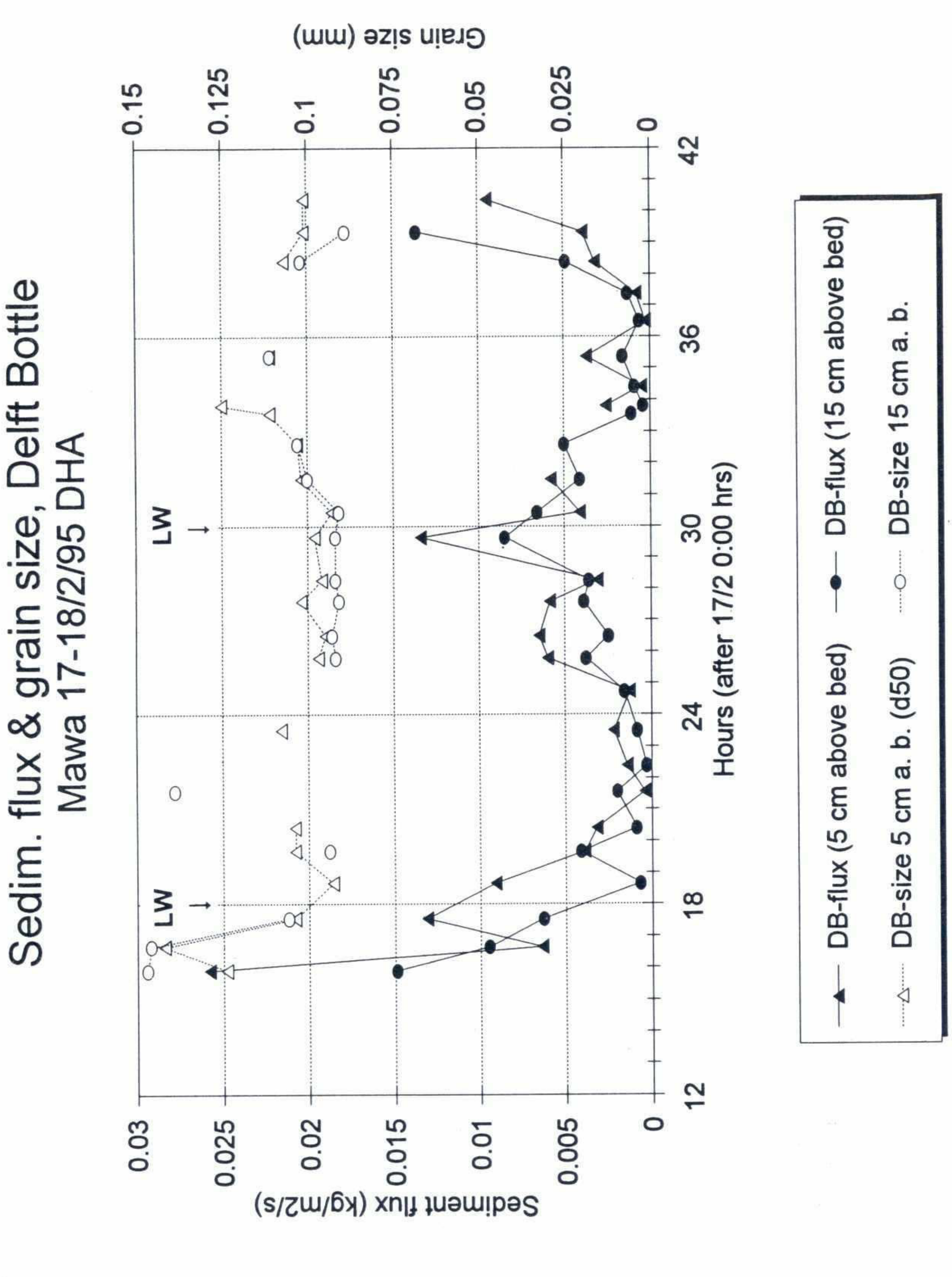

Figure D.16 Mawa. Sediment flux measured by Delft Bottle, shown together with median grain size of samples (Main channel, DHA).

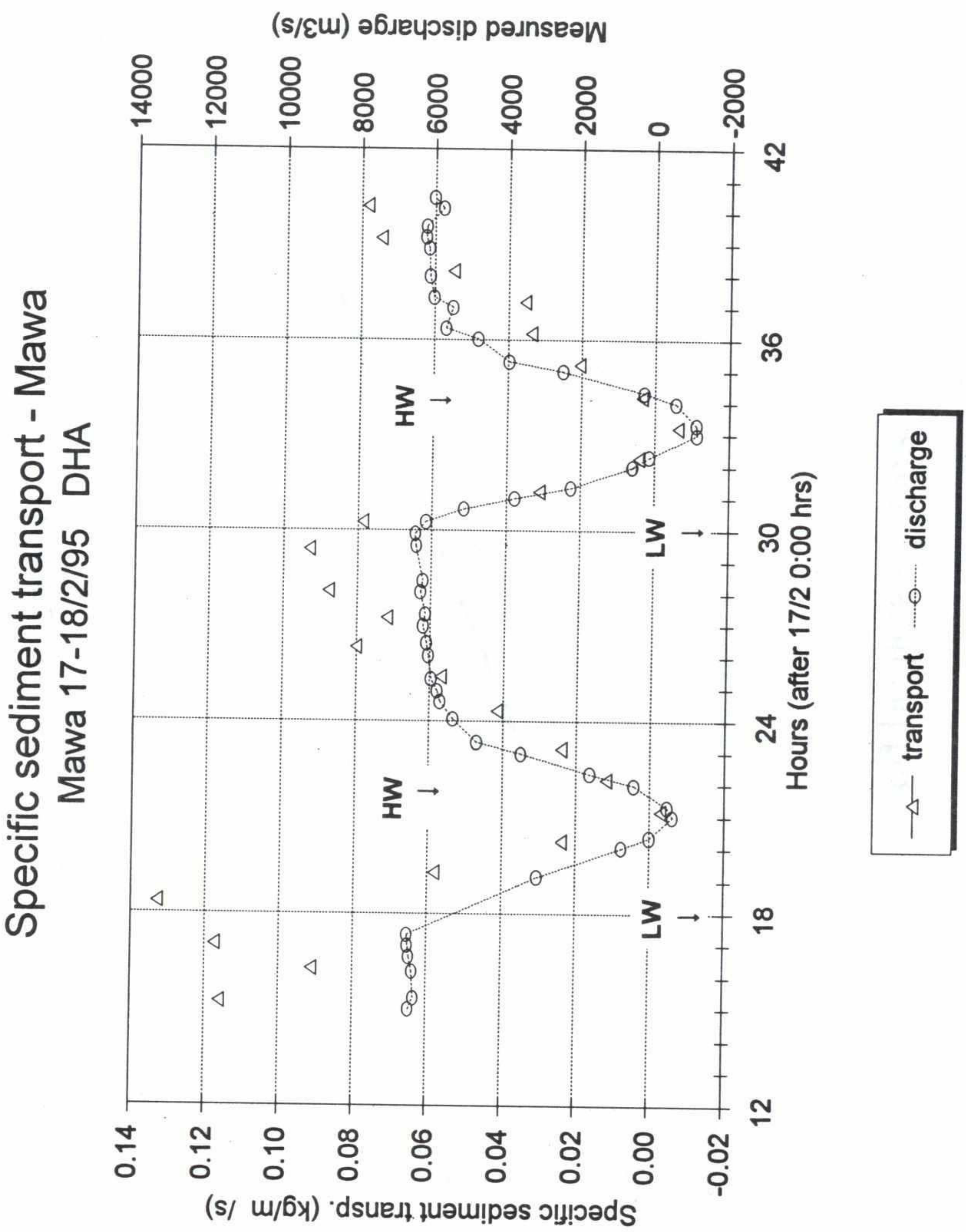

Figure D.17 Mawa. Specific transport of suspended sediment (at a vertical), from pump bottle samples and stationary velocity profiles.

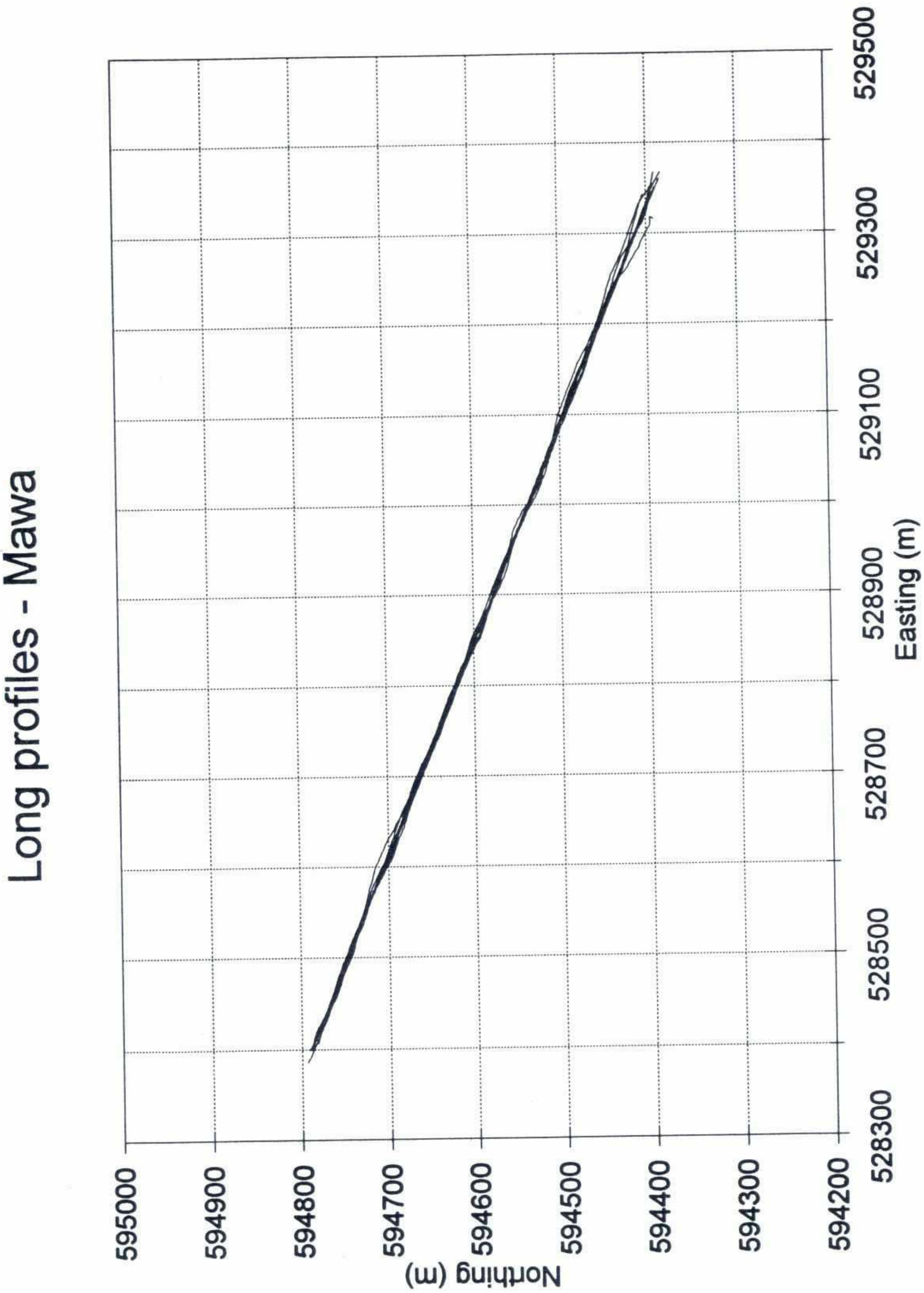

Figure D.18 Mawa. Dune tracking lines (9 surveys).

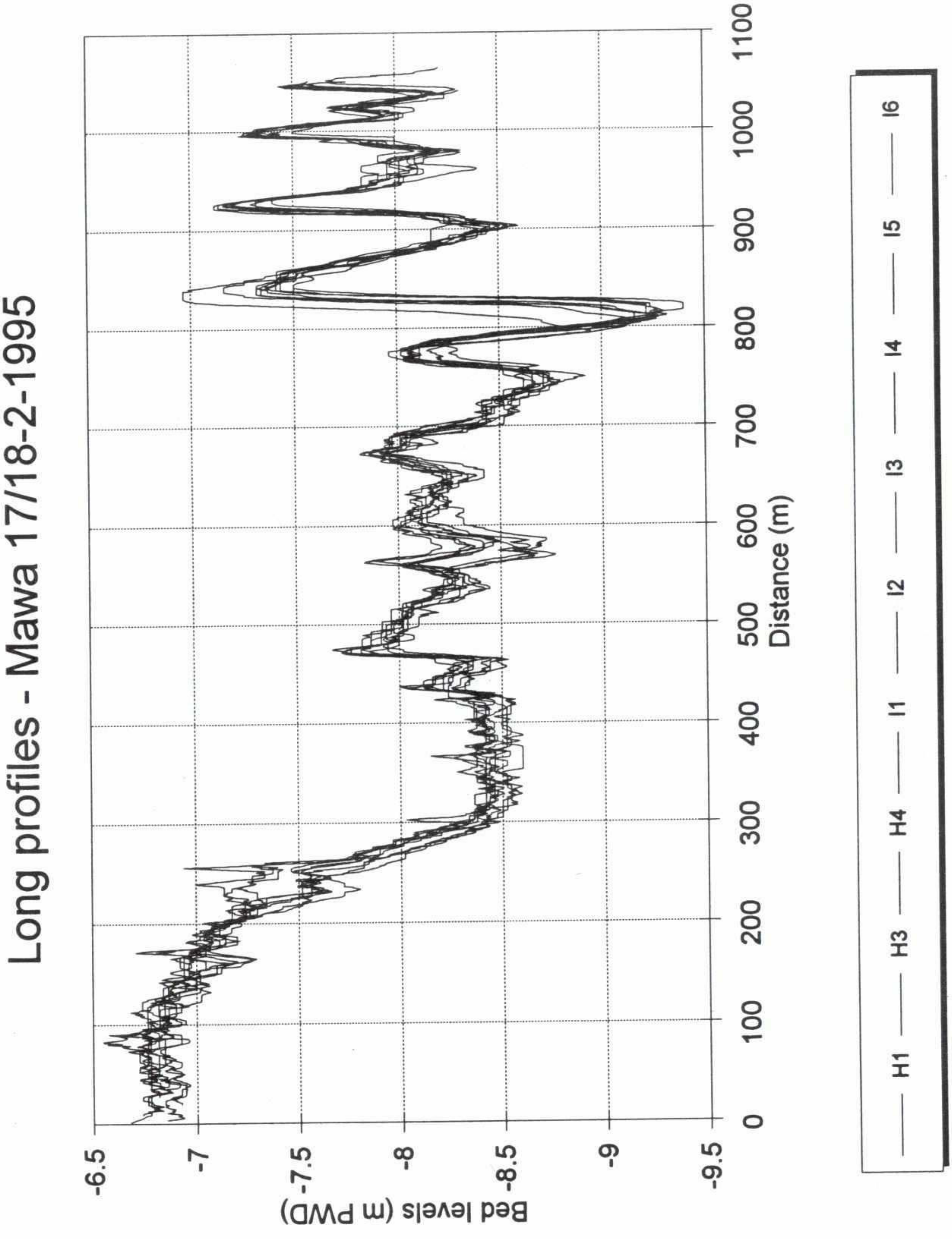

Figure D.19 Mawa. Comparison of dune trackings (after horizontal and vertical reduction). Note: The profiles are highly distorted.

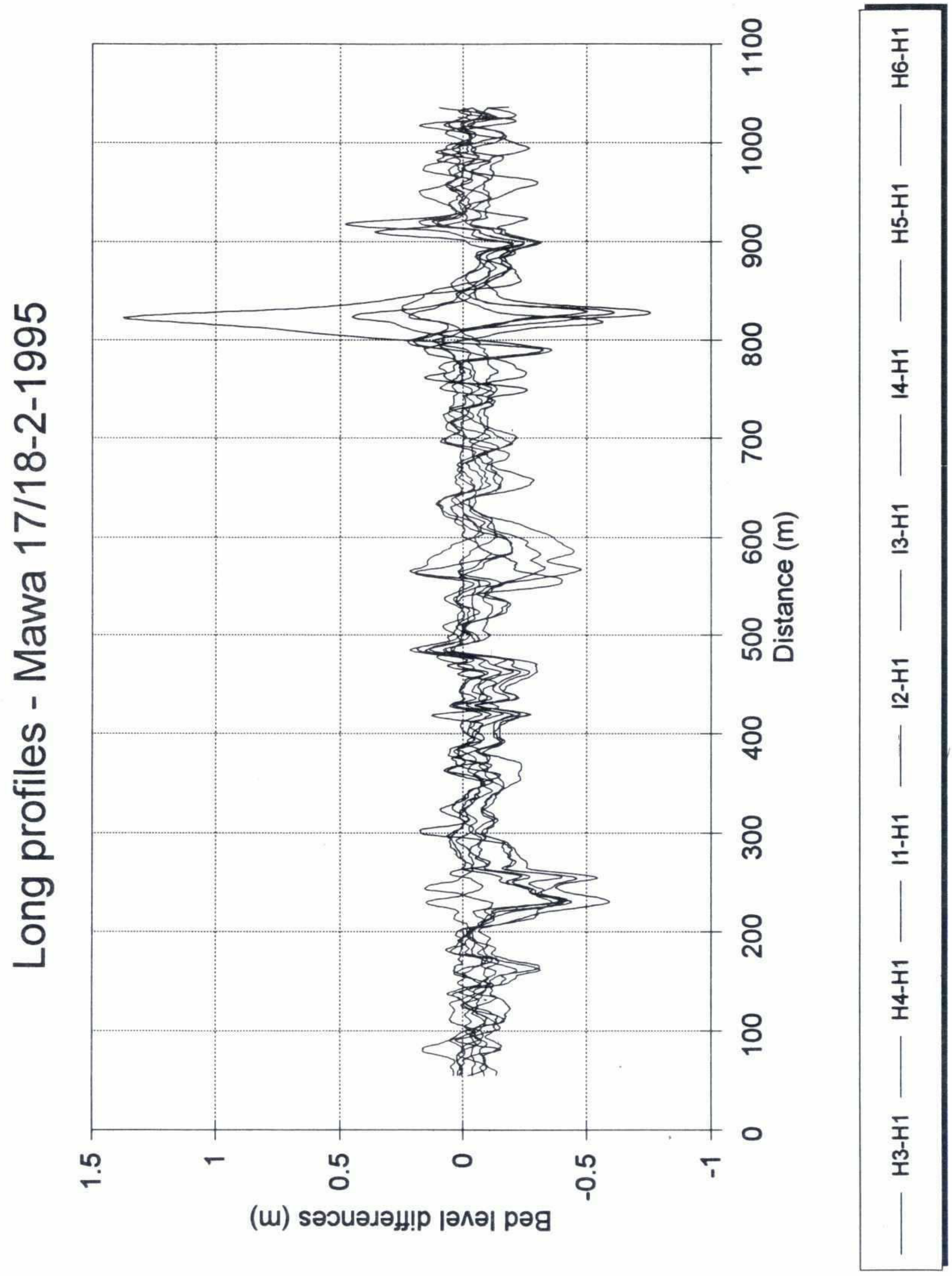

Figure D.20 Mawa. Smoothed differences in bed levels between each dune tracking and the first dune tracking.

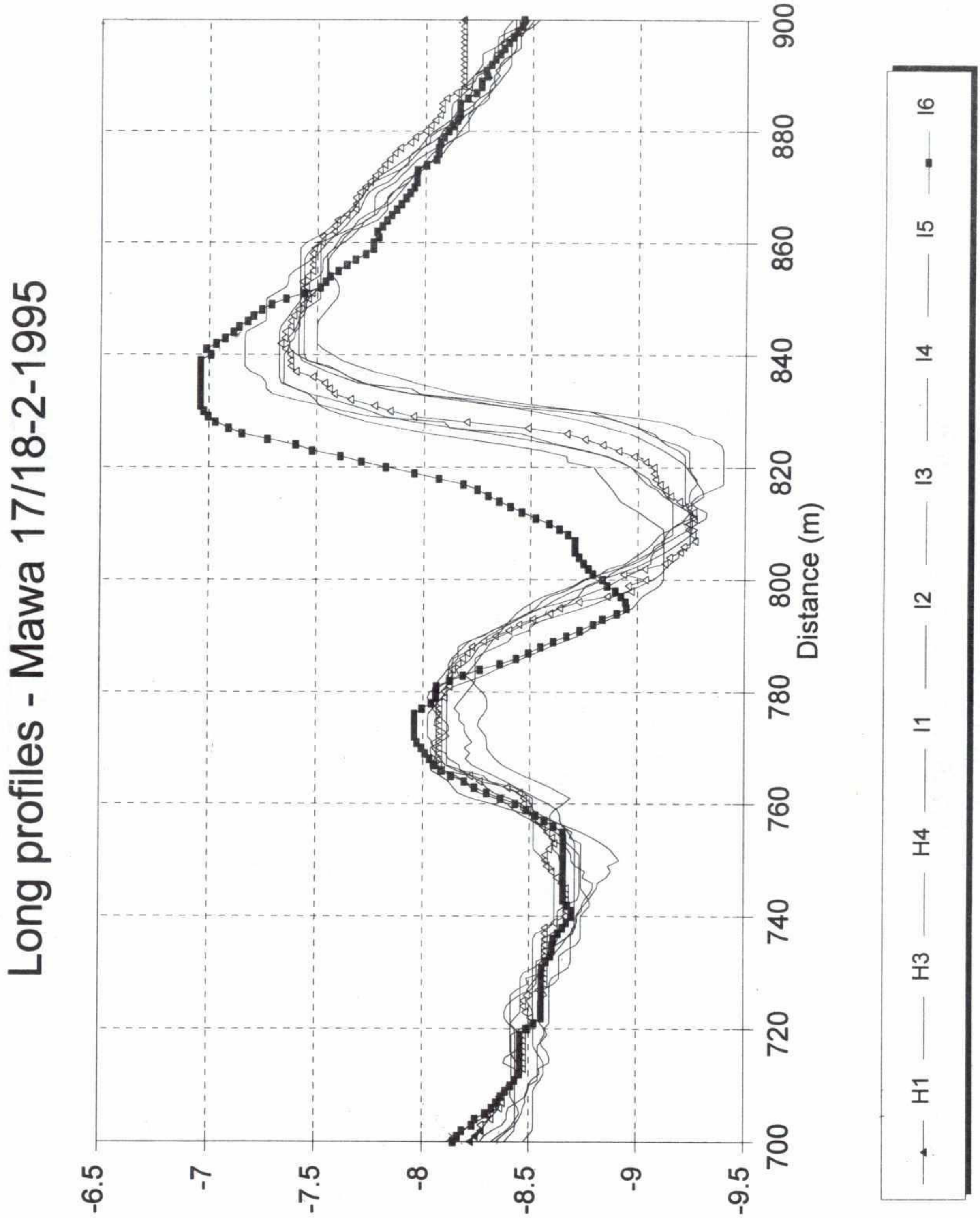

Figure D.21 Mawa. Comparison of dune trackings (after horizontal and vertical reduction) for a selected section of high changes. Note: The profiles are highly distorted.

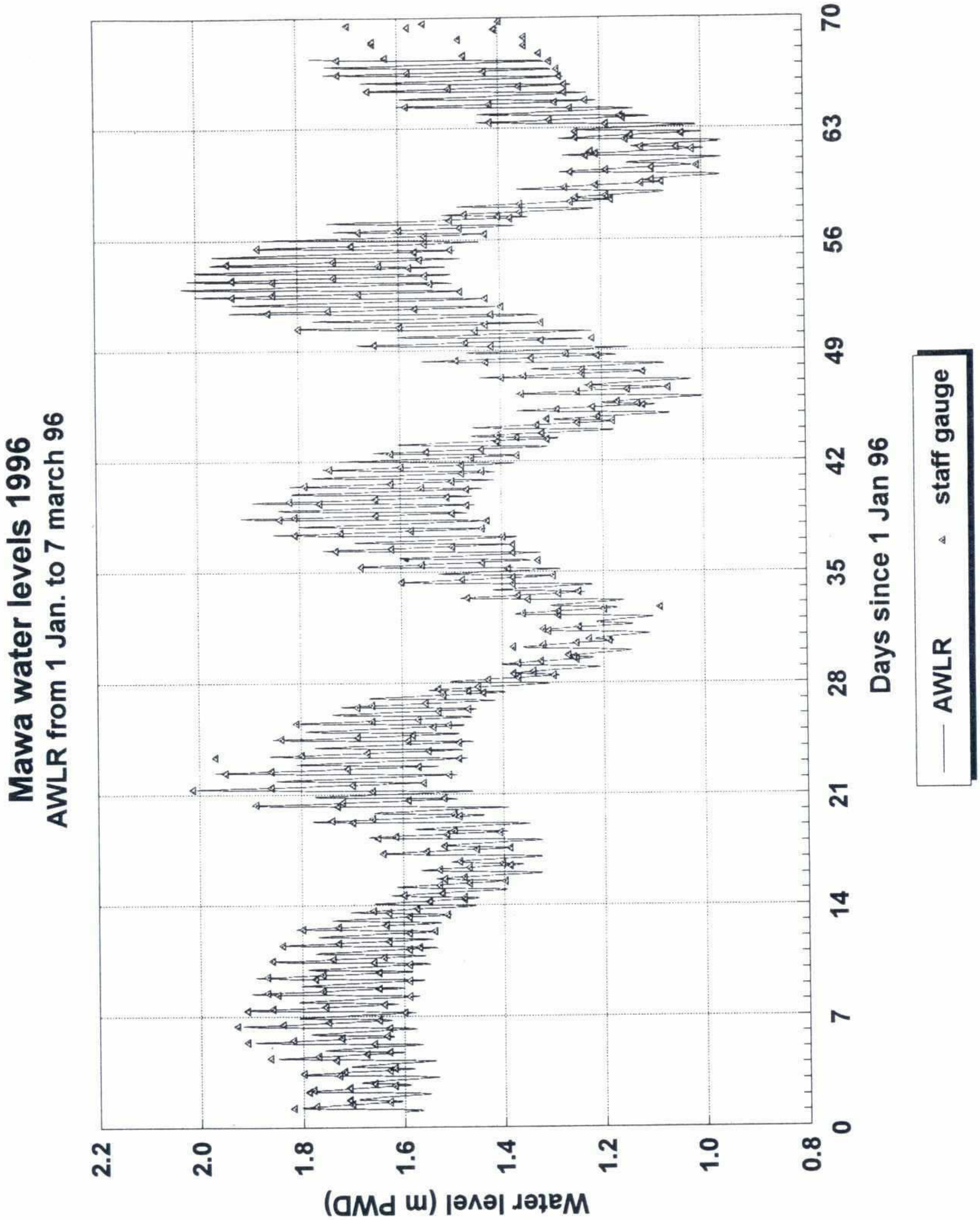

Figure D.22 Two months time series of water levels at Mawa. Automatic water level recorder and staff gauge (both left bank).

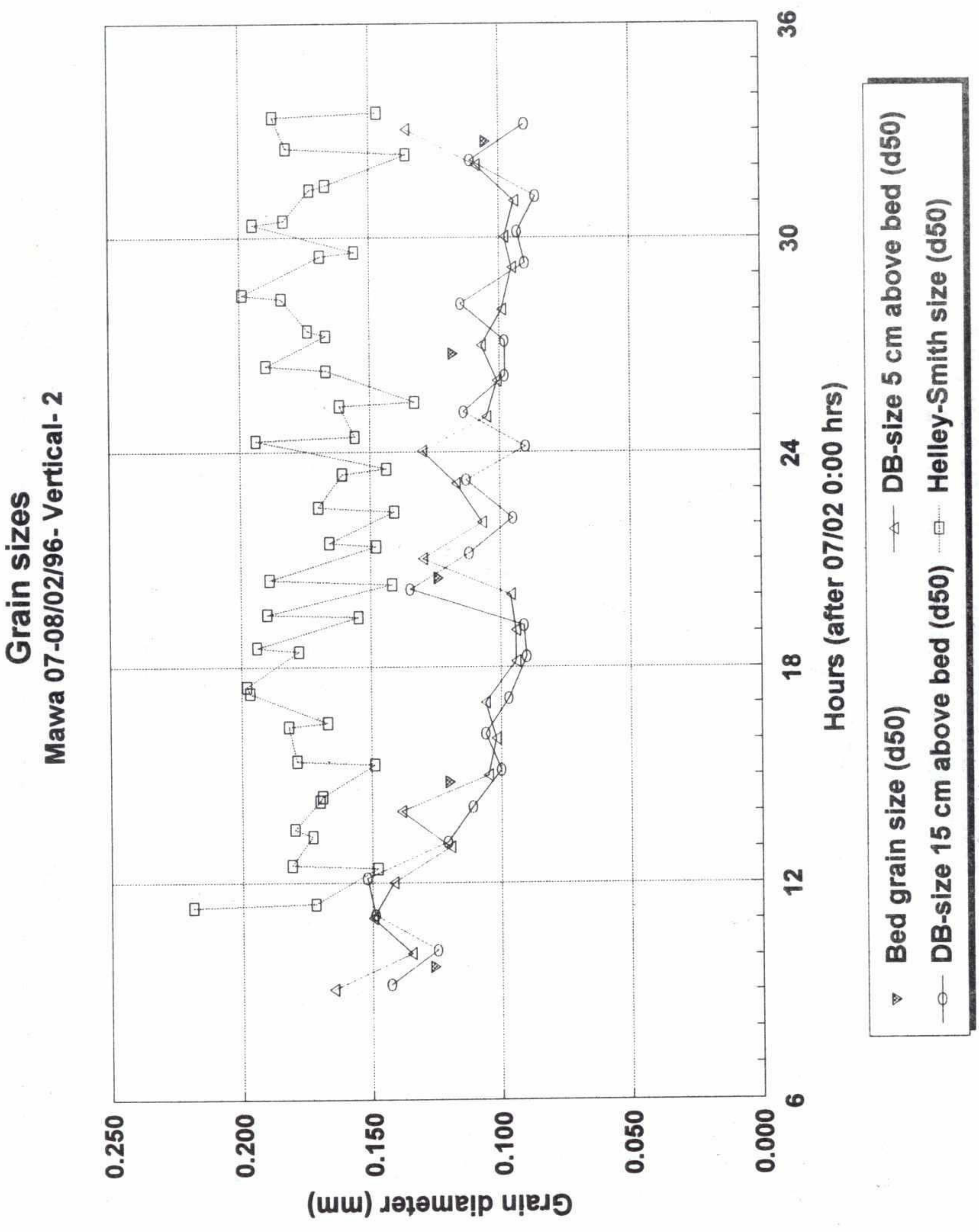

Figure D.23 Mawa. Median grain sizes of bed material samples, Helley Smith samples and Delft Bottle samples (Main channel, Vertical 2).

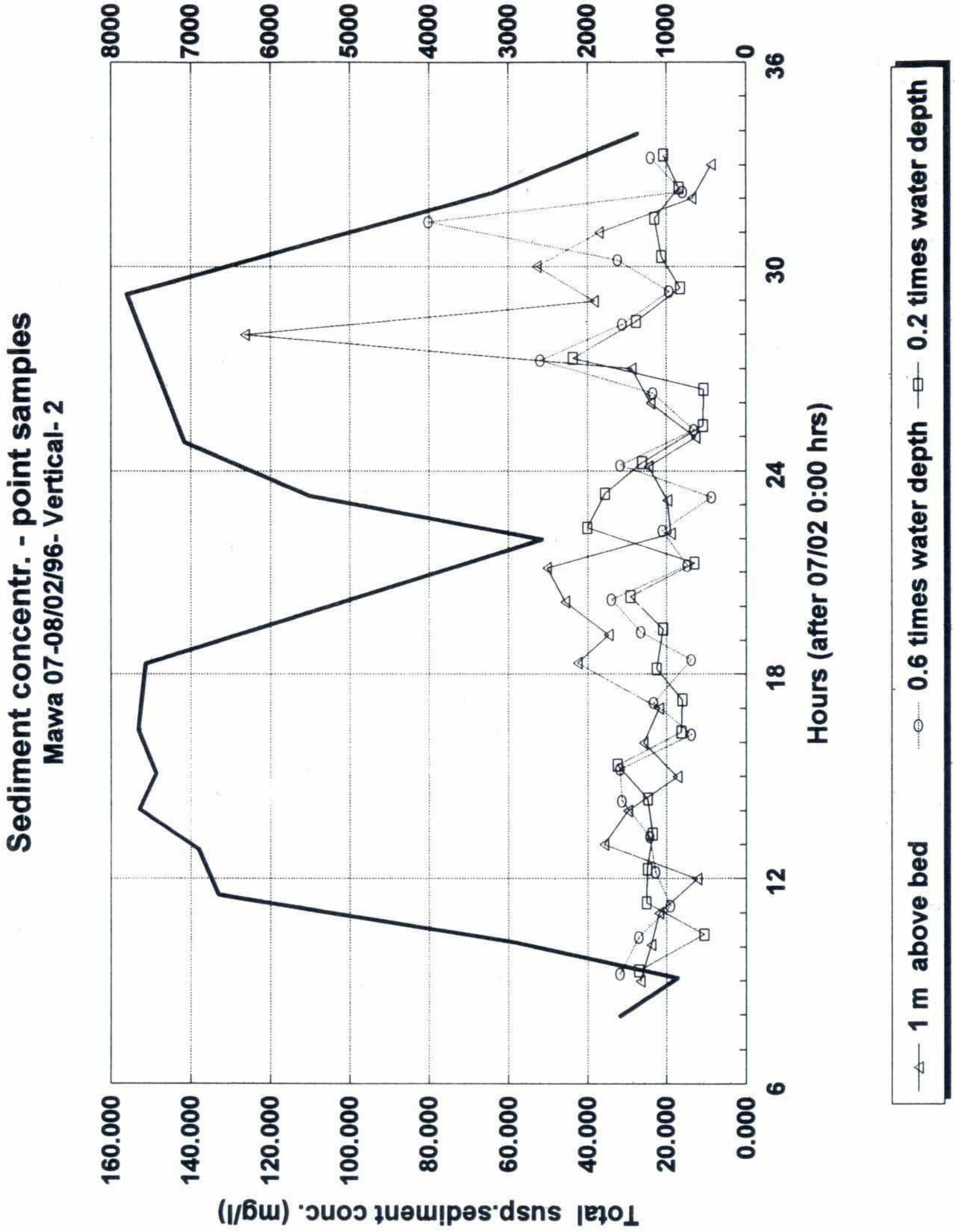

Figure D.24	Mawa. Measured sediment concentration time series (pump bottle samples) shown together with the discharge time series (Main channel, Vertical 2).

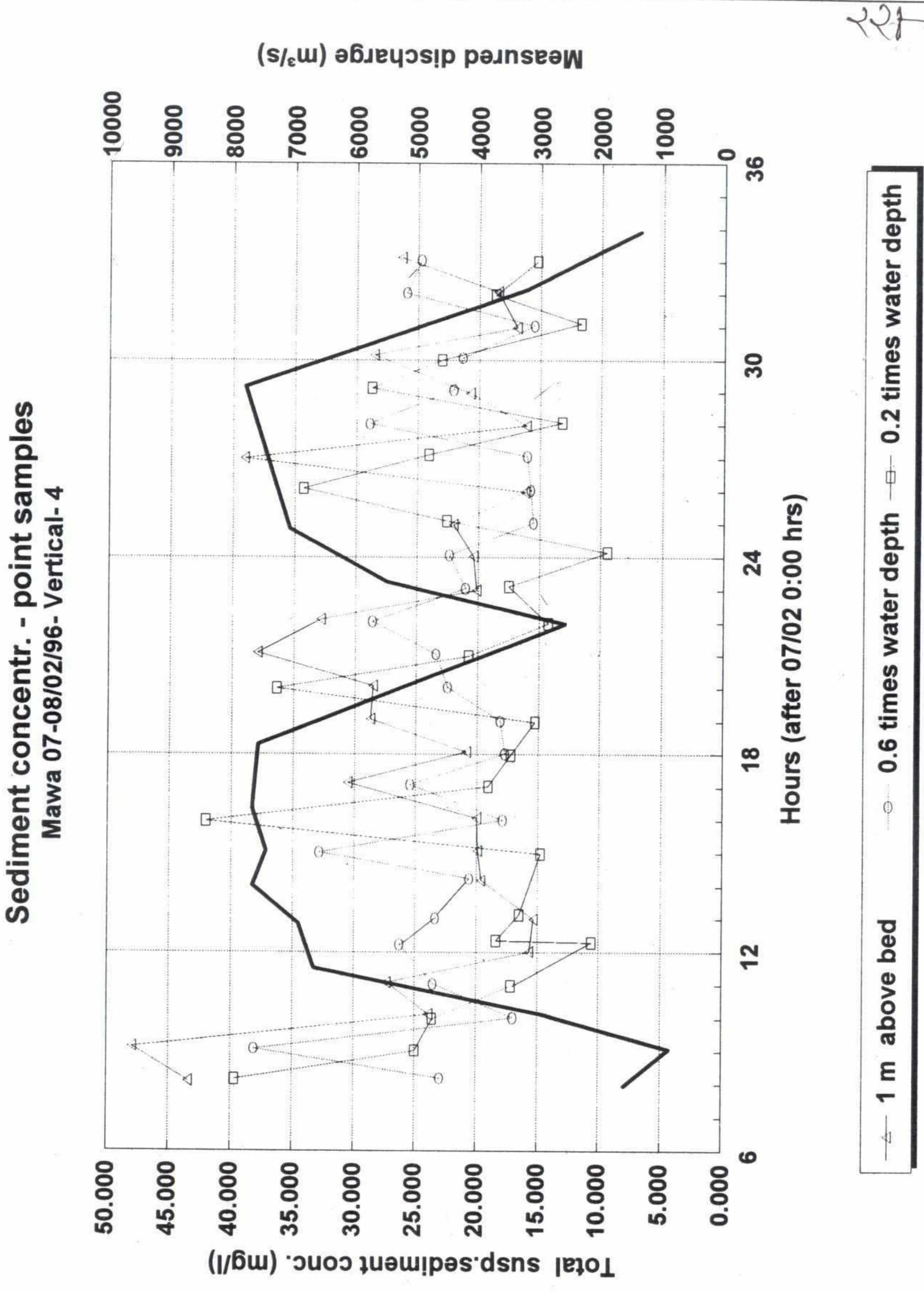

Figure D.25 Mawa. Measured sediment concentration time series (pump bottle samples) shown together with the discharge time series (Secondary channel, Vertical 4).

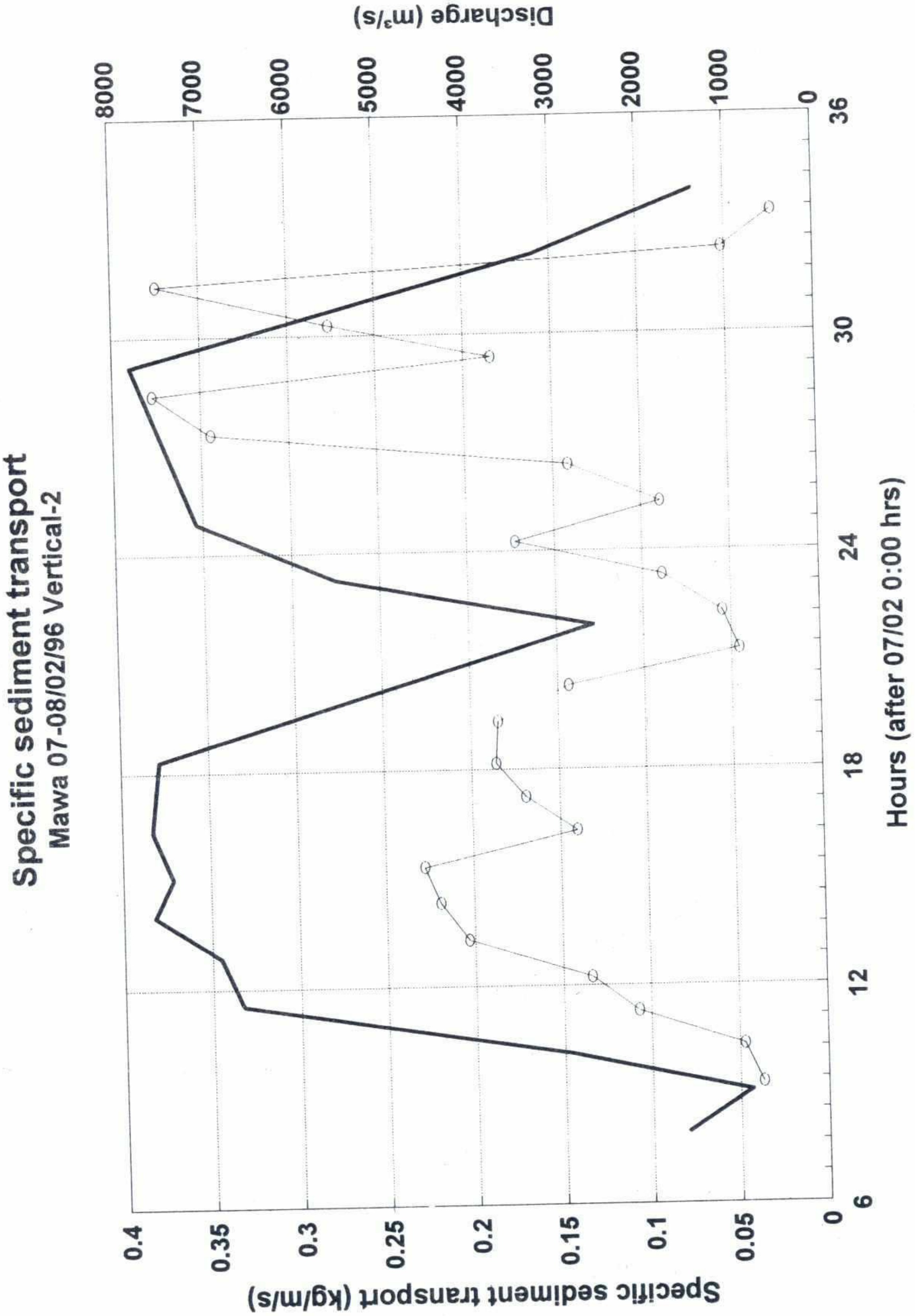

Figure D.26 Mawa. Specific transport of suspended sediment (at a vertical), from pump bottle samples and stationary velocity profiles.

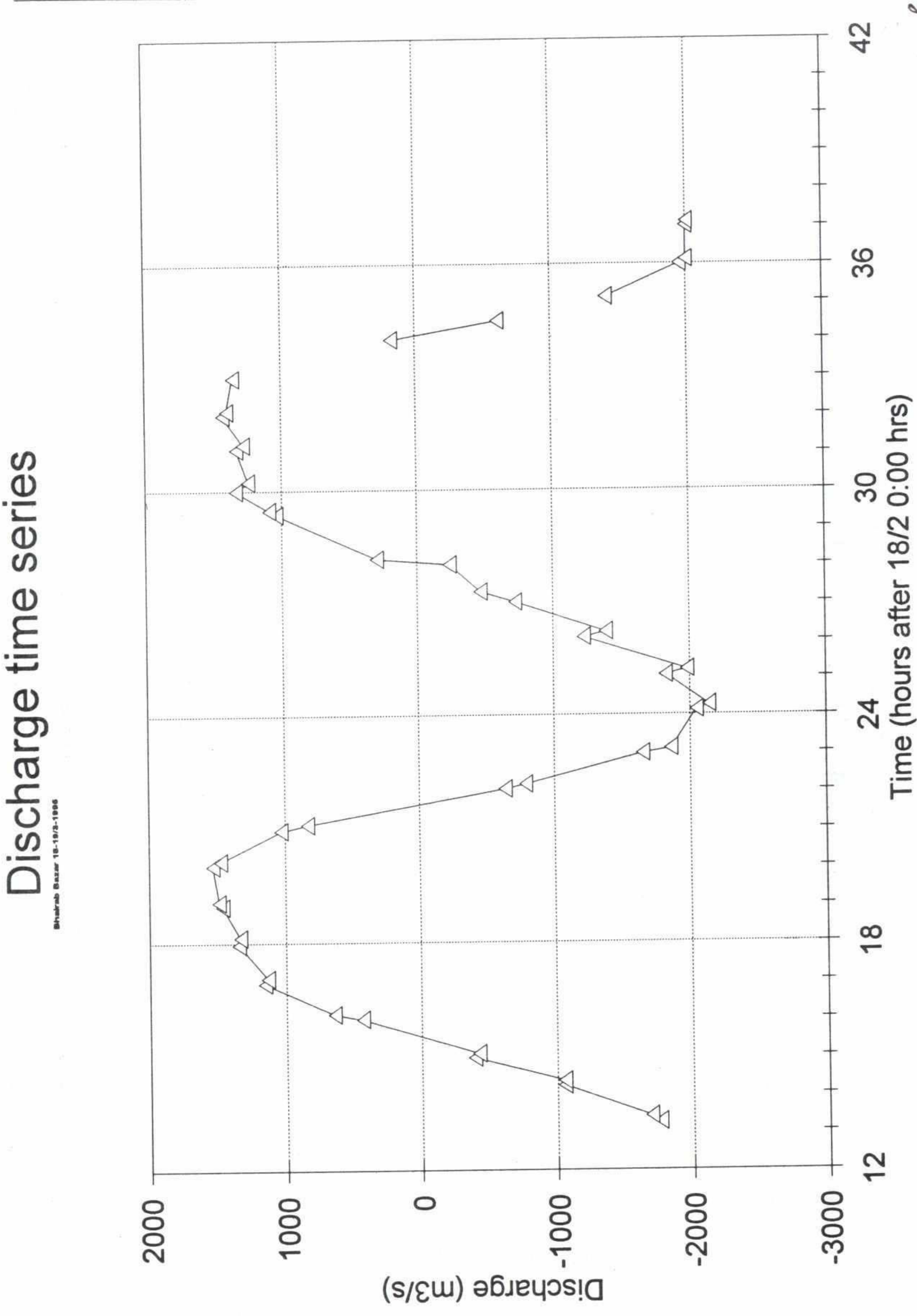

Figure D.27 Bhairab Bazar. Measured discharge time series 18-19/3 1995.

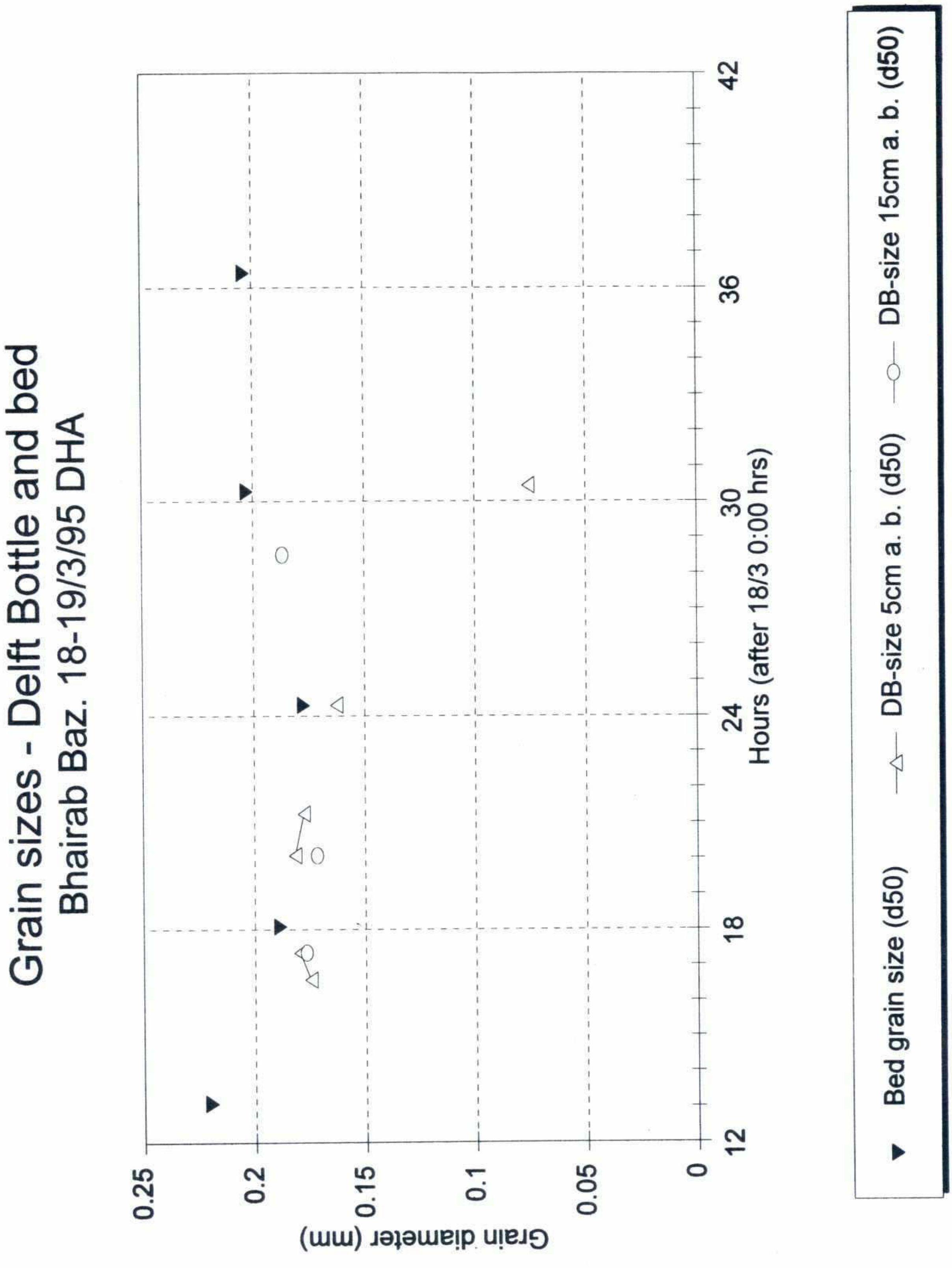

Figure D.28 Bhairab Bazar. Median grain sizes of bed material samples, Helley Smith samples and Delft Bottle samples (Main channel, DHA).

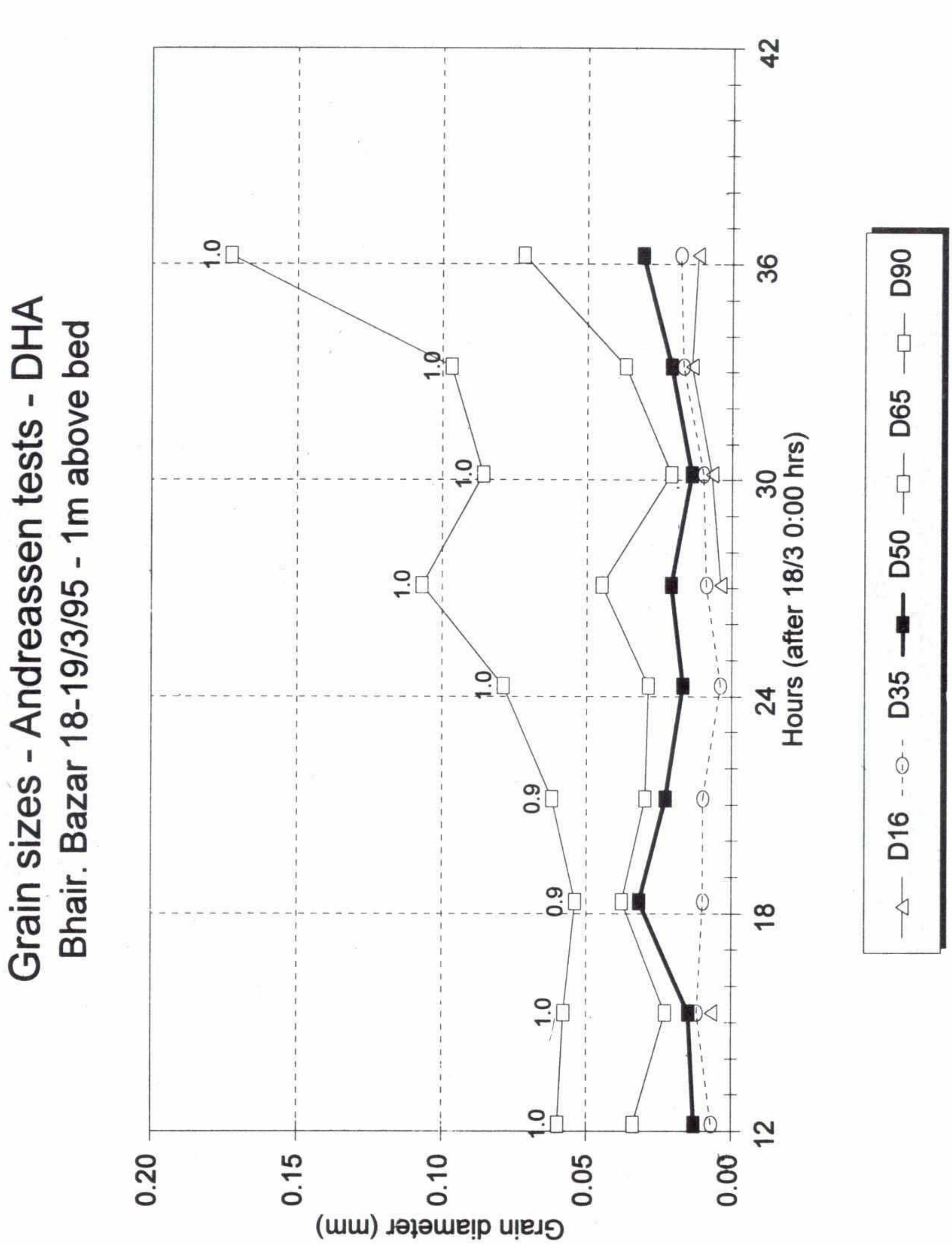

Figure D.29 Bhairab Bazar. Grain sizes fractions determined by Andreassen tests for bulk sediment samples taken approximately 1 m above bed (Main channel, DHA). The labels indicate sampling level above bed (m).

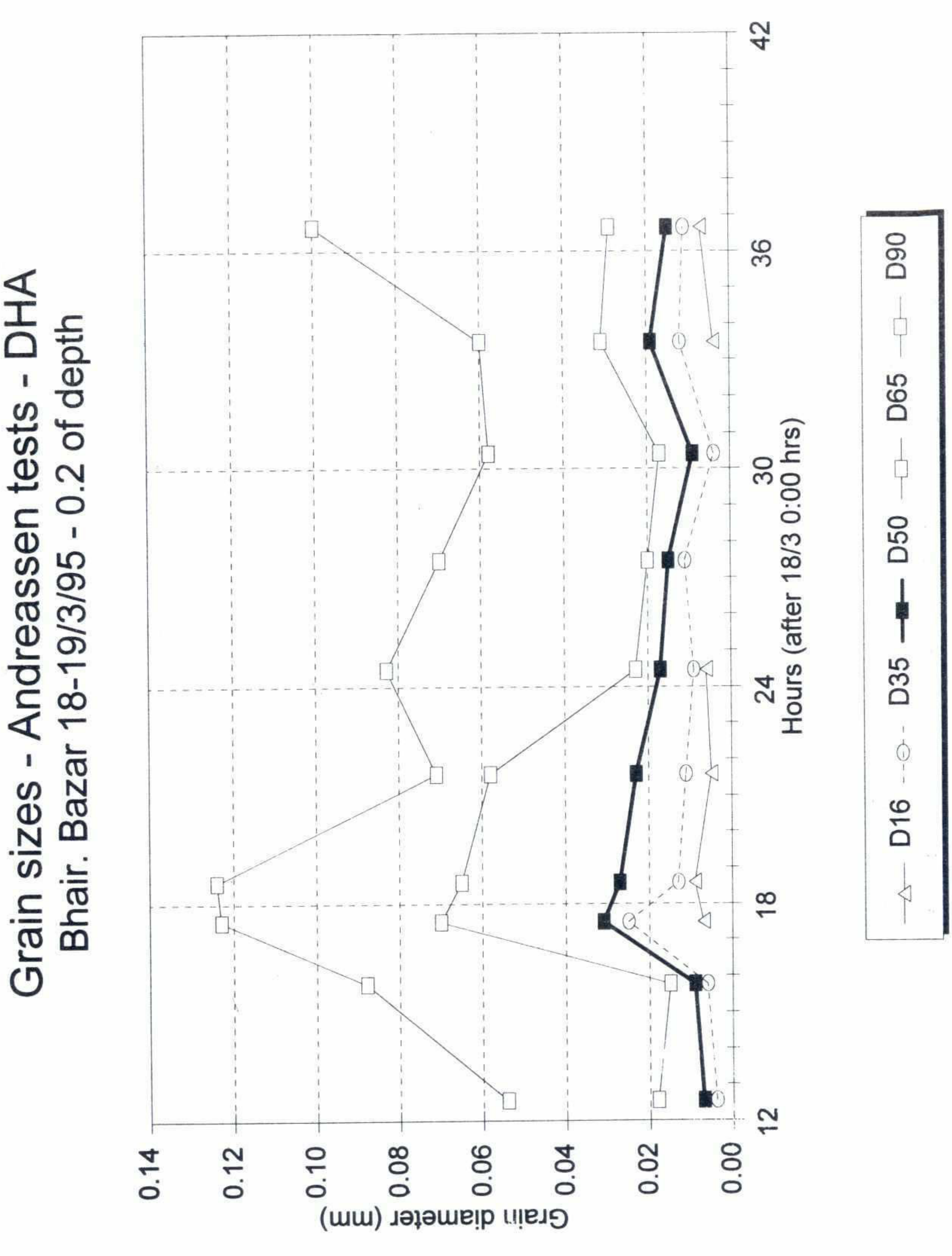

Figure D.30 Bhairab Bazar. Grain sizes fractions determined by Andreassen tests for bulk sediment samples taken approximately 0.2 of water depth below surface (Main channel, DHA).

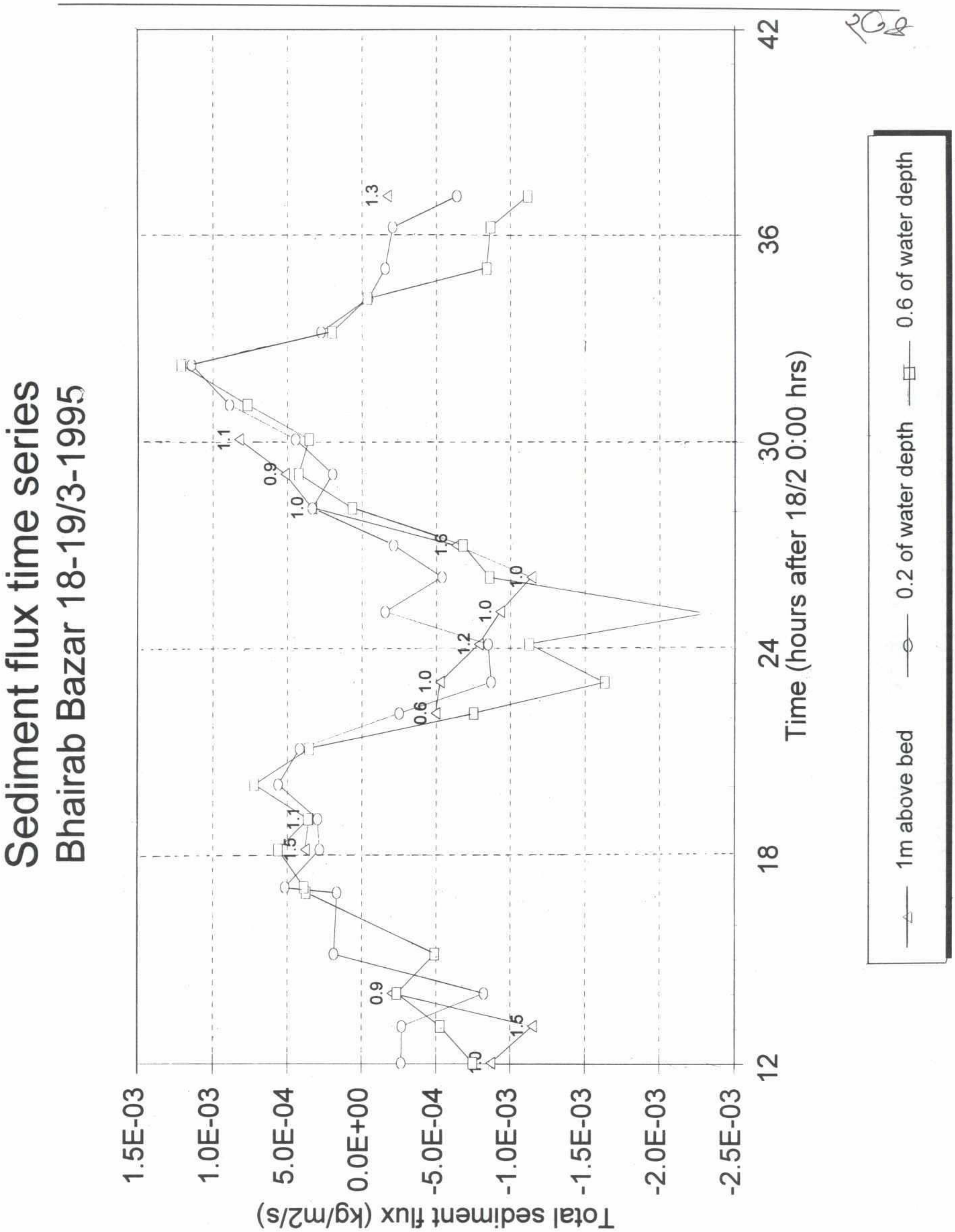

Figure D.31 Bhairab Bazar. Sediment flux at different levels of the vertical profile, determined as concentration multiplied by velocity. Total load. The labels indicate sampling level above bed for the measurement nearest to the bed (m).

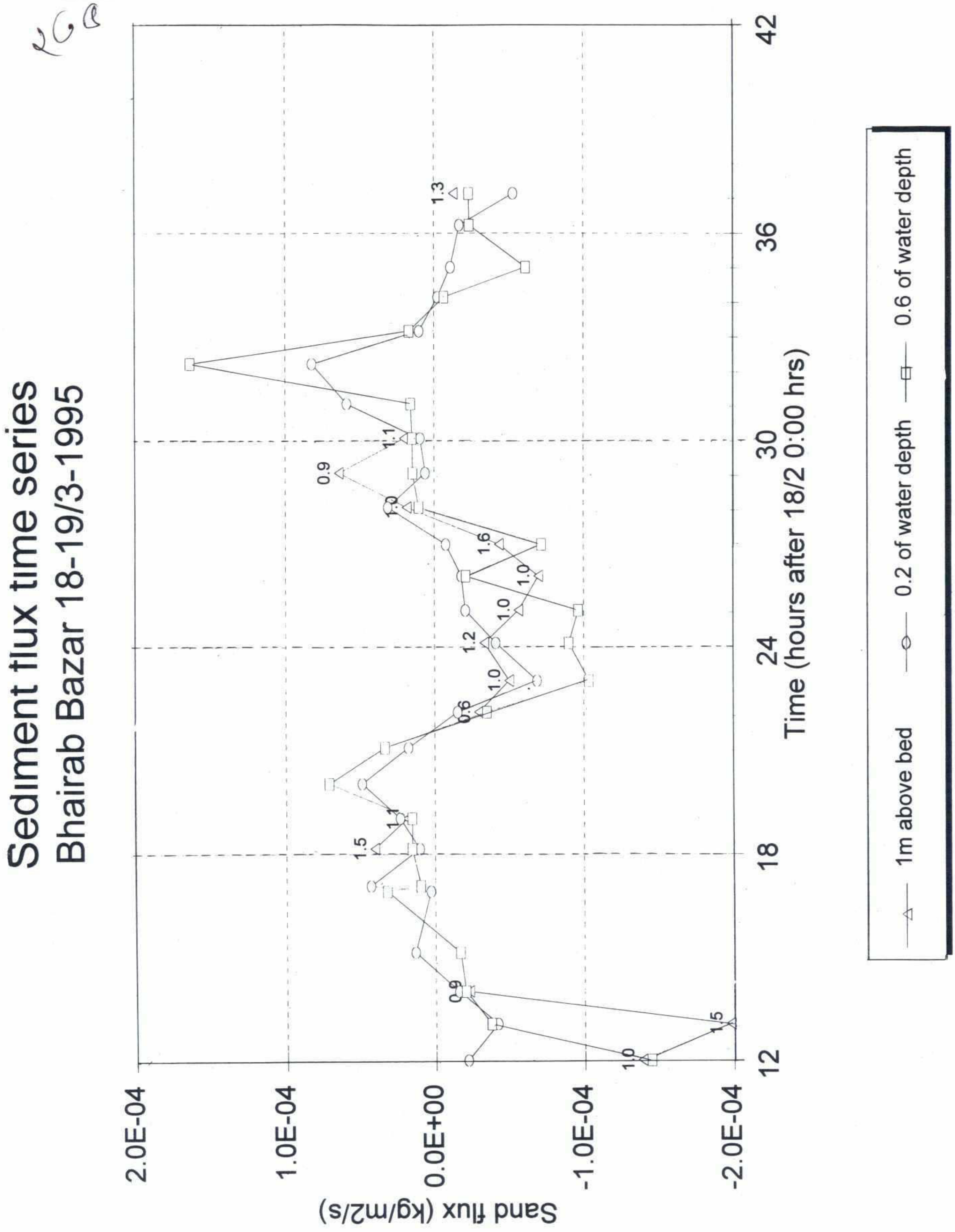

Figure D.32 Bhairab Bazar. Sediment flux at different levels of the vertical profile, determined as concentration multiplied by velocity. Sand fraction only. Labels indicate sampling level above bed for the measurement nearest to the bed (m).

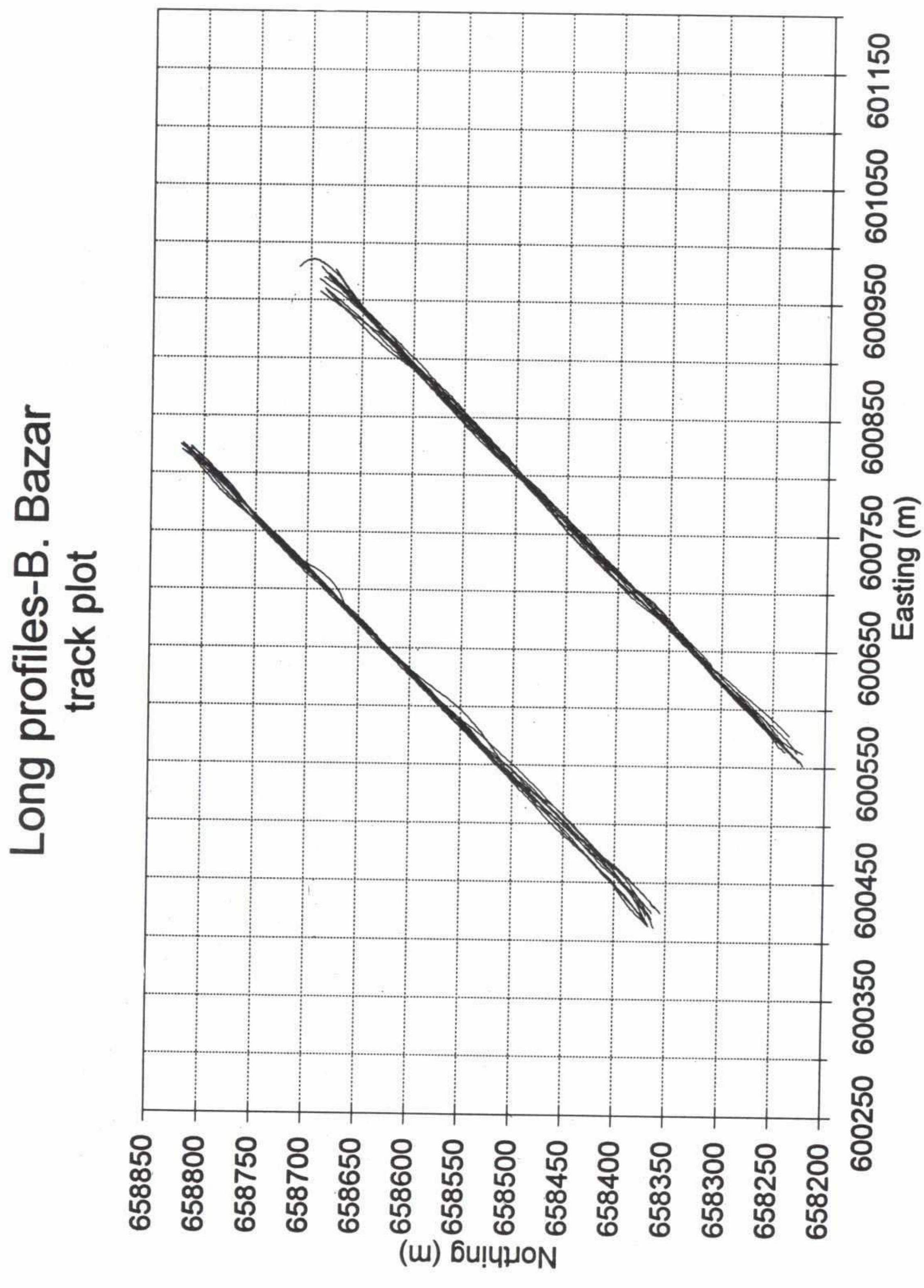

Figure D.33 Bhairab Bazar. Dune tracking lines.